

# Phenomenology of the BFKL Pomeron and Unitarity Corrections at low $x$

H. Lotter

II. Institut f. Theoretische Physik, Universität Hamburg,  
Luruper Chaussee 149, D-22761 Hamburg

The low  $x$  limit of deep inelastic electron proton scattering is considered using methods of perturbative QCD. In the first part we investigate the phenomenological consequences of the resummation of leading logarithms in  $1/x$  given by the BFKL pomeron. We apply the BFKL pomeron to the inclusive structure function  $F_2$ , to the diffractive production of vector mesons at large momentum transfer, to inclusive photon diffractive dissociation in DIS and to quark-antiquark production with large transverse momenta in DIS diffractive dissociation. For the last process we perform extensive numerical calculations based on the double logarithmic approximation.

The BFKL pomeron is known to violate unitarity. In the second part the first next-to-leading corrections which have to be taken into account to restore unitarity of the scattering amplitude are investigated. A compact configuration space representation of the two to four gluon transition vertex is derived. Conformal symmetry of the vertex is proven and its relation to a conformal covariant three point function is established. The important role of the spectral function  $\chi_4$  of the four gluon state is pointed out. We relate this function to the twist expansion of the four gluon amplitude. Motivated by this relation we develop a method to perform the twist expansion of the amplitude. Based upon first results of our analysis we draw conclusions concerning the singularity structure of the function  $\chi_4$ .



# Contents

<b>1</b>	<b>Introduction</b>	<b>3</b>
<b>2</b>	<b>Properties of the BFKL Pomeron</b>	<b>10</b>
2.1	The Bethe Salpeter equation in momentum space . . . . .	11
2.2	The configuration space representation . . . . .	12
2.2.1	Conformal invariance of the equation . . . . .	13
2.2.2	Conformal partial wave expansion . . . . .	15
2.2.3	Conformally invariant $n$ -point functions . . . . .	16
2.3	The momentum space representation of the conformal eigenfunctions . . . . .	17
2.3.1	The expansion in powers of the momentum transfer . . . . .	20
<b>3</b>	<b>Phenomenology of the BFKL Pomeron in Deep Inelastic Scattering</b>	<b>22</b>
3.1	Inclusive Scattering at small $x$ : Collinear and High Energy Factorization . . . . .	24
3.1.1	Collinear factorization . . . . .	24
3.1.2	High energy factorization and the BFKL equation for $F_2$ . . . . .	25
3.1.3	BFKL equation and transverse energy distribution . . . . .	29
3.2	Diffractive Production of Vector Mesons at large $t$ . . . . .	31
3.2.1	The result for the cross section . . . . .	31
3.2.2	Comparison of the exact formula with asymptotic expressions . . . . .	33
3.2.3	The slope of the BFKL amplitude . . . . .	36
3.3	The BFKL pomeron in DIS diffractive dissociation . . . . .	38
3.3.1	The production of $q\bar{q}$ -pairs . . . . .	38
3.3.2	The limit $\mathbf{q}^2 = 0$ . . . . .	42
3.3.3	The limit of large momentum transfer . . . . .	44
3.3.4	Additional gluons in the final state . . . . .	45
3.4	Production of $q\bar{q}$ pairs in DIS diffractive dissociation . . . . .	48
3.4.1	Kinematics and observables . . . . .	48
3.4.2	Formalism and result for the cross section . . . . .	49
3.4.3	Numerical results . . . . .	54
3.4.4	The angular asymmetry . . . . .	58
3.4.5	Production of charm quarks . . . . .	61
<b>4</b>	<b>Unitarity Corrections</b>	<b>64</b>
4.1	Generalized leading-log approximation . . . . .	66
4.1.1	Unitarity relations from the BFKL equation . . . . .	67
4.1.2	Higher order equations . . . . .	68
4.2	The transition vertex . . . . .	69
4.2.1	The operator representation . . . . .	70
4.2.2	Conformal invariance . . . . .	75
4.2.3	Projection on conformal three-point functions . . . . .	76
4.3	The four gluon state I: Introduction, Motivation and Examples . . . . .	79
4.3.1	The onset of unitarity . . . . .	79
4.3.2	Correlation functions, short distance limit and the BFKL amplitude as an example . . . . .	81
4.3.3	The twist expansion . . . . .	84
4.4	The four gluon state II: Beginning of the Twist Expansion . . . . .	86
4.4.1	The two reggeon intermediate state . . . . .	89
4.4.2	The effective interaction vertex . . . . .	93
4.4.3	Concluding remarks . . . . .	98
<b>5</b>	<b>Conclusions</b>	<b>100</b>

<b>A</b>	<b>Appendix</b>	<b>104</b>
A.1	Fourier transformation of the Bethe-Salpeter equation . . . . .	104
A.2	The eigenvalue of the configuration space kernel . . . . .	105
A.3	Properties of the BFKL eigenvalue $\chi(\nu, n)$ . . . . .	107
A.4	Expansion of the momentum space eigenfunction for small argument . . . . .	107
	<b>References</b>	<b>109</b>

# 1 Introduction

The physics of hadrons is the regime of the theory of the strong interaction. A realization of a theory of the strong interaction satisfying the requirements of general quantum theory and relativity is Quantum Chromodynamics (QCD). The objective of QCD is to describe the variety of strong interaction phenomena ranging from the spectrum of light meson states to high energetic hadronic collisions. Unfortunately, the mathematical structure of QCD is quite complicated so that a solution of QCD, e. g. the calculation of all correlation functions, appears impossible. Consequently, to make predictions in QCD, one has to make use of an approximation scheme. In a very coarse-grained distinction these approximation methods can be divided into two classes. One can distinguish between perturbative<sup>1</sup> methods on the one hand and nonperturbative methods on the other hand.

Perturbative calculations start from the elementary degrees of freedom of QCD, namely quarks and gluons. Perturbation theory begins with the observation that the coupling constant of QCD which specifies the strength of the interactions of quarks and gluons decreases when the energy of these particles increases (asymptotic freedom). The perturbative approach is therefore appropriate when the specific phenomenon under consideration can be shown to be describable in terms of the elementary interactions of highenergetic quarks and gluons. Nonperturbative methods have to be applied when such a description is not possible. Since the interaction of quarks and gluons is strong then, nonperturbative considerations often start from composite objects or collective excitations of quarks and gluons as e. g. condensates, mesons or instantons. It is a major challenge in QCD to find a connection between these nonperturbative composite objects and the perturbative quark and gluon degrees of freedom. This is the place where this thesis is settled. Using perturbative methods it attempts to approach a composite, probably nonperturbative, object of QCD, the pomeron.

The pomeron is a concept which originates from Regge theory. It has a mathematical definition as the rightmost singularity with vacuum quantum numbers of the proton-proton scattering amplitude in the complex angular momentum plane. Phenomenologically it admits the interpretation of an exchanged object mediating the proton proton interaction at very high center of mass energies. It leads to a slow rise of the total proton-proton cross section at high energies. From the theoretical point of view this rise can at most be logarithmic since a power rise would ultimately lead to a violation of unitarity bounds. Since in the bulk of the total proton-proton cross section processes which are determined by an underlying high energetic quark or gluon interaction cannot be identified, the pomeron is commonly considered to be of nonperturbative origin. Stated differently, perturbation theory is not the correct approximation scheme to describe the total proton-proton cross section. It should be emphasized that up to now the behavior which is associated with the pomeron has not been derived ab initio from QCD.

There are, on the other hand, processes which are describable in terms of elementary quark and gluon interactions, in which perturbation theory is thus applicable. It is then perfectly legitimate to ask for the behavior of these processes at high center of mass energy, i. e. in the regime of Regge theory.

An example of such a process is onium-onium scattering, i. e. the scattering of two colorless heavy quark - heavy antiquark states. When processes of this type are studied at high center of mass energy in the framework of QCD perturbation theory a problem arises. When perturbative contributions of higher order are considered they are found to be proportional to powers of the logarithm of the center of mass energy. Since one is interested in high energies, this logarithm is a large parameter and it is eventually sufficiently large to compensate the smallness of the coupling constant. Because of this observation it is of course senseless to apply fixed order perturbation theory to study the high energy behavior of the process. In this situation a possible escape is resummation. It is clearly not possible to resum all perturbative contributions but a sensible starting point is to isolate in each order the contribution with the highest power of the logarithm and to resum these leading terms. The result of this procedure is termed the leading logarithmic approximation. This resummation was performed, in perturbative QCD, for the first time by Balitskii and Lipatov [1]. They made use of results which were obtained by Lipatov and coworkers in the framework of the massive gauge theory some time before [2, 3, 4]. The infinitely many Feynman diagrams they resummed have the topology

---

<sup>1</sup>The term 'perturbative' is used in a narrow sense here denoting methods which are based on the expansion in powers of the coupling constant.

of ladder diagrams with reggeized gluons in the  $t$ -channel. The ladders are summed by an integral equation, the BFKL equation. The reggeized gluon itself also represents an infinite number of Feynman diagrams. In this sense it can be regarded as a collective excitation within perturbative QCD. The resummed amplitude turns out to have a cut in the complex angular momentum plane. It has been termed the perturbative or BFKL pomeron.

We now give an introduction to the investigations pursued in this thesis where we refer also to previous and related work. The original contributions contained in the present work are indicated in the end.

The BFKL pomeron has a number of remarkable properties which we summarize in the second chapter of this thesis. First of all it is an infrared finite quantity, i. e. all singularities which arise individually from real and virtual corrections cancel in the sum. A quite interesting property of the BFKL equation is its invariance w. r. t. global conformal transformations in two-dimensional transverse configuration space. Due to this property the equation can easily be solved in configuration space by a conformal partial wave expansion [5]. Furthermore the resummed scattering amplitude can be interpreted in the framework of an effective conformal field theory. In this interpretation the reggeized gluon appears as a primary field of conformal dimension and spin zero. The BFKL amplitude which depends only on the anharmonic ratios of the coordinates can consistently be interpreted as the four point function of this field.

With these interesting results in mind one can ask two questions

- Is the BFKL pomeron phenomenologically relevant, or, stated differently, is there a possibility to observe the effect of the resummation of perturbative leading logarithms in a physical process?
- What is the relation between the BFKL pomeron and the true QCD pomeron?

The first of these questions is addressed in chapter 3 of this work whereas chapter 4 discusses the present status of the second question.

Since onium-onium scattering is not experimentally feasible presently, a different physical process has to be used to study the phenomenological applications of the BFKL resummation. A class of processes which is for many reasons appropriate for this undertaking are deep inelastic electron-proton scattering (DIS) processes at low values of the Bjorken scaling variable  $x$ . In DIS perturbative QCD has been very successful in describing observable quantities at intermediate values of  $x$  due to the large virtuality  $Q^2$  of the photon which in many processes sets the energy scale for the strong coupling constant. The perturbative QCD approach to inclusive DIS, i. e. structure function calculations, is based on collinear factorization [7] which allows to separate perturbative and nonperturbative parts of the scattering amplitude, and on the DGLAP [8] evolution equations. The latter serve to calculate the scale dependence of the structure functions. This scale dependence is controlled by the purely perturbatively calculable evolution kernels while the nonperturbative part has been factored off in the initial conditions of the equations. DIS is of interest for our purposes since when  $x$  becomes small one is entering the Regge limit due to the fact that  $x$  is inversely proportional to the center of mass energy of the virtual photon-proton system. Keeping  $Q^2$  large one is entering this limit from a side where perturbation theory is applicable.

Repeating the reasoning sketched above one comes to the conclusion that logarithms of  $1/x$  are important in this region and eventually have to be summed up. For this reason the BFKL equation has been considered as an alternative to the DGLAP equations for the description of the scale and  $x$  dependence of the structure function at low  $x$ . The BFKL and DGLAP equations have their origin in quite different approximations of the phase space integration. The latter is an evolution equation in  $Q^2$  and takes into account the region of phase space in which the transverse momenta are strongly ordered, whereas the former is an evolution equation in  $1/x$  and takes into account the phase space with strongly ordered longitudinal momenta with the transverse momenta being disordered. There is an overlap region of both strongly ordered transverse and longitudinal momenta where these equations coincide, the so-called double logarithmic region.

We show in section 3.1 that by extending the framework of collinear factorization to high-energy (or  $\mathbf{k}$ -) factorization [9] the BFKL equation can be used to calculate DIS structure functions. We perform a calculation of the structure function  $F_2$  based on a numerical evaluation of the equation. It predicts a strong increase of the structure function with decreasing  $x$ . This is qualitatively in good agreement with HERA data [10, 11] in a region of  $x$  of  $10^{-4} \dots 10^{-2}$ . There is still an intense debate on the theoretical interpretation of the data. Section 3.1 gives an interpretation from the point of view of the BFKL equation.

The application of the BFKL equation to the inclusive structure function faces a serious problem, namely the separation of perturbative and nonperturbative scales which is in some sense perfect in the collinear factorization framework is limited here. A characteristic feature of the BFKL evolution is the diffusion in transverse momentum space which we display explicitly by calculating transverse momentum distributions. Starting from some characteristic momentum scale of an initial condition the transverse momenta diffuse during evolution into both the infrared and the ultraviolet region. This means that the evolution receives a contribution from a part of phase space which is certainly not treated correctly in the perturbative approach. This is a serious problem for the structure function calculation because on the proton side of the evolution one starts already deep in the nonperturbative regime and the diffusion tends to make it worse. As a potential way out of this problem we consider the possibility of imposing a modification of the infrared region to suppress the incorrectly treated region of phase space. With this procedure one can quite successfully describe the data, but it is not really conclusive since there is some arbitrariness inherent in it. This is demonstrated by the rather strong dependence of the result on the precise choice of the parameters of the modification. One should state, however, that the HERA data demonstrate the importance of the logarithms in  $1/x$ . This is emphasized by the success of the double logarithmic approximation (or the double asymptotic scaling approach) in which only terms are taken into account which contain both a logarithm of  $Q^2$  and of  $1/x$ . But it could not be unambiguously demonstrated that one needs the BFKL logarithms (the ones without the  $Q^2$ ) to describe the small  $x$  data presently available. This includes also studies [12] in which these logarithms were implemented into the evolution in form of higher order contributions to the gluon anomalous dimension.

To overcome the theoretical problem arising from diffusion in the BFKL equation one has to look for a process in which the contribution of infrared momenta is suppressed due to the kinematical characteristics of the process. One example for such a process is inclusive DIS with an associated jet in the final state [13]. In this case the large transverse momentum of the additional jet lifts the lower side of the evolution out of the infrared region [14]. Indeed first data on this process indicate a better agreement with BFKL based predictions than with fixed-order matrix element calculations, indicating the importance of higher order logarithms in  $1/x$  [15]. A related possibility is the study of the total cross section of virtual photon-photon scattering at  $e^+ - e^-$  colliders. Here the virtuality of the second photon takes the role of the jet transverse momentum in the example above. A discussion and estimate of event rates can be found in [6].

Another possibility to suppress the region of low momenta is to require a nonzero momentum transfer along the BFKL ladder. Such a finite  $t$  acts as an effective infrared momentum cut-off. If the momentum transfer is increased the cross section decreases rapidly due to the decrease of the proton formfactor. At small  $x$  one could still expect a sizeable effect in a region of moderate  $t$  due to the strong rise of the cross section as a function of  $x$  which could compensate the  $t$ -suppression. The study of the  $t$ -dependence of the BFKL pomeron is also interesting since it allows the investigation of the slope of the BFKL pomeron trajectory. As a consequence of the conformal invariance of the BFKL kernel its eigenvalues which control the energy dependence of the amplitude are momentum transfer independent. From this one would expect the trajectory associated with the BFKL pomeron to be fixed, i. e. to have no slope. In a physical process, however, conformal invariance is broken by characteristic mass scales of external particles. Due to this breaking of conformal symmetry one can indeed derive a small effective slope of physical amplitudes which contain the BFKL pomeron.

As a case study of a process of this kind we investigate in section 3.2 diffractive vector meson production at large momentum transfer in DIS which was proposed by Forshaw and Ryskin [16] (The study of large  $t$  diffractive processes was also considered earlier by Frankfurt and Strikman [17]). For these calculation it is required to have at hand the momentum space expression for the nonforward BFKL amplitude. It is derived from the configuration space representation in chapter 2 of this work.

A class of processes where Regge theory traditionally is successfully applied is diffractive dissociation. Single diffractive dissociation in hadron-hadron collisions denotes a process in which of two colliding hadrons one stays intact and is only weakly deflected after the scattering whereas the other one dissociates into a many particle hadronic system with vacuum quantum numbers. One can consider a related process in DIS by replacing the hadron which dissociates by the virtual photon. This type of process has received much attention after the HERA experiments have reported an excess of 'rapidity-gap' events compared with predictions from

standard DIS Monte-Carlo generators. These rapidity gap events at low  $x$  can be interpreted as diffractive dissociation of the photon. The 'gap' refers to a region in the detector in which no final state particles are observed. In terms of Regge theory this process is interpreted by assuming the exchange of a pomeron<sup>2</sup> between the proton and the photon. In the region of large invariant masses of the produced hadronic system also more general exchange processes have to be taken into account in which the photon does not couple to the pomeron directly but through another pomeron and a triple pomeron interaction vertex.

Since for large  $Q^2$  one is in a region where perturbation theory in principle is applicable one can raise the question to which extent perturbative QCD can describe photon diffractive dissociation in DIS. The simplest possibility to start with is to consider two gluon exchange between the photon and the proton. The gluons couple to the two quarks in which the photon dissociates in this picture. At low  $x$  one finds again that two gluon exchange is not enough since additional loops generate logarithms in  $1/x$ . The resummation of this logarithms finally leads to the BFKL pomeron as the object which is exchanged between the photon and the proton. By using the results of Bartels [18] and Bartels and Wüsthoff [19] on the triple Regge limit in perturbative QCD one can also extend this approach to the triple Regge region of large invariant masses of the hadronic system. This approach is pursued in section 3.3 of this thesis where the inclusive DIS diffractive cross section is calculated for finite and zero momentum transfer. As a result we find in this model that the  $x$ -dependence of the cross section is rather steep, it rises at low  $x$  with a power of about 1. Although the data are not yet conclusive one can say that this  $x$ -dependence is certainly too strong compared with the experimental observation [20, 21]. The applicability of the BFKL pomeron to integrated DIS diffractive dissociation therefore has to be questioned.

It is possible to understand this drawback by again considering the contribution of different regions of phase space to the evolution in this process. Numerical studies of the BFKL equation in diffractive dissociation have demonstrated [22] that almost the whole evolution takes place in the infrared region where the perturbative approach cannot be consistently applied. In particular it was shown that in inclusive diffractive DIS the virtuality  $Q^2$  of the photon does not act as a hard scale in the effective photon pomeron interaction. On the contrary, the coupling of the gluons to the quarks is dominated by very low scales<sup>3</sup>. Consequently, this process appears not to be appropriate to phenomenologically identify the effect of the large perturbative logarithms of  $1/x$ .

Since, on the other hand, the data on DIS diffractive dissociation show a rise of the cross section at low  $x$ , similar to the inclusive structure function, one can still ask if there is a subclass of events in which the effect of the large logarithms is visible.

In [22] it was shown that the scale of the effective photon pomeron vertex becomes hard if restrictions are imposed on the diffractively produced final state. The authors considered a large transverse momentum of the outgoing quarks but one could also think of heavy quarks or the production of a heavy vector meson. With such an effective large scale perturbation theory has a much better foundation compared to the inclusive case dominated by low scales.

As an example of such a process we consider the diffractive production of a quark-antiquark pair with either a large quark mass or a large transverse momentum of the (anti)quark [25]. Starting again from BFKL pomeron exchange we analyze the process in detail in the double logarithmic approximation in which the coupling of the two gluons to the proton can be expressed in terms of the gluon density. Within this approximation we perform an extensive numerical evaluation of the cross section. As a remarkable property of the two-gluon exchange model (see also [26]) we consider the azimuthal dependence of the cross section. This shows a pattern quite different from the one obtained in the photon-gluon fusion process. We propose to use this signal to reveal the two gluon exchange nature of the interaction underlying the process. For the case of heavy quarks (we consider charm) the transverse momentum integration can be performed without entering the infrared region. This allows the calculation of the charm contribution to the diffractive structure function in our model.

---

<sup>2</sup>We disregard secondary trajectories for the moment.

<sup>3</sup>The dominance of soft scales is emphasized in other models of diffractive dissociation. In the aligned jet model [23] one of the produced quarks is very soft and interacts with the proton like a hadronic constituent quark. In the model of [24] the proton is treated as a soft gluonic background field. The fluctuation of the photon into the  $q\bar{q}$ -pair is then calculated in this soft background.



So far we have specified the energy dependence of the BFKL pomeron only qualitatively. The cut in the complex angular momentum plane transforms into a power behavior (in  $1/x$ ) of the amplitude with the power being given by  $4 \log 2 N_c \alpha_s / \pi$ . For reasonable values of the strong coupling constants the numerical value of this power is 0.5. In numerical simulations in which the infrared region is suppressed by a cut-off the effective power turns out to be somewhat smaller. The common feature of all calculations of DIS processes based on BFKL pomeron exchange is accordingly the power rise of the cross section at low values of  $x$ . This behavior is in principle conflict with the unitarity bound which states that the cross section can at most increase logarithmically. The leading logarithmic approximation thus violates a fundamental principle of quantum theory. The same problem is observed when only double logarithmic terms are taken into account although the asymptotic rise turns out to be somewhat smaller then. Unitarity is therefore also violated in the DGLAP formalism for asymptotically low  $x$ .

The key problem of low  $x$  physics is therefore to identify the corrections which restore unitarity and to calculate them. The attractive feature of DIS is without doubt that one can use perturbation theory as a starting point here since this approximation is highly successful at intermediate  $x$ . It is therefore natural to ask first for the perturbative corrections which render the amplitude unitary. If one succeeds in constructing a unitary amplitude in perturbation theory one can expect that from such a highly constrained result one will get indications of potential nonperturbative corrections. Ultimately these considerations could then lead to the true QCD pomeron which applies also in hadron-hadron scattering. As an example of nonperturbative corrections which are related to perturbation theory, namely to ambiguities in the asymptotic QCD perturbation series, we mention renormalons [27] which have been intensively studied in the last few years. Let us shortly sketch a physically intuitive picture to motivate the necessity of corrections at low  $x$ . At fixed  $x$  and  $Q^2$  the proton as seen by the virtual photon can be regarded as a dilute gas of partons of transverse size  $1/Q^2$ . The partons are nearly noninteracting since the interaction strength is small. If, at fixed  $Q^2$ ,  $x$  is decreased the density of the gas starts to rise. The interaction strength, specified by the coupling constant evaluated at the scale  $Q^2$  is still weak but interactions occur frequently since the density is high. The state of the partons can now be regarded as a liquid. The frequent interactions now diminish the rise of the density eventually until a steady state is reached (saturation). This would then correspond to the unitarity limit of the scattering amplitude.

How is this picture realized in terms of higher order perturbative corrections? The key step is to extend the single parton evolution equations to take into account density reducing parton-parton interactions.

The first approach in this direction is due to Gribov, Levin and Ryskin [28]. They considered freely evolving parton cascades which merge at a triple ladder vertex (fan diagrams). The corresponding diagrams were resummed by a nonlinear evolution equation where the nonlinearity represents the parton screening. This approach already emphasizes the necessity to consider diagrams with more than two partons in the  $t$ -channel of the amplitude. In fact the relevant diagrams at small  $x$  contain only gluons in the  $t$ -channel due to the vector nature of the gluon. The contribution of spin- $\frac{1}{2}$  particles is suppressed at high energy.

A systematic program towards the calculation of higher order corrections of this kind has been initiated by Bartels [29, 30, 18]. In this program the BFKL amplitude represents the starting point and the guideline to calculate higher order corrections is unitarity. This implies that in each order only those corrections are taken into account which are absolutely necessary to restore unitarity. The corrections are calculated using unitarity integrals and dispersion relations. The outcome of this formalism are sets of coupled integral equations for amplitudes with  $n$  gluons in the  $t$ -channel, where  $n = 2$  corresponds to the BFKL equation. It should be strongly emphasized that the gluons are reggeized in this approach, i. e. the elementary degree of freedom is a composite object which resums infinitely many Feynman diagrams. In this way the reggeized gluon is the first example of what is called a reggeon. The ultimate aim of the program proposed here is to combine as many elementary interactions as possible into collective excitations, called reggeons, and to encode all higher order contributions in an effective reggeon field theory [31, 32, 33, 30]. A prerequisite for the inductive construction of such an effective field theory is the thorough understanding of the basic elements which arise in low orders.

Bartels [18] and Bartels and Wüsthoff [19] have considered the system of coupled equations up to  $n = 4$ . They succeeded in solving this system partially by reducing the  $n = 3$  system and parts of the  $n = 4$  system to the BFKL amplitude and they decomposed the remaining part of the  $n = 4$  system into two factors. The

first factor is an effective vertex which mediates the transition from the two (reggeized) gluon system to the four gluon system. The second part is the amplitude associated with the four gluon state.

Chapter 4 of this thesis is devoted to the investigation of these two elements. The transition vertex has originally been derived in momentum space but with regard to an effective field theory it is sensible to represent it in configuration space. This is the case since - as already indicated - the starting point of the formalism, the BFKL amplitude, has in configuration space an interesting interpretation in terms of a conformal field theory. Since conformal symmetry, especially in two dimensions, is known to be a powerful property, it is an essential question if this property persists in higher orders. If this turns out to be the case, one could think of conformal field theory as a potential effective field theory encoding all unitarity corrections. As an encouraging first step in this direction the proof of the conformal symmetry of the transition vertex has been given in [34]. In the present work we formulate an alternative and simpler proof which is based on the symbolic operator representation introduced by Lipatov [35] to prove holomorphic separability of the BFKL kernel. Unfortunately it turns out that holomorphic separability cannot be shown for the transition vertex. Using conformal symmetry we then elaborate on the interpretation of the vertex in terms of elements of a conformal field theory. It is demonstrated that in this framework the vertex admits the simple representation as a conformal three point function. The field entering this correlation function is a field which can be associated with the BFKL pomeron. A virtue of the configuration space representation as a three point function is that the number of terms contributing to the vertex function is drastically reduced.

Since the understanding of the transition vertex is rather satisfactory the calculation of the four (reggeized) gluon amplitude is an urgent task. The four gluon amplitude is defined as the solution of the four particle BKP [29, 36] equation which is of the form of a Bethe Salpeter equation with summation over all pairwise interactions of two gluons. These pairwise interactions are given by the BFKL kernel. The solution of this equation would complete the analysis of the first nontrivial unitarity corrections. It is of great phenomenological significance since it would allow to investigate in which region of  $x$  the corrections which reduce the rise of the cross section become sizeable. It would be highly interesting to see whether these terms, added to the BFKL amplitude, can describe experimental data, both for the structure function and for diffractive events. From the theoretical point of view the analysis of the four gluon state constitutes only the first step. Asymptotically this contribution will probably also generate a power behavior which violates unitarity. Only after resummation of all  $n$ -gluon contributions a unitary amplitude can be expected.

The  $n$ -gluon system is currently under intense study in the large  $N_c$ -approximation. In this limit the BKP equations in configuration space have been shown to be holomorphic factorizable [35, 37]. The holomorphic and the antiholomorphic part have been demonstrated [38] to be equivalent to the integrable model of the XXX Heisenberg spin chain for spin  $s = 0$  [39]. Accordingly one tries to solve the model using quantum inverse scattering methods [40, 41].

In this work we restrict ourselves to  $n = 4$  and we do not consider the large  $N_c$ -approximation. The aim is to derive the operator algebra [42] of the fields which we associate with reggeons constructed from the coupling of two gluons. The idea behind is that from the knowledge of the operator algebra further information can be obtained regarding a potential effective conformal field theory. To derive the operator algebra we consider the short-distance or twist expansion of the four gluon amplitude. There is another interesting information which one could obtain from this expansion. Namely, for the BFKL equation a very close relation between the anomalous dimensions appearing in the twist expansion and the spectrum of the BFKL kernel can be demonstrated. The anomalous dimensions correspond to the residues of the poles of the eigenvalue at integer points in the  $\nu$ -plane where  $\nu$  corresponds to the quantum number associated with the conformal symmetry. Postulating a similar relationship for the four gluon spectrum one could think of reproducing the spectrum from the anomalous dimensions with the help of a dispersion relation. The knowledge of the spectrum, i. e. the eigenvalues of the four-particle interaction operator would already allow important conclusions concerning the high energy behavior of the amplitude. It remains then of course to calculate the eigenfunctions.

Section 4.4 of this thesis concentrates on the twist expansion of the four gluon amplitude. We use the Faddeev reordering [43] and try to make use of conformal invariance of the two particle interaction kernels by resumming pairwise interactions with the BFKL amplitude. In this way the problem is formulated as an effective two reggeon problem. Our analysis of the twist expansion starts from identifying singularities of the reggeon propagators and the effective reggeon interaction vertices. For the simplest examples it is then

shown how the anomalous dimensions can be obtained from the iteration of these singularities.

Let us briefly recapitulate the organization of this thesis.

Chapter 2 collects some background material on the BFKL pomeron with the emphasis on the conformal properties of the amplitude. The sections 2.2 and 2.3 mainly review known results. The momentum space expressions discussed in section 2.3 constitute an original contribution of this thesis partly published in [44]. Chapter 3 is devoted to the phenomenological applications of the BFKL pomeron in DIS at low  $x$ . The numerical calculations on the structure function  $F_2$  in sections 3.1.2 and 3.1.3 are results of this work. Results similar to the ones in 3.1.2 have been reported in [45]. The calculation of the cross section of diffractive vector meson production at large  $t$  in section 3.2.1 is a new contribution of this thesis. The following sections 3.2.2 and 3.2.3 contain some corollaries and numerical evaluations. Results similar to the ones in 3.2.2 and 3.2.3 have been obtained in the joint publication [46]. Section 3.3 on inclusive diffractive dissociation is based on the joint publication [44]. The main contribution of the present work is the explicit momentum space calculation based on the results of section 2.3. The results of section 3.3.3 entered into the joint publication [47]. Section 3.4 on quark-antiquark production in DIS diffractive dissociation almost exclusively contains results which have been obtained independently by the author. They partly entered the joint publications [25]. The generalization to finite quark mass and the results of section 3.4.5 have not been published so far. Chapter 4 focusses on the unitarity corrections. The section 4.1 serves as an introduction and review of the background upon which the investigation is based. Apart from section 4.1.2 the material presented here is well-known. Section 4.2 is devoted to the analysis of the transition vertex. The content of the sections 4.2.1 and 4.2.2 has been obtained in the collaboration [48]. Section 4.2.3 is based on the author's independent research. Section 4.3 discusses the significance of the four-gluon state. The material contained therein has not been presented in this form before. In section 4.4 the four gluon state is considered in detail. Apart from a short review of the basic results of [18] the approach developed here constitutes an original contribution of this thesis which has not been published so far.

Some technical supplements are collected in the appendix.

## 2 Properties of the BFKL Pomeron

In 1976 a program was initiated [2] to investigate the ideas of Regge theory in the framework of QCD perturbation theory. The aim was to understand, in this framework, the nature of the leading singularity with vacuum quantum numbers in the complex angular momentum plane, the so-called Pomeron singularity (Pomeron). In the asymptotic region of large center of mass energy  $s$  large logarithms of  $s$  compensate the small value of the perturbative coupling  $\alpha_s$  and have to be resummed. In [2]-[1] the partial wave amplitude of gluon-gluon scattering was calculated in the leading-log( $s$ ) approximation, which takes into account contributions of the form  $s(\alpha_s \log s)^n \phi_n(Q^2)$  with a hard momentum scale  $Q^2$ . In the original papers the calculations were performed in a massive gauge theory in which the natural scale is the mass of the vector boson. In the massless theory the hard scale is given by the characteristic scale of perturbatively calculable impact factors with which the gluon-gluon scattering amplitude is convoluted. This partial wave amplitude satisfies a Bethe-Salpeter equation which generates a ladder-like structure with gluons being produced in the  $s$ -channel and reggeized gluons being exchanged in the  $t$ -channel. In the vacuum channel (color singlet exchange) the equation generates a fixed cut in the angular momentum plane. In the color octet channel (the channel with gluon quantum numbers) the equation is solved by a Regge-pole ansatz. This bootstrap property demonstrates the reggeization of the gluon in perturbative QCD. The BFKL equation with zero momentum transfer has been studied extensively in the last few years. Relatively little attention has been devoted to the generalization to finite momentum transfer (nonforward direction). This generalized equation is important for phenomenological applications and in particular for theoretical reasons since it appears as an essential building block in a systematic study of subleading corrections to the BFKL equation. The analysis of the generalized equation is highly facilitated by its symmetry w. r. t. two-dimensional conformal transformations, due to which it can be diagonalized by conformal partial waves [5]. The conformal symmetry reveals itself in the configuration space representation which is particularly well suited to study the conformal properties of the BFKL amplitude. In this representation the results of the leading-log approximation can be interpreted in the general framework of conformal field theory [42]. The reggeized gluon can be interpreted as an elementary field with conformal dimension zero and the BFKL amplitude has a natural interpretation as the four point function of that field. An interpretation along these lines might in the long run serve as a guideline to obtain an effective theory of QCD in the Regge limit as a conformal field theory. Further evidence for this conjecture will be given in the last chapter of this thesis.

The first part of this section serves as an introduction to these aspects of the BFKL theory. We will introduce the equation and derive its configuration space representation. The proof of conformal symmetry will be given and the interpretation in terms of a conformal field theory will be sketched.

The configuration space representation is elegant and allows for promising interpretations but using it one loses the connection to perturbation theory since QCD perturbation theory is usually performed in momentum space. The amplitudes of the scattering processes which are studied in chapter 3 and the subleading corrections to the BFKL theory which are the objective in chapter 4 are calculated within perturbative QCD in momentum space. To apply the BFKL amplitude to the calculation of these scattering amplitudes and the analysis of unitarity corrections a back transformation of the configuration space results to momentum space is desirable. This is the aim of the second part of this section. We will formulate the solution of the nonforward BFKL equation in momentum space and study some of its properties. These results will be used in forthcoming sections of this thesis.

The formulation of the BFKL equation as a two particle Schrödinger equation in two dimensions with a non-trivial kinetic term [35] which is a further development of the results of section 2.2 will be discussed in conjunction with the unitarity corrections in the last chapter of this work.

## 2.1 The Bethe Salpeter equation in momentum space

The results of the leading-log( $s$ ) approximation are the following. The amplitude for the scattering of colorless objects can be written in factorized form

$$A(s, t) = is \int_{\mathcal{C}} \frac{d\omega}{2\pi i} s^\omega \Phi_\omega(\mathbf{q}^2), \quad t = -\mathbf{q}^2 \quad (2.1)$$

$$\Phi_\omega(\mathbf{q}^2) = \int \frac{d^2\mathbf{k}}{(2\pi)^3} \frac{d^2\mathbf{k}'}{(2\pi)^3} \Phi_\omega(\mathbf{k}, \mathbf{k}'; \mathbf{q}) \phi_1(\mathbf{k}, \mathbf{q}) \phi_2(\mathbf{k}', \mathbf{q}) \quad (2.2)$$

The integration contour  $\mathcal{C}$  is located to the right of all singularities of  $\Phi_\omega$ . The function  $\Phi_\omega(\mathbf{k}, \mathbf{k}'; \mathbf{q})$  can be interpreted as the  $t$ -channel partial wave amplitude for the scattering of virtual gluons with virtualities  $-\mathbf{k}^2, -(\mathbf{q} - \mathbf{k})^2, -\mathbf{k}'^2$  and  $-(\mathbf{q} - \mathbf{k}')^2$  respectively. The functions  $\phi_{1,2}$  are the wave functions of the scattered colorless states. The color neutrality condition manifests itself in the following property of the wave functions

$$\phi_{1,2}(\mathbf{k} = 0, \mathbf{q}) = \phi_{1,2}(\mathbf{k} = \mathbf{q}, \mathbf{q}) = 0 \quad (2.3)$$

which is essential for the infrared finiteness of the amplitude. The partial wave amplitude  $\Phi_\omega$  is given in the leading-log approximation as the solution of a Bethe-Salpeter type of equation in the transverse momentum space

$$\begin{aligned} \omega \Phi_\omega(\mathbf{k}, \mathbf{k}'; \mathbf{q}) &= \frac{\delta^{(2)}(\mathbf{k} - \mathbf{k}')}{\mathbf{k}^2 \mathbf{k}'^2} + (\mathcal{K}_{\text{BFKL}} \otimes \Phi_\omega)(\mathbf{k}, \mathbf{k}'; \mathbf{q}) \\ &- [\beta(\mathbf{k}^2) + \beta((\mathbf{q} - \mathbf{k})^2)] \Phi_\omega(\mathbf{k}, \mathbf{k}'; \mathbf{q}) \end{aligned} \quad (2.4)$$

This equation resums the radiative corrections to the Born level two gluon exchange which is represented by the inhomogeneous term. The integral kernel  $\mathcal{K}_{\text{BFKL}}$  is given by the square of an effective real gluon production vertex and reads

$$(\mathcal{K}_{\text{BFKL}} \otimes \Phi_\omega)(\mathbf{k}, \mathbf{k}'; \mathbf{q}) = \frac{1}{\mathbf{k}^2 (\mathbf{q} - \mathbf{k})^2} \frac{N_c \alpha_s}{2\pi^2} \int d^2\mathbf{l} \left[ -\mathbf{q}^2 + \frac{\mathbf{l}^2 (\mathbf{q} - \mathbf{k})^2 + \mathbf{k}^2 (\mathbf{q} - \mathbf{l})^2}{(\mathbf{k} - \mathbf{l})^2} \right] \Phi_\omega(\mathbf{l}, \mathbf{k}'; \mathbf{q}) \quad (2.5)$$

The function  $\beta(\mathbf{k}^2)$  is the gluon trajectory function<sup>4</sup> which resums the virtual corrections

$$\beta(\mathbf{k}^2) = \frac{1}{2} \frac{N_c \alpha_s}{2\pi^2} \int d^2\mathbf{l} \frac{\mathbf{k}^2}{\mathbf{l}^2 (\mathbf{k} - \mathbf{l})^2} \quad (2.6)$$

The trajectory function as well as the production vertex contain infrared singularities. The sum of real and virtual corrections, however, gives a finite result in the case of color singlet exchange. This cancellation of singular contributions relies on the property (2.3) of the wavefunctions. It should be remarked that on the level of the leading-log accuracy  $\alpha_s$  is fixed and the scale is, strictly speaking, not determined. For consistency one should use the hard scale of the process as the argument of  $\alpha_s$ . Logarithms of a relevant scale  $M^2$  which are absorbed by introducing the running coupling  $\alpha_s(M^2)$  only appear in next-to-leading order. They are expected to be found in the complete NLO corrections to the BFKL equation which are studied presently by Lipatov and Fadin [49]. Iteration of the Bethe-Salpeter equation leads to a ladder like structure with reggeized gluons being exchanged in the  $t$ -channel and real gluons being produced in the  $s$ -channel. Setting the momentum transfer  $t$  equal to zero one obtains the BFKL equation in forward direction which can be diagonalized by power functions

$$e^{(\nu, n)}(\mathbf{k}) = 2\pi\sqrt{2} (\mathbf{k}^2)^{-\frac{3}{2} - i\nu} e^{-in\phi} \quad ; \quad \nu \in \mathbb{R}, n \in \mathbb{Z} \quad (2.7)$$

with eigenvalues

$$\chi(\nu, n) = \frac{N_c \alpha_s}{\pi} \left[ 2\psi(1) - \psi\left(\frac{1+|n|}{2} + i\nu\right) - \psi\left(\frac{1+|n|}{2} - i\nu\right) \right] \quad (2.8)$$

---

<sup>4</sup>Loosely speaking we call  $\beta$  the trajectory function of the gluon. The trajectory of the gluon in the sense of Regge theory is  $\alpha(\mathbf{k}^2) = 1 - \beta(\mathbf{k}^2)$ . It passes through the physical spin 1 for zero momentum transfer  $\alpha(0) = 1$ .

The function  $\psi$  is defined as the logarithmic derivative of the  $\Gamma$ -function:  $\psi(x) = \Gamma'(x)/\Gamma(x)$ . Some important properties of the function  $\chi(\nu, n)$  are given in appendix A.3. The solution of the BFKL equation consequently reads

$$\Phi_\omega(\mathbf{k}, \mathbf{k}') = \sum_{n=-\infty}^{+\infty} \int_{-\infty}^{\infty} \frac{d\nu}{2\pi} \frac{1}{\omega - \chi(\nu, n)} e^{(\nu, n)}(\mathbf{k}) e^{(\nu, n)*}(\mathbf{k}') \quad (2.9)$$

For the case of non-zero momentum transfer simple eigenfunctions are not known in momentum space. In that case it proves to be useful to discuss the equation in configuration space.

## 2.2 The configuration space representation

We define the Fourier transformation of the off-shell partial wave amplitude  $\Phi$

$$\delta^{(2)}(\mathbf{q} - \mathbf{q}') \Phi_\omega(\mathbf{k}, \mathbf{k}'; \mathbf{q}') = \int \prod_{i=1}^2 d^2 \rho_i \prod_{i=1}^2 d^2 \rho_{i'} \cdot \Phi_\omega(\rho_1, \rho_2; \rho_{1'}, \rho_{2'}) e^{i\mathbf{k}\rho_1 + i(\mathbf{q}-\mathbf{k})\rho_2 - i\mathbf{k}'\rho_{1'} - i(\mathbf{q}'-\mathbf{k}')\rho_{2'}} \quad (2.10)$$

Consequently we can express the partial wave amplitude as

$$\delta^{(2)}(\mathbf{q} - \mathbf{q}') \Phi_\omega(\mathbf{q}^2) = \frac{1}{(2\pi)^2} \int \prod_{i=1}^2 d^2 \rho_i \prod_{i=1}^2 d^2 \rho_{i'} \Phi_\omega(\rho_1, \rho_2; \rho_{1'}, \rho_{2'}) \phi_1(\rho_1, \rho_2; \mathbf{q}) \phi_2(\rho_{1'}, \rho_{2'}; \mathbf{q}) \quad (2.11)$$

with the configuration space representation of the wavefunctions

$$\phi_1(\rho_1, \rho_2; \mathbf{q}) = \frac{1}{(2\pi)^2} \int d^2 \mathbf{k} \phi_1(\mathbf{k}, \mathbf{q}) e^{i\mathbf{k}\rho_1 + i(\mathbf{q}-\mathbf{k})\rho_2} \quad (2.12)$$

In configuration space the color neutrality condition is equivalent to the vanishing of the space integral over the wavefunction

$$\int d^2 \rho_1 \phi_1(\rho_1, \rho_2; \mathbf{q}) = \int d^2 \rho_2 \phi_1(\rho_1, \rho_2; \mathbf{q}) = 0 \quad (2.13)$$

To proceed with the configuration space representation it will be convenient to introduce complex coordinates in the two-dimensional transverse momentum and configuration space <sup>5</sup>

$$\begin{aligned} \mathbf{k} &= (k_x, k_y) \\ k &= k_x + ik_y, \quad k^* = k_x - ik_y \\ \rho_i &= \rho_{ix} + i\rho_{iy}, \quad \rho_i^* = \rho_{ix} - i\rho_{iy} \\ \partial_i &= \frac{\partial}{\partial \rho_i}, \quad \partial_i^* = \frac{\partial}{\partial \rho_i^*} \\ \mathbf{k} \cdot \rho &= \frac{1}{2}(k\rho^* + k^*\rho) \end{aligned} \quad (2.14)$$

Rewriting the Bethe-Salpeter equation in terms of these coordinates and performing the Fourier transformation we obtain (cf. appendix A.1)

$$\begin{aligned} \omega |\partial_1|^2 |\partial_2|^2 \Phi_\omega(\rho_1, \rho_2; \rho_{1'}, \rho_{2'}) &= \frac{1}{(2\pi)^4} \delta^{(2)}(\rho_{11'}) \delta^{(2)}(\rho_{22'}) \\ &+ \frac{N_c \alpha_s}{\pi} \left[ \partial_1 \partial_2^* \frac{1}{2} \int \frac{d^2 \rho_0}{|\rho_{10}|^2} \theta \left( \frac{|\rho_{10}|}{|\rho_{12}|} - \epsilon \right) \partial_0^* \partial_2 \Phi_\omega(\rho_0, \rho_2; \rho_{1'}, \rho_{2'}) \right. \\ &+ \pi \log \epsilon |\partial_1|^2 |\partial_2|^2 \Phi_\omega(\rho_1, \rho_2; \rho_{1'}, \rho_{2'}) \\ &+ \text{(h.c.)} + (1 \leftrightarrow 2) \Big] \end{aligned} \quad (2.15)$$

---

<sup>5</sup>In the following, boldtype letters are used for vectors in two-dimensional transverse momentum space with positive euclidean metric. In configuration space normal type letters are used both for the two-dimensional vector  $\rho = (\rho_x, \rho_y)$  and the complex number  $\rho = \rho_x + i\rho_y$ . Which object is meant should be clear from the context in which the expression appears.

We have introduced the shorthand notation  $\rho_{ij} = \rho_i - \rho_j$ . The variable  $\epsilon$  is a fictitious parameter which regularizes the ultraviolet singularity of the integral arising from the region near  $\rho_{10} = 0$ . The kernel of the  $\rho_0$ -integral encodes in a compact form the contribution of the gluon production vertex and the gluon trajectory function.

### 2.2.1 Conformal invariance of the equation

In two dimensions the global conformal transformations can be represented by the mapping

$$\rho \rightarrow \frac{a\rho + b}{c\rho + d}, \quad a, b, c, d \in \mathbb{C}, \quad ad - bc \neq 0 \quad (2.16)$$

i. e. a linear fractional transformation. To be precise, global conformal transformations are well-defined on the compactified complex plane, i.e. the Riemannian sphere  $S^2$ . These transformations form the pseudoorthogonal group  $SO(3, 1)$  which is isomorphic to  $SL(2, \mathbb{C})/\{\pm 1\}$ . Each of the elements of this group is obtained by a superposition of transformations of the following types

$$\begin{aligned} \text{Translations: } & \rho \rightarrow \rho + b \\ \text{Rotations : } & \rho \rightarrow a\rho, |a| = 1 \\ \text{Dilatations : } & \rho \rightarrow \lambda\rho, \lambda \in \mathbb{R}_+ \\ \text{Inversions : } & \rho \rightarrow \frac{1}{\rho} \end{aligned}$$

We want to show that the group of linear fractional transformations is the invariance group of the Bethe-Salpeter equation. Conformal invariance implies restrictions on the form of the correlation functions of a theory. These restrictions and the interpretation of the amplitudes  $\Phi_\omega$  in the framework of a conformal invariant theory will be the subject of the next section.

First we show that the solution of the Born level equation ( $\alpha_s = 0$ ) can be written in conformally invariant form, then we show that the integral kernel is invariant under conformal transformations. From this we conclude that the general solution of the Bethe-Salpeter equation can be represented in conformally invariant form and that the solution can be obtained by conformal partial wave diagonalization.

First we note that the Bethe-Salpeter equation (2.15) reduces for  $\alpha_s = 0$  to a Poisson type equation in two dimensions the solution of which is given by

$$\Phi_\omega^{(0)}(\rho_1, \rho_2; \rho_{1'}, \rho_{2'}) = \frac{1}{\omega} \frac{1}{(2\pi)^6} \log |\rho_{11'} \rho_{22'}| \quad (2.17)$$

By adding logarithmic terms this solution can be transformed into an expression which depends only on the two independent conformally invariant anharmonic ratios which can be constructed from four coordinates

$$\Phi_\omega^{(0)}(\rho_1, \rho_2; \rho_{1'}, \rho_{2'}) = \frac{1}{2\omega} \frac{1}{(2\pi)^6} \log \frac{|\rho_{11'} \rho_{22'}|}{|\rho_{12} \rho_{1'2'}|} \log \frac{|\rho_{11'} \rho_{22'}|}{|\rho_{12'} \rho_{1'2}|} \quad (2.18)$$

When integrated with wave functions of color neutral systems due to the property eq. (2.13) the additional terms give no contribution. Hence we have shown that the zeroth order solution can be represented in conformally invariant form. Note that eq. (2.17) corresponds to two-gluon exchange whereas the terms which were added to obtain (2.18) do not have a counterpart in terms of Feynman diagrams.

Now we want to verify that the integral kernel of the configuration space representation is invariant under conformal transformations. It is obvious that the kernel in (2.15) remains invariant under rotations, translations and dilatations. It remains to show the invariance with respect to inversions. Let us perform

simultaneously the transformations

$$\rho_i \rightarrow \frac{1}{\rho_i} \quad (2.19)$$

$$\partial_i \rightarrow -\rho_i^2 \partial_i \quad (2.20)$$

$$d^2 \rho_0 \rightarrow \frac{d^2 \rho_0}{|\rho_0|^4} \quad (2.21)$$

$$|\rho_{i0}|^2 \rightarrow \frac{|\rho_{i0}|^2}{|\rho_i|^2 |\rho_0|^2} \quad (2.22)$$

Under these transformations the lhs and the inhomogeneous part of the eq. (2.15) are multiplied by the factor  $|\rho_1|^4 |\rho_2|^4$ . Applying these transformations to the integral kernel, i. e. the terms in brackets in (2.15), we obtain

$$\begin{aligned} & \frac{1}{2} \rho_1^2 \rho_2^{*2} \partial_1 \partial_2^* \int \frac{d^2 \rho_0}{|\rho_{10}|^2} \frac{|\rho_1|^2 |\rho_0|^2}{|\rho_0|^4} \theta \left( \frac{|\rho_{10}| |\rho_2|}{|\rho_{12}| |\rho_0|} - \epsilon \right) \rho_0^{*2} \rho_2^2 \partial_0^* \partial_2 \Phi_\omega(\rho_0, \rho_2) \\ & + \pi \log \epsilon |\rho_1|^4 |\rho_2|^4 |\partial_1|^2 |\partial_2|^2 \Phi_\omega(\rho_1, \rho_2) + [\text{h.c.}] + [1 \leftrightarrow 2] \\ = & |\rho_1|^4 |\rho_2|^4 \left[ \frac{1}{2} \partial_1 \partial_2^* \int \frac{d^2 \rho_0}{|\rho_{10}|^2} \frac{\rho_1 \rho_0^*}{\rho_0 \rho_1^*} \theta \left( \frac{|\rho_{10}| |\rho_2|}{|\rho_{12}| |\rho_0|} - \epsilon \right) \partial_0^* \partial_2 \Phi_\omega(\rho_0, \rho_2) \right. \\ & \left. + \pi \log \epsilon |\partial_1|^2 |\partial_2|^2 \Phi_\omega(\rho_1, \rho_2) + [\text{h.c.}] + [1 \leftrightarrow 2] \right] \end{aligned} \quad (2.23)$$

We rewrite the numerator in front of the  $\theta$ -function as

$$\begin{aligned} \rho_1 \rho_0^* &= (\rho_{01}^* + \rho_1^*)(\rho_{10} + \rho_0) \\ &= \rho_{01}^* \rho_{10} + \rho_{01}^* \rho_0 + \rho_1^* \rho_{10} + \rho_1^* \rho_0 \end{aligned} \quad (2.24)$$

and consider the four terms separately. For the first three terms the singularity in  $\rho_0 = \rho_1$  becomes integrable and the  $\theta$ -function can be removed. We obtain for the first term

$$\partial_1 \partial_2^* \int d^2 \rho_0 \frac{(-1)}{\rho_1^* \rho_0} \partial_0^* \partial_2 \Phi_\omega(\rho_0, \rho_2) = \pi \delta^{(2)}(\rho_1) |\partial_2|^2 \Phi_\omega(\rho_1, \rho_2) \quad (2.25)$$

where the rhs emerges after partial integration with respect to  $\rho_0$  and the use of the following identities ( $\Delta$  is the conventional twodimensional Laplace operator)

$$\Delta \log |\rho| = 4 \partial \partial^* \log |\rho| = 2 \pi \delta^{(2)}(\rho) \quad (2.26)$$

$$\partial \frac{1}{\rho^*} = \partial^* \frac{1}{\rho} = \pi \delta^{(2)}(\rho) \quad (2.27)$$

The second and third term of (2.24) are calculated in a similar way

$$\begin{aligned} & \partial_1 \partial_2^* \int d^2 \rho_0 \left[ \frac{1}{\rho_1^* \rho_{01}} + \frac{1}{\rho_0 \rho_{10}^*} \right] \partial_0^* \partial_2 \Phi_\omega(\rho_0, \rho_2) \\ = & \left[ -\partial_1 \frac{1}{\rho_1^*} + \frac{1}{\rho_1} \partial_1^* \right] |\partial_2|^2 \Phi_\omega(\rho_1, \rho_2) \end{aligned} \quad (2.28)$$

The conjugate expression gives

$$\left[ -\partial_1^* \frac{1}{\rho_1} + \frac{1}{\rho_1^*} \partial_1 \right] |\partial_2|^2 \Phi_\omega(\rho_1, \rho_2) \quad (2.29)$$

After commutation of derivatives we obtain terms proportional to  $\delta^{(2)}(\rho_1)$ -functions which cancel against (2.25); the remaining terms in (2.28) and (2.29) add up to zero. Consequently the only contribution comes



from the fourth term of (2.24), i. e. after inversion the kernel reads

$$|\rho_1|^4 |\rho_2|^4 \left[ \frac{1}{2} \partial_1 \partial_2^* \int \frac{d^2 \rho_0}{|\rho_{10}|^2} \theta \left( \frac{|\rho_{10}| |\rho_2|}{|\rho_{12}| |\rho_0|} - \epsilon \right) \partial_0^* \partial_2 \Phi_\omega(\rho_0, \rho_2) \right. \\ \left. + \pi \log \epsilon |\partial_1|^2 |\partial_2|^2 \Phi_\omega(\rho_1, \rho_2) + [\text{h.c.}] + [1 \leftrightarrow 2] \right] \quad (2.30)$$

Now we use the identity

$$\int \frac{d^2 \rho_0}{|\rho_{10}|^2} \theta \left( \frac{|\rho_{10}| |\rho_2|}{|\rho_{12}| |\rho_0|} - \epsilon \right) \psi(\rho_0) = \int \frac{d^2 \rho_0}{|\rho_{10}|^2} \theta \left( \frac{|\rho_{10}|}{|\rho_{12}|} - \epsilon \right) \psi(\rho_0) - 2\pi \log \frac{|\rho_2|}{|\rho_1|} \psi(\rho_1) \quad (2.31)$$

Where  $\psi$  is some testfunction to eliminate the factor  $|\rho_2|/|\rho_0|$  from the argument of the  $\theta$ -function. The extra term  $\log |\rho_2|/|\rho_1|$  cancels due to its antisymmetry with respect to the exchange of  $\rho_1$  and  $\rho_2$ .

After removing the overall factor  $|\rho_1|^4 |\rho_2|^4$  we recover the original expression (2.15). This completes the proof of conformal invariance of the Bethe-Salpeter equation in configuration space.

### 2.2.2 Conformal partial wave expansion

In the last section it was shown that the amplitude  $\Phi_\omega(\rho_1, \rho_2; \rho_{1'}, \rho_{2'})$  can be written in a conformally invariant way. It follows that the solutions of the Bethe-Salpeter equation can be classified according to the irreducible representations of the conformal group  $SO(3, 1)$ . The general solution is obtained as an expansion with respect to the representation functions of the corresponding irreducible representation, the conformal partial wave expansion

$$\Phi_\omega(\rho_1, \rho_2; \rho_{1'}, \rho_{2'}) = \sum_{n=-\infty}^{\infty} \int \frac{d\nu}{2\pi} \int d^2 \rho_0 E^{(\nu, n)}(\rho_{10}, \rho_{20}) \Gamma^{(\nu, n)}(\rho_{1'0}, \rho_{2'0}; \omega) \quad (2.32)$$

The representation functions  $E^{(\nu, n)}(\rho_{10}, \rho_{20})$  are the (up to a constant) uniquely defined conformally invariant three-point functions and will be given explicitly below. The representation is labeled by the parameters  $\nu \in \mathbb{R}$  and  $n \in \mathbb{Z}$  which enumerate the unitary irreducible principal series representation of the group  $SO(3, 1)$ . The coordinate  $\rho_0$  represents an additional quantum number. For a detailed mathematical discussion we refer to [50] and references given therein. The explicit form of the representation functions is

$$E^{(\nu, n)}(\rho_{10}, \rho_{20}) = c(\nu, n) \left( \frac{\rho_{12}}{\rho_{10} \rho_{20}} \right)^{\frac{1+n}{2} - i\nu} \left( \frac{\rho_{12}^*}{\rho_{10}^* \rho_{20}^*} \right)^{\frac{1-n}{2} - i\nu} \quad (2.33)$$

The constant  $c(\nu, n)$  is undetermined and for the moment set equal to unity. The functions  $E^{(\nu, n)}(\rho_{10}, \rho_{20})$  are the eigenfunctions of the two Casimir operators  $L^2 = -\rho_{12}^2 \partial_1 \partial_2$ ,  $L^{*2} = -\rho_{12}^{*2} \partial_1^* \partial_2^*$  of the global conformal group

$$\begin{aligned} L^2 E^{(\nu, n)} &= h(h-1) E^{(\nu, n)} \\ L^{*2} E^{(\nu, n)} &= \bar{h}(\bar{h}-1) E^{(\nu, n)} \\ h &= \frac{1-n}{2} + i\nu, \quad \bar{h} = \frac{1+n}{2} + i\nu \end{aligned} \quad (2.34)$$

where  $h$  and  $\bar{h}$  are the conformal weights of the representation. For the representation functions  $E^{(\nu, n)}(\rho_{10}, \rho_{20})$  the following orthonormalization condition holds

$$\begin{aligned} \int \frac{d^2 \rho_1 d^2 \rho_2}{|\rho_{12}|^4} E^{(\nu, n)}(\rho_{10}, \rho_{20}) E^{(\mu, m)}(\rho_{1'0}, \rho_{2'0}) &= a_{\nu, n} \delta_{n, m} \delta(\nu - \mu) \delta^{(2)}(\rho_{00'}) \\ &+ b_{\nu, n} \delta_{n, -m} \delta(\nu + \mu) \frac{1}{|\rho_{00'}|^{2+4i\nu}} \left( \frac{\rho_{00'}}{\rho_{00'}^*} \right)^n \end{aligned} \quad (2.35)$$

The proof of this relation can be found in the appendix of [5]. The coefficients  $a_{\nu,n}$  and  $b_{\nu,n}$  are determined as

$$a_{\nu,n} = \frac{2\pi^2}{4\nu^2 + n^2} \quad (2.36)$$

$$b_{\nu,n} = \pi^3 4^{2i\nu} \frac{\Gamma(-i\nu + \frac{|n|}{2})\Gamma(i\nu + \frac{|n|}{2})}{\Gamma(i\nu + \frac{|n|}{2})\Gamma(1 - i\nu + \frac{|n|}{2})} \quad (2.37)$$

The appearance of the second term on the rhs of the orthonormalization relation is due to the fact that the representations corresponding to the quantum numbers  $[\nu, n]$  and  $[-\nu, -n]$  are equivalent. We have the following intertwining relation

$$E^{(-\nu, -n)}(\rho_{10}, \rho_{20}) = \frac{b_{n, -\nu}}{a_{n, \nu}} \int d^2 \rho_{0'} E^{(\nu, n)}(\rho_{10'}, \rho_{20'}) |\rho_{00'}|^{-2+4i\nu} \left( \frac{\rho_{00'}^*}{\rho_{00'}} \right)^n \quad (2.38)$$

This relation can be proven with the methods used in appendix A.2. By insertion of the conformal partial wave expansion into the Bethe-Salpeter equation and use of eqs. (2.35) and (2.38) one can prove that the partial wave  $\Gamma(\rho_{1'0}, \rho_{2'0}; \omega)$  is proportional to the conjugate representation function  $E^{(\nu, n)*}(\rho_{1'0}, \rho_{2'0})$ . It follows that the explicit solution of the Bethe-Salpeter equation can be written in the following form

$$\begin{aligned} \Phi_\omega(\rho_1, \rho_2; \rho_{1'}, \rho_{2'}) &= \sum_{n=-\infty}^{\infty} \int_{-\infty}^{+\infty} \frac{d\nu}{2\pi} \frac{16\nu^2 + 4n^2}{[4\nu^2 + (n-1)^2][4\nu^2 + (n+1)^2]} \\ &\quad \cdot \frac{1}{\omega - \chi(\nu, n)} \int d^2 \rho_0 E^{(\nu, n)}(\rho_{10}, \rho_{20}) E^{(\nu, n)*}(\rho_{1'0}, \rho_{2'0}) \end{aligned} \quad (2.39)$$

Here  $\chi(\nu, n)$  is given by eq. (2.8) and corresponds to the eigenvalue of the integral kernel acting on the representation function  $E^{(\nu, n)}$ . Due to conformal invariance the eigenvalue has to be independent of the momentum transfer and hence has to coincide with the eigenvalue of the zero momentum transfer equation. An explicit calculation of this eigenvalue in configuration space is performed in appendix A.2. Note that for  $n = \pm 1$  the  $\nu$ -integral in the expression above is understood in the sense of the principal value.

### 2.2.3 Conformally invariant $n$ -point functions

In a general conformally invariant field theory there exists a set of primary fields  $\phi_{h, \bar{h}}$  which transform under a conformal transformation  $\rho \rightarrow f(\rho)$ ,  $\rho^* \rightarrow f^*(\rho^*)$  according to

$$\phi_{h, \bar{h}}(\rho, \rho^*) \rightarrow \left( \frac{\partial f}{\partial \rho} \right)^h \left( \frac{\partial f^*}{\partial \rho^*} \right)^{\bar{h}} \phi_{h, \bar{h}}(f(\rho), f^*(\rho^*)) \quad (2.40)$$

where  $h$  and  $\bar{h}$  are the conformal weights of the field. Conformal covariance then implies that the correlation functions of the theory satisfy

$$\begin{aligned} < \phi_{h_1, \bar{h}_1}(\rho_1, \rho_1^*) \cdots \phi_{h_n, \bar{h}_n}(\rho_n, \rho_n^*) > = \prod_{i=1}^n \left( \frac{\partial f}{\partial \rho_i} \right)^{h_i} \left( \frac{\partial f^*}{\partial \rho_i^*} \right)^{\bar{h}_i} \\ &\quad < \phi_{h_1, \bar{h}_1}(f(\rho_1), f^*(\rho_1^*)) \cdots \phi_{h_n, \bar{h}_n}(f(\rho_n), f^*(\rho_n^*)) > \end{aligned} \quad (2.41)$$

This covariance property imposes restrictions on the form of the correlation functions [51]. The two-point functions and the three-point functions of the primary fields are fixed up to a constant

$$\begin{aligned} < \phi_{h_1, \bar{h}_1}(\rho_1, \rho_1^*) \phi_{h_2, \bar{h}_2}(\rho_2, \rho_2^*) > &= \delta_{h_1, h_2} \delta_{\bar{h}_1, \bar{h}_2} \frac{c_{h_1, \bar{h}_1}}{\rho_{12}^{2h_1} \rho_{12}^{2\bar{h}_1}} \\ < \phi_{h_1, \bar{h}_1}(\rho_1, \rho_1^*) \phi_{h_2, \bar{h}_2}(\rho_2, \rho_2^*) \phi_{h_3, \bar{h}_3}(\rho_3, \rho_3^*) > &= \end{aligned} \quad (2.42)$$

$$c_{h_1 h_2 h_3, \bar{h}_1 \bar{h}_2 \bar{h}_3} \frac{1}{\rho_{12}^{h_1+h_2-h_3} \rho_{13}^{h_1+h_3-h_2} \rho_{23}^{h_2+h_3-h_1}} \frac{1}{\rho_{12}^{*h_1+\bar{h}_2-\bar{h}_3} \rho_{13}^{*h_1+\bar{h}_3-\bar{h}_2} \rho_{23}^{*h_2+\bar{h}_3-\bar{h}_1}} \quad (2.43)$$

The higher  $n$ -point functions are not completely fixed by conformal covariance but have to obey certain constraints. The four-point function takes the form

$$< \phi_{h_1, \bar{h}_1}(\rho_1, \rho_1^*) \cdots \phi_{h_4, \bar{h}_4}(\rho_4, \rho_4^*) > = \Psi(x, x^*) \prod_{i < j} \rho_{12}^{-h_i-h_j+\frac{1}{3}\sum_i h_i} \rho_{12}^{*-h_i-\bar{h}_j+\frac{1}{3}\sum_i \bar{h}_i} \quad (2.44)$$

where  $\Psi(x, x^*)$  is an undetermined function of the anharmonic ratio  $x = \frac{\rho_{12}\rho_{34}}{\rho_{13}\rho_{24}}$  and its conjugate. In general the  $n$ -point function ( $n \geq 4$ ) contains an a priori undetermined function which depends on the  $n(n-3)/4$  anharmonic ratios which can be constructed from  $n$  coordinates and their conjugate.

Let us now interpret the amplitudes which were calculated in the preceeding sections in terms of the general conformal  $n$ -point function. By comparing the conformal representation functions  $E^{(\nu, n)}$  (2.33) with the general three-point function (2.43) we note that the former can be interpreted as a conformal three-point function build up from two fields with conformal weights  $h = 0, \bar{h} = 0$  at the points  $\rho_1, \rho_2$  and a field with conformal weights  $h = (1+n)/2 - i\nu, \bar{h} = (1-n)/2 - i\nu$  at the point  $\rho_0$

$$E^{(\nu, n)}(\rho_{10}, \rho_{20}) = < \phi_{0,0}(\rho_1) \phi_{0,0}(\rho_2) O_{h, \bar{h}}(\rho_0) >_{\substack{h=(1-n)/2+i\nu \\ \bar{h}=(1+n)/2+i\nu}} \quad (2.45)$$

We interpret  $\phi_{0,0}$  as an elementary field representing the reggeized gluon and  $O(\rho_0)$  as a field which represents a composite state of two reggeized gluons which emerges from the solution of the dynamical equations of the theory. After having introduced an elementary field representing the reggeized gluon it is natural to interpret the off-shell scattering amplitude  $\Phi_\omega(\rho_1, \rho_2; \rho_{1'}, \rho_{2'})$  as the four-point function of the field  $\phi_{0,0}$ . It then follows from the general theory outlined above that this function can depend on the four points only as a function of the anharmonic ratio. This was already shown for the Born-level approximation of this function (2.18) and can be demonstrated for the exact four-point function (2.39) by integrating over the coordinate  $\rho_0$ . For this calculation we limit ourselves to the case  $n = 0$ . Since  $\Phi_\omega(\rho_1, \rho_2; \rho_{1'}, \rho_{2'})$  is conformally invariant the  $\rho_0$ -integration can be simplified by choosing e. g.  $\rho_{2'} = \infty$ . Then we use the methods and results of [52] to perform the integration and restore the  $\rho_{2'}$ -dependence afterwards by requiring the correct transformation properties. In this way we obtain

$$\begin{aligned} \Phi_\omega(\rho_1, \rho_2; \rho_{1'}, \rho_{2'}) &= \int_{-\infty}^{+\infty} \frac{d\nu}{2\pi} \frac{16\nu^2}{[4\nu^2 + 1]^2} \frac{\pi}{\omega - \chi(\nu, 0)} \\ &\left[ \eta^{\frac{1}{2}+i\nu} \eta^{*\frac{1}{2}+i\nu} \frac{\Gamma(2i\nu-1)\Gamma(2-2i\nu)}{\Gamma^2(1+2i\nu)} \frac{\Gamma^2(\frac{1}{2}+i\nu)}{\Gamma^2(\frac{1}{2}-i\nu)} {}_2F_1\left(\frac{1}{2}+i\nu, \frac{1}{2}+i\nu, 1+2i\nu, \eta\right) {}_2F_1\left(\frac{1}{2}+i\nu, \frac{1}{2}+i\nu, 1+2i\nu, \eta^*\right) \right. \\ &\left. + \eta^{\frac{1}{2}-i\nu} \eta^{*\frac{1}{2}-i\nu} \frac{\Gamma(-2i\nu-1)\Gamma(2+2i\nu)}{\Gamma^2(1-2i\nu)} \frac{\Gamma^2(\frac{1}{2}-i\nu)}{\Gamma^2(\frac{1}{2}+i\nu)} {}_2F_1\left(\frac{1}{2}-i\nu, \frac{1}{2}-i\nu, 1-2i\nu, \eta\right) {}_2F_1\left(\frac{1}{2}-i\nu, \frac{1}{2}-i\nu, 1-2i\nu, \eta^*\right) \right] \end{aligned} \quad (2.46)$$

with the anharmonic ratios

$$\eta = \frac{\rho_{12}\rho_{1'2'}}{\rho_{11'}\rho_{22'}}, \quad \eta^* = \frac{\rho_{12}^*\rho_{1'2'}^*}{\rho_{11'}^*\rho_{22'}^*} \quad (2.47)$$

Eq. (2.47) confirms that the four-point function of four fields associated with the reggeized gluon depends on the coordinates only through the two anharmonic ratios in agreement with the general theory. The representation above could be useful in the study of the short-distance limits of the BFKL amplitude in configuration space.

## 2.3 The momentum space representation of the conformal eigenfunctions

In the preceding sections the non-forward Bethe-Salpeter equation was solved in configuration space by conformal partial wave expansion. An interpretation in terms of a conformal field theory in two dimensions

was sketched. Although the resulting expression looks elegant and compact it seems preferable for many reasons to work with a momentum space representation.

To this end we apply the inverse Fourier transformation to the configuration space solution (2.39) of the Bethe Salpeter equation. The  $\rho_0$ -integration can be performed easily to give the  $\delta^{(2)}(\mathbf{q} - \mathbf{q}')$ -function. The resulting expression factorizes in two terms, one depending only on  $\mathbf{k}$  and the other one depending only on  $\mathbf{k}'$ . The  $\mathbf{k}$ -dependent term reads

$$E^{(\nu, n)}(\mathbf{k}, \mathbf{q} - \mathbf{k}) = c(\nu, n) \int d^2 \rho_1 d^2 \rho_2 e^{i\mathbf{k}\rho_1 + i(\mathbf{q} - \mathbf{k})\rho_2} \left( \frac{\rho_{12}}{\rho_1 \rho_2} \right)^{\frac{1+n}{2} - i\nu} \left( \frac{\rho_{12}^*}{\rho_1^* \rho_2^*} \right)^{\frac{1-n}{2} - i\nu} \quad (2.48)$$

and corresponds to the momentum space representation of the conformal three-point function. We reintroduced the constant  $c(\nu, n)$  which will be adjusted in the end to match the eigenfunction (2.7) in the forward direction. The  $\mathbf{k}$ -factorization is of course broken by the  $\nu$ -integration as will be seen in a moment. In the following we restrict ourselves to the case  $n = 0$ . As we will show later, results for nonzero  $n$  can be obtained in a very similar fashion. Introducing center of mass coordinates  $\rho = \rho_{12}$ ,  $R = \rho_1 + \rho_2$ , we first obtain the mixed representation for the three-point function

$$E^{(\nu, 0)}(\rho, \mathbf{q}) = c(\nu, 0) (|\rho|^2)^{\frac{1}{2} - i\nu} \int d^2 R e^{i\mathbf{q}R} \left( \frac{1}{|\rho + R|^2 |\rho - R|^2} \right)^{\frac{1}{2} - i\nu} \quad (2.49)$$

$$= c(\nu, 0) 2\pi \frac{4^{i\nu}}{\Gamma^2(\frac{1}{2} - i\nu)} |\rho| (\mathbf{q}^2)^{-i\nu} \int_0^1 dx [x(1-x)]^{-\frac{1}{2}} e^{-i\mathbf{q}\rho(1-x)} K_{-2i\nu}(|\mathbf{q}||\rho|\sqrt{x(1-x)}) \quad (2.50)$$

where  $K$  denotes the modified Bessel function of the second kind. Now we perform the  $\rho$ -integration using polar coordinates which results in

$$E^{(\nu, 0)}(\mathbf{k}, \mathbf{q} - \mathbf{k}) = c(\nu, 0) (\mathbf{q}^2)^{-i\nu} \int_0^\infty d|\rho|^2 |\rho| J_0(|\rho||\mathbf{k} - (1-x)\mathbf{q}|) K_{-2i\nu}(|\mathbf{q}||\rho|\sqrt{x(1-x)}) \quad (2.51)$$

$$= c(\nu, 0) 8\pi^2 4^{i\nu} \frac{\Gamma(\frac{3}{2} + i\nu) \Gamma(\frac{3}{2} - i\nu)}{\Gamma^2(\frac{1}{2} - i\nu)} (\mathbf{q}^2)^{-\frac{3}{2} - i\nu} \int_0^1 dx [x(1-x)]^{-2} \cdot {}_2F_1\left(\frac{3}{2} + i\nu, \frac{3}{2} - i\nu, 1; -\frac{x(1-x)\mathbf{q}^2}{(\mathbf{k} - x\mathbf{q})^2}\right) \quad (2.52)$$

$$= c(\nu, 0) 8\pi^2 4^{i\nu} \frac{\Gamma(\frac{3}{2} + i\nu) \Gamma(\frac{3}{2} - i\nu)}{\Gamma^2(\frac{1}{2} - i\nu)} \int_0^1 dx [x(1-x)]^{-\frac{1}{2} + i\nu} [x(1-x)\mathbf{q}^2 + (\mathbf{k} - x\mathbf{q})^2]^{-\frac{3}{2} - i\nu} \cdot {}_2F_1\left(\frac{3}{2} + i\nu, -\frac{1}{2} + i\nu, 1; \frac{(\mathbf{k} - x\mathbf{q})^2}{x(1-x)\mathbf{q}^2 + (\mathbf{k} - x\mathbf{q})^2}\right) \quad (2.53)$$

where in the last line a transformation of the hypergeometric function was used which leading to a result in which the argument of the  ${}_2F_1$ -function is bounded by 1 from above for every value of  $\mathbf{k}, \mathbf{q}$  and  $x$ . By performing the transformation  $x \rightarrow 1 - x$  we establish the symmetry w. r. t. the exchange of  $\mathbf{k}$  and  $\mathbf{q} - \mathbf{k}$ . Now we want to recover the result for the forward direction ( $\mathbf{q} = 0$ ) from this expression. In the limit  $\mathbf{q} = 0$  the argument of the hypergeometric function moves on the unit circle where the convergence properties of the hypergeometric series depend on the values of the first three arguments. To make this more transparent we use an analytic transformation [53] for the hypergeometric function which gives in the limit  $\mathbf{q} \rightarrow 0$

$$\begin{aligned} & {}_2F_1\left(\frac{3}{2} + i\nu, -\frac{1}{2} + i\nu, 1; \frac{(\mathbf{k} - x\mathbf{q})^2}{x(1-x)\mathbf{q}^2 + (\mathbf{k} - x\mathbf{q})^2}\right) \\ &= \left[ \frac{\Gamma(-2i\nu)}{\Gamma(-\frac{1}{2} - i\nu) \Gamma(\frac{3}{2} - i\nu)} + \left(x(1-x) \frac{\mathbf{q}^2}{\mathbf{k}^2}\right)^{-2i\nu} \cdot \frac{\Gamma(2i\nu)}{\Gamma(\frac{3}{2} + i\nu) \Gamma(-\frac{1}{2} + i\nu)} \right] [1 + O(\mathbf{q}^2)] \end{aligned} \quad (2.54)$$

Inserting this into eq. (2.53) we find

$$E^{(\nu,0)}(\mathbf{k}, \mathbf{q} - \mathbf{k}) = c(\nu, n) 4\pi^2 (\mathbf{k}^2)^{-\frac{3}{2}-i\nu} \left[ 4^{-i\nu} \frac{\Gamma(-i\nu)}{\Gamma(1+i\nu)} \frac{\Gamma(\frac{3}{2}+i\nu)\Gamma(\frac{1}{2}+i\nu)}{\Gamma(\frac{1}{2}-i\nu)\Gamma(-\frac{1}{2}-i\nu)} \right. \\ \left. + \left( \frac{\mathbf{q}^2}{\mathbf{k}^2} \right)^{-2i\nu} 4^{i\nu} \frac{\Gamma(i\nu)}{\Gamma(1-i\nu)} \frac{\Gamma(\frac{3}{2}-i\nu)\Gamma(\frac{1}{2}+i\nu)}{\Gamma(\frac{1}{2}-i\nu)\Gamma(-\frac{1}{2}+i\nu)} \right] [1 + O(\mathbf{q}^2)] \quad (2.55)$$

We choose the normalization  $c(\nu, n)$  to cancel the first term in square brackets

$$E^{(\nu,0)}(\mathbf{k}, \mathbf{q} - \mathbf{k}) = 4\pi^2 (\mathbf{k}^2)^{-\frac{3}{2}-i\nu} \left[ 1 + 4^{2i\nu} \left( \frac{\mathbf{q}^2}{\mathbf{k}^2} \right)^{-2i\nu} \frac{\Gamma(i\nu)\Gamma(1+i\nu)}{\Gamma(-i\nu)\Gamma(1-i\nu)} \frac{\Gamma(\frac{3}{2}-i\nu)\Gamma(-\frac{1}{2}-i\nu)}{\Gamma(\frac{3}{2}+i\nu)\Gamma(-\frac{1}{2}+i\nu)} \right] \quad (2.56)$$

From this representation we conclude that the momentum space eigenfunction  $E^{(\nu,0)}$  has a well defined limit in the forward direction only if  $Im(\nu) > 0$ . In the opposite case,  $Im(\nu) < 0$ , the function  $E^{(\nu,0)}$  becomes singular in the forward direction. For the conjugate eigenfunction  $E^{(\nu,0)*}$  the converse is true. Thus the  $\mathbf{q} = 0$ -limit of the product  $E^{(\nu,0)} E^{(\nu,0)*}$  which enters into the momentum space expression of the BFKL amplitude seems to be ill-defined in the whole strip  $-1 < Im(\nu) < 1$  in which the coefficient of the second term in eq. (2.55) and its conjugate are analytic functions of  $\nu$ . However, according to this equation in the limit  $\mathbf{q} \rightarrow 0$  the product  $E^{(\nu,0)} E^{(\nu,0)*}$  can be decomposed into a sum of four terms and we can deform the contour of the  $\nu$ -integration for each term separately. Explicitly we have

$$E^{(\nu,0)}(\mathbf{k}, \mathbf{q} - \mathbf{k}) E^{(\nu,0)*}(\mathbf{k}', \mathbf{q} - \mathbf{k}') = \frac{16\pi^4}{\nu^2} \left( \nu^2 + \frac{1}{4} \right)^2 (\mathbf{k}^2)^{-\frac{3}{2}-i\nu} (\mathbf{k}'^2)^{-\frac{3}{2}+i\nu} \\ \left[ 1 + \left( \frac{\mathbf{k}^2}{\mathbf{k}'^2} \right)^{2i\nu} + 4^{2i\nu} \left( \frac{\mathbf{q}^2}{\mathbf{k}^2} \right)^{-2i\nu} C(\nu) + 4^{-2i\nu} \left( \frac{\mathbf{q}^2}{\mathbf{k}'^2} \right)^{2i\nu} C^*(\nu) \right] [1 + O(\mathbf{q}^2)] \quad (2.57)$$

with  $C(\nu)$  representing the combination of  $\Gamma$ -functions in eq. (2.56). For the third and the fourth term we can shift the integration contour to the lower, resp. upper half of the complex  $\nu$ -plane. This shift is legitimate due to the analyticity properties of  $C(\nu)$ . After this deformation the limit  $\mathbf{q} \rightarrow 0$  of these terms can be performed and yields zero. The first and the second term are identical since in the second term we can shift from  $\nu$  to  $-\nu$ . With this prescription we end up with

$$E^{(\nu,0)}(\mathbf{k}, -\mathbf{k}) E^{(\nu,0)*}(\mathbf{k}', -\mathbf{k}') = 2 \frac{16\pi^4}{\nu^2} \left( \nu^2 + \frac{1}{4} \right)^2 (\mathbf{k}^2)^{-\frac{3}{2}-i\nu} (\mathbf{k}'^2)^{-\frac{3}{2}+i\nu} \quad (2.58)$$

The  $\nu$ -dependent prefactors cancel after inserting this into eq. (2.39). To match the solution in the forward direction we finally have to divide by  $4\pi^2$ . This is done by absorbing an additional factor  $\sqrt{2}/(2\pi)$  in  $c(\nu, 0)$ . Consequently the normalization factor  $c(\nu, 0)$  is determined as

$$c(\nu, 0) = \frac{\sqrt{2}}{2\pi} 4^{i\nu} \frac{\Gamma(1+i\nu)}{\Gamma(-i\nu)} \frac{\Gamma(\frac{1}{2}-i\nu)\Gamma(-\frac{1}{2}-i\nu)}{\Gamma(\frac{3}{2}+i\nu)\Gamma(\frac{1}{2}+i\nu)} \quad (2.59)$$

For the  $\mathbf{q} = 0$ -limit of the eigenfunctions we prescribe to neglect the  $(\mathbf{q}^2)^{-2i\nu}$ -term in eq. (2.55) by choosing  $Im(\nu) > 0$ . With this effective prescription we reproduce the correct result. When this normalization is used for the eigenfunctions in momentum space the factor  $\nu^2/(\nu^2 + 1/4)^2$  which appears in the solution of the configuration space equation has to be omitted. It is absorbed into the eigenfunctions.

In eq. (2.53) we have realized a rather compact form of the momentum space expression of the conformal three-point function for  $n = 0$ . We were not able to give a similar representation for  $n \neq 0$ . Of course for  $n \neq 0$  the momentum space expressions can be obtained by linear combination of functions generated from expressions similar to eq. (2.53) by partial differentiation. Switching from complex to cartesian coordinates in configuration space, for  $n = \pm 1$  we can construct the linear combinations

$$\frac{1}{2} [E^{(\nu,+1)} \pm E^{(\nu,-1)}] (\rho_1, \rho_2) = \frac{(|\rho_{12}|)^{-i\nu}}{(|\rho_1|^2 |\rho_2|^2)^{1-i\nu}} \left[ \left( \frac{\rho_2^x}{-i\rho_2^y} \right) |\rho_1|^2 + \left( \frac{-\rho_1^x}{i\rho_1^y} \right) |\rho_2|^2 \right] \quad (2.60)$$

Changing from cartesian components to partial derivatives we find the momentum space representation of the above expression

$$\frac{1}{2} \left[ E^{(\nu, +1)} \pm E^{(\nu, -1)} \right] (\mathbf{k}, \mathbf{q} - \mathbf{k}) = -2i c(\nu, 1) \left[ \left( \frac{\partial_{\mathbf{q}_x}}{-i\partial_{\mathbf{q}_y}} \right) I_0^{(\nu, 1)}(\mathbf{k}, \mathbf{q} - \mathbf{k}) + \left( \frac{-\partial_{\mathbf{k}_x} - \partial_{\mathbf{q}_x}}{i\partial_{\mathbf{k}_y} + i\partial_{\mathbf{q}_y}} \right) I_1^{(\nu, 1)}(\mathbf{k}, \mathbf{q} - \mathbf{k}) \right] \quad (2.61)$$

where we have introduced the function

$$I_m^{(\nu, 1)}(\mathbf{k}, \mathbf{q} - \mathbf{k}) = 4\pi^2 4^{i\nu} \frac{\Gamma(1 + i\nu)}{\Gamma(-i\nu)} \int_0^1 dx x^{i\nu-1+m} (1-x)^{i\nu-m} [\mathbf{q}^2 x(1-x) + (\mathbf{k} - x\mathbf{q})^2]^{-1-i\nu} {}_2F_1 \left( 1 + i\nu, i\nu, 1; \frac{(\mathbf{k} - x\mathbf{q})}{\mathbf{q}^2 x(1-x) + (\mathbf{k} - x\mathbf{q})^2} \right) \quad (2.62)$$

It is clear that representations of this type can also be generated for higher  $n$  but the explicit expressions become rather complicated. For use at a later stage of this work it will still be useful to know explicitly the normalization factors  $c(\nu, n)$  for arbitrary  $n$ . For  $n = 1$  this factor can be found by performing first the differentiations in eq. (2.61) and following the steps described above for  $n = 0$ .

### 2.3.1 The expansion in powers of the momentum transfer

There is an alternative approach which allows to obtain a closed formula for the factor  $c(\nu, n)$ . It turns out that it is possible to compute the complete expansion of  $E^{(\nu, n)}(\mathbf{k}, \mathbf{q} - \mathbf{k})$  in  $|\mathbf{q}|$  for arbitrary  $n$ . From this expansion  $c(\nu, n)$  is obtained by normalizing the zero-order contribution.

To construct the expansion we go back to the definition of the momentum space representation in eq. (2.48)

$$E^{(\nu, n)}(\mathbf{k}, \mathbf{q} - \mathbf{k}) = c(\nu, n) \int d^2\rho e^{i\mathbf{k}\rho} (\rho^2)^{\frac{1}{2}-i\nu} \left( \frac{\rho}{\rho^*} \right)^{\frac{n}{2}} \int d^2\rho_2 \frac{e^{i\mathbf{q}\rho_2}}{(\rho_2^2(\rho + \rho_2)^2)^{\frac{1}{2}-i\nu}} \left[ \frac{\rho_2^*(\rho + \rho_2)^*}{\rho_2(\rho_2 + \rho)} \right]^{\frac{n}{2}} \quad (2.63)$$

It is essential to realize that there are two regions in the  $\rho_2$ -integration which give contributions of the same order in the limit  $\mathbf{q} \rightarrow 0$ . The first region is  $|\rho_2| > |\rho|$  and the coefficients are obtained by first expanding the integrand of the  $\rho_2$  integral in powers of  $|\rho|/|\rho_2|$  and then integrating the coefficients over  $\rho_2$  and  $\rho$ . The second region is  $|\mathbf{q}| < |\rho_2|$  and the coefficients are obtained by first expanding the exponential in powers of  $|\mathbf{q}|$  and integrating then again the coefficients over  $\rho_2$  and  $\rho$ . As to the first region we obtain from the  $\rho_2$ -integration

$$c(\nu, n) \int d^2\rho e^{i\mathbf{k}\rho} (|\rho^2|)^{\frac{1}{2}-i\nu} \left( \frac{\rho}{\rho^*} \right)^{\frac{n}{2}} \sum_{M=0}^{\infty} (|\mathbf{q}||\rho|)^M \sum_{m=0}^M \left( \frac{q}{q^*} \right)^{\frac{M}{2}-m-n} \left( \frac{\rho}{\rho^*} \right)^{m-\frac{M}{2}} \beta_{M,m}^{(\nu, n)} \left( \frac{q}{q^*}, \frac{\rho}{\rho^*} \right) \quad (2.64)$$

with

$$\beta_{M,m}^{(\nu, n)} \left( \frac{q}{q^*}, \frac{\rho}{\rho^*} \right) = \pi 4^{2i\nu - \frac{M}{2}} \frac{(-1)^M}{\Gamma(1+M)} i^{|2n+2m-M|} \binom{M}{m} \frac{\Gamma(\frac{1}{2} - i\nu + \frac{n}{2} + m) \Gamma(\frac{1}{2} - i\nu - \frac{n}{2} + M - m)}{\Gamma(\frac{1}{2} - i\nu + \frac{n}{2}) \Gamma(\frac{1}{2} - i\nu - \frac{n}{2})} \frac{\Gamma(2i\nu + |n+m - \frac{M}{2}| - \frac{M}{2})}{\Gamma(1 - 2i\nu + |n+m - \frac{M}{2}| + \frac{M}{2})} \quad (2.65)$$

As to the second integration region we expand the exponential function in the  $\rho_2$ -integral, use a complex representation for the scalar product  $\mathbf{q}\rho = 1/2(q\rho^* + q^*\rho)$  and expand the higher orders of this expression using the binomial theorem. This gives us in each order of  $(|\mathbf{q}|^2)^M$  a sum over  $M+1$  contributions of the form

$$\int d^2\rho_2 \left( \frac{1}{\rho_2} \right)^{\frac{1}{2}-i\nu+\frac{n}{2}-(M-m)} \left( \frac{1}{\rho_2^*} \right)^{\frac{1}{2}-i\nu-\frac{n}{2}-m} \left( \frac{1}{\rho_2 + \rho} \right)^{\frac{1}{2}-i\nu+\frac{n}{2}} \left( \frac{1}{\rho_2^* + \rho^*} \right)^{\frac{1}{2}-i\nu-\frac{n}{2}} \quad (2.66)$$

This integral can be calculated by reducing it to a product of two contour integrals, a method which is also used in appendix A.2 to calculate the eigenvalues of the BFKL-kernel and is described in detail in [52]. After

introducing the rescaled variables  $\sigma = \rho_2/\rho$ ,  $\sigma^* = \rho_2^*/\rho^*$  one performs a Wick rotation  $\sigma_y \rightarrow i \exp(-2i\epsilon)\sigma_y \simeq i(1-2i\epsilon)\sigma_y$  and turns over to light-cone coordinates  $\sigma_+ = \sigma_x + \sigma_y$ ,  $\sigma_- = \sigma_x - \sigma_y$ . The integrals over  $\sigma_+$  and  $\sigma_-$  then factorize up to terms of order  $\epsilon$  which define the way in which the contours of integration by-pass the singular points. Deformation of the contours then leads to the product of two integrals which reduce to  $\Gamma$ -functions. Eq. (2.66) can be expressed as

$$\pi(|\rho|^2)^{2i\nu} \rho^M \left(\frac{\rho^*}{\rho}\right)^{n+m} (-1)^{M+n} \frac{\Gamma(-2i\nu - n - m)}{\Gamma(1 + 2i\nu - n + M - m)} \frac{\Gamma(\frac{1}{2} + i\nu - \frac{n}{2})\Gamma(\frac{1}{2} + i\nu - \frac{n}{2} + M - m)}{\Gamma(\frac{1}{2} - i\nu - \frac{n}{2})\Gamma(\frac{1}{2} - i\nu - \frac{n}{2} - m)} \quad (2.67)$$

This leads to the following contribution to the expansion of eq. (2.63) in  $|\mathbf{q}|$

$$c(\nu, n) \int d^2\rho e^{i\mathbf{k}\rho} (|\rho^2|)^{\frac{1}{2}+i\nu} \left(\frac{\rho}{\rho^*}\right)^{\frac{M}{2}} \sum_{M=0}^{\infty} (|\mathbf{q}||\rho|)^M \sum_{m=0}^M \left(\frac{q}{q^*}\right)^{m-\frac{M}{2}} \left(\frac{\rho}{\rho^*}\right)^{-m-n+\frac{M}{2}} \alpha_{M,m}^{(\nu,n)}\left(\frac{q}{q^*}, \frac{\rho}{\rho^*}\right) \quad (2.68)$$

with coefficients

$$\alpha_{M,m}^{(\nu,n)}\left(\frac{q}{q^*}, \frac{\rho}{\rho^*}\right) = \frac{\pi}{\Gamma(1+M)} \left(\frac{i}{2}\right)^M (-1)^{M+n} \binom{M}{m} \cdot \frac{\Gamma(-2i\nu - n - m)}{\Gamma(1 + 2i\nu - n + M - m)} \frac{\Gamma(\frac{1}{2} + i\nu - \frac{n}{2})\Gamma(\frac{1}{2} + i\nu - \frac{n}{2} + M - m)}{\Gamma(\frac{1}{2} - i\nu - \frac{n}{2})\Gamma(\frac{1}{2} - i\nu - \frac{n}{2} - m)} \quad (2.69)$$

It remains to perform the  $\rho$ -integration. This is straightforward and we obtain the complete expansion of the momentum space eigenfunction in powers of  $|\mathbf{q}|/|\mathbf{k}|$  for arbitrary  $n$ .

$$E^{(\nu,n)} = c(\nu, n) (|\mathbf{k}|^2)^{-\frac{3}{2}-i\nu} \left(\frac{k}{k^*}\right)^{-\frac{n}{2}} \sum_{M=0}^{\infty} \left(\frac{|\mathbf{q}|}{|\mathbf{k}|}\right)^M \sum_{m=0}^M \left(\frac{k}{k^*}\right)^{-m+\frac{M}{2}} \left(\frac{q}{q^*}\right)^{m-\frac{M}{2}} \cdot \left[ a_{M,m}^{(\nu,n)} + \left(\frac{\mathbf{q}^2}{\mathbf{k}^2}\right)^{-2i\nu} \left(\frac{q^*k}{qk^*}\right)^n b_{M,m}^{(\nu,n)} \right] \quad (2.70)$$

with coefficients

$$\begin{aligned} a_{M,m}^{(\nu,n)} &= 2\pi 4^{1+i\nu+\frac{M}{2}} (-1)^{|\frac{n}{2}-m+\frac{M}{2}|} \frac{\Gamma(\frac{3}{2} + i\nu + \frac{M}{2} + |\frac{n}{2} - m + \frac{M}{2}|)}{\Gamma(-\frac{1}{2} - i\nu - \frac{M}{2} + |\frac{n}{2} - m + \frac{M}{2}|)} \alpha_{M,m}^{(\nu,n)} \\ b_{M,m}^{(\nu,n)} &= 2\pi 4^{1-i\nu+\frac{M}{2}} (-1)^{|\frac{n}{2}+m-\frac{M}{2}|} \frac{\Gamma(\frac{3}{2} - i\nu + \frac{M}{2} + |\frac{n}{2} + m - \frac{M}{2}|)}{\Gamma(-\frac{1}{2} + i\nu - \frac{M}{2} + |\frac{n}{2} + m - \frac{M}{2}|)} \beta_{M,m}^{(\nu,n)} \end{aligned} \quad (2.71)$$

For  $n = 0$  and low orders in  $M$  this can be compared with the expansion which can be worked out starting from eq. (2.53).

A comment is in order concerning the existence of the integrals which determine the coefficients of the expansion. These integrals converge only in a strip in the complex  $\nu$ -plane the location of which depends on the order  $M$ . The value outside this strip is obtained from the result of the integration by analytical continuation.

By repeating the same line of arguments as given for the case  $n = 0$  we determine the normalization factor  $c(\nu, n)$  for general  $n$  to be

$$c(\nu, n) = i^n \frac{\sqrt{2}}{2\pi} 4^{i\nu} \frac{\Gamma(1 + i\nu + \frac{|n|}{2})}{\Gamma(-i\nu + \frac{|n|}{2})} \frac{\Gamma(-\frac{1}{2} - i\nu + \frac{|n|}{2})}{\Gamma(\frac{1}{2} + i\nu + \frac{|n|}{2})} \frac{\Gamma(\frac{1}{2} - i\nu + \frac{|n|}{2})}{\Gamma(\frac{3}{2} + i\nu + \frac{|n|}{2})} \quad (2.72)$$

For the  $\mathbf{q} = 0$ -limit of the eigenfunction we use the same prescription as before, namely to give  $\nu$  a small imaginary part. The second term in brackets in eq. (2.71) then vanishes in the limit  $\mathbf{q} = 0$ .

### 3 Phenomenology of the BFKL Pomeron in Deep Inelastic Scattering

The past few years have seen a renewed interest in the BFKL theory from the phenomenological point of view. In deep inelastic scattering (DIS) QCD perturbation theory, in particular the resummation of large logarithms of  $Q^2$ , has been successfully applied for a long time. It was then realized that with DIS entering the regime of small Bjorken- $x$  there might be the need to resum also logarithms of  $1/x$  which - in leading order approximation - is done by the BFKL equation. Processes at small  $x$  - which corresponds to large photon-proton cms energy - are traditionally described within Regge theory. In Regge theory scattering processes are mediated by Regge trajectories - singularities of the partial wave amplitude in the complex angular momentum plane. The leading singularity at high energies - the pomeron - has been regarded as an object of nonperturbative origin in QCD. Since, on the other hand, DIS is successfully described within perturbation theory, the question arises if in DIS at small  $x$  a novel object, a 'hard' pomeron appears, which emerges from the resummation of large logarithms in  $1/x$  within perturbation theory. To leading order this 'hard' pomeron has to be identified with the BFKL pomeron. In this chapter the idea that in DIS at small  $x$  large logarithms of  $1/x$  have to be resummed is pursued.

The BFKL resummation is first used to determine the inclusive DIS structure function  $F_2$ . The conventional approach towards hard scattering processes in DIS is based on the collinear factorization theorem which allows to separate perturbative and nonperturbative contributions. In order to resum the logarithms in  $1/x$  this framework has to be extended to the more general formalism of high energy factorization. The key difference is that in the latter the gluon <sup>6</sup> distribution of the proton becomes transverse momentum dependent and a convolution in transverse momentum space has to be carried out. In section 3.1 we give a short introduction to collinear and high energy factorization and show how the BFKL equation can be used to calculate the unintegrated (transverse momentum dependent) gluon density.

In the transverse momentum convolution the integration is performed also over nonperturbative scales. This raises the question of the consistency of this approach since it uses perturbative results in a region where perturbation theory is not applicable. Even worse, it can be shown that in principle one has to expect a finite contribution from this region. The logarithms in  $1/x$  are built up in the multi-Regge region of phase space to which hard and low scales contribute equally. The evolution which resums these contributions can be regarded as a diffusion process in transverse momentum space. The center of the diffusion is set by the characteristic external scales of the process. In inclusive DIS there are two scales, the virtuality  $Q^2$  of the photon and the inverse size  $1/R_P^2$  of the proton. The diffusion process which starts from the proton side is centered around  $Q_0^2 = 1/R_P^2$  in the nonperturbative region and consequently the part of the phase space which is treated incorrectly in the BFKL theory gives a substantial contribution. This dependence on the nonperturbative region is investigated in detail in section 3.1. We will furthermore discuss modifications of the infrared region of the BFKL equation and show their effect on the evolution and the results for  $F_2$ . An additional part of section 3.1 is devoted to the transverse energy distribution of the gluons which evolve according to the BFKL equation. The measurement of the transverse energy distribution has been advocated as a possible 'footprint' of BFKL dynamics, especially of the characteristic gaussian distribution of transverse momenta.

The sections 3.2 - 3.4 deal with exclusive processes in deep inelastic scattering. In section 3.2 diffractive production of vector mesons at large momentum transfer  $t$  and small  $x$  is investigated. This process deserves interest for two reasons. First, for large  $t$  the physical picture of the BFKL evolution changes drastically. The scale  $\mathbf{q}^2 = -t$  acts as a lower cutoff for the diffusion in transverse momentum space, i. e. we have diffusion with a boundary. This means that the serious infrared problem which the application of BFKL to inclusive DIS ( $F_2$ ) faces is absent here and the BFKL prediction has a much better theoretical foundation. Second, this process allows to investigate the  $t$ -dependence of the hard pomeron trajectory. It was stated in the first chapter of this work that due to conformal symmetry the BFKL singularity is a fixed cut, i. e. there is no  $t$ -dependence. The conformal symmetry is broken when the BFKL amplitude is convoluted with the impact factors of external particles and in principle a  $t$ -dependence of the trajectory can be observed. We

---

<sup>6</sup>The quark distribution has not been considered in this framework up to now.



parametrize such a dependence in terms of the slope of the trajectory and derive an effective slope for the amplitude under consideration.

In section 3.3 we turn to diffractive dissociation of the photon in DIS. Diffractive dissociation is well-known from hadron-hadron scattering and is traditionally described in terms of Regge singularity exchange. Given the presence of the large scale  $Q^2$  one can ask again to which extent QCD perturbation theory can describe these processes. The perturbative analysis of diffractive dissociation is fairly complicated especially if one turns to large masses of the diffractively produced system and consistent approximation schemes exist only for specific limiting cases. In the simplest case the virtual photon dissociates into a quark-antiquark pair which scatters off the proton. We will use the BFKL pomeron to describe this scattering at large and zero momentum transfer. The result for this simplest case shows some specific properties which are expected to hold also when more complicated final states are taken into account. From the phenomenological point of view the results for zero momentum transfer are not so interesting since it has been shown that in the diffractive case the infrared problem of the BFKL equation is even more severe than in inclusive DIS. It turns out that the effective scale at the photon side is much lower than the virtuality  $Q^2$ . Therefore the BFKL evolution is driven deeply into the nonperturbative domain. From the theoretical point of view these calculations are nevertheless important since they represent the first steps towards the perturbative unitarization of the BFKL pomeron. For finite momentum transfer the theoretical foundation of the perturbative results is better. For this case we discuss some subtleties concerning the coupling of the BFKL pomeron to quarks.

We will then generalize the calculation to include also more complicated final states. Use will be made of results which were obtained for the triple Regge limit in which the final state mass  $M^2$  is very large. We will show that the  $q\bar{q}$ -calculation can easily be extended and we derive interesting results for the energy dependence of the cross section in the zero momentum transfer limit. These results can be shown to follow from a conservation law for the conformal dimension of the BFKL pomerons at an effective triple pomeron vertex. In this last part the analysis will, however, remain incomplete in so far as we will not consider a certain group of contributions which is beyond theoretical reach at the moment.

In section 3.4 we turn to exclusive photon diffractive dissociation. It has been shown that a large momentum scale in the diffractively produced final state acts as a hard scale at the effective photon pomeron vertex in diffraction. In this case the diffusion scenario of the BFKL evolution is comparable to inclusive DIS with the proton scale  $Q_0^2$  at the lower end and the hard scale at the upper end. Examples for such hard scales are a heavy vector meson mass, a large transverse momentum of the produced quark-antiquark pair or the mass of a produced charm quark. We will concentrate on the last two cases, namely we will consider the production of  $q\bar{q}$ -pairs with either large transverse momentum or large mass. Our starting point will be the exchange of the BFKL pomeron and we will show how to apply high energy factorization in this context. It is known that in the double logarithmic limit in which the large logarithms in  $Q^2$  and  $1/x$  are resummed the collinear factorization and the high-energy factorization coincide. This limit provides a very accurate approximation to the data on inclusive  $F_2$  at small  $x$ . Based upon this observation we perform the double logarithmic limit of the leading-log( $1/x$ ) results. This allows us to express the cross section for the processes under consideration in terms of the conventional gluon density and in turn to obtain a parameter free prediction. Several properties of the result are studied in detail numerically and predictions for event rates are given. The azimuthal dependence which is obtained within our two-gluon model might be of special interest since a remarkable difference to the azimuthal dependence of the photon-gluon fusion process is found.

It has been argued that the process of diffractive heavy vector meson production might serve as a tool to constrain the gluon density since the square of this quantity enters the cross section. The same is true for diffractive  $q\bar{q}$ -production and this process could even be better suited for that purpose since ambiguities associated with the undetermined vector meson wave function are absent.

## 3.1 Inclusive Scattering at small $x$ : Collinear and High Energy Factorization

### 3.1.1 Collinear factorization

The well-established framework to study deep inelastic scattering or more general hard processes in perturbative QCD is the formalism of collinear factorization [7]. This formalism applies whenever there is a strong interaction process with one large momentum scale  $Q^2$  at which the coupling constant  $\alpha_s$  of QCD is small. Collinear factorization then allows a clean separation of the contribution of large (hard) scales, for which perturbation theory is applicable from the contribution of low (soft) scales which are determined by nonperturbative dynamics of QCD. This separation is made explicit by representing the cross section of the process as a convolution of a hard quark- or gluon-subprocess cross section with a universal probability distribution of finding a quark (gluon) in the hadron which enters the process. The master formula of collinear factorization for DIS processes with hard scale  $Q^2$  reads <sup>7</sup>

$$F(x, Q^2) = \sum_i \int_x^1 dz C_i(\alpha_s(Q^2), \frac{x}{z}, Q^2) f_i(z, Q^2) \quad (3.1)$$

In this expression the function  $C_i$  represents the hard subprocess cross section for an incoming parton of type  $i$ . These coefficient functions are calculable in perturbative QCD as a power series in  $\alpha_s$  and have been calculated for the important processes at least to next-to-leading order. The quantity  $f_i(z, Q^2)$  represents the probability to pick the parton of type  $i$  with longitudinal momentum fraction  $z$  and virtuality  $\leq Q^2$  out of the hadron. In the following we prefer the moment space representation of the factorization formula which unfolds the  $z$ -convolution

$$F(N, Q^2) = \sum_i C_i(\alpha_s(Q^2), N, Q^2) f_i(N, Q^2) \quad , \text{ with } F(N, Q^2) = \int_0^1 dx x^{N-1} F(x, Q^2) \quad (3.2)$$

The scale dependence of the parton distribution functions is governed by the renormalization group equations, the so-called DGLAP evolution equations [8], which read in the moment representation

$$\frac{d}{d \log Q^2} f_i(N, Q^2) = \sum_j \gamma_{ij}(\alpha_s(Q^2), N) f_j(N, Q^2) \quad (3.3)$$

The important quantity entering here is the anomalous dimension matrix  $\gamma_{ij}(N)$  which controls the scaling violations of the process. The scale dependence of the parton densities which follows from eq. (3.3) is <sup>8</sup>

$$f_k(N, Q^2) = f_k(N, Q_0^2) \left( \frac{Q^2}{Q_0^2} \right)^{\hat{\gamma}_k(\alpha_s, N)} \quad (3.4)$$

with  $\hat{\gamma}_k(\alpha_s, N)$  being the eigenvalues of the anomalous dimension matrix and the index  $k$  referring to the corresponding eigenvectors. The elements of the anomalous dimension matrix are also computable perturbatively as a power series in  $\alpha_s$  and are known explicitly up to  $\mathcal{O}(\alpha_s^2)$ . The nonperturbative contribution enters into the formalism as the initial condition of the coupled evolution equations (3.3) at a lower momentum scale  $Q_0^2$ . These input distributions have to be obtained from experimental data by means of global analysis. With coefficient functions and anomalous dimensions evaluated in leading order the above formalism can be shown to resum the leading logarithms in  $Q^2$  (the hard scale), i. e. all perturbative contributions of the form  $(\alpha_s \log(Q^2/Q_0^2))^n$  are taken into account. This is due to the fact that the evolution equations (3.3) resum logarithmic contributions (collinear logarithms) of an infinite number of Feynman diagrams. In a physical gauge these diagrams correspond to ladder diagrams with strong ordering of parton transverse momenta along the ladder.

If, for fixed  $Q^2$ , the variable  $x$  is decreased one approaches the Regge limit of DIS. Using the inversion formula for the moments of parton densities one notices that the leading contribution in the limit of small  $x$

<sup>7</sup>Here we have set the factorization scale  $\mu^2$  equal to the hard scale  $Q^2$  for simplicity.

<sup>8</sup>For simplicity the solution with fixed  $\alpha_s$  is given.

is determined through the part of the gluon anomalous dimension which is singular<sup>9</sup> at  $N = 0$ . This leads to the following behavior of the gluon distribution at small  $x$

$$xf_G(x, Q^2) = \sqrt{\frac{\pi}{4}} \left[ \frac{3\alpha_s}{\pi} \frac{\log Q^2/Q_0^2}{\log 1/x} \right]^{\frac{1}{4}} \exp \sqrt{4 \frac{N_c \alpha_s}{\pi} \log \frac{1}{x} \log \frac{Q^2}{Q_0^2}} \cdot \text{const.} \quad (3.5)$$

Rewritten in the variables  $\rho = \sqrt{\log(1/x)/\log(Q^2/Q_0^2)}$  and  $\sigma = \sqrt{\log(1/x) \cdot \log(Q^2/Q_0^2)}$  this behavior has been termed double asymptotic scaling [54, 55] and has been shown to be in good agreement with small- $x$  data from the HERA collider [55].

The presence of the singularity at  $N = 0$  in the gluon anomalous dimension is due to the fact that the diagrams which are resummed by the anomalous dimension do not only contain the collinear logarithm (in  $Q^2$ ) in each order of  $\alpha_s$  but also a logarithm in  $1/x$  (soft logarithm). In eq. (3.5) all contributions of the form  $(\alpha_s \log(Q^2/Q_0^2) \log 1/x)^n$  are summed, consequently the corresponding approximation is referred to as the double logarithmic approximation.

### 3.1.2 High energy factorization and the BFKL equation for $F_2$

Given the presence of the singularity at  $N = 0$  one may ask for the importance of higher order contributions to the anomalous dimension which also contain a singularity at  $N = 0$ . The presence of these singularities might spoil the convergence of the perturbative expansion of the anomalous dimension at small  $x$ . This is the reason why the BFKL equation was considered to describe inclusive deep inelastic scattering in the small- $x$  region. The BFKL equation effectively resums all singularities at  $N = 0$ , or, formulated in  $x$ -space, it sums the perturbative contributions of the form  $(\alpha_s \log 1/x)^n$ . Transformed to  $x$ -space the BFKL equation (3.4) in the forward direction has the form of an evolution equation<sup>10</sup> with the logarithm of  $x$  being the evolution parameter

$$-\frac{d}{d \log x} \mathcal{F}_G(x, \mathbf{k}) = \frac{N_c \alpha_s}{2\pi^2} \int d^2 \mathbf{k}' \left[ \frac{1}{(\mathbf{k} - \mathbf{k}')^2} - \delta^{(2)}(\mathbf{k} - \mathbf{k}') \int \frac{d^2 \mathbf{l}}{\mathbf{l}^2} \frac{\mathbf{k}^2}{[\mathbf{l}^2 + (\mathbf{l} - \mathbf{k})^2]} \right] \mathcal{F}_G(x, \mathbf{k}') \quad (3.6)$$

The function  $\mathcal{F}_G(z, \mathbf{k})$  has to be interpreted as the unintegrated (w. r. t. to  $\mathbf{k}$ ) gluon density. In order to obtain the hadronic cross section (the structure function in DIS) the unintegrated gluon density has to be convoluted with a  $\mathbf{k}$ -dependent coefficient function.

$$F(x, Q^2) = \int d^2 \mathbf{k} \int_x^1 \frac{dz}{z} \hat{C}(\alpha_s, z, \mathbf{k}, Q^2) \mathcal{F}_G(z, \mathbf{k}) \quad (3.7)$$

This equation constitutes the high-energy, or  $\mathbf{k}$ -factorization theorem [9]. It is a generalization of the collinear factorization theorem in eq. (3.1) which allows for the inclusion of leading-log( $1/x$ ) contributions in the structure function. The double logarithmic result is recovered by assuming dominance of the region  $\mathbf{k}^2 \ll Q^2$  in the  $\mathbf{k}$ -integration by means of which one obtains

$$F(x, Q^2) = \int_x^1 dz C(\alpha_s, \frac{x}{z}, Q^2) f_G(z, Q^2) \quad , \text{ with } z f_G(z, Q^2) = \int_{\mathbf{k}^2 \leq Q^2} d^2 \mathbf{k} \mathcal{F}_G(z, \mathbf{k}) \quad (3.8)$$

i. e. the collinear factorization.

The main theoretical problem which one faces when using the BFKL equation to predict the behavior of the structure function at small  $x$  is the fact that the BFKL evolution does not separate perturbative and nonperturbative scales. In the DGLAP evolution the partons transverse momenta  $\mathbf{k}^2$  increase starting from a lower but still perturbative scale  $Q_0^2$  to the hard scale  $Q^2$ , i. e. the whole evolution process takes place in the perturbative domain. In the BFKL evolution there is no  $\mathbf{k}^2$ -ordering, since the leading logarithms

<sup>9</sup>The effect of the singularity of the anomalous dimension matrix element  $\gamma$  at  $N = 0$  is of higher order in  $\log 1/x$  since the gluon does not couple directly to the photon.

<sup>10</sup>This equation is obtained from eq. (3.4) by inverse mellin transform w. r. t.  $N = \omega - 1$  and removing one propagator from the function  $\Phi_\omega(\mathbf{k})$ . The function that results from this operation is then termed  $\mathcal{F}_G$ .

in  $x$  are built up in the multi-Regge region of strongly ordered longitudinal momenta with the transverse momenta being disordered. To be more specific we recall that the rescaled (with  $\sqrt{\mathbf{k}^2}$ ) solution of the BFKL equation for asymptotically small values of  $x$  reads

$$\psi(z, \mathbf{k}) = \sqrt{\mathbf{k}^2} \mathcal{F}_G(x, \mathbf{k}) = \frac{a}{\sqrt{\Lambda_0^2}} \left( \frac{1}{x} \right)^{\frac{N_c \alpha_s}{\pi} 4 \log 2} \frac{1}{\sqrt{14 N_c \alpha_s \zeta(3) \log 1/x}} e^{-\pi \frac{\log \mathbf{k}^2 / \Lambda_0^2}{N_c \alpha_s 56 \zeta(3) \log 1/x}} \quad (3.9)$$

with  $a$  and  $\Lambda_0^2$  being related to the normalization and mass scale of an initial condition at large  $x$ . From this solution one concludes first that the BFKL equation predicts a power rise of the unintegrated gluon structure function at small  $x$  with the famous exponent  $4 \log 2 N_c \alpha_s / \pi$ , which has to be compared with the exponential rise in eq. (3.5). In the second place one realizes that the transverse momenta are distributed according to a normal distribution in  $\log \mathbf{k}^2$  with mean value  $\log \Lambda_0^2$  and width  $\sqrt{N_c \alpha_s / \pi \cdot 28 \zeta(3) \log 1/x}$ . This normal distribution is the outcome of the diffusion mechanism underlying the BFKL evolution. The partons perform a random walk in  $\log \mathbf{k}^2$ -space. As a result there will inevitably be a contribution of nonperturbative momentum scales to the evolution. In this region the perturbative BFKL results are of course not valid and the application of the evolution equation becomes inconsistent<sup>11</sup>.

In order to overcome this infrared consistency problem it was proposed [45, 58] to modify the infrared sector of the BFKL equation. Several *ad hoc*-prescriptions are described in the literature which were designed to exclude nonperturbative effects from the BFKL evolution, or, more ambitious, to model contributions from the nonperturbative region. The common feature of these prescriptions is that they introduce additional parameters the precise value of which is not under theoretical control. The results obtained with these modified BFKL evolution equations of course depend on the values chosen for the parameters. With this freedom one gets on the one hand more room to describe successfully the experimental data, but, on the other hand, the theoretical foundation of this description becomes somewhat obscure. The uncertainty associated with this model- and parameter-dependence is related to the magnitude of the contribution which the BFKL evolution receives from the infrared region in a given application. Therefore, a first estimate of the reliability of a BFKL prediction requires an investigation of this quantity.

To illustrate this we perform a calculation of the structure function  $F_2$  at small  $x$  based on the  $\mathbf{k}$ -factorization formalism with the unintegrated gluon density being calculated from the BFKL equation. We use eqs. (3.6) and (3.7) with the well-known coefficient function  $\hat{C}$  [59] representing the coupling of a gluon to the virtual photon. To solve the BFKL equation we have to specify an initial condition at a starting point  $x_0$ . In order to be consistent with the  $F_2$ -calculations for  $x > x_0$  we express the unintegrated gluon distribution at  $x_0$  as the logarithmic derivative of the gluon density (cf. eq. (3.8)) and take the latter from one of the current parameterizations in the literature. These parameterizations give the gluon density only above a boundary value  $Q_0^2$  and for our purposes we have to continue it down to  $Q^2 = 0$ . There is a freedom in this continuation and here we follow [45] by taking  $\mathcal{F}_G(x_0, \mathbf{k}) = c/(\mathbf{k}^2 + \mathbf{k}_a^2)$  for  $\mathbf{k}^2 \leq \mathbf{k}_0^2$  and  $\mathcal{F}_G(x_0, \mathbf{k}) = 1/(\mathbf{k}^2 + \mathbf{k}_a^2) \partial/(\partial \log \mathbf{k}^2) x_0 f_G(x_0, \mathbf{k}^2)$  for  $\mathbf{k}^2 \geq \mathbf{k}_0^2$  with  $c$  determined from continuity and  $\mathbf{k}_0^2, \mathbf{k}_a^2$  two momentum scales to be specified later. This ansatz guarantees consistency with the gluon density for large  $\mathbf{k}^2$  and respects the gauge invariance constraint  $\lim_{\mathbf{k}^2 \rightarrow \infty} \mathbf{k}^2 \mathcal{F}_G(x_0, \mathbf{k}) = 0$ . Now we solve the BFKL equation with a particular modification of the infrared region. We evolve the initial condition down from  $x = x_0$  but after each evolution step cut off the infrared tail of the distribution  $\mathcal{F}_G(x, \mathbf{k})$  with  $\mathbf{k}^2 \leq \mathbf{k}_0^2$  and replace it with the model function  $c/(\mathbf{k}^2 + \mathbf{k}_a^2)$  with  $c$  again determined by continuity and  $\mathbf{k}_0^2, \mathbf{k}_a^2$  as above.

In fig. 3.1 we show the results of this calculation for different values of  $Q^2$  where we have taken  $\mathbf{k}_0^2 = 1 \text{ GeV}^2$  and two different values for  $\mathbf{k}_a^2$ ,  $\mathbf{k}_a^2 = 1 \text{ GeV}^2$  and  $\mathbf{k}_a^2 = 2 \text{ GeV}^2$ . In addition the result is displayed which is obtained without the modification of the infrared region.

One recognizes that the normalization of the result depends strongly on the value of the infrared parameter  $\mathbf{k}_a^2$  whereas the slope is rather stable. This dependence becomes weaker with increasing  $Q^2$ . It should be remarked that these results were obtained from a calculation with fixed  $\alpha_s = \alpha_s(Q^2)$ . Corrections which introduce a scale dependence of  $\alpha_s$  are subleading in  $\log(1/x)$  and hence beyond the scope of the BFKL formalism. We choose here  $\alpha_s = \alpha_s(Q^2)$  because  $Q^2$  is the only hard scale in the present context. The value

<sup>11</sup>We do not discuss here the additional problem of violation of energy conservation due to the contribution of very large scales which has been studied in [56] and [57].

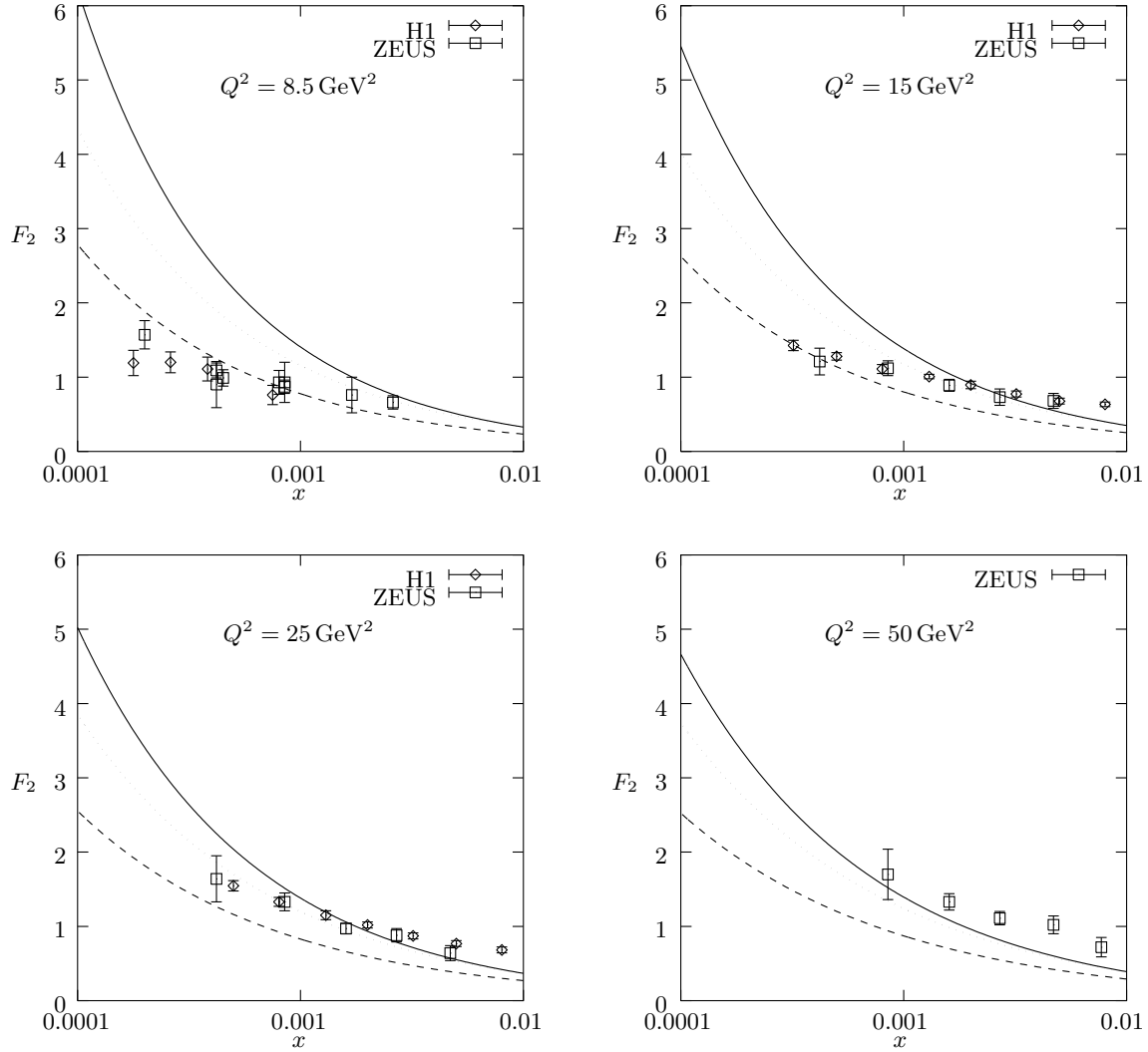


Figure 3.1: Results of the BFKL-based  $F_2$ -calculation for  $Q^2 = 8.5, 15, 25$  and  $50 \text{ GeV}^2$ . Displayed are the non-modified solution (solid line) and the modified solution with  $\mathbf{k}_a^2 = 1 \text{ GeV}^2$  (dotted line) and  $\mathbf{k}_a^2 = 2 \text{ GeV}^2$  (dashed line) in comparison with data from the H1 [10], ZEUS [11] and E665 [60] collaborations.

of  $\alpha_s$  enters in the global normalization and in the  $x$ -slope in the calculation. One sees that this produces a wrong scaling behaviour in  $Q^2$  for very small  $x$ . It was shown [45] that after introduction of running  $\alpha_s$  a more realistic  $Q^2$ -scaling is obtained. One should however keep in mind that all attempts to implement running  $\alpha_s$  into the BFKL evolution remain preliminary unless the analysis of the complete NLO-corrections (see [49] and references therein) is completed.

In the following we concentrate on the interpretation of the observed strong sensitivity of the results to the infrared parameters. To this end we notice [14] that we can represent  $F_2$  as

$$F_2(x, Q^2) = \sqrt{Q^2 \Lambda_0^2} \int_{-\infty}^{+\infty} d\xi \psi_1(Q^2, \xi; \frac{x}{z}) \psi_2(\Lambda_0^2, \xi, \frac{z}{x_0}) , \quad \xi = \log \frac{\mathbf{k}^2}{\mathbf{k}_0^2}, \quad x \leq z \leq x_0 \quad (3.10)$$

and calculate, for every  $z$  the function  $\psi_1 \psi_2$  which determines the transverse momentum distribution inside the BFKL evolution. For these distributions we calculate the mean value  $\langle \xi \rangle$  and the width  $\Delta(\xi) =$

$(\langle \xi^2 \rangle - \langle \xi \rangle^2)^{\frac{1}{2}}$ . In figs. 3.2, 3.3 we display for the extreme values of  $Q^2$  the results for  $\langle \xi \rangle$  and  $\xi_{\pm} = \langle \xi \rangle \pm \Delta(\xi)$  translated back to the variable  $\mathbf{k}^2$  as a function of  $z$ . Fig. 3.2 illustrates the basic diffusion

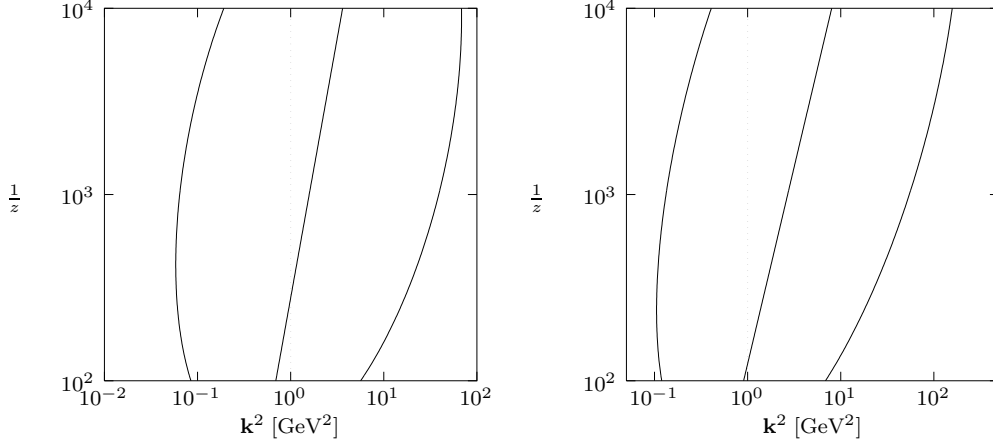


Figure 3.2: Mean value  $\langle \xi \rangle$  and width  $\Delta(\xi)$  of the distribution of  $\xi = \log \mathbf{k}^2 / \mathbf{k}_0^2$  inside the non-modified BFKL evolution for  $F_2$  with  $x = 10^{-4}$ ,  $x_0 = 10^{-2}$  and  $Q^2 = 8.5 \text{ GeV}^2$  (left diagram) resp.  $Q^2 = 50 \text{ GeV}^2$  (right diagram).

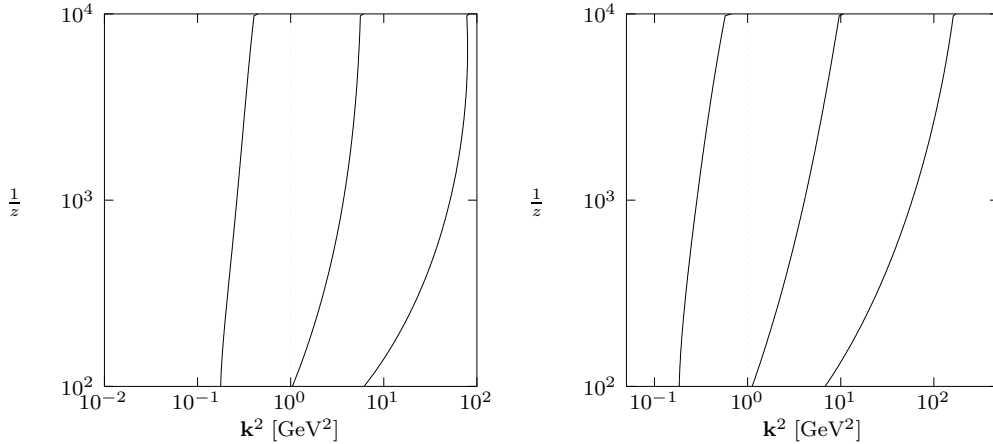


Figure 3.3: The same as in fig. 3.2 but with the BFKL evolution modified in the infrared region with  $\mathbf{k}_a^2 = 1 \text{ GeV}^2$ .

mechanism of the BFKL evolution. Starting from the initial distributions at  $z = x_0$  and  $z = x$  the transverse momenta diffuse into the infrared and ultraviolet region. Coming from below the center of diffusion drifts to the right since the hard scale at the upper end pulls the evolution out of the infrared domain which is to the left of the dotted vertical line. The contribution which comes from this nonperturbative region is clearly increasing with decreasing  $Q^2$ . Assuming as an approximation gaussian distributions for  $\psi_1$  and  $\psi_2$  the pattern of fig. 3.2 can be reproduced analytically. The evolution picture changes drastically if the modification of the infrared region is applied. Fig. 3.3 shows that in this case the diffusion into the infrared is cut off whereas there is still diffusion into the ultraviolet. Given that in the application to  $F_2$  the contribution from the infrared region is large as observed in fig. 3.2 it is clear that the result of the evolution is rather sensitive to the details of the infrared modifications. It is also easy to realize that this sensitivity becomes

stronger if  $Q^2$  is decreased in agreement with the behavior observed in fig. 3.1.

To summarize one can say that by using the BFKL equation and  $\mathbf{k}$ -factorization one obtains predictions for  $F_2$  at small  $x$  which are seriously affected by the way in which one treats the infrared region leading to a large theoretical uncertainty. In the preasymptotic region  $x \simeq 10^{-3}$  good agreement with data can be achieved but for smaller  $x$  the slope generated by the BFKL evolution becomes too steep. It should be recalled that we are calculating only the gluonic contribution to  $F_2$ . Agreement with data in the preasymptotic region requires of course the addition of a non-gluonic background contribution.

### 3.1.3 BFKL equation and transverse energy distribution

In the context of the  $F_2$ -measurements at HERA it has been advocated [61] to use the transverse energy flow in the final state as a window to examine the nature of the parton evolution in the deep inelastic scattering process. In particular one would expect an enhanced energy flow in the central rapidity region for a BFKL type of evolution compared to conventional evolution due to disordered transverse momenta. In order to study the transverse energy flow, the transverse energy weighted single parton inclusive cross section has been calculated in the BFKL formalism [61]. It should be remarked that the single parton inclusive cross section is not a well-defined quantity within the BFKL approximation since the collinear singularities present in the real and virtual corrections cancel only at the fully inclusive level. For the one-parton inclusive case an infrared finite result is obtained only after energy weighting. A more consistent definition of the transverse energy flow requires the analysis of associated distributions at small  $x$  based on the color coherence approach [62].

As a preparatory study we examine in the following the transverse energy distribution of the gluons which are exchanged in the  $t$ -channel in the BFKL evolution. From this one should obtain at least a qualitative impression of the energy distribution of the final state particles. We focus on the center of rapidity in the photon proton cms frame which is defined by the relation  $z = (x_B \cdot \mathbf{k}^2/Q^2)^{\frac{1}{2}}$ . For  $\mathbf{k}^2$  we take a mean value of the transverse momentum which can be read off from fig. 3.2. The results for the transverse energy distribution for  $Q^2 = 50 \text{ GeV}^2$  and three different values of  $x_B$  are shown in fig. 3.4.

On the left hand side the product distribution  $\psi_1(\xi)\psi_2(\xi)$  is shown as a function of  $\xi$ . On the right

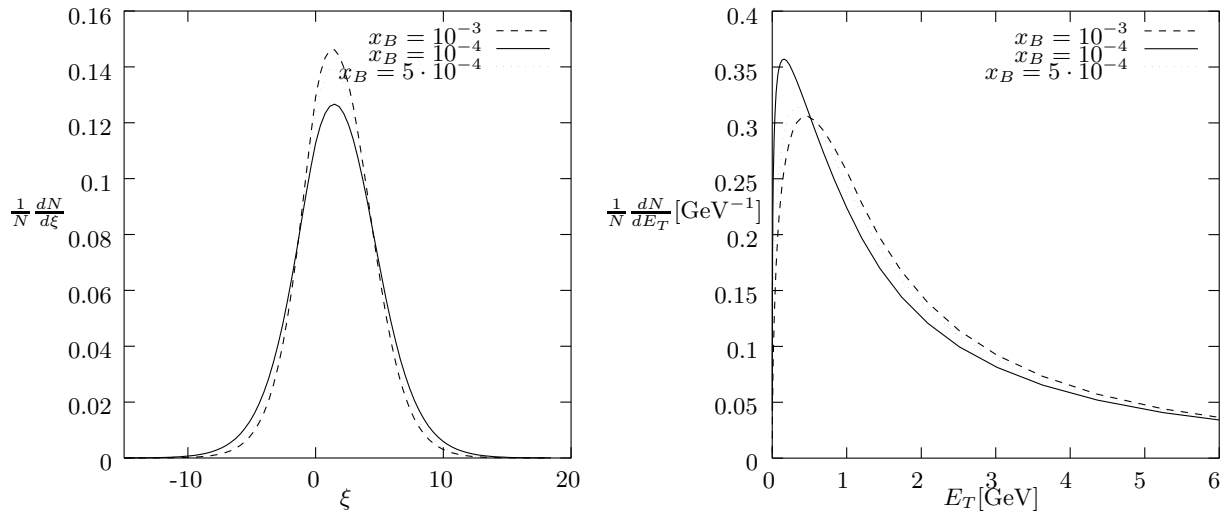


Figure 3.4: The  $\xi$ -distributions in the central rapidity region for different values of  $x_B$  and the corresponding transverse energy distributions.

hand side we display the transverse energy distribution calculated from the product distributions. The characteristic feature of the  $\xi$ -distributions is the increase of the width with increasing rapidity interval which is a manifestation of the diffusion mechanism. The width of these distributions is shown as a function of  $x_B$

for two values of  $Q^2$  on the left hand side of fig. 3.5. The increase of the width transforms into an increase of the mean transverse energy which is shown on the right hand side of fig. 3.5.

Based on the asymptotic solution (3.9) of the BFKL equation simple analytic estimates for the observables

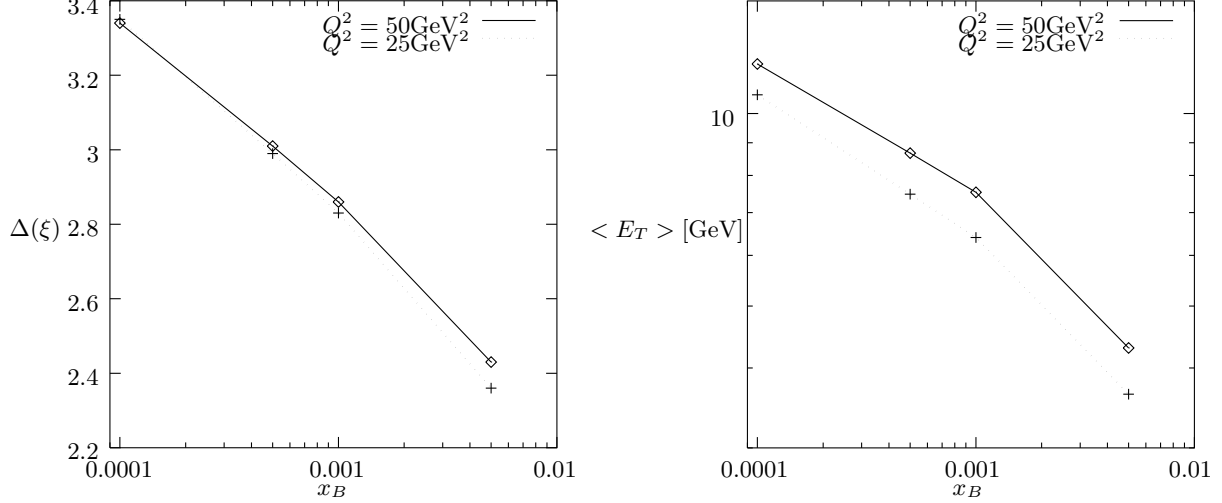


Figure 3.5: Width of the  $\xi$ -distributions and mean value of the  $E_T$  distributions for  $Q^2 = 25 \text{ GeV}^2$  and  $Q^2 = 50 \text{ GeV}^2$ .

studied above can be obtained. Characterizing the initial distributions  $\psi_i(\xi)$  at  $x_B$  and  $x_0$  by their mean value  $\langle \xi_i \rangle$  and width  $\delta_i(\xi)$  we find for the mean value of the product distribution in the central rapidity region

$$\xi = \frac{\langle \xi_1 \rangle (\delta_1(\xi) + \frac{1}{2} \log \frac{1}{x_B} \frac{\mathbf{k}^2}{Q^2}) + \langle \xi_2 \rangle (\delta_2(\xi) + \frac{1}{2} \log \frac{x_0^2}{x_B} \frac{Q^2}{\mathbf{k}^2})}{\delta_1(\xi) + \delta_2(\xi) + \frac{1}{2} \log \frac{1}{x_B} \frac{\mathbf{k}^2}{Q^2} + \frac{1}{2} \log \frac{x_0^2}{x_B} \frac{Q^2}{\mathbf{k}^2}} \quad (3.11)$$

For small  $x_B$  it becomes constant as observed in fig. 3.4. For the width we find

$$\Delta(\xi) = \left[ \frac{N_c \alpha_s}{\pi} 28 \zeta(3) \frac{(\delta_1(\xi) + \frac{1}{2} \log \frac{1}{x_B} \frac{\mathbf{k}^2}{Q^2})(\delta_2(\xi) + \frac{1}{2} \log \frac{x_0^2}{x_B} \frac{Q^2}{\mathbf{k}^2})}{\delta_1(\xi) + \delta_2(\xi) + \frac{1}{2} \log \frac{1}{x_B} \frac{\mathbf{k}^2}{Q^2} + \frac{1}{2} \log \frac{x_0^2}{x_B} \frac{Q^2}{\mathbf{k}^2}} \right]^{\frac{1}{2}} \quad (3.12)$$

The width becomes independent of the details of the boundary conditions for small  $x_B$  and thus represents a characteristic BFKL signal. Asymptotically it rises with the square root of the rapidity. The latter can thus be interpreted as the time coordinate of the gluon's random walk. The analytic prediction for the asymptotic mean transverse energy  $\langle E_T \rangle$  is

$$\langle E_T \rangle = \exp \left[ \frac{1}{8} \Delta^2(\xi) + \frac{1}{2} \langle \xi \rangle \right] \quad (3.13)$$

Since  $\langle \xi_1 \rangle$  increases with increasing  $Q^2$  the mean  $E_T$  increases with  $Q^2$  in accordance with the behavior observed in fig. 3.5.

To conclude, we want to stress that it is the square root increase of the width of the  $\log \mathbf{k}^2$ -distribution with rapidity which is the fundamental manifestation of the diffusion mechanism underlying the BFKL equation. An experimental study of this observable might provide valuable insight into the parton evolution at small  $x$ . The problem with this quantity, however, could be its large sensitivity to hadronization effects which wash out the characteristics of the parton level distributions.



### 3.2 Diffractive Production of Vector Mesons at large $t$

In the preceeding section it was shown that the diffusion of gluon momenta in the BFKL evolution leads to a large theoretical uncertainty associated with the contribution of nonperturbative momentum scales. This is not the case if there is a large momentum scale present all along the ladder which keeps the diffusion in the perturbative domain. An immediate example for such a large scale is the momentum transfer  $-t$ . The authors of [16, 46] introduced a reaction in which colorless exchange at large momentum transfer applies. They studied the process  $\gamma^*(Q) + P(p) \rightarrow V(Q+q) + X(p-q)$  where  $V$  is a vector meson with mass  $M_V$ , e. g. a  $J/\Psi$ , which is produced with large momentum transfer  $t = q^2$  and  $X$  is a final state resulting from the dissociation of the proton. If the hadronic energy  $W^2 = (p+Q)^2$  becomes large logarithmic corrections become important which are resummed by the BFKL amplitude (represented by the blob in fig. 3.6).

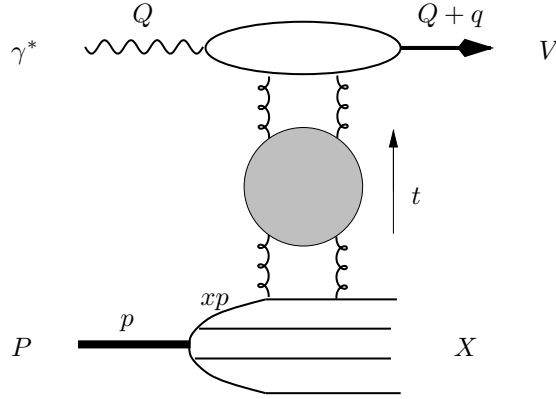


Figure 3.6: Graphical representation of the process of diffractive vector meson production in DIS.

#### 3.2.1 The result for the cross section

The cross section for the process can be written in the following factorized form [16]

$$x \frac{d\sigma^{\gamma^* P}}{dx dt} = \frac{d\sigma^{\gamma^* q}}{dt}(x, t) \left[ \sum_f (x q_f(x, -t) + x \bar{q}_f(x, -t)) + \frac{81}{16} x G(x, -t) \right] \quad (3.14)$$

This factorization means that the photon scatters off a single parton with longitudinal momentum  $xp$  and virtuality  $\leq t$ . It is expected to hold as long as  $-t$  is larger than the inverse size  $Q_0^2$  of the proton.

The photon-parton subprocess energy is  $s = xW^2$  and the subprocess cross section reads

$$\frac{d\sigma^{\gamma^* q}}{dt}(x, t) = \pi \left( \frac{4}{9} \right)^2 \frac{\alpha_s^4}{t^4} \left| \int \frac{d\omega}{2\pi i} \left( \frac{s}{Q^2 + M_V^2 - t} \right)^\omega \Phi_\omega(\mathbf{q}^2) \right|^2 \quad ; \quad \mathbf{q}^2 = -t \quad (3.15)$$

with  $\Phi_\omega$  being given as the convolution of the BFKL amplitude with the impact factors of the incoming particles

$$\Phi_\omega(\mathbf{q}^2) = |\mathbf{q}|^4 \int \frac{d^2 \mathbf{k}}{(2\pi)^3} \frac{d^2 \mathbf{k}'}{(2\pi)^3} \Phi_\omega(\mathbf{k}, \mathbf{k}'; \mathbf{q}) \phi_V(\mathbf{k}, \mathbf{q}) \phi_q(\mathbf{k}', \mathbf{q}) \quad (3.16)$$

Here  $\phi_V$  is the impact factor for the photon producing a vector meson and  $\phi_q$  is the impact factor for the incoming parton. The photon-vector meson transition can be described in terms of a non-relativistic form factor [63]

$$\phi_V(\mathbf{k}, \mathbf{q}) = -\frac{C}{2} \left[ \frac{1}{\Delta^2 + (\mathbf{k} - \mathbf{q}/2)^2} - \frac{1}{\Delta^2 + \mathbf{q}^2/4} \right] \quad (3.17)$$

where  $4\Delta^2 = Q^2 + M_V^2$  and the coefficient is determined through the electromagnetic width of the vector meson

$$\mathcal{C}^2 = 3\Gamma_V^{ee} \frac{M_V^3}{\alpha_{\text{em}}} \quad (3.18)$$

This transition is helicity conserving and it is given here for transverse polarization of the photon. For the longitudinal polarization one has to multiply the right hand side of eq. (3.15) with  $Q^2/M_V^2$ .

The parton formfactor deserves more discussion. An incoming parton is not a colorless state and hence eq. 3.16 seems to be in contradiction with the results of section 2.1. . The description in terms of a parton formfactor constitutes an effective prescription, valid for  $-t \gg Q_0^2$ , which requires a particular modification of the BFKL amplitude  $\phi_\omega(\mathbf{k}, \mathbf{k}'; \mathbf{q})$ . For the conformal eigenfunction  $E^{(\nu,0)}$  which couples to the parton line the Mueller-Tang subtraction [64] has to be performed

$$E^{(\nu,0)}(\rho_1, \rho_2) = \left( \frac{\rho_{12}^2}{\rho_1^2 \rho_2^2} \right)^{\frac{1}{2}-i\nu} \longrightarrow E_{MT}^{(\nu,0)}(\rho_1, \rho_2) = E^{(\nu,0)}(\rho_1, \rho_2) - \left( \frac{1}{\rho_1^2} \right)^{\frac{1}{2}-i\nu} - \left( \frac{1}{\rho_2^2} \right)^{\frac{1}{2}-i\nu} \quad (3.19)$$

This modification subtracts  $\delta$ -function like contributions from the conformal eigenfunction which are not present in perturbation theory. These  $\delta$ -function terms have implicitly been added to the BFKL equation to ensure conformal invariance. They are not present in the physical amplitude since they give zero after convolution with color neutral impact factors. In the effective prescription in which the BFKL pomeron couples to a colored state, however, they have to be subtracted. It should be emphasized here that the Mueller-Tang prescription does not apply in general [47]. We postpone a more detailed discussion to the following section. With the above prescription the quark formfactor becomes unity and insertion of the general solution of the nonforward BFKL equation with the Mueller-Tang subtraction performed gives

$$\Phi_\omega(\mathbf{q}^2) = |\mathbf{q}|^4 \int_{-\infty}^{+\infty} \frac{d\nu}{2\pi} \frac{\nu^2}{(\nu^2 + 1/4)^2} \frac{1}{\omega - \chi(\nu)} \int \frac{d^2\mathbf{k}}{(2\pi)^3} E^{(\nu,0)}(\mathbf{k}, \mathbf{q} - \mathbf{k}) \phi_V(\mathbf{k}, \mathbf{q}) \int \frac{d^2\mathbf{k}'}{(2\pi)^3} E_{MT}^{(\nu,0)*}(\mathbf{k}', \mathbf{q} - \mathbf{k}') \quad (3.20)$$

We consider only conformal spin  $n = 0$  since this gives the dominant contribution in the high-energy limit. The integration of the Mueller-Tang eigenfunction gives the simple result

$$\int \frac{d^2\mathbf{k}'}{(2\pi)^3} \int d^2\rho_1 d^2\rho_2 e^{i\mathbf{k}'\rho_1 + i(\mathbf{q}-\mathbf{k}')\rho_2} \left[ \left( \frac{\rho_{12}^2}{\rho_1^2 \rho_2^2} \right)^{\frac{1}{2}+i\nu} - \left( \frac{1}{\rho_1^2} \right)^{\frac{1}{2}+i\nu} - \left( \frac{1}{\rho_2^2} \right)^{\frac{1}{2}+i\nu} \right] \quad (3.21)$$

$$= -2 \, 4^{-i\nu} (\mathbf{q}^2)^{-\frac{1}{2}+i\nu} \frac{\Gamma(\frac{1}{2} - i\nu)}{\Gamma(\frac{1}{2} + i\nu)} \quad (3.22)$$

The evaluation of the  $\mathbf{k}$ -integration is more complicated. Instead of using the explicit representation for the momentum space eigenfunctions we prefer to work with the mixed representation (3.50). The  $\mathbf{k}$ -integration then gives a modified Bessel-function

$$\int \frac{d^2\mathbf{k}}{(2\pi)^3} \phi_V(\mathbf{k}, \mathbf{q}) e^{i\mathbf{k}\rho} = -\frac{\mathcal{C}}{2} \frac{1}{(2\pi)^2} \left[ K_0(|\rho|\Delta) e^{\frac{i}{2}\mathbf{q}\rho} - 2\pi \delta^{(2)}(\rho) \frac{1}{\Delta^2 + \mathbf{q}^2/4} \right] \quad (3.23)$$

If we assume  $\text{Re}(i\nu) < 1/2$  the only non-zero contribution comes from the first term and for the  $\mathbf{k}$ -integral in eq. (3.20) we find

$$-\frac{\mathcal{C}}{2} \frac{1}{2\pi} 4^{i\nu} \frac{(\mathbf{q}^2)^{-\frac{3}{2}-i\nu}}{\Gamma^2(\frac{1}{2}-i\nu)} \int_0^\infty d\xi \xi^2 K_0(\xi \frac{\Delta}{|\mathbf{q}|}) \int_0^1 dx [x(1-x)]^{-\frac{1}{2}} J_0(\xi |x - \frac{1}{2}|) K_{2i\nu}(\xi \sqrt{x(1-x)}) \quad (3.24)$$

where the the integral over the angle of  $\rho = \rho_{12}$  was performed and the dimensionless variable  $\xi$  was introduced. The next step is the insertion of the following representation of a  $\delta$ -function

$$\delta(\xi - \xi') = \int_{-\infty}^{+\infty} \frac{d\lambda}{\pi} \frac{1}{\xi} \left( \frac{\xi'}{\xi} \right)^{2i\lambda} \quad (3.25)$$

which allows to separate the  $K_0$  function from the  $x$ -dependent factors

$$-\frac{\mathcal{C}}{2} \frac{1}{2\pi} 4^{i\nu} \frac{(\mathbf{q}^2)^{-\frac{3}{2}-i\nu}}{\Gamma^2(\frac{1}{2}-i\nu)} \int \frac{d\lambda}{\pi} \left( \frac{|\mathbf{q}|}{\Delta} \right)^{3+2i\lambda} \int_0^\infty d\xi' \xi'^{2+2i\lambda} K_0(\xi') \cdot \int_0^\infty d\xi \xi^{-1-2i\lambda} \int_0^1 dx [x(1-x)]^{-\frac{1}{2}} J_0(\xi|x-\frac{1}{2}|) K_{2i\nu}(\xi\sqrt{x(1-x)}) \quad (3.26)$$

$$= -\frac{\mathcal{C}}{2} \frac{1}{2\pi} 4^{i\nu} \frac{(\mathbf{q}^2)^{-\frac{3}{2}-i\nu}}{\Gamma^2(\frac{1}{2}-i\nu)} \int \frac{d\lambda}{\pi} \left( \frac{|\mathbf{q}|}{\Delta} \right)^{3+2i\lambda} 2^{1+2i\lambda} \Gamma^2(\frac{3}{2}+i\lambda) \cdot \int_0^\infty d\xi \xi^{-1-2i\lambda} \int_0^1 dx [x(1-x)]^{-\frac{1}{2}} J_0(\xi|x-\frac{1}{2}|) K_{2i\nu}(\xi\sqrt{x(1-x)}) \quad (3.27)$$

Here the contour of the  $\lambda$ -integration has been shifted in the complex plane such that the condition  $-3/2 < \text{Re}(i\lambda) < \pm \text{Re}(i\nu)$  is fulfilled. Now the remaining  $\xi$  and  $x$  integrations can be performed. The  $\xi$ -integral gives

$$2^{-2-2i\lambda} \Gamma(-i\lambda+i\nu) \Gamma(-i\lambda-i\nu) \int_0^1 dx [x(1-x)]^{-\frac{1}{2}+i\lambda} {}_2F_1(-i\lambda-i\nu, -i\lambda+i\nu, 1; -\frac{(1-2x)^2}{4x(1-x)}) \quad (3.28)$$

After changing the integration variable to  $z = (1-2x)^2$  and using an analytic continuation of the hypergeometric function the remaining integral can be performed to give

$$4^{-1-2i\lambda} \Gamma(-i\lambda+i\nu) \Gamma(-i\lambda-i\nu) \frac{\Gamma(\frac{1}{2})\Gamma(\frac{1}{2}-i\nu)}{\Gamma(1-i\nu)} {}_3F_2(-i\lambda-i\nu, 1+i\lambda-i\nu, \frac{1}{2}; 1, 1-i\nu; 1) \quad (3.29)$$

$$= 4^{-1-2i\lambda} \pi \frac{\Gamma(\frac{1}{2}+i\nu)\Gamma(\frac{1}{2}-i\nu)\Gamma(-i\lambda+i\nu)\Gamma(-i\lambda-i\nu)}{\Gamma(\frac{1}{2}-\frac{1}{2}(i\lambda+i\nu))\Gamma(\frac{1}{2}-\frac{1}{2}(i\lambda-i\nu))\Gamma(1+\frac{1}{2}(i\lambda+i\nu))\Gamma(1+\frac{1}{2}(i\lambda-i\nu))} \quad (3.30)$$

where the last identity follows from Watson's theorem [53]. Collecting everything together we arrive at the following expression for the partial wave amplitude

$$\Phi_\omega(\mathbf{q}) = 4\pi\mathcal{C} \int_{-\infty}^{+\infty} \frac{d\nu}{2\pi} \frac{\nu^2}{(\nu^2+1/4)^2} \frac{1}{\omega-\chi(\nu)} \cdot \int \frac{d\lambda}{\pi} \left( \frac{\mathbf{q}^2}{4\Delta^2} \right)^{\frac{3}{2}+i\lambda} \frac{\Gamma^2(\frac{3}{2}+i\lambda)\Gamma(-i\lambda+i\nu)\Gamma(-i\lambda-i\nu)}{\Gamma(\frac{1}{2}-\frac{1}{2}(i\lambda+i\nu))\Gamma(\frac{1}{2}-\frac{1}{2}(i\lambda-i\nu))\Gamma(1+\frac{1}{2}(i\lambda+i\nu))\Gamma(1+\frac{1}{2}(i\lambda-i\nu))} \quad (3.31)$$

### 3.2.2 Comparison of the exact formula with asymptotic expressions

The remaining contour integral  $I(\nu)$  (the second line in eq. (3.31) over  $\lambda$  can either be performed numerically or evaluated as a power series in the ratio  $|\mathbf{q}|/(2\Delta)$  (resp.  $2\Delta/|\mathbf{q}|$ ). In the limit of large momentum transfer, when  $|\mathbf{q}|/(2\Delta) \gg 1$ , the dominant contribution is obtained by shifting the contour past the singularity at  $i\lambda = -3/2$ . The residue of the double pole leads to the leading behavior

$$I(\nu) = 8 \frac{\Gamma(\frac{1}{2}+i\nu)\Gamma(\frac{1}{2}-i\nu)}{\Gamma^2(\frac{1}{4}+\frac{1}{2}i\nu)\Gamma^2(\frac{1}{4}-\frac{1}{2}i\nu)} \left[ \log \frac{\mathbf{q}^2}{4\Delta^2} - 2\gamma_E - 2\text{Re} \psi(\frac{1}{2}+i\nu) \right] \quad (3.32)$$

In the opposite limit we have two poles at  $i\lambda = \pm i\nu$  which contribute equally as long as the imaginary part of  $\nu$  is small which is true in the high-energy limit. For  $|\mathbf{q}|/(2\Delta) \ll 1$  we thus have

$$I(\nu) = \frac{4}{\sqrt{\pi}} \left( \frac{\mathbf{q}^2}{4\Delta^2} \right)^{\frac{3}{2}} \text{Re} \left[ \left( \frac{\mathbf{q}^2}{4\Delta^2} \right)^{i\nu} \frac{\Gamma^2(\frac{3}{2}+i\nu)\Gamma(-2i\nu)}{\Gamma(\frac{1}{2}-i\nu)\Gamma(1+i\nu)} \right] \quad (3.33)$$

In fig. 3.7 the result of a numerical calculation of  $I(\nu)$  is compared with the asymptotic formulas eqs. (3.32)

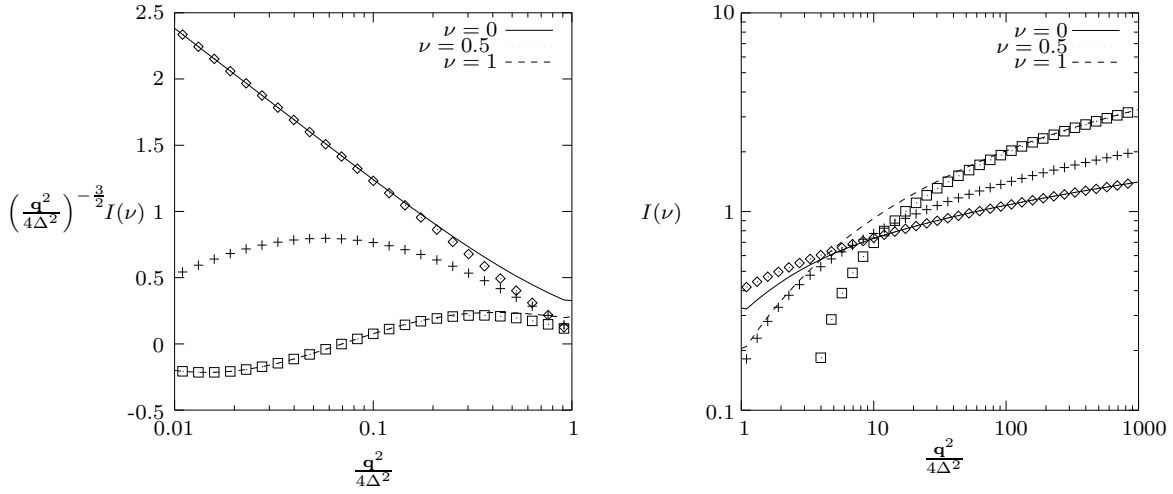


Figure 3.7: Comparison of a numerical evaluation of  $I(\nu)$  (lines) with the asymptotic analytic predictions (symbols) for different values of  $\nu$ .

and (3.33) for different values of  $\nu$ .

It remains to find the energy dependence of the cross section by performing the  $\nu$  and  $\omega$  integration. The  $\omega$  integration leads to the familiar exponential factor  $\exp[y\chi(\nu)]$  ( $y = \log s/(Q^2 + M_V^2 - t)$ ) and we end with

$$\frac{d\sigma^{\gamma^* q}}{dt}(x, t) = \pi \left(\frac{4}{9}\right)^2 \frac{\alpha_s^4}{t^4} \left| 4\pi C \int \frac{d\nu}{2\pi} \frac{\nu^2}{(\nu^2 + 1/4)^2} \frac{1}{\omega - \chi(\nu)} I(\nu) \right|^2 \quad (3.34)$$

where  $I(\nu)$  is given by the second line in eq. (3.31). Analytic results can again be obtained in certain kinematical limits. First we conclude from eq. (3.32) that for large  $|\mathbf{q}|/(2\Delta)$  the  $|\mathbf{q}|$  and the  $y$  dependence factorize. For large  $y$  the  $\nu$  integral is then dominated by the exponential  $\exp[y \cdot \chi(\nu)]$  and the asymptotic behavior is obtained by expansion around the saddle point which is located at  $\nu = 0$

$$\chi(\nu) = \frac{N_c \alpha_s}{\pi} [4 \log 2 - 28\zeta(3) \nu^2] + O(\nu^4) \quad (3.35)$$

The saddle point approximation then gives the following result in the limit of  $y \gg 1$  for fixed  $|\mathbf{q}|/(2\Delta) \gg 1$

$$\frac{d\sigma^{\gamma^* q}}{dt}(x, t) = \pi \left(\frac{4}{9}\right)^2 \frac{\alpha_s^4}{t^4} \left| C 128 \frac{\pi^3}{\Gamma^4(1/4)} \left[ \log \left( \frac{|\mathbf{q}|^2}{4\Delta^2} \right) + 4 \log 2 \right] \frac{e^{\frac{N_c \alpha_s}{\pi} 4 \log 2 \cdot y}}{[N_c \alpha_s 14 \zeta(3) y]^{\frac{3}{2}}} \right|^2 \quad (3.36)$$

Note the  $y^{\frac{3}{2}}$  in the denominator which has to be compared with the  $(\log 1/x)^{\frac{1}{2}}$  in the denominator of eq. (3.9). This difference is a manifestation of the different types of leading  $\omega$ -plane singularities of the  $t = 0$  and  $t \neq 0$  solutions of the BFKL equation.

For the case  $|\mathbf{q}|/(2\Delta) \ll 1$  the analysis is more complicated since we have from eq. (3.33) an additional factor  $[|\mathbf{q}|/(2\Delta)]^{2i\nu}$  in the  $\nu$  integral which leads to a correlation between the  $|\mathbf{q}|$  and the  $y$  dependence. Now we have to find the saddle point of the function  $y \cdot \chi(\nu) \pm i\nu \log |\mathbf{q}|^2/(4\Delta^2)$ . If we assume  $y \gg \log(4\Delta^2)/|\mathbf{q}|^2$  the saddle point is found at  $\nu = \pm i \log |\mathbf{q}|^2/(4\Delta^2) \cdot 1/(y |\chi''(0)|)$  and the corresponding result for the cross section reads

$$\frac{d\sigma^{\gamma^* q}}{dt}(x, t) = \pi \left(\frac{4}{9}\right)^2 \frac{\alpha_s^4}{t^4} \left| C 16\pi^2 \left( \frac{|\mathbf{q}|^2}{4\Delta^2} \right)^{\frac{3}{2}} (-2 + 3 \log 2) \frac{e^{\frac{N_c \alpha_s}{\pi} 4 \log 2 \cdot y}}{[N_c \alpha_s 14 \zeta(3) y]^{\frac{3}{2}}} e^{-\pi \frac{\log^2 \frac{|\mathbf{q}|^2}{4\Delta^2}}{N_c \alpha_s 56 \zeta(3) y}} \right|^2 \quad (3.37)$$

The last exponential factor induces a (rather weak) correlation between  $y$  and  $|\mathbf{q}|$ , i. e. the cms energy and the momentum transfer of the process. The above approximation can be valid only in a limited range. In the

formal limit of  $y \rightarrow \infty$  one has to perform the integrations over  $\lambda$  and  $\nu$  in reverse order. Integrating over  $\nu$  first one obtains the saddle point at  $\nu = 0$  and evaluating the integral in the corresponding approximation one finds that the singularity structure of the integrand of the  $\lambda$  integration has changed. Instead of two separated poles at  $\lambda = \pm\nu$  one double pole at  $\lambda = 0$  is found. In the case  $|\mathbf{q}|/(2\Delta) \ll 1$  the residue of this pole dominates and one gets the result

$$\frac{d\sigma^{\gamma^* q}}{dt}(x, t) = \pi \left( \frac{4}{9} \right)^2 \frac{\alpha_s^4}{t^4} \left| C 16\pi^2 \left( \frac{|\mathbf{q}|^2}{4\Delta^2} \right)^{\frac{3}{2}} \left( 3 \log 2 - 2 - \frac{1}{2} \log \frac{|\mathbf{q}|^2}{4\Delta^2} \right) \frac{e^{y \frac{N_c \alpha_s}{\pi} 4 \log 2}}{[N_c \alpha_s 14 \zeta(3) y]^{\frac{3}{2}}} \right|^2 \quad (3.38)$$

In this limit the  $y$  and  $|\mathbf{q}|$  dependence again factorize, i. e. there is no energy-momentum transfer correlation. The last interesting case to be studied is the limit of small momentum transfer at fixed  $y$ , i. e. we start from the approximation eq. (3.33) and assume  $\log(4\Delta^2)/|\mathbf{q}|^2 \gg y$ . The saddle point of the  $\nu$  integration is then found at  $i\nu = \pm 1/2 \mp [N_c \alpha_s / \pi \cdot y \log^{-1}(4\Delta^2)/|\mathbf{q}|^2]^{\frac{1}{2}}$  and the cross section is expressed through the amplitude in the double-leading-log limit

$$\frac{d\sigma^{\gamma^* q}}{dt}(x, t) = \pi \left( \frac{4}{9} \right)^2 \frac{\alpha_s^4}{t^4} \left| C \frac{2}{\sqrt{\pi}} \left( \frac{|\mathbf{q}|^2}{4\Delta^2} \right)^2 \frac{e^{\sqrt{4 \frac{N_c \alpha_s}{\pi} y \log \frac{4\Delta^2}{|\mathbf{q}|^2}}} \log \frac{4\Delta^2}{|\mathbf{q}|^2}}{[N_c \alpha_s / \pi y \log 4\Delta^2 / |\mathbf{q}|^2]^{\frac{3}{4}}} \right|^2 \quad (3.39)$$

In this expression  $|\mathbf{q}|^2$  no longer has the meaning of the momentum transfer. In the limit which is considered here  $|\mathbf{q}|$  can be neglected along the gluon ladder and the result for the amplitude becomes identical to the  $t = 0$  result for the gluon density in the double logarithmic (DL) limit with the upper large scale  $4\Delta^2$  and the virtuality of the incoming parton being of the order of  $t$ . Thus  $|\mathbf{q}|^2$  becomes the lower scale of the gluon evolution and it is clear that the amplitude diverges in the formal limit  $|\mathbf{q}| \rightarrow 0$  since we are considering a colored initial state. To obtain a finite  $t = 0$  cross section one has to go beyond the simple factorization formula (3.14) and has to couple the two gluon ladder to the proton in a gauge invariant way. An example for such a coupling will be presented and discussed in the next section. The above expression gives a higher twist contribution to DIS since it scales as  $1/Q^8$ . The accuracy of the large  $y$  approximations can be read

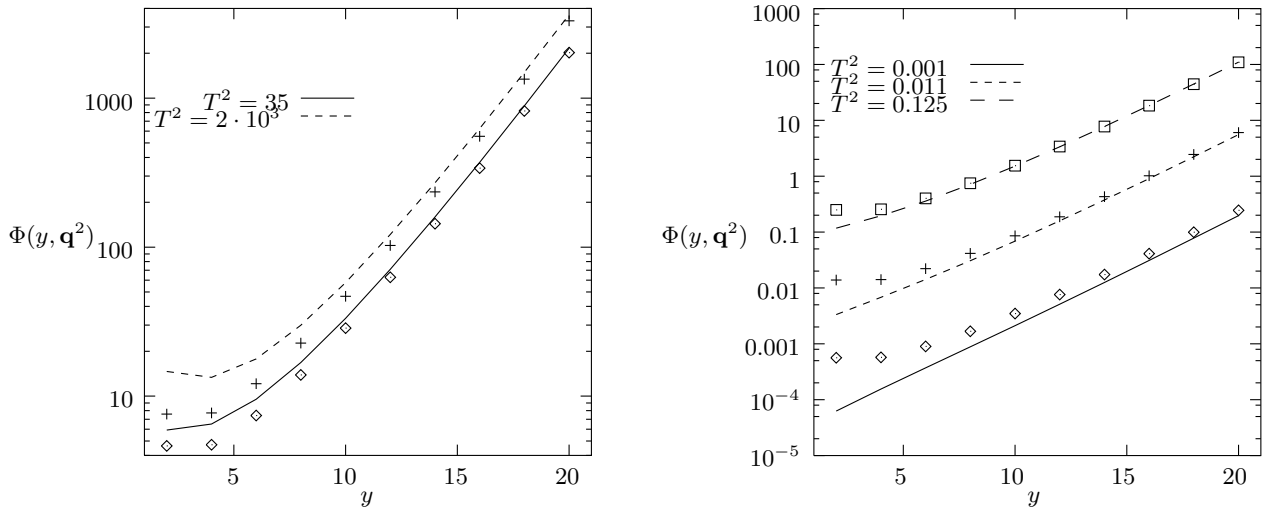


Figure 3.8: Comparison of the analytic results (symbols) contained in eq. (3.36) (left hand side) and eq. (3.37) (right hand side) with the exact numerical evaluation (lines) of  $\Phi(y, \mathbf{q}^2)$  based on eq. (3.31) for different value of  $T^2 = |\mathbf{q}|^2/(4\Delta^2)$ .

off from fig. 3.8. We display the inverse Mellin transformed partial wave amplitude  $\Phi(y, \mathbf{q}^2)$  as a function

of  $y$  for different values of  $|\mathbf{q}|/(2\Delta)$  and compare with the analytic results eqs. (3.36) and (3.38). One finds very good agreement for  $y \gtrsim 10$ . From the right hand figure one can conclude that the approximation contained in eq. (3.37) is rather bad in the kinematic range considered here. This approximation misses the  $\log |\mathbf{q}|/(2\Delta)$  contribution which is very important since  $3 \log 2 - 2 \simeq 0.079$  is a very small coefficient. Hence this approximation largely underestimates the true result. In fig. 3.9 we compare the approximations

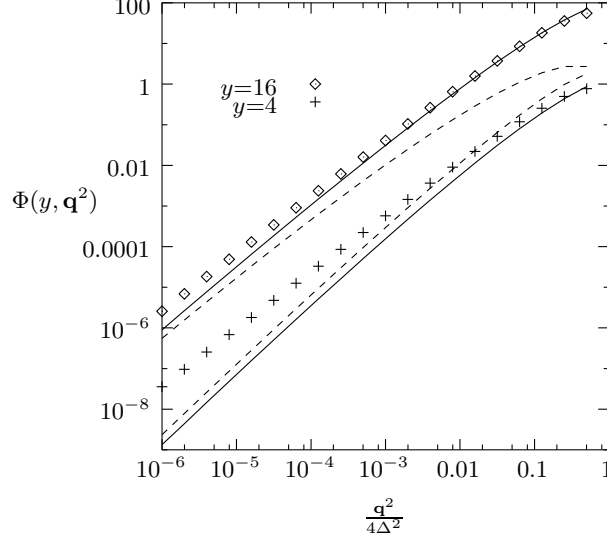


Figure 3.9: Comparison of the  $|\mathbf{q}|$ -dependence of the analytical results in eq. (3.38) (symbols) and eq. (3.39) (dashed line) with the numerical result (solid line).

contained in eqs. (3.38) and (3.39) with the exact numerical result. One sees that for very small  $|\mathbf{q}|/(2\Delta)$  the double logarithmic approximation indeed becomes valid, whereas in the range of not so small  $|\mathbf{q}|/(2\Delta)$  the BFKL type approximation is better, especially for large  $y$ .

### 3.2.3 The slope of the BFKL amplitude

The fact that for very small  $|\mathbf{q}|/(2\Delta)$  the double logarithmic approximation provides a good description is remarkable since it implies a correlation of the momentum transfer and the energy. Such a behavior is usually related to the slope of the Regge trajectory which is exchanged in the process. The slope  $\alpha'$  is defined as the coefficient of the term linear in  $t$  in the small- $t$  expansion of the trajectory function  $\alpha(t) = \alpha_0 + \alpha' \cdot t$ . Assuming dominance of this trajectory the amplitude behaves as  $(s/s_0)^{\alpha(t)} = (s/s_0)^{\alpha_0} \exp(\alpha' y t)$  ( $y = \log s/s_0$ ) and  $\alpha'$  determines the shrinkage of the diffraction peak, i. e. the increase of the slope of the  $t$ -dependence with increasing energy. Using the above expression the slope <sup>12</sup>  $\delta$  of the diffraction peak equals

$$\delta = \alpha' \log s/s_0 + \delta_0 \quad (3.40)$$

where  $\delta_0$  is determined through the  $t$ -dependent residue function. Due to conformal invariance the BFKL-singularity is a fixed ( $t$ -independent) cut and *prima facie* there is no shrinkage. An effective slope is found if the conformal invariance is broken by introducing running  $\alpha_s$  and additional scale parameters to modify the infrared region as discussed in [65] and [66]. In our approach conformal symmetry is maintained but there are scale parameters which enter through the convolution with the impact factors of the scattered particles. The correlation with energy is mediated through the  $\nu$  integration. For large energy the saddle point of this integration becomes constant and the  $s$  and  $t$  dependence factorize as in eq. (3.38), i. e. there is indeed no

<sup>12</sup>The term 'slope' appears here with two different meanings. On the one hand we have the slope parameter  $\alpha'$  of the Regge trajectory function. The slope of the diffraction peak on the one hand is a measure for the steepness of the decrease of the diffractive cross section as a function of  $t$  in the small- $t$  region.

shrinkage. In the subasymptotic region the saddle point is a function of  $s$  and  $t$  and the behavior of eq. (3.39) is found which implies an effective slope. Using the general formulae given above we can define the effective slope parameter  $\alpha'_{\text{eff}}$  through the relation

$$\alpha'_{\text{eff}} = -\frac{\partial}{\partial y} \frac{\partial}{\partial \mathbf{q}^2} \log \Phi(y, \mathbf{q}^2) \quad (3.41)$$

and find from eq. (3.39)

$$\alpha'_{\text{eff}} = \frac{1}{|\mathbf{q}^2|} \frac{N_c \alpha_s}{2\pi} \frac{1}{\sqrt{N_c \alpha_s / \pi} y \log 4\Delta^2 / |\mathbf{q}|^2}}, \quad (3.42)$$

i. e. the slope is a function of  $t$  and  $s$ . The same energy dependence of the effective slope was found in [65] by using the diffusion approximation in impact parameter space for an infrared modified BFKL equation. It seems reasonable to assume that this effective slope is universal, i. e. it does not depend on the specific process. The process enters only through the scale which is  $4\Delta^2$  here. It should be stressed, however, that the result in eq. (3.42) is obtained in a limit which does not correspond to the diffusion limit of the BFKL equation. Using eq. (3.42) as an estimate for the slope and inserting the realistic values  $-t = 1 \text{ GeV}^2$ ,  $y = 8$ ,  $4\Delta^2 = 10 \text{ GeV}^2$  we find  $\alpha'_{\text{eff}} \simeq 0.05 \text{ GeV}^{-2}$  which has to be regarded as very small in comparison with the slope  $\alpha_{\text{soft}} = 0.25 \text{ GeV}^{-2}$  of the soft (Donnachie-Landshoff) pomeron [67]. A more accurate calculation [46] based on the exact numerical evaluation of  $\Phi(y, \mathbf{q}^2)$  in eq. (3.31) leads to a similar result. It should be stressed here again that in the small- $t$  limit which is considered here one should go beyond the Mueller-Tang prescription. We will come back to this point in the next section.

Finally in fig. 3.10 we present the full differential partonic cross section normalized to its value at  $-t = 1 \text{ GeV}^2$  for small values of  $-t$ . These curves illustrate the shrinkage phenomenon. For large energy the slope of the

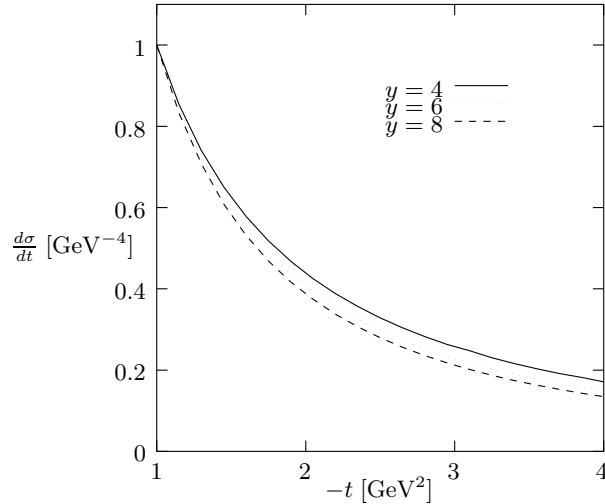


Figure 3.10: The normalized photon-parton cross section as a function of  $t$  for different values of  $y$ .

$t$ -dependence increases. Based on the starting formula (3.14) an absolute prediction for the cross section is possible. To obtain an estimate for the total cross section we perform a fourfold numerical integration over the auxiliary parameter  $\lambda$ , the conformal dimension  $\nu$  and the phase space variables  $x$  and  $t$ . We have chosen to integrate  $\lambda$  and  $\nu$  by iteratively using conventional methods based on the interpolation of the integrand between a discrete set of points. The phase space integration is done with a Monte-Carlo algorithm [68]. For the photoproduction case  $Q^2 = 0$  and the vector meson being the  $J/\Psi$  with mass  $M_{J/\Psi} = 3.10 \text{ GeV}$  we integrate over  $x$  from 0.2 to 0.6 and over  $|t|$  from  $1 \text{ GeV}^2$  to  $20 \text{ GeV}^2$ . We find for the total photon proton cross section values of 480 nb, 99 nb and 24 nb for  $W = 200 \text{ GeV}$ ,  $100 \text{ GeV}$  and  $50 \text{ GeV}$ , respectively.

### 3.3 The BFKL pomeron in DIS diffractive dissociation

The subject of this section is a study of deep inelastic diffractive dissociation at zero and finite momentum transfer based on the BFKL pomeron, or, more general, the leading  $\log(1/x)$  resummation of perturbative QCD. We investigate the process  $\gamma^*(q) + P(p) \rightarrow X(q+\xi) + P(p-\xi)$ . Experimentally, e. g. in electron-proton collisions at HERA, these processes show the characteristic signature of a rapidity gap. There is a region between the outgoing proton and the system  $X$  in which no particles are observed. In the first step we will consider the system  $X$  as being made up of a quark-antiquark pair, afterwards we will generalize to  $q\bar{q} + n$  gluon final states. The analysis presented here is to a large extent based on the results on the triple Regge limit in perturbative QCD contained in [18] and [19].

The interest in this type of process stems from the fact that it is closely related to the unitarization problem. Both the leading-log ( $Q^2$ ) (eq. (3.5)) and the leading-log ( $1/x$ ) (eq. (3.9)) asymptotics at small  $x$  violate unitarity, i. e. they grow too fast with decreasing  $x$ . From unitarity, at most a logarithmic increase at small  $x$  is expected<sup>13</sup>. The first subleading corrections which serve to restore unitarity have been classified and analyzed in [18] and [19]. It turns out that a large part of these corrections contributes to diffractive dissociation. In other words, DIS diffractive dissociation is the appropriate process to study, both theoretically and experimentally, properties of unitarity corrections at small  $x$ . It will be shown that the BFKL four-gluon amplitude constitutes a very important element of these corrections.

From the start we will assume that the large scale  $Q^2$  of deep inelastic scattering justifies the perturbative approach. A critical discussion of this assumption will be given after the results have been stated.

#### 3.3.1 The production of $q\bar{q}$ -pairs

We begin with the discussion of diffractive  $q\bar{q}$ -production. Photon diffractive dissociation means that the virtual photon which is radiated off a fast electron dissociates into a  $q\bar{q}$ -pair which in turn scatters diffractively off the proton, i. e. the photon stays intact or is weakly excited after the collision. No color is exchanged between the proton and the  $q\bar{q}$ -pair and consequently in the framework of perturbative QCD the amplitude in lowest order contains a two-gluon exchange. At high photon-proton cms (or small  $x$  equivalently) the dominant higher order corrections to the amplitude are resummed by the BFKL equation. The general structure of the squared amplitude is represented graphically in fig. 3.11. The shaded blobs represent the BFKL

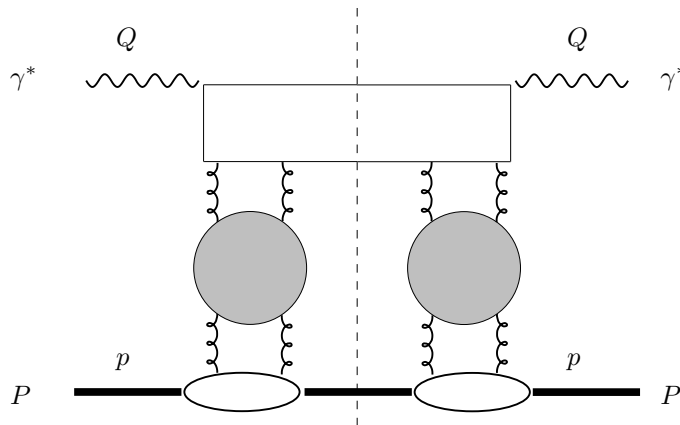


Figure 3.11: Photon diffractive dissociation into a  $q\bar{q}$ -pair.

amplitude which is coupled to the proton through an impact factor to be specified below. Mathematically,

<sup>13</sup> A rigorous proof of this statement has not been given up to now. It is however commonly accepted, based on the proof for hadron-hadron scattering and the use of vector meson dominance. For recent attempts towards a proof see [69] and [70].



we use the partial wave representation for the cross section

$$\frac{d\sigma^{\gamma^*P}}{dt}(x, t) = \frac{1}{Q^4} \int \frac{d\omega_1}{2\pi i} \int \frac{d\omega_2}{2\pi i} \left(\frac{1}{x}\right)^{\omega_1+\omega_2} \Phi_{\omega_1\omega_2}(\mathbf{q}^2) \quad ; \quad \mathbf{q}^2 = -t \quad (3.43)$$

where the partial wave amplitude  $\Phi_{\omega_1\omega_2}$  has the following form

$$\begin{aligned} \frac{1}{Q^4} \Phi_{\omega_1\omega_2}(\mathbf{q}^2) &= \int \frac{d^2\mathbf{k}_1}{(2\pi)^3} \int \frac{d^2\mathbf{k}_2}{(2\pi)^3} D_{(4,0)}(\mathbf{k}_1, \mathbf{q} - \mathbf{k}_1, \mathbf{k}_2, -\mathbf{q} - \mathbf{k}_2) \\ &\int \frac{d^2\mathbf{l}_1}{(2\pi)^3} \Phi_{\omega_1}(\mathbf{k}_1, \mathbf{l}_1; \mathbf{q}) \phi_P(\mathbf{l}_1, \mathbf{q}) \int \frac{d^2\mathbf{l}_2}{(2\pi)^3} \Phi_{\omega_2}(\mathbf{k}_2, \mathbf{l}_2; -\mathbf{q}) \phi_P(\mathbf{l}_2, -\mathbf{q}) \end{aligned} \quad (3.44)$$

Here  $\Phi_{\omega_i}$  is the BFKL amplitude,  $D_{(4,0)}$  represents the quark-loop diagram with four gluons attached and  $\phi_P$  is the coupling of the BFKL amplitude to the proton. This coupling is not determined theoretically and one has to use a phenomenological model. A convenient choice is the rescaled photon-meson formfactor  $\Delta^2\phi_V$  from the previous section (eq. (3.17)) with  $\Delta^2$  a characteristic proton scale of the order of  $1 \text{ GeV}^2$  and  $\mathcal{C}$  an undetermined dimensionless constant. As to the four gluon amplitude  $D_{(4,0)}$ , one has to consider 16 diagrams corresponding to the different ways to couple four gluons to a quark-antiquark pair [71, 72, 73]. In the inclusive case which is under study here the momentum structure of these diagrams simplifies considerably and can be reduced to the two gluon amplitude  $D_{(2,0)}$ . This is due to the fact that two or three gluons which couple to the same quark line collapse into one reggeon. The reggeon is a composite object consisting of two or more gluons, but it behaves effectively like a single gluon. The expression for the four gluon amplitude then reads

$$D_{(4,0)}(\mathbf{k}_1, \mathbf{k}_2, \mathbf{k}_3, \mathbf{k}_4) = 4\pi\alpha_s \frac{\sqrt{2}}{3} \left[ \sum_{i=1}^4 D_{(2,0)}(\mathbf{k}_i, -\mathbf{k}_i) - \sum_{i=2}^4 D_{(2,0)}(\mathbf{k}_1 + \mathbf{k}_i, -\mathbf{k}_1 - \mathbf{k}_i) \right], \left( \sum_{i=1}^4 \mathbf{k}_i = 0 \right) \quad (3.45)$$

The coefficient in front results from the projection of the color structure of the four gluon amplitude on color zero in the subsystems of the gluons with momenta  $(\mathbf{k}_1, \mathbf{k}_2)$  and  $(\mathbf{k}_3, \mathbf{k}_4)$ . For further details see [19]. The function  $D_{(2,0)}(\mathbf{k}, -\mathbf{k})$  is well known [59]. It is identical to the coefficient function in DIS in the  $\mathbf{k}$ -factorization formalism as discussed in section 3.1. We consider transverse and longitudinal photons separately and use the Mellin representation

$$D_{(2,0)}(\mathbf{k}, -\mathbf{k}) = \int \frac{d\nu}{2\pi} \left( \frac{\mathbf{k}^2}{Q^2} \right)^{\frac{1}{2}+i\nu} D_{(2,0)}(\nu) \quad (3.46)$$

$$D_{(2,0)T}(\nu) = \sum_f e_f^2 \alpha_{\text{em}} \alpha_s \frac{1}{\sqrt{8}} \frac{\Gamma(5/2 - i\nu)}{\Gamma(2 - i\nu)} \frac{\Gamma(1/2 - i\nu)}{1/2 - i\nu} \frac{\Gamma(1/2 + i\nu)}{1/2 + i\nu} \frac{\Gamma(5/2 + i\nu)}{\Gamma(2 + i\nu)} \quad (3.47)$$

$$D_{(2,0)L}(\nu) = \sum_f e_f^2 \alpha_{\text{em}} \alpha_s \frac{1}{\sqrt{8}} \frac{\Gamma(5/2 - i\nu)}{\Gamma(2 - i\nu)} \frac{\Gamma(1/2 - i\nu)}{3/2 - i\nu} \frac{\Gamma(1/2 + i\nu)}{3/2 + i\nu} \frac{\Gamma(5/2 + i\nu)}{\Gamma(2 + i\nu)} \quad (3.48)$$

The key difference between the transverse and the longitudinal part is the double pole of  $D_{(2,0)T}(\nu)$  at  $i\nu = 1/2$  where  $D_{(2,0)L}(\nu)$  has a simple pole. It means that at large  $Q^2$  the transverse part is logarithmically enhanced relative to the longitudinal part. This is well known in standard DIS where the longitudinal cross section is an order  $\alpha_s$  contribution (it is zero in the naive parton model). It should be mentioned that a compact expression for the four gluon amplitude  $D_{(4,0)}$  is obtained if the configuration space representation is used [71, 72]. This corresponds to Fourier transformation of eq. (3.45)

$$D_{(4,0)}(\mathbf{k}_1, \mathbf{k}_2, \mathbf{k}_3, \mathbf{k}_4) = 4\pi\alpha_s \frac{\sqrt{2}}{3} \int d^2\rho |\Psi(\rho)|^2 \prod_{i=1}^4 (1 - e^{i\mathbf{k}_i\rho}) \quad (3.49)$$

Here  $\Psi(\rho)$  is the light cone wave function of the photon. The explicit expression for  $|\Psi(\rho)|^2$  which involves generalized Bessel functions can be found in [71, 72, 44]. One can see that the rule for constructing  $n$ -gluon

amplitudes is simple. For every additional gluon with momentum  $\mathbf{k}_j$  a factor  $(1 - \exp(i\mathbf{k}_j\rho))$  has to be added.

Now we are ready to calculate the partial wave  $\Phi_{\omega_1\omega_2}$ . We insert the factorizing momentum space expressions for the BFKL (i. e. the momentum space analogue of eq. (3.39)) amplitudes into eq. (3.44). The partial wave then decomposes into three parts. We have two factors which result from integrating the lower factor of the BFKL amplitude with the pomeron-proton coupling

$$\Lambda^{(\nu_i, n_i)}(\mathbf{q}^2) = \int \frac{d^2\mathbf{l}_i}{(2\pi)^3} \phi_P(\mathbf{l}_i, \mathbf{q} - \mathbf{l}_i) E^{(\nu_i, n_i)*}(\mathbf{l}_i, \mathbf{q} - \mathbf{l}_i) \quad (i = 1, 2) \quad (3.50)$$

The key element results from integrating the four gluon amplitude with the upper factors of the BFKL amplitudes. This defines a vertex function  $\Theta^{(\nu, \nu_1, \nu_2; n_1, n_2)}(\mathbf{q}^2)$

$$\begin{aligned} \Theta^{(\nu, \nu_1, \nu_2; n_1, n_2)}(\mathbf{q}^2) = \int \frac{d^2\mathbf{k}_1}{(2\pi)^3} \int \frac{d^2\mathbf{k}_3}{(2\pi)^3} \left[ \sum_{i=1}^4 \left( \frac{\mathbf{k}_i^2}{Q^2} \right)^{\frac{1}{2} + i\nu} - \sum_{i=2}^4 \left( \frac{(\mathbf{k}_1 + \mathbf{k}_i)^2}{Q^2} \right)^{\frac{1}{2} + i\nu} \right] \\ \cdot E^{(\nu_1, n_1)}(\mathbf{k}_1, \mathbf{q} - \mathbf{k}_1) E^{(\nu_2, n_2)}(\mathbf{k}_3, -\mathbf{q} - \mathbf{k}_3) \end{aligned} \quad (3.51)$$

where from momentum conservation we have  $\mathbf{k}_2 = \mathbf{q} - \mathbf{k}_1$ ,  $\mathbf{k}_4 = -\mathbf{q} - \mathbf{k}_3$ .

The partial wave amplitude is then given as

$$\frac{1}{Q^4} \Phi_{\omega_1\omega_2}(\mathbf{q}^2) = \sum_{n_1, n_2=-\infty}^{+\infty} \int \frac{d\nu}{2\pi} \int \frac{d\nu_1}{2\pi} \int \frac{d\nu_2}{2\pi} D_{(2,0)}(\nu) \Theta^{(\nu, \nu_1, \nu_2; n_1, n_2)}(\mathbf{q}^2) \prod_{i=1}^2 \frac{\Lambda^{(\nu_i, n_i)}(\mathbf{q}^2)}{\omega_i - \chi(\nu_i, n_i)} \quad (3.52)$$

In the following we drop the index  $n$  since we restrict the calculation to zero conformal spin. For the function  $\Lambda^{(\nu)}(\mathbf{q}^2)$  the results from the previous section can be used. Performing the steps that led to eq. (3.31) we obtain

$$\begin{aligned} \Lambda^{(\nu)}(\mathbf{q}^2) = -\mathcal{C} \frac{\Delta^2}{\mathbf{q}^2} (\mathbf{q}^2)^{-\frac{1}{2} + i\nu} 4^{-2i\nu} \pi \frac{\Gamma(1 - i\nu) \Gamma(-\frac{1}{2} + i\nu)}{\Gamma(i\nu) \Gamma(\frac{3}{2} - i\nu)} \\ \int \frac{d\lambda}{\pi} \left( \frac{\mathbf{q}^2}{4\Delta^2} \right)^{\frac{3}{2} + i\lambda} \frac{\Gamma^2(\frac{3}{2} + i\lambda) \Gamma(-i\lambda + i\nu) \Gamma(-i\lambda - i\nu)}{\Gamma(\frac{1}{2} - \frac{1}{2}(i\lambda + i\nu)) \Gamma(\frac{1}{2} - \frac{1}{2}(i\lambda - i\nu)) \Gamma(1 + \frac{1}{2}(i\lambda + i\nu)) \Gamma(1 + \frac{1}{2}(i\lambda - i\nu))} \end{aligned} \quad (3.53)$$

The core of this section is the calculation of the vertex function. The first point to realize is that out of the seven terms in the sum in eq. (3.51) only two give a nonzero contribution. This is however true only if we keep  $\mathbf{q}^2 \neq 0$ . If we set  $\mathbf{q}^2 = 0$  in (3.51) it is crucial to keep all seven terms to obtain a finite result [74]. For finite  $\mathbf{q}^2$  on the other hand we can go back to the mixed representation for  $E^{(\nu)}$  (with arguments  $\mathbf{q}, \rho$ ) and find that for the cases in which the two gluons from the BFKL amplitude are coupled to the same quark line a  $\delta^{(2)}(\rho)$ -function is obtained. If then  $\text{Re}(i\nu) < 1/2$  is assumed the  $\rho$ -integration of the corresponding term gives zero. In the end an analytic continuation to  $\text{Re}(i\nu) > 1/2$  can be performed. The same reasoning was used in the previous section when the second term in eq. (3.23) was omitted. This shows that the contributions in which two gluons couple to the same quark line serve as pure subtraction terms which are needed for convergence but give no finite contribution. Calculating with finite  $\mathbf{q}^2$  provides a regularization in which these terms can be omitted from the beginning. Furthermore by shifting the integration variable it can be shown that the two terms which survive are in fact identical. After all one nontrivial two-loop integration has to be carried out in (3.51). We use the representation (3.53) for the  $E^{(\nu)}$  functions and get

the following expression

$$\begin{aligned}
\Theta^{(\nu, \nu_1, \nu_2)}(\mathbf{q}^2) &= -2 \int \frac{d^2 \mathbf{k}_1}{(2\pi)^3} \int \frac{d^2 \mathbf{k}_3}{(2\pi)^3} \left( \frac{(\mathbf{k}_1 + \mathbf{k}_3)^2}{Q^2} \right)^{\frac{1}{2} + i\nu} \\
&4\pi 4^{2i\nu_1} \frac{\Gamma(1 + i\nu_1)}{\Gamma(-i\nu_1)} \frac{\Gamma(\frac{3}{2} - i\nu_1) \Gamma(-\frac{1}{2} - i\nu_1)}{\Gamma(\frac{1}{2} + i\nu_1) \Gamma(\frac{1}{2} - i\nu_1)} \int_0^1 dx [x(1-x)]^{-\frac{1}{2} + i\nu_1} [\mathbf{q}^2 x(1-x) + (\mathbf{k}_1 - x\mathbf{q})^2]^{-\frac{3}{2} - i\nu_1} \\
&4\pi 4^{2i\nu_2} \frac{\Gamma(1 + i\nu_2)}{\Gamma(-i\nu_2)} \frac{\Gamma(\frac{3}{2} - i\nu_2) \Gamma(-\frac{1}{2} - i\nu_2)}{\Gamma(\frac{1}{2} + i\nu_2) \Gamma(\frac{1}{2} - i\nu_2)} \int_0^1 dy [y(1-y)]^{-\frac{1}{2} + i\nu_2} [\mathbf{q}^2 y(1-y) + (\mathbf{k}_3 + y\mathbf{q})^2]^{-\frac{3}{2} - i\nu_2} \\
&{}_2F_1 \left( \begin{matrix} \frac{3}{2} + i\nu_1, -\frac{1}{2} + i\nu_1 \\ 1 \end{matrix}; \frac{(\mathbf{k}_1 - x\mathbf{q})^2}{\mathbf{q}^2 x(1-x) + (\mathbf{k}_1 - x\mathbf{q})^2} \right) {}_2F_1 \left( \begin{matrix} \frac{3}{2} + i\nu_2, -\frac{1}{2} + i\nu_2 \\ 1 \end{matrix}; \frac{(\mathbf{k}_3 + y\mathbf{q})^2}{\mathbf{q}^2 y(1-y) + (\mathbf{k}_3 + y\mathbf{q})^2} \right)
\end{aligned} \tag{3.54}$$

It is now necessary to use the usual Mellin-Barnes representation for the hypergeometric function [53]. The momentum dependence then appears in terms of the form  $[\mathbf{q}^2 x(1-x) + (\mathbf{k} - x\mathbf{q})^2]^\gamma$  with some exponent  $\gamma$ . To perform the momentum integration it is then convenient to use a Mellin-Barnes representation also for these factors. Performing these steps we end with the following expression for the last three lines in eq. (3.54)

$$\begin{aligned}
&\prod_{i=1}^2 4\pi 4^{2i\nu_i} \frac{\Gamma(1 + i\nu_i)}{\Gamma(-i\nu_i)} \frac{\Gamma(\frac{3}{2} - i\nu_i) \Gamma(-\frac{1}{2} - i\nu_i)}{\Gamma(\frac{1}{2} + i\nu_i) \Gamma(\frac{1}{2} - i\nu_i)} \int_0^1 dx [x(1-x)]^{-\frac{1}{2} + i\nu_1} \int_0^1 dy [y(1-y)]^{-\frac{1}{2} + i\nu_2} \\
&\frac{1}{|\Gamma(\frac{3}{2} + i\nu_1)|^2 |\Gamma(\frac{3}{2} + i\nu_2)|^2} \int \frac{ds_1}{2\pi i} \int \frac{ds_2}{2\pi i} \prod_{i=1}^2 \frac{\Gamma(-s_i) \Gamma(-s_i - 2i\nu_i) \Gamma(s_i + \frac{3}{2} + i\nu_i)}{\Gamma(-s_i - \frac{1}{2} - i\nu_i)} \\
&[\mathbf{q}^2 x(1-x)]^{s_1} [\mathbf{q}^2 y(1-y)]^{s_2} [(\mathbf{k}_1 - x\mathbf{q})^2]^{-s_1 - \frac{3}{2} - i\nu_1} [(\mathbf{k}_3 + y\mathbf{q})^2]^{-s_2 - \frac{3}{2} - i\nu_2}
\end{aligned} \tag{3.55}$$

Now we can perform a shift of the integration variable and the momentum integration takes the simple form

$$(Q^2)^{-\frac{1}{2} - i\nu} \int \frac{d^2 \mathbf{k}_1}{(2\pi)^3} \int \frac{d^2 \mathbf{k}_3}{(2\pi)^3} \frac{[(\mathbf{k}_1 + \mathbf{k}_3 + (x-y)\mathbf{q})^2]^{\frac{1}{2} + i\nu}}{(\mathbf{k}_1^2)^{s_1 + \frac{3}{2} + i\nu_1} (\mathbf{k}_3^2)^{s_2 + \frac{3}{2} + i\nu_2}} \tag{3.56}$$

$$\begin{aligned}
&= \frac{(Q^2)^{-\frac{1}{2} - i\nu}}{(2\pi)^6} \pi^2 [\mathbf{q}^2 |x-y|^2]^{-\frac{1}{2} - s_1 - s_2 + i\nu - i\nu_1 - i\nu_2} \frac{\Gamma(\frac{3}{2} + i\nu)}{\Gamma(-\frac{1}{2} - i\nu)} \\
&\cdot \prod_{i=1}^2 \frac{\Gamma(-s_i - \frac{1}{2} - i\nu_i)}{\Gamma(s_i + \frac{3}{2} + i\nu_i)} \frac{\Gamma(\frac{1}{2} + s_1 + s_2 - i\nu + i\nu_1 + i\nu_2)}{\Gamma(\frac{1}{2} - s_1 - s_2 + i\nu - i\nu_1 - i\nu_2)}
\end{aligned} \tag{3.57}$$

This result is now inserted in eq. (3.54) and it remains to perform the integration of the Feynman parameters. Due to the symmetry properties of the integrand the integral can be readily expressed as a  ${}_3F_2$  generalized hypergeometric function which can be reduced to  $\Gamma$ -functions using Whittaker's theorem [53]

$$\begin{aligned}
&\int_0^1 dx [x(1-x)]^{-\frac{1}{2} + s_1 + i\nu_1} \int_0^1 dy [y(1-y)]^{-\frac{1}{2} + s_2 + i\nu_2} [|x-y|^2]^{-\frac{1}{2} - s_1 - s_2 + i\nu - i\nu_1 - i\nu_2} \\
&= 4^{1+s_1+s_2+i\nu_1+i\nu_2-2i\nu} \frac{\pi}{\Gamma(\frac{1}{2} + i\nu)} \prod_{i=1}^2 \frac{\Gamma(\frac{1}{2} + s_i + i\nu_i)}{\Gamma(\frac{1}{2} - s_i - i\nu_i + i\nu)} \\
&\cdot \frac{\Gamma(-2s_1 - 2s_2 - 2i\nu_1 - 2i\nu_2 + 2i\nu) \Gamma(-s_1 - s_2 - i\nu_1 - i\nu_2 + 2i\nu)}{\Gamma(\frac{1}{2} - s_1 - s_2 - i\nu_1 - i\nu_2 + i\nu)}
\end{aligned} \tag{3.58}$$

Collecting then the terms from eqs. (3.54) - (3.58) and performing all possible cancellations we obtain the final result for the vertex function

$$\begin{aligned} \Theta^{(\nu, \nu_1, \nu_2)}(\mathbf{q}^2) = & -2 \frac{(\mathbf{q}^2)^{-\frac{1}{2} + i\nu - i\nu_1 - i\nu_2}}{16\pi^3 (Q^2)^{\frac{1}{2} + i\nu}} 4^{i\nu_1 + i\nu_2 - 2i\nu} \frac{\Gamma(\frac{3}{2} + i\nu)}{\Gamma(-\frac{1}{2} - i\nu)\Gamma(\frac{1}{2} + i\nu)} \\ & \prod_{i=1}^2 \left[ 4\pi 4^{2i\nu_i} \frac{\Gamma(1 + i\nu_i)}{\Gamma(-i\nu_i)} \frac{\Gamma(-\frac{1}{2} - i\nu_i)}{\Gamma(\frac{3}{2} + i\nu_i)\Gamma(\frac{1}{2} + i\nu_i)\Gamma(\frac{1}{2} - i\nu_i)} \right] \prod_{i=1}^2 \left[ \int \frac{ds_i}{2\pi i} \Gamma(-s_i)\Gamma(-s_i - 2i\nu_i) \frac{4^{s_i}\Gamma(\frac{1}{2} + s_i + i\nu_i)}{\Gamma(\frac{1}{2} - s_i - i\nu_i + i\nu)} \right] \\ & \frac{\Gamma(\frac{1}{2} + s_1 + s_2 - i\nu + i\nu_1 + i\nu_2)}{\Gamma(\frac{1}{2} - s_1 - s_2 + i\nu - i\nu_1 - i\nu_2)} \frac{\Gamma(-2s_1 - 2s_2 - 2i\nu_1 - 2i\nu_2 + 2i\nu)\Gamma(-s_1 - s_2 - i\nu_1 - i\nu_2 + 2i\nu)}{\Gamma(\frac{1}{2} - s_1 - s_2 - i\nu_1 - i\nu_2 + i\nu)} \end{aligned} \quad (3.59)$$

The partial wave amplitude  $\Phi_{\omega_1\omega_2}(\mathbf{q}^2)$  can now be determined by inserting the expression for the vertex function  $\Theta^{(\nu, \nu_1, \nu_2)}$  and the functions  $\Lambda^{(\nu_i)}$  into eq. (3.52). The result is fairly complicated and even a numerical evaluation does not seem to be a simple task. We will investigate in the following the limits  $\mathbf{q}^2 \rightarrow 0$  and  $\mathbf{q}^2 \rightarrow \infty$ .

### 3.3.2 The limit $\mathbf{q}^2 = 0$

Let us first observe that the  $\mathbf{q}^2$ -dependence of the vertex function is simply  $(\mathbf{q}^2)^{-\frac{1}{2} + i\nu - i\nu_1 - i\nu_2}$  which follows of course from purely dimensional considerations. From this dependence it can be concluded that a finite limit of the vertex function in the limit  $\mathbf{q}^2 \rightarrow 0$  implies a constraint on the conformal dimensions  $\nu, \nu_1, \nu_2$ . A well-defined, nonzero limit requires  $-\frac{1}{2} + i\nu - i\nu_1 - i\nu_2 = 0$ , otherwise the vertex function would either be zero or infinity. To show how this works in detail one has to consider the singularity structure of the  $\nu$ -integration in (3.52)

It is important to recall first from the previous section that the  $\mathbf{q}^2 \rightarrow 0$  limit of the functions  $\Lambda^{(\nu_i)}$  is determined by the poles at  $i\lambda = \pm i\nu$  in the integrand in eq. (3.53). This means that for  $\mathbf{q}^2 \rightarrow 0$  we have  $\Lambda^{(\nu_i)}(\mathbf{q}^2) = (\Delta^2)^{-1/2} [a(\nu_i) + b(\nu_i)(\mathbf{q}^2)^{2i\nu_i}]$ .

As to the  $\nu$ -integration, the  $\nu$ -contour in (3.52) runs on the real axis and the relevant part of the integrand is  $(\mathbf{q}^2)^{-1/2 + i\nu}$ . For  $\mathbf{q}^2 \rightarrow 0$  one has to shift the contour into the lower half plane in order to obtain a power series in  $\mathbf{q}^2$ . The integrand has two factors which generate singularities in the lower half plane. From combining the coefficient function  $D_{(2,0)}(\nu)$  with the three  $\Gamma$ -functions in the first line of eq. (3.59) one gets simple poles at  $i\nu = 1/2, 3/2, \dots$  (these poles are absent in the longitudinal case). Furthermore one has a string of simple poles from the function  $\Gamma(1/2 + s_1 + s_2 + i\nu_1 + i\nu_2 - i\nu)$  in the third line of (3.59). The other two  $\Gamma$ -functions generate poles in the upper half plane. One has to consider only the first pole of each of these strings since the following ones are  $\mathbf{q}^2$ -suppressed. For the first group taking the residue at  $i\nu = 1/2$  leads to a remaining  $\mathbf{q}$ -dependence  $(\mathbf{q}^2)^{-i\nu_1 - i\nu_2}$ . If this factor is combined with the results for the functions  $\Lambda^{(\nu_i)}(\mathbf{q}^2)$  (see above) we end with the result

$$\Phi_{\omega_1\omega_2}(\mathbf{q}^2) = C(\nu_1, \nu_2) \cdot \prod_{i=1}^2 \int_{-\infty}^{+\infty} \frac{d\nu_i}{2\pi} \frac{1}{\omega_i - \chi(\nu_i)} [a(\nu_i)(\mathbf{q}^2)^{-i\nu_i} + b(\nu_i)(\mathbf{q}^2)^{i\nu_i}] \quad (3.60)$$

Since  $C(\nu_1, \nu_2)$ ,  $a(\nu_i)$  and  $b(\nu_i)$  can be shown to be analytic in a strip around the real  $\nu_i$ -axis we can shift each  $\nu_i$ -contour either into the upper or lower  $\nu_i$ -plane. In that way each term in (3.60) can be shown to vanish for  $\mathbf{q}^2 = 0$ . The pole for the coefficient function hence gives no contribution for zero momentum transfer.

As to the leading pole of the second string of singularities we take the residue at  $i\nu = 1/2 + i\nu_1 + i\nu_2 + s_1 + s_2$ . This leads to the factor  $(\mathbf{q}^2/Q^2)^{s_1 + s_2}$  where  $s_1$  and  $s_2$  still have to be integrated. Since we are interested in the limit  $\mathbf{q}^2 \rightarrow 0$  we have to shift the  $s_i$ -contours to the right, past the poles at  $s_i = 0$ ,  $s_i = -2i\nu_i$ , i. e. we get a sum of four contributions. Combining these with the results for the functions  $\Lambda(\nu_i)$  one gets 16 terms. Four of these are independent of  $\mathbf{q}^2$  and the other 12 have a  $\mathbf{q}^2$ -dependence analogous to eq. (3.60) and vanish after deforming the contours of the  $\nu_i$ -integration. Finally one can show that due to the symmetry properties of the integrand the remaining four terms are in fact identical and the result for the partial wave

amplitude in the limit  $\mathbf{q}^2 = 0$  reads

$$\Phi_{\omega_1\omega_2}(\mathbf{q}^2)|_{\mathbf{q}^2=0} = \frac{\mathcal{C}^2}{64\pi^2} \frac{Q^2}{\Delta^2} \prod_{i=1}^2 \int \frac{d\nu_i}{2\pi} \frac{(\Delta^2/Q^2)^{i\nu_i}}{\omega_i - \chi(\nu_i)} \Gamma\left(\frac{1}{2} + i\nu_i\right) \Gamma\left(\frac{1}{2} - i\nu_i\right) \cdot D_{(2,0)}\left(\frac{1}{2} + i\nu_1 + i\nu_2\right) \cdot \frac{\Gamma(2 + i\nu_1 + i\nu_2)}{\Gamma(-1 - i\nu_1 - i\nu_2)} \frac{\Gamma(-\frac{1}{2} - i\nu_1)\Gamma(-\frac{1}{2} - i\nu_2)}{\Gamma(\frac{3}{2} + i\nu_1)\Gamma(\frac{3}{2} + i\nu_2)} \quad (3.61)$$

Here the factors in the second line correspond to the zero momentum transfer expression of the vertex function. We have seen that the constraint on the conformal dimensions which was anticipated above is implemented in the vertex function through the pole of the  $\Gamma$ -function  $\Gamma(1/2 + i\nu_1 + i\nu_2 + s_1 + s_2 - i\nu)$ . In the  $\mathbf{q}^2 = 0$ -limit one is forced to take this pole which expresses the conservation of conformal dimensions. The remaining  $\nu_i$ -integrals in eq. (3.61) have to be evaluated numerically. For small  $x$  we can obtain an approximate analytical result by using the saddle point approximation. It is convenient to use the integration variables  $\nu_{\pm} = \nu_1 \pm \nu_2$ . The saddle point of the  $\nu_-$ -integration is then found at  $\nu_- = 0$  and the corresponding integration is straightforward. The saddle point of the  $\nu_+$ -integration is found at  $i\nu_+ = 1/2 \log(\Delta^2/Q^2)/\log(1/x)/|\chi''(0)| \ll 1$ . For the longitudinal part the corresponding integration is simple since the non-exponential parts of the integrand are analytic in a neighbourhood of the saddle point. For the transverse case we have a pole at  $i\nu_+ = 0$ , i. e. in the limit of small  $x$  the saddle point approaches a pole of the integrand. In this case the saddle point contour consists of two parts. We have the principal value of the  $\nu_+$ -integration and the contribution of a small semicircle around the pole at  $\nu = 0$ . In the limit of small  $x$  the semicircle contribution is dominant and the principal value integral can be neglected. The results for the photon-proton cross sections in the small- $x$  limit then read

$$\frac{d\sigma_T^{\gamma^*P}}{dt}(x, t)|_{t=0} = \frac{1}{Q^2\Delta^2} \mathcal{C}^2 \sum_f e_f^2 \alpha_{\text{em}} \alpha_s^2 \frac{2}{9} \frac{e^{2\frac{N_c\alpha_s}{\pi} 4\log 2 \log 1/x}}{\sqrt{7N_c\alpha_s\zeta(3)} \log 1/x} \quad (3.62)$$

$$\frac{d\sigma_L^{\gamma^*P}}{dt}(x, t)|_{t=0} = \frac{1}{Q^2\Delta^2} \mathcal{C}^2 \sum_f e_f^2 \alpha_{\text{em}} \alpha_s^2 \frac{1}{9} \frac{e^{2\frac{N_c\alpha_s}{\pi} 4\log 2 \log 1/x}}{7N_c\alpha_s\zeta(3) \log 1/x} e^{-\frac{\log \Delta^2/Q^2}{28N_c\alpha_s/\pi\zeta(3) \log 1/x}} \quad (3.63)$$

The ratio of the longitudinal to the transverse cross section is approximately (disregarding the exponential factor which is close to unity)  $1/(2\sqrt{7N_c\alpha_s\zeta(3)} \log(1/x))$ , i. e. the longitudinal part can be neglected.

The calculation above was based on the assumption that the large photon virtuality  $Q^2$  justifies the perturbative approach to diffractive dissociation at  $t = 0$ . At first sight one could think that the large scale plays a similar role as in inclusive DIS, namely it pulls the diffusion of transverse momenta in the BFKL ladder out of the infrared region. In this case one would conclude that for high  $Q^2$  a large part of the phase space is treated correctly and that corrections which are important in the infrared region lead to a reduction of the exponent of  $1/x$  from 1 to 0.4...0.5, which is twice the exponent of the observed rise of  $F_2$ . Numerical investigations of the BFKL evolution in diffractive dissociation [22] however show that these expectations are not correct. It turns out that  $Q^2$  is not the relevant scale at the upper end of the BFKL ladders, but that on the contrary the diffusion is driven to even lower momentum scales than the proton scale at the lower end. Almost the whole phase space which is covered by the evolution is located in the infrared domain where perturbation theory is not applicable. This shows that in inclusive diffractive dissociation corrections to the BFKL pomeron in the infrared region are even more important than in ordinary DIS and that the deviation of the experimentally observed  $x$ -dependence from the BFKL prediction should be large, in other words, the BFKL based calculation provides no reasonable approximation to inclusive diffractive DIS. The findings of [22] thus confirm the physical picture of the aligned jet model [23]. In this model one of the quarks into which the virtual photon dissociates carries almost the whole momentum of the photon whereas the other one carries almost none. Both quarks have almost zero transverse momentum (they are aligned to the photon-proton direction). The slow quark interacts with the proton after it has travelled a long time from the point where it was produced. During this time it evolves nonperturbatively and there is no hard scale which can be associated with the quark-proton interaction. It was also shown in [22] that the situation changes when restrictions are imposed on the  $q\bar{q}$  final state. An additional hard scale in the  $q\bar{q}$  final state,

e. g. a large transverse momentum or the mass of a formed vector meson acts similarly to the scale  $Q^2$  in ordinary DIS. It pulls the diffusion out of the infrared and increases the contribution of perturbative scales. Consequently a steeper  $x$ -dependence is expected for processes of this type (for the production of quarks with large transverse momenta see the next section).

### 3.3.3 The limit of large momentum transfer

We now turn to the investigation of the large momentum transfer limit of the partial wave amplitude. In this region perturbation theory is applicable and the BFKL prediction has a better theoretical foundation. This consideration is also interesting for another reason. If we turn the diagram in fig. 3.11 upside down and replace the virtual photon with a proton we end with a model for diffractive vector meson production at large  $t$ , where the BFKL amplitude is now coupled to the proton in a gauge invariant way. Clearly one has to reinterpret the function  $D_{(4,0)}$  in this model. One could think of  $D_{(4,0)}$  as the momentum space expression of the square of the inclusive  $q\bar{q}$  wavefunction of the proton. With  $Q^2$  being replaced by a hadronic scale  $\Lambda^2$  one then has a consistent model for the coupling of the BFKL amplitude to a hadron which does not need the effective Mueller-Tang [64] prescription. The investigation of the limit  $\mathbf{q} \rightarrow \infty$  allows us to discuss the validity of this prescription.

The starting point is again eq. (3.52) with  $\Theta^{(\nu, \nu_1, \nu_2)}$  and  $\Lambda^{(\nu_i)}$  being given by (3.53) and (3.59). Using the results from the previous section we derive that  $\Lambda^{(\nu_i)}$  behaves for large  $\mathbf{q}^2$  as

$$\Lambda^{(\nu_i)} = (\mathbf{q}^2)^{-3/2+i\nu_i} \log \mathbf{q}^2 / (4\Delta^2) a(\nu_i) \quad (3.64)$$

with some analytic function  $a(\nu_i)$ . For the  $\mathbf{q}^2$ -dependence of the vertex function we again have to consider the singularity structure of the  $\nu$ -integration. The essential factor is  $(\mathbf{q}^2/Q^2)^{i\nu}$  and for  $\mathbf{q}^2 \rightarrow \infty$  we have to shift the  $\nu$ -contour into the upper half plane. The Mellin transform  $D_{(2,0)}(\nu)$  has a pole at  $i\nu = -1/2$ . It seems as if the  $\Gamma$ -functions in the denominator of eq. (3.59) cancel this singularity. But closer inspection shows that this is not the case. Let us assume that the pole at  $i\nu = -1/2$  is the one which is nearest to the  $\nu$ -contour, i. e. we have to take it first. Then with  $i\nu = -1/2 + \epsilon$  and as  $\epsilon \rightarrow 0$  one finds that both the contours of the  $s_1$  and  $s_2$  integrations are pinched by the poles of the  $\Gamma$ -functions inside the  $s_i$ -integrations in eq. (3.59). Each pinching implies a pole at  $\epsilon = 0$  or, equivalently, at  $i\nu = -1/2$ . We conclude that the  $s_i$ -integrals in fact contain a double pole at  $i\nu = -1/2$  which cancels the pole of the  $\Gamma$ -functions in the denominator. Hence we can calculate the vertex function  $\Theta^{(\nu, \nu_1, \nu_2)}$  for  $i\nu = -1/2$

$$\Theta^{(\nu=i\frac{1}{2}, \nu_1, \nu_2)} = \frac{2}{16\pi^3} (\mathbf{q}^2)^{-1+i\nu_1+i\nu_2} \prod_{i=1}^2 \left[ 4\pi 4^{2i\nu_i} \frac{\Gamma(1+i\nu_i)}{\Gamma(-i\nu_i)} \frac{\Gamma(-\frac{1}{2}-i\nu_i)}{\Gamma(\frac{3}{2}+i\nu_i)} \right] \frac{1}{2\pi} \quad (3.65)$$

The precise  $\mathbf{q}$ -behaviour of the partial wave amplitude depends on the nature of the singularity of  $D_{(2,0)}(\nu)$  at  $i\nu = -1/2$ . If it has a single pole, like in the longitudinal case, the result is

$$\Phi_{\omega_1 \omega_2 L}(\mathbf{q}^2) = \sum_f e_f^2 \alpha_{\text{em}} \alpha_s^2 \frac{(Q^2 \Delta^2)^2}{(\mathbf{q}^2)^4} \log^2 \frac{\mathbf{q}^2}{4\Delta^2} \frac{64}{9} \mathcal{C}^2 \prod_{i=1}^2 \int \frac{d\nu_i}{2\pi} \frac{\nu_i^2}{\omega_i - \chi(\nu_i)} \frac{\Gamma(-\frac{1}{2}+i\nu_i) \Gamma(-\frac{1}{2}+i\nu_i)}{|\Gamma(\frac{5}{4}+i\frac{\nu_i}{2})|^2 |\Gamma(\frac{1}{4}+i\frac{\nu_i}{2})|^2} \quad (3.66)$$

If there is a double pole at  $i\nu = -1/2$ , like in the transverse case then there is an additional  $\log \mathbf{q}^2/Q^2$ -enhancement

$$\Phi_{\omega_1 \omega_2 T}(\mathbf{q}^2) = 2 \log \frac{\mathbf{q}^2}{Q^2} \Phi_{\omega_1 \omega_2 L}(\mathbf{q}^2) \quad (3.67)$$

The small- $x$  asymptotics of the cross section can now be calculated in the usual way by evaluating the  $\nu_i$ -integrals in the saddle point approximation with the saddle point at  $\nu_{i,s} = 0$ . Note the factor  $\nu_i^2$  in the numerator of the integrand which is characteristic for the BFKL pomeron in the non-forward direction.

Now let us comment on the Mueller-Tang prescription. As anticipated in the last section this prescription states to consider only the diagram in which both gluons from the BFKL amplitude couple to the same quark line and to subtract from the conformal eigenfunctions  $E^{(\nu)}$   $\delta$ -function like terms which are not present in

perturbation theory. In our case this corresponds to keeping only one term in the sum in eq. (3.45) with momentum dependence  $(\mathbf{q}^2/Q^2)^{1/2+i\nu}$  and to substitute the functions  $E^{(\nu)}$  with the Mueller-Tang subtracted eigenfunctions in momentum space

$$E_{MT}^{(\nu)}(\mathbf{k}, \mathbf{q} - \mathbf{k}) = E^{(\nu)}(\mathbf{k}, \mathbf{q} - \mathbf{k}) - \left[ \delta^{(2)}(\mathbf{k}) + \delta^{(2)}(\mathbf{q} - \mathbf{k}) \right] 4^{2i\nu} 4\pi^2 (\mathbf{q}^2)^{-\frac{1}{2}-i\nu} \frac{\Gamma(1+i\nu)}{\Gamma(-i\nu)} \frac{\Gamma(-\frac{1}{2}-i\nu)}{\Gamma(\frac{3}{2}+i\nu)} \quad (3.68)$$

Using the same arguments as presented below eq. (3.53) it can be shown that only the  $\delta$ -function terms give a finite contribution and the result for the vertex function is exactly the expression in eq. (3.65) multiplied by  $(\mathbf{q}^2/Q^2)^{1/2+i\nu}$ . Taking then the pole of  $D_{(2,0)}(\nu)$  at  $i\nu = -1/2$  one arrives at the large- $\mathbf{q}^2$  limit of the exact calculation. This shows that the Mueller-Tang prescription indeed gives the correct large- $\mathbf{q}^2$  asymptotics. The effective parton formfactor which was used in the last section to calculate diffractive vector meson production therefore gives a correct description for large  $\mathbf{q}^2$ . For smaller  $\mathbf{q}^2$ , however, a gauge invariant coupling like the one presented in this section should be used.

In contrast to the open  $q\bar{q}$ -pair production, the Mueller-Tang prescription fails when applied to the coupling of the BFKL amplitude to the photon - vector meson vertex  $\phi_V$  (eq. (3.17)). It was shown in the last section that the large- $\mathbf{q}^2$  behavior in this case contains a  $\log(\mathbf{q}^2)$  which is not obtained when the Mueller-Tang subtraction is used. This demonstrates that the Mueller-Tang prescription does not apply universally but has to be checked in each single case. From the examples which have been studied here one can conjecture [47] that the prescription works in inclusive cases, where configurations with far separated quarks dominate. In exclusive cases where the quarks stay close together the prescription fails.

It remains to discuss the  $\delta$ -function terms which are subtracted in the Mueller-Tang prescription. It is clear from the definition that the momentum space eigenfunctions  $E^{(\nu)}(\mathbf{k}, \mathbf{q} - \mathbf{k})$  are singular for  $\mathbf{k} \rightarrow 0$  and  $\mathbf{k} \rightarrow \mathbf{q}$ . To investigate this singularity it is useful to introduce a small positive conformal dimension  $\lambda$  for the (reggeized) gluon field as a regularization parameter [44]. The regularized momentum space expression  $E^{(\nu,\lambda)}$  can be obtained in the same way as for  $\lambda = 0$ . Investigation of the limit  $\mathbf{k} \rightarrow 0$  of this expression shows that the most singular term is

$$E^{(\nu)}(\mathbf{k}, \mathbf{q} - \mathbf{k}) \xrightarrow{\mathbf{k} \rightarrow 0} \lambda \cdot (\mathbf{k}^2)^{-1+\lambda} (\mathbf{q}^2)^{-\frac{1}{2}-i\nu} 4\pi \frac{\Gamma(1+i\nu)}{\Gamma(-i\nu)} \frac{\Gamma(-\frac{1}{2}-i\nu)}{\Gamma(\frac{3}{2}+i\nu)} [1 + O(\lambda)] \quad (3.69)$$

which can be regarded as a smeared  $\delta^{(2)}(\mathbf{k})$ -function. The origin of these terms which cannot be associated with Feynman diagrams is clear. When proving conformal invariance of the BFKL equation it was necessary to add logarithms of differences of coordinates to the solution of the zero order ( $\alpha_s = 0$ ) equation to ensure conformal symmetry of the initial condition. These fictitious terms cancel when the BFKL amplitude is integrated with color neutral impact factors. The same is true for the  $\delta$ -function terms which do not appear in the physical amplitude as long as the wave functions of the external particles obey the color neutrality condition. One can therefore conclude that the presence of the  $\delta$ -functions is due to the addition of these logarithmic terms to the configuration space amplitude.

### 3.3.4 Additional gluons in the final state

In this part we will generalize the above results to final states which contain also gluons in addition to the  $q\bar{q}$ -pair. The considerations are based on the analysis of photon diffractive dissociation in the triple Regge limit [18, 19] in which  $s \gg M^2 \gg Q^2$ , where  $M^2$  is the invariant mass of the produced hadronic system. The partial wave representation of the cross section now reads

$$\frac{d\sigma^{\gamma^*P}}{dtdM^2} = \frac{1}{M^2 Q^4} \int \frac{d\omega}{2\pi i} \int \frac{d\omega_1}{2\pi i} \int \frac{d\omega_2}{2\pi i} \left( \frac{s}{M^2} \right)^{\omega_1+\omega_2} \left( \frac{M^2}{Q^2} \right)^\omega \Phi_{\omega\omega_1\omega_2} \quad (3.70)$$

It was shown in [18, 19] that the partial wave amplitude  $\Phi_{\omega\omega_1\omega_2}$  comes as a sum of two terms. In both terms the additionally produced gluons are described by a BFKL ladder which is coupled to the quark loop. In the first term this BFKL amplitude couples to the lower two BFKL pomerons through a disconnected vertex. This vertex results from the reggeization of pairs and triplets of gluons in the same way as described

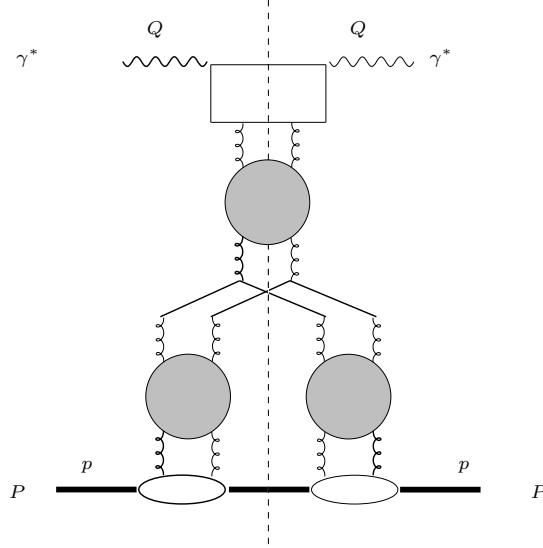


Figure 3.12: Disconnected contribution to photon diffractive dissociation into  $q\bar{q} + n$  gluons.

in the discussion of the four gluon amplitude  $D_{(4,0)}$ . A typical contribution is displayed in fig. 3.12. In the second term a connected vertex appears which couples the upper BFKL ladder to an interacting four gluon state. This interacting four gluon state splits into two BFKL ladders which couple to the proton. Due to our incomplete understanding of the connected vertex and the interacting four gluon state we cannot treat the second term exactly and restrict our considerations to the first term. The vertex and the four gluon state will be studied in the last chapter of this thesis.

Given the results of the  $q\bar{q}$ -case it is not difficult to obtain the partial wave amplitude for the diagrams in fig. 3.12. We have to insert a factor  $1/(\omega - \chi(\nu))$  into the expression for the partial wave amplitude, corresponding to the Mellin transform of the upper BFKL pomeron. The vertex function  $\Theta^{(\nu, \nu_1, \nu_2)}$  which now has the interpretation of a triple pomeron vertex is the same as before. The constraint on the conformal dimensions which holds for  $\mathbf{q}^2 = 0$  now leads to a remarkable interplay between the energy and the momentum transfer dependence in the region of small  $\mathbf{q}^2$ . After performing the  $\omega$ -integrations the energy dependence of the  $\gamma^* - P$  cross section is encoded in the function

$$\exp[y_M \chi(\nu) + y_s(\chi(\nu_1) + \chi(\nu_2))] \quad (3.71)$$

where  $y_M = \log M^2/Q^2$  and  $y_s = \log s/M^2$  were introduced and  $\chi(\nu)$  is the BFKL eigenvalue. In addition to the exponential we have also the factor  $(\mathbf{q}^2/Q^2)^{i\nu}$  which becomes important if  $\mathbf{q}^2$  becomes small. First we keep  $\mathbf{q}^2 \approx Q^2$ , i. e.  $\log \mathbf{q}^2/Q^2 \ll 1$ , and  $y_M$  and  $y_s$  are large. Then all  $\nu$  integrals are determined by the respective stationary point of the exponent in (3.71) which is found at  $\nu_s = \nu_{1s} = \nu_{2s} = 0$ . From this one can conclude that the triple pomeron vertex  $\Theta$  behaves as  $(\mathbf{q}^2)^{-\frac{1}{2}}$  in the triple Regge limit. This behavior was also observed in the color dipole formalism [75]. One can also expect that this result holds for the connected vertex since the  $\mathbf{q}^2$ -behavior follows from purely dimensional arguments. Upon saddle point integration the following expression for the cross section is finally found

$$\begin{aligned} \frac{d\sigma^{\gamma^* P}}{dt dM^2} = & \frac{1}{M^2} \frac{Q^4}{|\mathbf{q}|^6} \frac{1}{\sqrt{\mathbf{q}^2 Q^2}} \log^2 \frac{\mathbf{q}^2}{4\Delta^2} \left( \frac{M^2}{Q^2} \right)^{4 \log 2 \frac{N_c \alpha_s}{\pi}} \left( \frac{s}{M^2} \right)^{8 \log 2 \frac{N_c \alpha_s}{\pi}} \\ & \sqrt{\pi} \mathcal{S} \frac{1}{(14 N_c \alpha_s \zeta(3))^3} \frac{1}{\sqrt{y_M y_s^6}} \frac{2\mathcal{C}^2}{\Gamma^2(1/4) \Gamma^2(5/4)} \end{aligned} \quad (3.72)$$



where the functions  $\Lambda^{(\nu_i)}$  (eq. (3.53)) have been evaluated in the limit  $4\Delta^2 \ll \mathbf{q}^2$  and  $\mathcal{S}$  is a constant resulting from the  $s_i$  integration in eq. (3.59) when all conformal dimensions are zero.

Now if  $\mathbf{q}^2$  becomes small the factor  $(\mathbf{q}^2/Q^2)^{i\nu}$  becomes dominant again. In the limit  $\mathbf{q}^2 = 0$  we are again forced to perform the  $\nu$ -integration by taking the conservation pole at  $i\nu = 1/2 + i\nu_1 + i\nu_2$  in the same way as described before eq. (3.61). Performing the  $\omega$ -integrations we end with the energy dependence

$$\exp \left[ y_M \chi(\nu_1 + \nu_2 - i\frac{1}{2}) + y_s (\chi(\nu_1) + \chi(\nu_2)) + (i\nu_1 + i\nu_2) \log \frac{\Delta^2}{Q^2} \right] \quad (3.73)$$

Depending on the relative magnitude of  $y_M$ ,  $y_s$  and  $\log \Delta^2/Q^2$  very different energy dependences are obtained. We will assume that  $y_s$  is the largest parameter, i. e.  $\nu_1$  and  $\nu_2$  are close to zero. Introducing then again  $\nu_+$  and  $\nu_-$  we find the saddle point of  $\nu_-$  at  $\nu_- = 0$ . Imposing the condition  $(\log Q^2/\Delta^2)^3 \gg y_M y_s^2$  we find a saddle point of the  $\nu_+$ -integration at

$$i\nu_{+s} = \sqrt{\frac{N_c \alpha_s}{\pi} \frac{y_M}{\log Q^2/\Delta^2}} \quad (3.74)$$

which leads to the energy dependence

$$\frac{d\sigma^{\gamma^*P}}{dt dM^2}|_{t=0} \sim \left( \frac{s}{M^2} \right)^{8 \log 2 \frac{N_c \alpha_s}{\pi}} \exp \left[ 2 \sqrt{\frac{N_c \alpha_s}{\pi} \log \frac{Q^2}{\Delta^2} \cdot y_M} \right] \quad (3.75)$$

If we instead impose the condition  $\log(\log Q^2/\Delta^2)^3 \ll y_M y_s^2$  the saddle point is located at

$$i\nu_{+s} = - \left[ \frac{1}{14\zeta(3)} \frac{y_M}{y_s} \right]^{\frac{1}{3}} \quad (3.76)$$

from which follows the energy dependence

$$\frac{d\sigma^{\gamma^*P}}{dt dM^2}|_{t=0} \sim \left( \frac{s}{M^2} \right)^{8 \log 2 \frac{N_c \alpha_s}{\pi}} \exp \left[ \frac{3}{2} \frac{N_c \alpha_s}{\pi} (y_M^2 y_s 14\zeta(3))^{\frac{1}{3}} \right] \quad (3.77)$$

In both cases we have retained only the part which follows from the zero order term of the expansion of the exponent around the saddle point. The contribution of the fluctuations have been left out since their treatment depends on the singularity structure of the coefficient function as already shown in the  $q\bar{q}$ -case. Further saddle points have been discussed in [44].

These results demonstrate that the conservation law for the conformal dimensions at  $\mathbf{q}^2 = 0$  has remarkable implications on the energy dependence of the cross section. In particular it is excluded that in all three BFKL amplitudes the point  $\nu = 0$  (the BFKL point) dominates. In the case (3.75) we find the energy dependence of the double-logarithmic (DLA) limit for the upper BFKL-ladder. This corresponds to a large ratio  $Q^2/\Delta_0^2$  where  $\Delta_0^2$  is the effective scale at the triple pomeron vertex. This result confirms the assertion that for  $\mathbf{q}^2 = 0$  the scale at the upper end of the BFKL amplitudes coupling to the proton is not  $Q^2$  but a nonperturbative scale. In (3.77) the upper ladder is also near the DLA limit since  $\nu$  is close to -1. From the energy dependence one can derive an effective scale  $\Delta_0^2 = Q^2 \cdot \exp(-\sqrt[3]{y_M y_s^2} c)$  which determines the scale at the vertex ( $c$  is a constant of order unity). An increase of the mass hence leads to a lowering of the effective scale at the vertex. From both results we conclude that should expect serious modifications of our  $\mathbf{q}^2 = 0$  results from nonperturbative corrections.

### 3.4 Production of $q\bar{q}$ pairs in DIS diffractive dissociation

This section is devoted to the study of deep inelastic diffractive reactions with a final state consisting of the diffracted proton and two jets with large transverse momenta. In lowest order perturbative QCD the jets originate from a quark-antiquark pair which is produced by the virtual photon. We calculate the cross section for the process  $\gamma^*(q) + P(p) \rightarrow q(k) + \bar{q}(q - k + \zeta) + P(p - \zeta)$  (fig. 3.13). We are interested in the limit

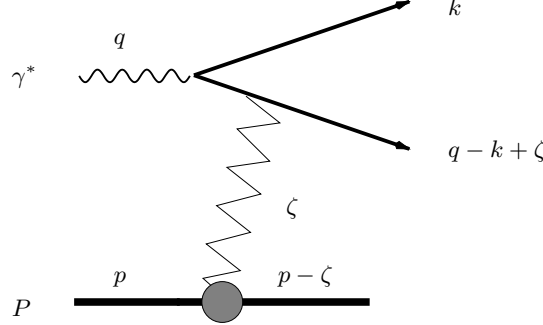


Figure 3.13: Diffractive production of a quark-antiquark pair.

of high photon-proton center of mass energy  $W^2 = (p + q)^2$ , in which the outgoing proton is well separated in rapidity from the  $q\bar{q}$ -pair. Since we regard the process as being mediated by the exchange of a composite object of gluons between the  $q\bar{q}$ -pair and the proton we are forced to conclude that this object is colorless because otherwise the formation of the rapidity gap would be exponentially suppressed, or, stated differently, a produced gap would be filled by final state radiation. As the lowest order contribution we take two-gluon exchange and since we require the transverse momentum  $\mathbf{k}^2$  of the (anti)quark to be large ( $\mathbf{k}^2 \gg \Lambda_{QCD}^2$ ) we treat both gluons perturbatively. A similar approach has been reported in [76] and [77], whereas in [78] the process was studied assuming the exchange of nonperturbative gluons. A different approach towards jet production in diffractive DIS has been pursued in [79] using a semiclassical picture in which the proton is treated as a classical color field.

#### 3.4.1 Kinematics and observables

We begin with some kinematical considerations limiting ourselves to the case of zero momentum transfer  $t = -\zeta^2 = 0$ . For the momenta  $k$  and  $\zeta$  we use a Sudakov decomposition w. r. t. the light cone momenta  $p$  and  $q' = q + xp$  ( $x = Q^2/(2pq)$ )

$$k = \alpha q' + \beta p + \mathbf{k} \quad (3.78)$$

$$\zeta = \alpha_\zeta q' + x_P p + \Delta \quad (3.79)$$

Using the mass shell conditions and the fact that  $W^2$  is the large variable one can show that  $\alpha_\zeta$  and  $\Delta^2$  can be neglected. The phase space can be cast into the form

$$d\Gamma = \frac{\pi}{8pq} \frac{1}{M^2} \frac{1}{\sqrt{1 - 4 \frac{\mathbf{k}^2 + m_f^2}{M^2}}} dM^2 dt d^2\mathbf{k} \quad (3.80)$$

with the quark mass  $m_f$  and  $M^2$  being the invariant mass of the  $q\bar{q}$  pair which is related to the light cone momentum fraction  $\alpha$  through the important relation

$$\alpha(1 - \alpha)M^2 = \mathbf{k}^2 + m_f^2 \quad (3.81)$$

Energy-momentum conservation leads to the phase space restriction  $M^2 \geq 4(\mathbf{k}^2 + m_f^2)$ . Furthermore the longitudinal momentum fraction  $x_P$  transferred from the proton to the  $q\bar{q}$  pair is fixed as

$$x_P = \frac{M^2 + Q^2}{W^2 + Q^2} \quad (3.82)$$

Another variable often used is  $\beta$  defined as

$$\beta = \frac{Q^2}{Q^2 + M^2} \quad (3.83)$$

and one has  $\beta = x/x_P$ . In addition we introduce two angular observables which can be defined from scalar products of the quark momentum with the momenta of the incoming particles. Going to the  $q\bar{q}$  cms in which quark and antiquark are produced back-to-back we define the angle  $\theta$  between the proton direction and the outgoing quark (or antiquark) which points into the proton hemisphere. One should remark here that the cross section of the process is symmetric w. r. t. to the exchange of quark and antiquark. For  $\theta$  we find the relation  $\sin^2 \theta = 4\mathbf{k}^2/M^2$ . In terms of  $\alpha$  one has  $\cos \theta = 1 - 2\alpha$ . The second angle  $\phi$  is defined between the particle which points into the proton hemisphere and the plane formed by the incoming and outgoing electron. The definition of the variables is summarized in fig. 3.14. Introducing the angle  $\phi$  as an additional observable

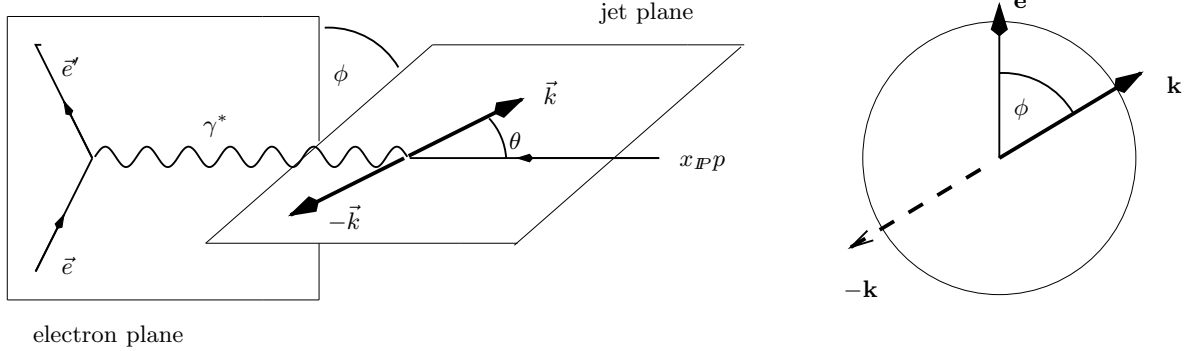


Figure 3.14: Definition of planes and angles in the  $q\bar{q}$  cms. The right hand side displays the projection onto the transverse plane perpendicular to the proton direction.

one obtains a more complicated expression for the electron-proton cross section than in inclusive (angle integrated) DIS. Using the Sudakov decomposition of the electron momentum  $e = 1/yq' + x(1-y)/yp + \mathbf{e}$  one finds for the lepton tensor

$$\begin{aligned} L_{\mu\nu} &= \frac{1}{2} \left[ 2e_\mu e_\nu - g_{\mu\nu} \frac{Q^2}{2} \right] \\ &= \left[ 4(1-y) \frac{x^2}{y^2} p_\mu p_\nu + \mathbf{e}_\mu \mathbf{e}_\nu - g_{\mu\nu}^\perp \frac{Q^2}{4} + (2-y) \frac{x}{y} (p_\mu \mathbf{e}_\nu + p_\nu \mathbf{e}_\mu) \right] \\ g_{\mu\nu}^\perp &= g_{\mu\nu} - (p_\mu q'_\nu + p_\nu q'_\mu)/pq' \end{aligned} \quad (3.84)$$

The different terms in this expression represent the contributions of photons with different polarization states. The first term correspond to the scattering of longitudinal photons, the second and third term belong to transversely polarized photons and the fourth term is an interference term.

### 3.4.2 Formalism and result for the cross section

As to the hadronic tensor we use the high energy factorization theorem to express the amplitude of the photon-proton scattering in terms of the unintegrated gluon density of the proton, which was discussed in

section 3.1. The relevant diagrams for the amplitude are shown in fig. 3.15 and the hadronic tensor has the form

$$H^{\mu\nu} = \left| \int d\mathbf{l}^2 C(\mathbf{l}^2; \mathbf{k}^2, Q^2, M^2) \mathcal{F}_G(x_P, \mathbf{l}^2) \right|_{\mu\nu}^2 \quad (3.85)$$

with the coefficient function  $C_\mu$ <sup>14</sup>. This factorization is valid in the leading-log ( $1/x_P$ ) approximation, in which the imaginary part of the diagrams in fig. 3.15 contributes. In contrast to inclusive DIS where the

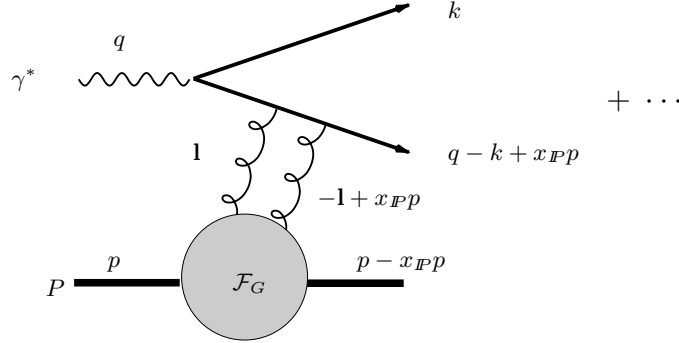


Figure 3.15: Representation of the amplitude in terms of the unintegrated gluon structure function. The dots represent three other diagrams which are generated by attaching the gluons to the quark lines in all possible ways.

cross section is given as the imaginary part of a true forward amplitude, in the present case the longitudinal momenta of the gluons coupling to the quarks are not symmetric. Their difference in longitudinal momentum fraction is  $x_P$  which is needed to transform the virtual photon into a real  $q\bar{q}$  - state. Consequently the longitudinal momentum argument of  $\mathcal{F}_G$  is not well-defined. To leading-log ( $1/x_P$ ) accuracy, to which this study is restricted, this difference does not contribute since in this approximation the longitudinal momenta of both gluons are neglected relative to the longitudinal momenta of the gluons one rung below (strongly ordered longitudinal momenta). In order to go beyond this approximation one has to take into account one gluon rung below the  $q\bar{q}$ -pair in a more accurate fashion. One should remark that in the leading-log ( $1/x$ ) approximation the longitudinal momentum argument of the gluon density is not well-defined as a matter of principle.

The calculation of the diagrams in fig. 3.15 is straightforward as soon as one realizes that the gluon polarization proportional to  $p^\mu$  gives the dominant contribution in the small- $x$  limit [71, 72, 73]. Contraction of the lepton tensor and the hadron tensor then gives the following structure for the electron-proton cross section

$$\begin{aligned} \frac{d\sigma^{eP}}{dydQ^2dM^2d\mathbf{k}^2d\phi dt} \Big|_{t=0} &= \frac{\alpha_{\text{em}}}{2yQ^2\pi^2} \left[ \frac{1 + (1-y)^2}{2} \frac{d\sigma_{D,T}^{*p}}{dM^2d\mathbf{k}^2dt} \Big|_{t=0} - 2(1-y) \cos 2\phi \frac{d\sigma_{D,A}^{*p}}{dM^2d\mathbf{k}^2dt} \Big|_{t=0} \right. \\ &\quad \left. + (1-y) \frac{d\sigma_{D,L}^{*p}}{dM^2d\mathbf{k}^2dt} \Big|_{t=0} + (2-y) \sqrt{1-y} \cos \phi \frac{d\sigma_{D,I}^{*p}}{dM^2d\mathbf{k}^2dt} \Big|_{t=0} \right] \quad (3.86) \end{aligned}$$

where the indices T, L, and I refer to the contributions of transverse and longitudinal photons and the interference term, respectively. The term with index A is an angular asymmetric contribution which also

<sup>14</sup>The notation in eq. (3.85) has to be understood in the sense that  $C$  carries one Lorentz index.

comes from transverse photons. The expressions for the photon-proton cross sections read

$$\begin{aligned} \frac{d\sigma_{D,T}^{\gamma^*P}}{dM^2 d\mathbf{k}^2 dt}|_{t=0} &= \frac{1}{M^4} \frac{1}{\mathbf{k}^2} \frac{1}{12} \sum_f e_f^2 \alpha_{\text{em}} \pi^2 \alpha_s^2 \frac{\mathbf{k}^2 + m_f^2}{\sqrt{1 - 4 \frac{\mathbf{k}^2 + m_f^2}{M^2}}} \left[ \left( 1 - 2 \frac{\mathbf{k}^2 + m_f^2}{M^2} \right) [I_T(Q^2, M^2, \mathbf{k}^2, m_f^2)]^2 \right. \\ &\quad \left. + 4m_f^2 \frac{\mathbf{k}^2 M^4}{(\mathbf{k}^2 + m_f^2)^2 Q^4} [I_L(Q^2, M^2, \mathbf{k}^2, m_f^2)]^2 \right] \end{aligned} \quad (3.87)$$

$$\frac{d\sigma_{D,L}^{\gamma^*P}}{dM^2 d\mathbf{k}^2 dt}|_{t=0} = \frac{1}{M^4} \frac{1}{Q^2} \frac{4}{3} \sum_f e_f^2 \alpha_{\text{em}} \pi^2 \alpha_s^2 \frac{\mathbf{k}^2 + m_f^2}{\sqrt{1 - 4 \frac{\mathbf{k}^2 + m_f^2}{M^2}}} [I_L(Q^2, M^2, \mathbf{k}^2, m_f^2)]^2 \quad (3.88)$$

$$\frac{d\sigma_{D,I}^{\gamma^*P}}{dM^2 d\mathbf{k}^2 dt}|_{t=0} = \frac{1}{M^4} \frac{1}{\sqrt{\mathbf{k}^2 Q^2}} \frac{1}{3} \sum_f e_f^2 \alpha_{\text{em}} \pi^2 \alpha_s^2 (\mathbf{k}^2 + m_f^2) I_T(Q^2, M^2, \mathbf{k}^2, m_f^2) I_L(Q^2, M^2, \mathbf{k}^2, m_f^2) \quad (3.89)$$

$$\frac{d\sigma_{D,A}^{\gamma^*P}}{dM^2 d\mathbf{k}^2 dt}|_{t=0} = \frac{1}{M^6} \frac{1}{\mathbf{k}^2} \frac{1}{12} \sum_f e_f^2 \alpha_{\text{em}} \pi^2 \alpha_s^2 \frac{(\mathbf{k}^2 + m_f^2)^2}{\sqrt{1 - 4 \frac{\mathbf{k}^2 + m_f^2}{M^2}}} [I_T(Q^2, M^2, \mathbf{k}^2, m_f^2)]^2 \quad (3.90)$$

The essential dynamics is contained in the universal functions  $I_T, I_L$  for which we have the following expressions

$$I_L(Q^2, M^2, \mathbf{k}^2, m_f^2) = - \int \frac{d\mathbf{l}^2}{\mathbf{l}^2} \mathcal{F}_G(x_P, \mathbf{l}^2) \left[ \frac{Q^2}{M^2 + Q^2} - \frac{(\mathbf{k}^2 + m_f^2) Q^2}{M^2 \sqrt{P_{\mathbf{k},1}}} \right] \quad (3.91)$$

$$\begin{aligned} I_T(Q^2, M^2, \mathbf{k}^2, m_f^2) &= - \int \frac{d\mathbf{l}^2}{\mathbf{l}^2} \mathcal{F}_G(x_P, \mathbf{l}^2) \left[ \frac{2M^2 \mathbf{k}^2}{(\mathbf{k}^2 + m_f^2)(Q^2 + M^2)} - 1 \right. \\ &\quad \left. + \frac{\mathbf{l}^2 + \frac{\mathbf{k}^2}{M^2}(Q^2 - M^2) + m_f^2(1 + \frac{Q^2}{M^2})}{\sqrt{P_{\mathbf{k},1}}} \right] \end{aligned} \quad (3.92)$$

with  $P_{\mathbf{k},1}$  being defined as

$$P_{\mathbf{k},1} = (\mathbf{l}^2 + \frac{\mathbf{k}^2}{M^2}(Q^2 - M^2) + \frac{m_f^2}{M^2}(Q^2 + M^2))^2 + 4\mathbf{k}^2(\frac{\mathbf{k}^2}{M^2}Q^2 + \frac{m_f^2}{M^2}(Q^2 + M^2)) \quad (3.93)$$

These expressions simplify considerably in the case of massless flavors ( $m_f^2 = 0$ ) [25]. To proceed we need an explicit representation for the unintegrated gluon structure function  $\mathcal{F}_G$ . One could in principle use the relation in eq. (3.8) to calculate  $\mathcal{F}_G$  from the usual gluon density by differentiation and evaluate the  $\mathbf{l}$ -integral numerically [80]. For this one has to introduce an infrared cutoff  $\mathbf{l}_0^2$  since the gluon density is not known for momenta  $\mathbf{l}^2 \lesssim 1 \text{ GeV}^2$ . In this section we prefer to work consistently in the leading-log ( $1/x_P$ ) approximation in which  $\mathcal{F}_G$  is determined by the BFKL resummation. Using the results of section 2.1 we have the following representation for the unintegrated structure function

$$\mathcal{F}_G(x_P, \mathbf{l}^2) = \frac{1}{\Lambda_0^2} \int_{-\infty}^{+\infty} \frac{d\nu}{2\pi} \left( \frac{\mathbf{l}^2}{\Lambda_0^2} \right)^{-\frac{1}{2} - i\nu} \phi(\nu) \exp \left[ \chi(\nu) \log \frac{1}{x_P} \right] \quad (3.94)$$

with  $\Lambda_0^2$  being a nonperturbative scale,  $\phi(\nu)$  an integrable function of  $\nu$  which is analytic in the strip  $-1/2 < \text{Im}(\nu) < 1/2$  and  $\chi(\nu)$  the eigenvalue of the BFKL kernel. This representation is inserted into the  $\mathbf{l}$ -integrals in eqs. (3.91), (3.92). It is useful to define the scaling variable

$$\xi = \frac{1}{M^2} \left( Q^2 + \frac{m_f^2}{\mathbf{k}^2} (Q^2 + M^2) \right) \quad (3.95)$$

The results for  $I_L, I_T$  then read

$$I_L(Q^2, M^2, \mathbf{k}^2, m_f^2) = \frac{1}{\Lambda_0^2} \frac{(\mathbf{k}^2 + m_f^2)Q^2}{\mathbf{k}^2 M^2} \frac{1}{1 + \xi} \int_{-\infty}^{+\infty} \frac{d\nu}{2\pi} \phi(\nu) e^{\chi(\nu) \log 1/x_P} \Gamma\left(\frac{1}{2} + i\nu\right) \Gamma\left(\frac{1}{2} - i\nu\right) \left[ \frac{\mathbf{k}^2}{\Lambda_0^2} (1 + \xi) \right]^{-\frac{1}{2} - i\nu} {}_2F_1\left(\frac{3}{2} + i\nu, -\frac{1}{2} - i\nu, 1; \frac{1}{1 + \xi}\right) \quad (3.96)$$

$$I_T(Q^2, M^2, \mathbf{k}^2, m_f^2) = \frac{1}{\Lambda_0^2} \frac{2}{1 + \xi} \int_{-\infty}^{+\infty} \frac{d\nu}{2\pi} \phi(\nu) e^{\chi(\nu) \log 1/x_P} \Gamma\left(\frac{1}{2} + i\nu\right) \Gamma\left(\frac{1}{2} - i\nu\right) \left(\frac{3}{2} + i\nu\right) \left[ \frac{\mathbf{k}^2}{\Lambda_0^2} (1 + \xi) \right]^{-\frac{1}{2} - i\nu} {}_2F_1\left(\frac{3}{2} + i\nu, -\frac{1}{2} - i\nu, 2; \frac{1}{1 + \xi}\right) \quad (3.97)$$

Note that since  $\xi > 0$  (for  $Q^2 \neq 0$ ) the argument of the hypergeometric function is in the unit circle, which means that this part of the integrand is an analytic function of  $\nu$ , even for imaginary  $\nu$ . The important variable which emerges from the calculation is the dimensionless ratio

$$\Delta = \frac{\mathbf{k}^2}{\Lambda_0^2} (1 + \xi) = \frac{Q^2 + M^2}{M^2} \cdot \frac{\mathbf{k}^2 + m_f^2}{\Lambda_0^2} \quad (3.98)$$

For the perturbative QCD calculation to be reliable one should postulate  $\Delta \gg 1$ . If we set  $m_f^2 = m_c^2$  (charm quarks) this relation is fulfilled for all  $\mathbf{k}^2$ , but for the three light flavours the result has to be restricted to large transverse momenta  $\mathbf{k}^2 \geq 1 \text{ GeV}^2$ . For DIS ( $Q^2 > 0$ ) the 'hardness' of the process is enhanced due to multiplication with the ratio  $(Q^2 + M^2)/M^2$ .

The  $\nu$ -integration in eqs. (3.96), (3.97) can be performed using the saddle point approximation. In the case  $\log 1/x_P \gg \log \Delta$  the saddle point is located at  $i\nu = 0$  and one obtains the usual BFKL results with the power rise in  $1/x_P$ . We give them here for completeness, although this is not the main objective of the section.

$$I_L = \frac{(\mathbf{k}^2 + m_f^2)Q^2}{M^2 \sqrt{\Lambda_0^2 [\mathbf{k}^2 (1 + \xi)]^3}} \pi {}_2F_1\left(\frac{3}{2}, -\frac{1}{2}, 1; \frac{1}{1 + \xi}\right) \left(\frac{1}{x_P}\right)^{\frac{N_c \alpha_s}{\pi} 4 \log 2} \frac{e^{-\frac{N_c \alpha_s}{\pi} \frac{\log^2 \Delta}{\log 1/x_P 56 \zeta(3)}}}{\sqrt{N_c \alpha_s \log 1/x_P 56 \zeta(3)}} \quad (3.99)$$

$$I_T = \frac{1}{\sqrt{\Lambda_0^2 [\mathbf{k}^2 (1 + \xi)]^3}} 3\pi {}_2F_1\left(\frac{3}{2}, -\frac{1}{2}, 2; \frac{1}{1 + \xi}\right) \left(\frac{1}{x_P}\right)^{\frac{N_c \alpha_s}{\pi} 4 \log 2} \frac{e^{-\frac{N_c \alpha_s}{\pi} \frac{\log^2 \Delta}{\log 1/x_P 56 \zeta(3)}}}{\sqrt{N_c \alpha_s \log 1/x_P 56 \zeta(3)}} \quad (3.100)$$

In the opposite case,  $\log 1/x_P \ll \log \Delta$ , the exponent becomes stationary at

$$i\nu_s = 1/2 - \sqrt{\frac{N_c \alpha_s}{\pi} \frac{\log(1/x_P)}{\log \Delta}} \quad (3.101)$$

which leads to the double-logarithmic approximation for  $I_L, I_T$

$$I_L = \frac{(\mathbf{k}^2 + m_f^2)Q^2}{\mathbf{k}^4 M^2} \frac{\xi - 1}{(1 + \xi)^3} x_P f_G(x_P, \mathbf{k}^2 (1 + \xi)) \quad (3.102)$$

$$I_T = \frac{4}{\mathbf{k}^2} \frac{\xi}{(1 + \xi)^3} x_P f_G(x_P, \mathbf{k}^2 (1 + \xi)) \quad (3.103)$$

where we have used the identity (cf. eq. (3.5))

$$x_P f_G(x_P, \mathbf{k}^2 (1 + \xi)) = \sqrt{\frac{\pi}{4}} \left[ \frac{N_c \alpha_s}{\pi} \frac{\log(1 + \xi) \mathbf{k}^2 / \Lambda_0^2}{\log 1/x_P} \right]^{\frac{1}{4}} \exp \sqrt{4 \frac{N_c \alpha_s}{\pi} \log(1 + \xi) \frac{\mathbf{k}^2}{\Lambda_0^2} \log \frac{1}{x_P}} \phi(\nu_s) \quad (3.104)$$

This double logarithmic approximation (in  $1/x_P$  and  $\mathbf{k}^2 (1 + \xi)$ ) could have been obtained directly from eqs. (3.91), (3.92) by assuming dominance of the phase space region  $\mathbf{l}^2 \ll \mathbf{k}^2 (1 + \xi)$  and corresponding expansion

of the integrand. Retaining the leading term of this expansion and using the basic relation (3.8) then leads to the above results. The scale of the gluon structure function emerges as the upper limit of the  $\mathbf{l}^2$ -integration which in turn is determined by the consistency of the expansion.

We will first concentrate on the case of massless flavors ( $m_f^2 = 0$ ) in which we have  $\xi = Q^2/M^2$ . Then we find that in the photoproduction limit ( $Q^2 = 0$ ) or, equivalently, in the large mass limit ( $M^2 \rightarrow \infty$ ) both  $I_L$  and  $I_T$  vanish. For  $I_L$  this has to be the case, of course, since longitudinally polarized real photons do not exist. Since, on the other hand, we expect a contribution from transversely polarized real photons, we have to conclude that the double logarithmic approximation is a poor one for  $Q^2 \rightarrow 0$  ( $M^2 \rightarrow \infty$ ). In the extreme case  $Q^2 = 0$  the term in squared brackets in eq. (3.92) equals  $2\theta(\mathbf{l}^2 - \mathbf{k}^2)$ , i. e. the DLA phase space does not contribute. Since  $\mathcal{F}_G(x_P, \mathbf{l}^2)$  decreases as  $1/\mathbf{l}^2$  (mod. logarithms) for large  $\mathbf{l}^2$  the integrand in eq. (3.92) is  $2\theta(\mathbf{l}^2 - \mathbf{k}^2)$  times a rapidly decreasing function of  $\mathbf{l}^2$  and consequently is dominated by the region  $\mathbf{l}^2 \simeq \mathbf{k}^2$ . It follows that one gets the result  $I_T \sim \mathcal{F}_G(x_P, \mathbf{k}^2) \sim \partial/\partial \mathbf{k}^2 x_P f_G(x_P, \mathbf{k}^2)$ . Such subleading corrections (in the DLA sense) can be obtained from the exact expressions (3.96), (3.97) if we, for  $i\nu = 1/2 - \delta$ , do not only retain the pole term (proportional to  $1/\delta$ ) of the coefficient function, but also the constant. Using the fact that the constant can be associated with the unintegrated structure function we find the following correction terms for  $I_L$  and  $I_T$

$$I_L^{(c)} = \frac{(\mathbf{k}^2 + m_f^2)Q^2}{\mathbf{k}^2 M^2} \frac{1}{(1 + \xi)^3} \left( 2 + (1 - \xi) \log \frac{\xi}{1 + \xi} \right) \frac{\partial}{\partial \mathbf{k}^2} x_P f_G(x_P, \mathbf{k}^2(1 + \xi)) \quad (3.105)$$

$$I_T^{(c)} = 2 \frac{1}{(1 + \xi)^3} \left( 1 - \xi - 2\xi \log \frac{\xi}{1 + \xi} \right) \frac{\partial}{\partial \mathbf{k}^2} x_P f_G(x_P, \mathbf{k}^2(1 + \xi)) \quad (3.106)$$

where we have restored the mass dependence for the moment. Indeed for  $I_T$  the correction is finite in the limit  $Q^2 = 0$  ( $M^2 \rightarrow \infty$ ). These correction terms represent only a small subset of the complete next-to-leading order corrections. Their numerical significance will be studied below.

If we now insert the above results for  $I_L$  and  $I_T$  into the cross section formulae (3.87)-(3.90) we obtain a parameter free prediction for  $q\bar{q}$ -production in diffractive DIS. It is on the level of double leading logarithmic accuracy with a subset of next-to-leading order corrections included, which means that an uncertainty in the absolute normalization cannot be excluded. The essential feature of the result is the dependence of the cross section on the square of the gluon density, with the scale of the latter being given by a specific combination of the kinematical parameters. The perturbative approach should be justified as long as either  $\mathbf{k}^2$  or  $m_f^2$  (or both) are larger than  $\simeq 1 \text{ GeV}^2$ .

In the perturbative QCD approach used here Regge factorization is explicitly violated. Regge factorization was introduced in [81] to describe diffractive processes with a hard subprocess. Regge factorization states that the diffractive cross section can be written as the product of a  $x_P$ -dependent flux factor (pomeron flux) and a partonic structure function of the pomeron which depends only on  $M^2$  and  $Q^2$ . In our model the  $x_P$ -dependence enters through the function  $x_P f_G(x_P, \mathbf{k}^2(1 + \xi))$  which depends also on  $\mathbf{k}^2$ ,  $Q^2$ ,  $M^2$  and  $m_f^2$ , i. e. the flux is controlled by the hard scales of the process and factorization is broken. Our analysis is of course limited to specific final states (jets or heavy flavors) and we cannot make a statement on the fully inclusive diffractive cross section which might well be described approximately by Regge factorization.

We now turn to the numerical evaluation of the cross section formulae (3.87)-(3.90). In all subsequent calculations we have used running  $\alpha_s$  with the scale being given by the scale of the gluon structure function. The results above have been given for  $t = 0$  where the cross section has its maximum. Experiments, however, cover a finite  $t$ -range and to obtain more realistic event rates we should integrate over  $t$ . The continuation of the results to finite  $t$  can be done by using the non-forward BFKL pomeron for the unintegrated gluon structure function. This leads to quite complicated expressions which do not allow for a straightforward evaluation. In order to keep the analysis simple we continue to finite  $t$  by simply multiplying our expressions for  $t = 0$  with the elastic proton form factor which has been given by Donnachie and Landshoff [82] and a factor which takes into account the  $t$ -dependence of the soft pomeron trajectory [67]

$$F_P(x_P, t) = \frac{4 - 2.8 \frac{t}{\text{GeV}^2}}{4 - \frac{t}{\text{GeV}^2}} \left( 1 - \frac{t}{0.7 \text{ GeV}^2} \right)^{-0.25 \frac{t}{\text{GeV}^2}} x_P \quad (3.107)$$

With this continuation the  $t$ -integration can even be done analytically.

Since our results depend on the gluon density, for a numerical evaluation we have to decide which parametrization to use. We choose the gluon density of GRV [83] because it allows for a simple implementation using the explicit formula which covers the whole  $x, Q^2$  range. A more fundamental question is whether the leading or the next-to-leading order gluon density should be used. Since we have included at least some subleading corrections the use of the next-to-leading order parameterization is not totally inconsistent. For comparison we have performed a calculation of  $F_2$  with the same type of approximations as done above, i.e. we have calculated the DLA-contribution and the first subleading corrections given by the constant parts of the coefficient function. The results are shown in fig. 3.16 where comparison is made with experimental data. For

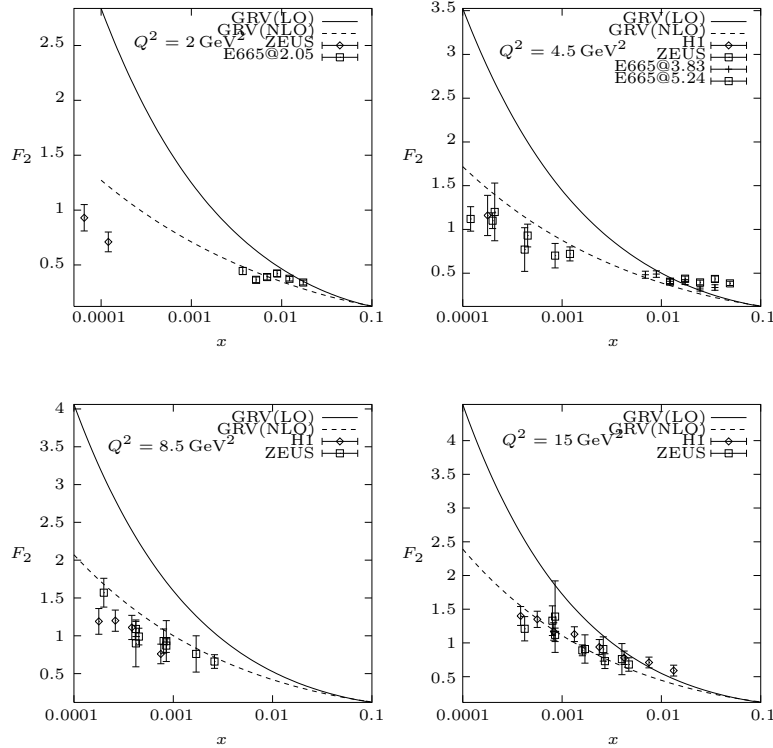


Figure 3.16: Comparison of  $F_2$  calculated with the leading order (solid line) and next-to-leading order (dashed line) GRV gluon density with experimental data from H1 [10], ZEUS [11] and E665 [60].

$F_2$  we get a much better description by using the next-to-leading order parameterization and we take this as a justification to use it in the calculation of diffractive DIS as well, admitting of course that we do not have a solid theoretical foundation for this prescription.

### 3.4.3 Numerical results

We start our numerical analysis with giving integrated electron-proton cross sections for  $q\bar{q}$ -pair production in DIS diffractive dissociation for three massless flavors. All phase space variables are integrated using a Monte-Carlo integration algorithm [68]. The available phase space is constrained by the cuts  $Q^2 > 10 \text{ GeV}^2$ ,  $x_P < 10^{-2}$  and  $50 \text{ GeV} < W < 220 \text{ GeV}$  ( $W^2 = (p + q)^2$ ), corresponding to typical HERA values. For  $\mathbf{k}^2$  we have chosen three different lower cut-offs  $2 \text{ GeV}^2$ ,  $4 \text{ GeV}^2$  and  $8 \text{ GeV}^2$ . In table 3.1 we show the results both for the GRV leading and the next-to-leading order gluon density. To demonstrate the magnitude of the corrections we compare the result containing the corrections with the pure DLA result. The numbers show that the jet cross section is strongly suppressed at large  $\mathbf{k}^2$ . The ratio of the longitudinal cross section



	$\mathbf{k}_0^2 = 2\text{GeV}^2$		$\mathbf{k}_0^2 = 4\text{GeV}^2$		$\mathbf{k}_0^2 = 8\text{GeV}^2$	
	GRV(LO)	GRV(NLO)	GRV(LO)	GRV(NLO)	GRV(LO)	GRV(NLO)
DLA + corrections						
$\sigma_T^{eP}$	193	108	49	30	8	6
$\sigma_L^{eP}$	15	9	3	2	1	0.6
$\sum_{i=T,L} \sigma_i^{eP}$	208	117	52	32	9	6.6
DLA						
$\sigma_T^{eP}$	113	56	28	16	5	3
$\sigma_L^{eP}$	10	5	4	2	1.5	0.9
$\sum_{i=T,L} \sigma_i^{eP}$	123	61	32	18	6.5	3.9

Table 3.1: Results for total  $eP$ -cross sections (in pbarn) of diffractive dijet production for two different parameterizations of the gluon density and three different cuts on the transverse momentum of the jets.

to the transverse one is of the order of 1:10. The other conclusion to be drawn is that the corrections are substantial, especially for the transverse cross section, where they are almost as large as the leading term. It becomes clear from the numbers that an experimental analysis of the process requires a very good transverse momentum resolution.

Next we turn to the most prominent feature of the cross section, namely its  $x_P$ -distribution. Being proportional to the gluon density squared the cross section rises steeply at small  $x_P$ . Mainly due to this enhancement there might be a chance to observe this type of event at HERA, although it is strongly momentum suppressed (it is a higher twist effect). Due to the strong sensitivity to the gluon density the process might in the long run serve as a means to discriminate between different sets of gluon distributions. Compared with diffractive vector meson production [84] it has the advantage that the cross section does not depend on a theoretically poorly determined quantity like the vector meson wave function. The  $x_P$ -dependence of the  $\gamma^*$ -proton cross section is displayed in fig. 3.17, separately for the transverse and the longitudinal part. The kinematical parameters are chosen as  $Q^2 = 50\text{GeV}^2$ ,  $\beta = 2/3$  and  $\mathbf{k}^2$  is integrated from  $2\text{GeV}^2$  to the phase space boundary. We show both the results based on the leading order and next-to-leading order gluon densities to demonstrate the strong sensitivity to this quantity. In fig. 3.18 we take a closer look on the slope of the cross section and its dependence on the parameters  $\mathbf{k}^2$  and  $\beta$ . For massless flavors the scale of the gluon density is  $\mathbf{k}^2/(1-\beta)$  and it is known that an increase of the momentum scale leads to an increase of the slope. We choose three different combinations of  $\mathbf{k}^2$  and  $\beta$  and display the normalized transverse cross section, calculated with the GRV next-to-leading order gluon density. The results from a fit to the function  $(1/x_P)^\alpha$  confirm the expectation. The slope increases with increasing  $\mathbf{k}^2/(1-\beta)$ , demonstrating the breaking of Regge factorization.

Next we want to present a more detailed discussion of the  $\mathbf{k}^2$ -dependence of the transverse and longitudinal cross section, again for massless flavors. From the expressions for  $I_L$  and  $I_T$  and the cross section formulae (3.87), (3.88) we see that for large  $\mathbf{k}^2$  the transverse cross section falls roughly as  $1/\mathbf{k}^4$  whereas the longitudinal one decreases like  $1/\mathbf{k}^2$ . This power behavior is modified by the  $\mathbf{k}^2$ -dependent scaling violations of the gluon density which cause a logarithmic enhancement for larger  $\mathbf{k}^2$  and a flattening of the power behavior for small  $\mathbf{k}^2$ . In addition we have the (integrable) Jacobi singularity  $1/\sqrt{1-4\mathbf{k}^2/M^2}$  which changes the power fall-off, although in a region where the cross section is rather small. The situation for  $d\sigma_T^{\gamma^*P}$  and  $d\sigma_L^{\gamma^*P}$  is summarized in figs. 3.19 - 3.22 where we display  $\mathbf{k}$ -spectra for different  $Q^2$  at fixed  $\beta$  and for different  $\beta$  at fixed  $Q^2$ . In the figures we give results of a fit to a behavior  $(\mathbf{k}^2)^{-\delta}$  for each curve. From fig. 3.21 it can be seen that a variation in  $\beta$  indeed has a substantial effect on the slope. Due to the scaling violations an increase in  $1/(1-\beta)$  leads to a drastic modification of the global power behavior  $(\mathbf{k}^2)^{-2}$ . What is seen in fig. 3.22 is a zero of the longitudinal cross section in  $(\mathbf{k}^2, Q^2, M^2)$ -space. In the DLA the longitudinal cross section has a zero at  $Q^2 = M^2$  ( $\xi = 1$ ), but when the corrections are taken into account, this zero becomes

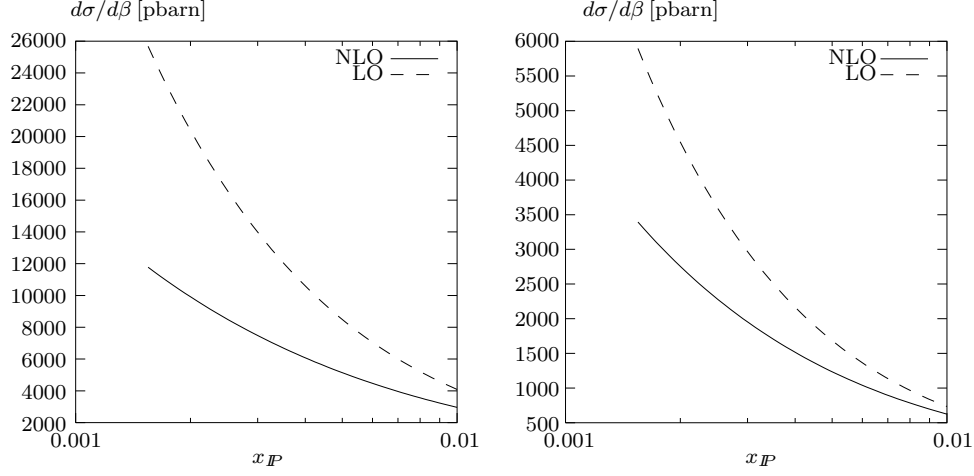


Figure 3.17:  $x_P$ -distribution of  $d\sigma_{T,L}^{\gamma^*P}/d\beta$  for fixed  $Q^2 = 50 \text{ GeV}^2$ ,  $\beta = 2/3$  and  $\mathbf{k}^2$  integrated from  $2 \text{ GeV}^2$  to  $M^2/4$ . The transverse cross section is on the left and the longitudinal one on the right hand side.

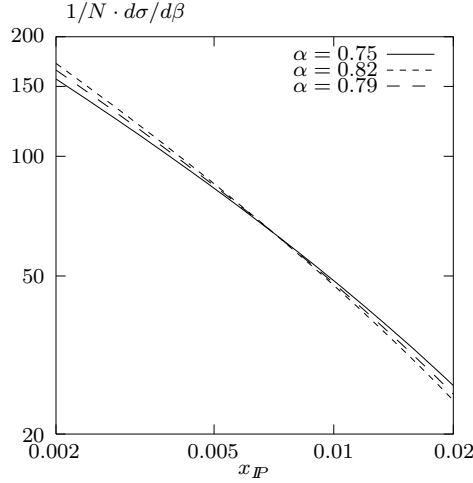


Figure 3.18:  $x_P$ -distribution of  $1/N d\sigma_T^{\gamma^*P}/d\beta$  ( $N$  is the integral of the cross section over the  $x_P$ -range displayed). The kinematical parameters are:  $Q^2 = 80 \text{ GeV}^2$ ,  $\beta = 2/3$ ,  $\mathbf{k}^2$  integrated between 2 and  $4 \text{ GeV}^2$ ;  $Q^2 = 80 \text{ GeV}^2$ ,  $\beta = 2/3$ ,  $\mathbf{k}^2$  integrated between 4 and  $8 \text{ GeV}^2$  and  $Q^2 = 80 \text{ GeV}^2$ ,  $\beta = 5/6$ ,  $\mathbf{k}^2$  integrated between 2 and  $4 \text{ GeV}^2$ . The variable  $\alpha$  denotes the slope of each curve.

$\mathbf{k}^2$ -dependent, due to the nontrivial  $\mathbf{k}^2$ -dependence of the ratio  $f_G(x_P, \mathbf{k}^2(1+\xi))/\partial_{\mathbf{k}^2} f_G(x_P, \mathbf{k}^2(1+\xi))$ .

The angular asymmetric term  $d\sigma_A^{\gamma^*P}$  which will be discussed in detail later has the same  $\mathbf{k}^2$ -dependence as the longitudinal cross section (for  $m_f^2 = 0$ ). This means that the asymmetry is enhanced at larger  $\mathbf{k}^2$ .

It is also worthwhile to have a closer look on the small  $\mathbf{k}^2$ -behavior of the cross section, although this does not correspond to the production of jets anymore. First, for  $m_f^2 = 0$ , we observe from eqs. (3.96) and (3.97) that  $I_L$  and  $I_T$  behave the same for  $\mathbf{k}^2 \rightarrow 0$ , up to constants. For  $\mathbf{k}^2 \ll \Lambda_0^2$  one can expand around the saddle point at  $i\nu_s = -1/2 + \sqrt{N_c\alpha_s/\pi} \log(1/x_P)/\bar{\Delta}$  and finds  $I_L, I_T \sim \text{const.}$  up to logarithms and the usual double logarithmic exponent(cf. eq. (3.104)). Inserting this into the cross section formulae (3.87),

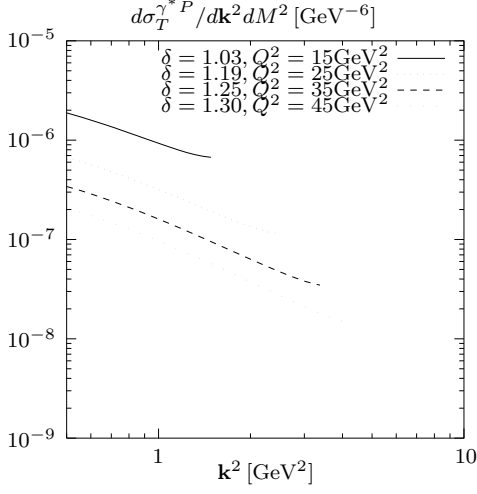


Figure 3.19:  $\mathbf{k}^2$ -spectra for transverse photons:  $x_P = 5 \cdot 10^{-3}$ , fixed  $\beta = 2/3$ .

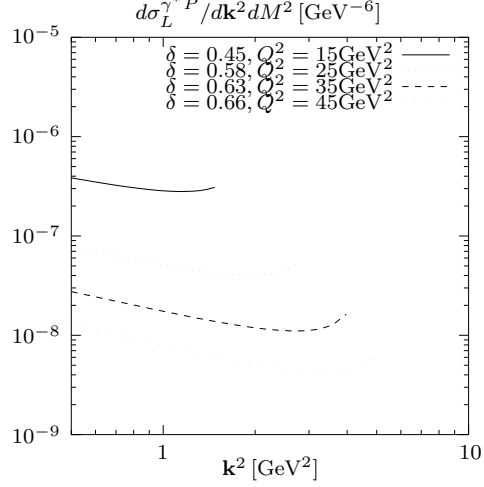


Figure 3.20:  $\mathbf{k}^2$ -spectra for longitudinal photons:  $x_P = 5 \cdot 10^{-3}$ , fixed  $\beta = 2/3$ .

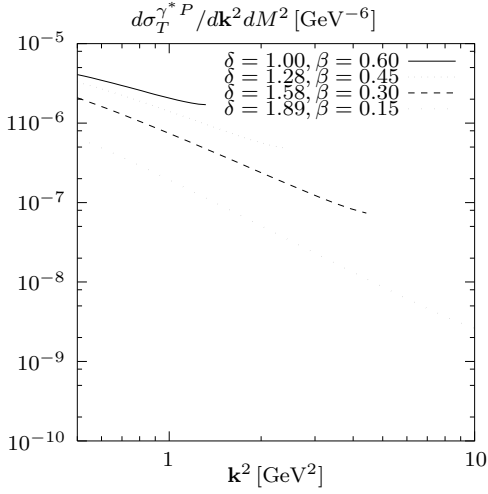


Figure 3.21:  $\mathbf{k}^2$ -spectra for transverse photons:  $x_P = 5 \cdot 10^{-3}$ , fixed  $Q^2 = 10 \text{ GeV}^2$ .

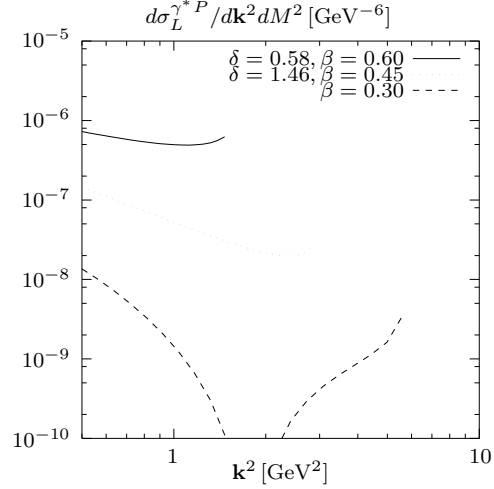


Figure 3.22:  $\mathbf{k}^2$ -spectra for longitudinal photons:  $x_P = 5 \cdot 10^{-3}$ , fixed  $Q^2 = 10 \text{ GeV}^2$ .

(3.88) one finds that  $d\sigma_L^{\gamma^*P}$  vanishes for  $\mathbf{k}^2 \rightarrow 0$  and that  $d\sigma_T^{\gamma^*P}$  approaches a constant. This can be traced back to the fact that the photon wave function has a different end-point behavior in the longitudinal and transverse case. The wave function of a  $\gamma_L^*$  is proportional to  $\alpha(1-\alpha) \sim \mathbf{k}^2$  and vanishes at the end-points  $\alpha = 0, \alpha = 1$ . The wave function of a  $\gamma_T^*$ , on the other hand is proportional to  $\alpha^2 + (1-\alpha)^2 \sim 1 - 2\mathbf{k}^2/M^2$  and does not vanish at the end points. Nonvanishing end-point contributions can be associated with large non-perturbative effects because the cross section is then dominated by the region where  $\mathbf{k}^2$  is small. One can conclude that in cases where one would like to integrate over  $\mathbf{k}^2$ , e. g. in vector meson production or in inclusive diffractive scattering, the transverse cross section receives large nonperturbative contributions whereas the perturbative result for the longitudinal cross section is rather stable.

We finish the numerical calculations with the  $\beta$ -spectra for the longitudinal and transverse case, shown in fig. 3.23. We have kept  $x_P$  fixed and have integrated  $\mathbf{k}^2$  from  $2 \text{ GeV}^2$  to the phase space boundary. The minimal  $\mathbf{k}^2$  leads to a maximal  $\beta$ . The transverse cross section has a maximum at  $\beta \simeq 0.4$  and tends to zero

for  $\beta \rightarrow 0$  and  $\beta \rightarrow 1$ . The longitudinal cross section has a zero at  $\beta \simeq 0.4$  and also goes to zero for  $\beta \rightarrow 0$  and  $\beta \rightarrow 1$ . The zero at  $\beta \simeq 0.4$  is the zero of the DLA at  $\beta = 1/2$  shifted due to the subleading corrections. Only for  $\beta \rightarrow 1$  the longitudinal cross section becomes comparable in magnitude to the transverse one.

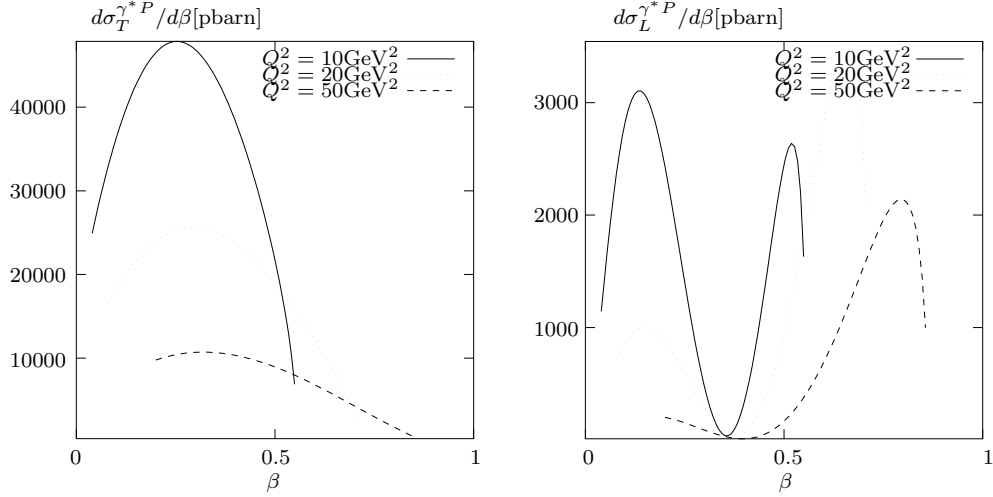


Figure 3.23: The  $\beta$ -dependence of the transverse and longitudinal cross section for  $x_P = 5 \cdot 10^{-3}$ ,  $\mathbf{k}^2$  integrated from  $2 \text{ GeV}^2$  to the phase space boundary and for different values of  $Q^2$ .

### 3.4.4 The angular asymmetry

We now come to the discussion of the angular dependence of the electron-proton cross section. The dependence upon the angle  $\theta$  is not so interesting since this can be derived easily from the dependence upon  $\mathbf{k}^2$  due to the simple relation  $\sin^2 \theta = 4\mathbf{k}^2/M^2$ . It is clear that the jets are concentrated near the incoming proton direction and large angle scattering is strongly suppressed.

The dependence upon  $\phi$  is more interesting, not alone since a measurement of the  $\phi$ -distribution allows to disentangle the transverse and the longitudinal contribution. We have two asymmetric terms, the term  $d\sigma_A^{\gamma^*P} \sim \cos 2\phi$  which is symmetric w. r. t.  $\phi = \pi$  and the interference term  $d\sigma_I^{\gamma^*P} \sim \cos \phi$  which is antisymmetric w. r. t.  $\phi = \pi$ . It follows that the interference contribution can be eliminated by adding the contributions at  $\phi$  and  $\phi + \pi$ . For  $d\sigma_A^{\gamma^*P}$  we note that this term has an additional factor  $(\mathbf{k}^2 + m_f^2)/M^2$  compared to the angular symmetric transverse term  $d\sigma_T^{\gamma^*P}$ . This offers the possibility to enhance the  $\phi$ -asymmetry by restricting measurements to larger  $\mathbf{k}^2$ . It is remarkable that the  $d\sigma_A^{\gamma^*P}$  contribution enters the electron-proton cross section with a negative sign, i. e. the jets which are produced in DIS diffractive dissociation prefer to lie in a plane perpendicular to the plane defined by the incoming and outgoing electron. These features of the  $\cos 2\phi$  asymmetry are illustrated in fig. 3.24. We have again calculated the integrated electron proton cross section with cuts  $Q^2 > 10 \text{ GeV}^2$ ,  $x_P < 10^{-2}$ ,  $50 \text{ GeV} < W < 220 \text{ GeV}$  and three different bins in  $\mathbf{k}^2$ . The contributions at  $\phi$  and  $\phi + \pi$  are added, hence the interference term drops out and the total cross section is recovered by integrating  $\phi$  from 0 to  $\pi$ . As expected for larger  $\mathbf{k}^2$  the asymmetry becomes enhanced. We find a factor of 8/5 between  $\phi = \pi/2$  and  $\phi = 0$  for the lowest  $\mathbf{k}^2$ -bin and a factor of 3 for the highest  $\mathbf{k}^2$ -bin.

The point which deserves further discussion is the peak of the diffractive cross section at  $\phi = \pi/2$ , i. e. the negative sign of the  $\cos 2\phi$ -term. Inspection of  $q\bar{q}$ -pair production in the photon-gluon fusion process (i. e. one-gluon exchange between the  $q\bar{q}$ -pair and the proton) shows [85] that in this case the  $\cos 2\phi$ -term has a positive sign, i. e. the cross section has a minimum at  $\phi = \pi/2$ . Adding a further gluon in the  $t$ -channel hence

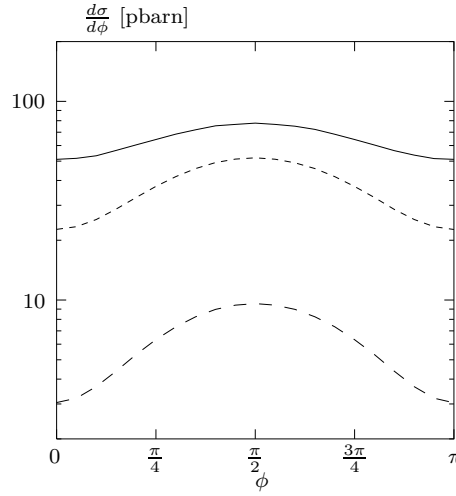


Figure 3.24: The total  $eP$ -cross section as a function of  $\phi$  with  $\mathbf{k}^2$  integrated from  $1 \text{ GeV}^2$  to  $2 \text{ GeV}^2$  (solid curve), from  $2 \text{ GeV}^2$  to the phase space boundary (dotted curve) and from  $5 \text{ GeV}^2$  to the phase space boundary (dashed curve).

completely changes the orientation of the final state. Clearly this striking phenomenon makes the azimuthal distribution a very interesting experimental signal which could be used to test the two-gluon nature of the hard diffractive interaction. We sketch below the derivation of the photon-gluon fusion result to elucidate the origin of the sign change, although a simple physical interpretation, based on angular momentum arguments for example, is not at our hand at the moment.

We use the same formalism as in the two-gluon case, namely  $\mathbf{k}$ -factorization, to calculate the process  $\gamma^*(q) + P(p) \rightarrow q(k) + \bar{q}(q - k + \xi) + X(p - \xi)$  and take  $\xi = \eta p + \mathbf{l}$  ( $\eta = x(1 + M^2/Q^2)$ ). Here in the leading-log( $1/x$ )-approximation the transverse momentum  $\mathbf{l}$  of the exchanged gluon goes into the  $q\bar{q}$ -state, i. e. when we integrate over  $\mathbf{l}$  we do not describe back-to-back  $q\bar{q}$ -production, but inclusive one-jet production (the other jet is integrated). The analogous situation to the diffractive case is only recovered in the collinear (or DLA) limit, when  $\mathbf{l} \rightarrow 0$ . In the photon-gluon case the cross section, not the amplitude, is proportional to the unintegrated gluon structure function. Now, for photon-gluon fusion the contraction of  $\mathbf{e}_\mu \mathbf{e}_\nu$  with the hadronic tensor results in

$$\mathbf{e}^2 [\Phi(\mathbf{k}) - \Phi(\mathbf{k} - \mathbf{l})]^2 - 4\alpha(1 - \alpha) [\mathbf{e} \cdot \Phi(\mathbf{k}) - \mathbf{e} \cdot \Phi(\mathbf{k} - \mathbf{l})]^2 \quad (3.108)$$

$$\text{with } \Phi(\mathbf{k}) = \frac{\mathbf{k}}{\alpha(1 - \alpha)Q^2 + \mathbf{k}^2} \quad (3.109)$$

The corresponding term in the diffractive case reads

$$\begin{aligned} & \mathbf{e}^2 [2\Phi(\mathbf{k}) - \Phi(\mathbf{k} - \mathbf{l}) - \Phi(\mathbf{k} + \mathbf{l})] [2\Phi(\mathbf{k}) - \Phi(\mathbf{k} - \mathbf{l}') - \Phi(\mathbf{k} + \mathbf{l}')] \\ & - 4\alpha(1 - \alpha) [\mathbf{e} \cdot \Phi(\mathbf{k}) - \mathbf{e} \cdot \Phi(\mathbf{k} - \mathbf{l}) - \mathbf{e} \cdot \Phi(\mathbf{k} + \mathbf{l})] [\mathbf{e} \cdot \Phi(\mathbf{k}) - \mathbf{e} \cdot \Phi(\mathbf{k} - \mathbf{l}') - \mathbf{e} \cdot \Phi(\mathbf{k} + \mathbf{l}')] \end{aligned} \quad (3.110)$$

The structures in brackets can be related to the quark-antiquark-gluon components of the light cone wave function of a transversely polarized virtual photon [25]. Now we concentrate on the term proportional to  $\alpha(1 - \alpha)$  since this one will lead to the  $\cos 2\phi$ -dependence. In the collinear limit we have to extract the  $O(\mathbf{l}^2)$  contribution in eq. (3.108) and the  $O(\mathbf{l}^2 \cdot \mathbf{l}'^2)$  contribution in eq. (3.111). In the latter case we can expand

in each bracket separately and get from each bracket an identical coefficient  $\sim \cos \phi$ . The result is

$$-4\alpha(1-\alpha)16\pi^2\mathbf{e}^2\frac{(\mathbf{k}^2)^3}{(\alpha(1-\alpha)Q^2+\mathbf{k}^2)^6}\cos^2\phi \quad (3.111)$$

$$= -4\frac{\mathbf{k}^2}{M^2}16\pi^2\mathbf{e}^2\left(\frac{M^2}{M^2+Q^2}\right)^6\frac{1}{(\mathbf{k}^2)^3}(\cos 2\phi+1) \quad (3.112)$$

where we have used the relation  $\mathbf{k}^2 = M^2\alpha(1-\alpha)$ . The coefficient which contributes in the collinear approximation is a square and as such positive definite. In the photon-gluon fusion situation we have

$$4\alpha(1-\alpha)\pi\mathbf{e}^2\frac{1}{(\alpha(1-\alpha)Q^2+\mathbf{k}^2)^4}(\mathbf{k}^4+\alpha^2(1-\alpha)^2Q^4-2\cos 2\phi\alpha(1-\alpha)Q^2\mathbf{k}^2) \quad (3.113)$$

$$= -4\frac{\mathbf{k}^2}{M^2}\pi\mathbf{e}^2\left(\frac{M^2}{M^2+Q^2}\right)^2\frac{1}{(\mathbf{k}^2)^2}\left(1+\frac{Q^4}{M^4}-2\frac{Q^2}{M^2}\cos 2\phi\right) \quad (3.114)$$

Here the coefficient of the collinear approximation has a more complicated structure in which the  $\cos 2\phi$ -term happens to have a negative sign. This leads to the relative sign compared to the diffractive case.

We compare the (normalized) two-gluon and the one-gluon cross section in fig. 3.25. Several interesting features can be read off from these graphs. The difference between the  $\cos 2\phi$  and the  $-\cos 2\phi$  behavior is clearly visible. Since we have, in contrast to fig. 3.24, not added the contributions at  $\phi$  and  $\phi + \pi$  the effect of the interference term can be seen (we display only the interval of  $\phi$  between 0 and  $\pi$  since the cross section for  $\phi > \pi$  can be obtained by reflection w. r. t. the line  $\phi = \pi$ ). We have  $\beta = 1/3$  on the left hand side and  $\beta = 2/3$  on the right hand side. It is obvious that the  $\cos \phi$ -term has a different sign in these two situations which is due to the zero of  $I_L$  located at  $\beta \simeq 0.4$ . It is furthermore encouraging that the asymmetry is stronger for the diffractive situation than for photon-gluon fusion (corresponding to normal DIS). Since we have no color rearrangement between the jets and the proton in the diffractive case (in contrast to normal DIS), one can expect that the signal is rather stable against hadronization effects. For the normal DIS situation it is known [86] that hadronization effects considerably modify the asymmetry created on the partonic level.

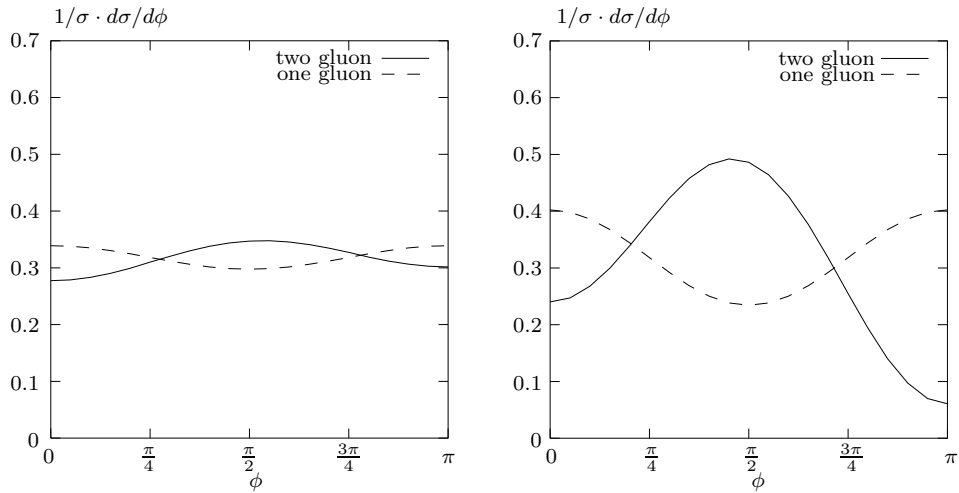


Figure 3.25: The  $\phi$ -distribution of  $q\bar{q}$ -pair production based on one-gluon and two-gluon exchange. The parameters are  $\beta = 1/3$  (left hand side),  $\beta = 2/3$  (right hand side),  $Q^2 = 100 \text{ GeV}^2$  and  $\mathbf{k}^2$  is integrated above  $5 \text{ GeV}^2$ . The normalization is the integral of the cross section from 0 to  $\pi$ .

### 3.4.5 Production of charm quarks

We now generalize our analysis to finite quark mass  $m_f$ . All previous numerical calculations have been done for three massless flavors but now we will calculate the contribution that can be expected from charm quarks with mass  $m_c = 1.5 \text{ GeV}$ . For this mass the characteristic scale  $(\mathbf{k}^2 + m_f^2)(Q^2 + M^2)/M^2$  is always large, even for small  $\mathbf{k}^2$ . This offers the possibility to integrate the double-logarithmic results (including the corrections) over  $\mathbf{k}^2$  and to obtain in this way the charm contribution to the diffractive structure function. Note that for  $m_f^2 \neq 0$  the DLA expression for  $I_L$  (3.102) becomes a constant and the DLA expression for  $I_T$  (3.103) vanishes in the limit  $\mathbf{k}^2 \rightarrow 0$ . The  $\mathbf{k}^2$ -integration is therefore infrared finite. Before we turn to the

	$\mathbf{k}_0^2 = 2\text{GeV}^2$		$\mathbf{k}_0^2 = 4\text{GeV}^2$		$\mathbf{k}_0^2 = 8\text{GeV}^2$	
	GRV(LO)	GRV(NLO)	GRV(LO)	GRV(NLO)	GRV(LO)	GRV(NLO)
DLA + corrections						
$\sigma_T^{eP}$	39	27	16	11	5	3.4
$\sigma_L^{eP}$	3.4	2.3	0.6	0.4	0.2	0.1
$\sum_{i=T,L} \sigma_i^{eP}$	42.4	29.3	16.6	11.4	5.2	3.5
DLA						
$\sigma_T^{eP}$	34	22	14	9	3.8	2.6
$\sigma_L^{eP}$	2.5	1.7	0.5	0.4	0.2	0.1
$\sum_{i=T,L} \sigma_i^{eP}$	36.5	23.7	14.5	9.4	4	2.7

Table 3.2: Results for total  $eP$ -cross sections (in pbarn) of diffractive dijet production for charm quarks. The cuts are the same as in table 3.1 .

calculation of the structure function we give in table 3.2 the charm contribution to the jet cross section. The total  $eP$  cross section was calculated with the same cuts as in table 3.1. Depending on the momentum cut, charm gives a contribution between 25 and 50 percent relative to the three massless flavors. It is obvious that the suppression for large transverse momenta is not as strong as in the massless case. This is due to the nontrivial  $\mathbf{k}^2$ -dependence of  $\xi$  in the results for  $I_L$  and  $I_T$  which damps the  $1/\mathbf{k}^2$  decrease. It is also noticeable that the relative importance of the correction terms is much smaller than in the massless case.

We now turn to the charm contribution to the diffractive structure function  $F_2^D$ . The latter has been introduced in analogy to the inclusive structure function  $F_2$  to describe diffractive events (events with a rapidity gap) in electron-proton collisions. In terms of  $F_2^D$  the diffractive cross section reads

$$\frac{d\sigma_{\text{DIFF}}^{eP}}{d\beta dQ^2 dx_P} = \frac{2\pi\alpha_{\text{em}}^2}{\beta Q^4} [1 + (1-y)^2] F_2^D(\beta, Q^2, x_P) \quad (3.115)$$

where the longitudinal contribution has been neglected. With this definition of  $d\sigma_{\text{DIFF}}^{eP}$ ,  $F_2^D$  can be obtained from the photon-proton cross section in the following way

$$F_2^D(\beta, Q^2, x_P) = \frac{Q^2}{4\pi^2\alpha_{\text{em}}} \int_0^\infty dt \int_0^{M^2/4-m_c^2} d\mathbf{k}^2 \left[ \frac{d\sigma_T^{*P}}{dx_P d\mathbf{k}^2 dt} + \frac{d\sigma_L^{*P}}{dx_P d\mathbf{k}^2 dt} \right] \quad (3.116)$$

In fig. 3.26 the  $x_P$ -dependence of the diffractive structure function  $F_2^{D(\text{charm})}$  is shown. What is seen here is again the steep rise in  $x_P$  which is determined by the square of the gluon distribution. Compared with experimental data on  $F_2^D$  this rise is too strong but our analysis is of course only valid for heavy quarks. For the light quarks which make up the larger part of the cross section a slower rise is expected since nonperturbative contributions dominate. The ZEUS collaboration [87] quotes a value of  $\sim 30$  for  $F_2^D$  at  $Q^2 = 16 \text{ GeV}^2$ ,  $\beta = 0.65$ , and  $x_P \simeq 10^{-3}$ . From the right hand side of fig. 3.26 we read off a value of  $\sim 2.3$ , i. e. at first sight we predict a 10 % contribution of charm in  $F_2^D$ . It would of course be interesting to isolate the charm contribution to  $F_2^D$  experimentally to confirm the perturbative character of this type of events. It

can be seen from the graphs that the  $Q^2$ -dependence is rather weak, i. e.  $F_2^D$  shows a leading-twist behavior<sup>15</sup>. This is true, however, only for the transverse part of  $F_2^D$ . As can be seen from eq. (3.88) the longitudinal cross section has a  $1/Q^2$  suppression. The most striking effect of the variation of  $Q^2$  is again the change in the slope. These curves thus demonstrate again the breaking of Regge-factorization. In fig. 3.27 we display

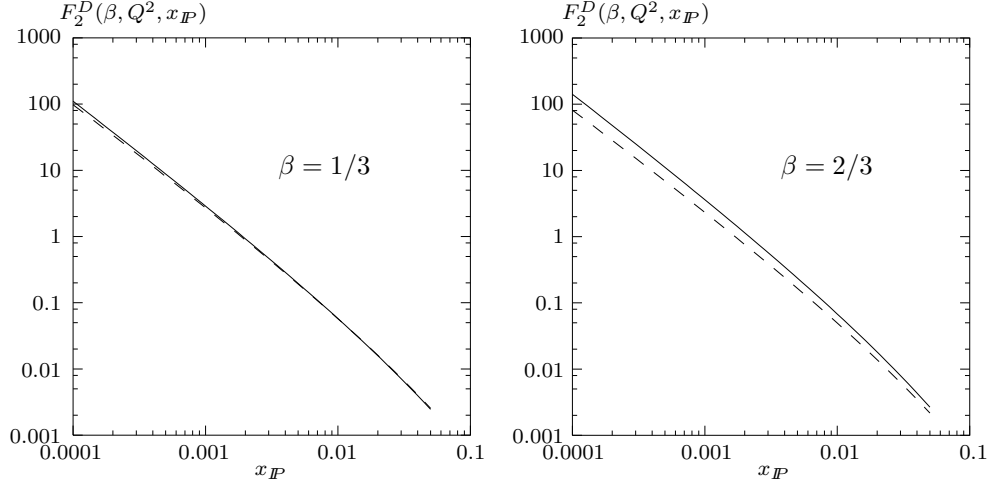


Figure 3.26: The  $x_P$ -dependence of the diffractive structure function for  $\beta = 1/3$ ,  $\beta = 2/3$  and  $Q^2 = 50 \text{ GeV}^2$  (solid line) and  $Q^2 = 20 \text{ GeV}^2$  (dashed line).

the  $\beta$ -dependence of  $F_2^D$  for  $x_P = 10^{-3}$  and two values of  $Q^2$ , separating the transverse and the longitudinal part. On the right hand side of each figure the charm-threshold can be seen, i. e. there is no phase space left if  $M^2$  becomes equal to the threshold mass  $M_{th}^2 = 4m_c^2$ . Increasing the mass from the threshold, i. e. going from higher to lower  $\beta$ , one sees first an increase in  $F_2^D$  due to the increasing phase space, but ultimately with growing masses the cross section is mass-suppressed and  $F_2^D$  goes to zero for  $\beta \rightarrow 0$ . Again we see that for large  $\beta$  there is a region where the longitudinal contribution becomes larger than the transverse one. When one compares the  $\beta$ -dependence of fig. 3.27 with experimental data one realizes one major shortcoming of our approach. The measured  $F_2^D$  does not vanish for  $\beta \rightarrow 0$ . For large masses quark-antiquark-gluon final states give the dominant (and for  $\beta = 0$  non-vanishing) contribution. These contributions are beyond the reach of the present analysis. It should therefore be realized that all calculations presented here are limited to the quark-antiquark component of the of  $F_2^{D(\text{charm})}$ . Including higher order components will above all modify the  $\beta$ -spectrum and the overall normalization. The  $x_P$ -dependence is not expected to change.

<sup>15</sup>It is understood that all statements are referring to the case of charm production. The index  $(\text{charm})$  will be omitted in the following.



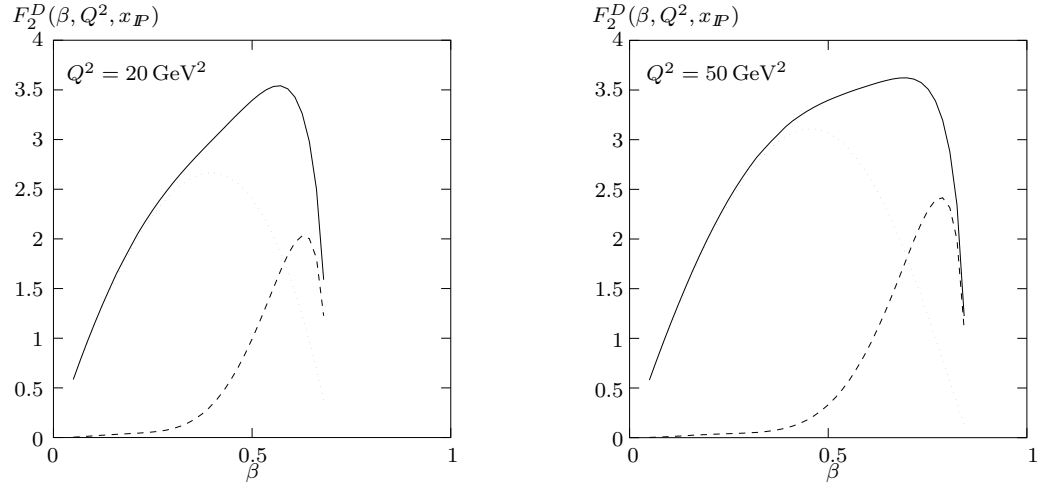


Figure 3.27: The  $\beta$ -dependence of the diffractive structure function for  $Q^2 = 20 \text{ GeV}^2$  and  $Q^2 = 50 \text{ GeV}^2$  and  $x_P = 10^{-3}$ . The dotted line is the transverse contribution the dashed line is the longitudinal part and the solid lines represent the sum.

## 4 Unitarity Corrections

In the preceding chapter we have discussed phenomenological implications of the resummation of large logarithms of  $1/x$ . The basic principle of these calculations was the insertion of the BFKL amplitude which resums the leading logarithms into a specific environment corresponding to respective initial and final states of a deep inelastic electron proton scattering process. The common feature of the results is the steep increase of the cross section as  $x$  decreases, either according to a power behavior with a power of order unity or - when only double logarithms are taken into account - according to the  $\exp(\sqrt{\log 1/x})$  behavior. This steep increase cannot persist down to arbitrarily low values of  $x$  since it violates a fundamental principle of quantum theory, i. e. unitarity. In the context of relativistic quantum field theory of the strong interaction unitarity implies that the cross section of a hadronic scattering reaction cannot increase with increasing energy  $s$  stronger than  $\log^2(s)$ . This statement is usually referred to as Froissart's theorem [88]. Applied to deep inelastic scattering <sup>16</sup> this theorem states that at small  $x$  the total cross section (the structure function) cannot increase faster than  $\log^2 1/x$ . This shows that the results of the preceding chapter can be valid only in a limited range of  $x$  since for arbitrarily small  $x$  they are in conflict with unitarity. This is one of the major shortcomings of the leading logarithmic approximation. Although consistent from the point of view of a perturbative expansion this approximation scheme violates a fundamental principle of quantum field theory. To fulfill the unitarity requirement one inescapably has to go beyond the leading logarithmic approximation.

In this chapter we introduce and investigate contributions that arise when subleading logarithms are taken into account in the perturbative expansion.

One should remark that the program which is pursued in the following constitutes only one of the many recent (effective actions [89, 90], eikonal approximation in soft gluon background [91], operator expansion [92], semiclassical approach [79, 24]) approaches to the unitarization problem in QCD. It is however the only approach which starts from the well-established and consistent framework of perturbative QCD which has been highly successful in describing strong interaction physics in deep inelastic scattering and elsewhere. On the other hand, it is not expected that a solely perturbative approach will be sufficient to restore unitarity. Ultimately one will certainly need some nonperturbative information regarding the structure of the colliding hadrons. Perturbation theory might nevertheless be a sensible starting point since it is known that a connection to nonperturbative physics might be drawn from ambiguities associated with the QCD perturbation series [27].

So far the most complete approach to subleading perturbative logarithms has been formulated by Bartels [29, 30, 18]. It is based on using unitarity and dispersion relations from the start as a tool to construct higher order amplitudes. As the main outcome of this approach one finds that it is necessary to take into account contributions with higher numbers of reggeized gluons in the  $t$ -channel, compared to the BFKL amplitude with two reggeized gluons. Ultimately it will be required to consider general  $n$ -reggeized gluon states in the  $t$ -channel and to sum over  $n$ . To this end it will be sensible to decompose the  $n$ -gluon problem into two major sectors. First one identifies transition vertices which mediate the transition between states with a different number of reggeized gluons. Second one has to solve the  $n$ -gluon problem. There is hope that one can find an effective field theory which incorporates all these elements and which might be solvable. If one recalls the symmetry properties of the BFKL amplitude which constitutes the first step in this program, one might even conjecture that this effective field theory is conformally symmetric.

In order to gain insight into the structure of a potential field theory one has in a first step to investigate the simplest new elements which arise beyond the leading logarithmic approximation. This is the objective of the present chapter.

We start with an introduction and review the basic concepts underlying the approach of [18]. In this introductory part we stress the importance of the notion of a reggeon as a collective excitation of elementary degrees of freedom in QCD. The reggeon which contains an infinite number of Feynman diagrams might be the right candidate for the basic field in an effective theory. At the present stage it is at least convenient to interpret the amplitudes which emerge from the calculation as reggeon amplitudes. To illustrate this we start with an interpretation of the BFKL equation in this framework. Since  $t$ -channel unitarity will ulti-

---

<sup>16</sup>Although it is not proven that the theorem is applicable to DIS this is generally believed to be the case. Compare footnote 13 in chapter 2.

mately be an important requirement to construct amplitudes of physical processes from reggeon amplitudes we demonstrate as an example the  $t$ -channel unitarity relations which follow from the BFKL equation.

We then give the coupled system of equations for reggeon amplitudes with up to  $n = 4$  reggeized gluons in the  $t$ -channel. The principle how to build equations with higher numbers of reggeons will become clear then. The step which was anticipated before, namely the identification of transition vertices has for this case been accomplished by Bartels and Wüsthoff [18, 19] and we describe the outcome of their analysis. Having isolated the two most important elements of the first subleading corrections, namely the transition vertex and the interacting four reggeized gluon state we then turn to the detailed investigation of these objects. We first derive a compact symbolic representation for the transition vertex. This representation is in the spirit of Lipatov's Hamilton operator formulation of the BFKL kernel [35]. The symbolic representation allows on the one hand a quite straightforward proof of conformal invariance of the vertex [34] and on the other hand the adressation of the property of holomorphic separability which has been shown to hold for the BFKL kernel [35]. We then show that after projection with the elementary conformal three point functions which were introduced in chapter 2 to diagonalize the BFKL kernel, the transition vertex can be consistently interpreted as the conformal three point function of a composite operator. This demonstrates that the interpretation of the amplitudes in the framework of a conformal field theory which was sketched for the BFKL amplitude in chapter 2 can be extended to the first corrections. The coordinate representation of the vertex is then completely fixed. The nontrivial part of the vertex in this representation is a dimensionless function of three conformal dimension which is given in terms of two-dimensional integrals.

The remaining sections of this chapter are devoted to the investigation of the four reggeized gluon state. We state the defining equation, namely the four particle BKP equation [29, 36] and discuss its properties. The phenomenological and theoretical significance of the solution of this equation is then discussed in some detail. We stress that a fully unitary amplitude requires the resummation of all contributions with arbitrarily large number of reggeized gluons in the  $t$ -channel. From the point of view of a potential effective conformal field theory the four gluon amplitude already contains interesting information. Performing a short-distance expansion of the amplitude it should be possible to derive the operator algebra of the composite operators associated with the BFKL pomeron. We discuss the concept of short-distance expansion and show using the BFKL amplitude as an example the relation between the anomalous dimensions and the spectrum of the system. This then leads us to our approach to the spectrum which is based on the twist expansion, i. e. the short-distance expansion of the amplitude in momentum space. The basic idea is to reconstruct the spectrum from the anomalous dimensions.

In the concluding section we then show how in principle the twist expansion of the four gluon state can be derived. We reformulate the defining equation using a method which goes back to Faddeev [43]. Using this method one can reformulate the problem as an effective two particle problem with highly complicated propagators and interaction vertices. We show how the singularities that are needed for the twist expansion can be extracted from the propagators and the vertices. For the simplest case we demonstrate how these singularities can be iterated to obtain the singularity of the four reggeized gluon amplitude. These singularities can be interpreted as the anomalous dimension of a corresponding operator associated with the four gluon state. We discuss its relation to the spectrum of the four reggeized gluon state. The complications which arise for the subleading singularities are finally indicated.

One final remark is in order here. In our investigations we keep the full color structure of the four gluon problem. In this case only conformal symmetry of the elementary interaction kernel can be and is used to simplify the problem. It has been shown that a remarkable simplification occurs in the large- $N_c$  approximation [93]. The key observation is that in this approximation the  $n$ -gluon system becomes holomorphic separable and in turn reduces to the product of two one-dimensional problems. After Lipatov had proven [37] the existence of nontrivial conserved quantities of the  $n$ -gluon system, Faddeev and Korchemsky [38, 40] have shown that the system can be identified with the XXX Heisenberg model for spin  $s = 0$ . From this follows that the system is completely solvable in the sense that there exists a sufficiently large number of integrals of motion. Using these results one can try to employ the quantum inverse scattering method and solve the system with the Bethe ansatz [40, 41]. We do not follow this direction in the present work.

## 4.1 Generalized leading-log approximation

Let us first show where the amplitudes which are investigated in the following parts of this chapter have their origin and sketch the role they play in the program towards an unitary effective high energy theory derived from QCD. The term 'generalized leading-log approximation' which appears here in the title is not really well defined. It is intended to denote the approximation scheme in which a minimal subset of next-to-leading logarithmic terms is taken into account which are needed to construct a unitary amplitude.

The fundamental idea is to obtain an effective description of QCD in the Regge limit in terms of a reggeon field theory [31, 32] in which unitarity is built in from the start. The reggeon is a collective excitation of the underlying field theory (QCD) that can be associated with singularities of partial wave amplitudes. It can be regarded as a nonrelativistic field in two transverse space dimensions which carries signature and belongs to an irreducible representation of the gauge group of the underlying theory. The immediate example is the reggeized gluon which emerges from an infinite order resummation of elementary gluon diagrams. It can be associated with a pole of the partial wave amplitude in the color octet channel and it has negative signature. The basic objects of the effective theory are the  $n$ -reggeon amplitudes. To be specific we consider two-particle to  $n$ -reggeon amplitudes  $D_n(\omega)$  where the reggeons<sup>17</sup> are coupled to a species of external elementary particles of the theory. Here  $\omega$  is a complex angular momentum variable which admits the interpretation as the energy of the  $n$ -reggeon system. These amplitudes arise from multiple discontinuities of multigluon amplitudes and can be shown to obey a set of coupled integral equations. The solutions of these equations are then plugged into the reggeon unitarity equations - which are unitarity equations in the  $t$ -channel - to calculate partial wave amplitudes [33, 30]. In the intermediate step in which the  $t$ -channel unitarity is applied one has to go to the physical region in the  $t$ -channel, i. e.  $t > 0$ . Afterwards an analytical continuation to  $t < 0$  has to be performed. In this way the partial wave amplitude is obtained as a sum of contributions with different numbers of reggeons in the  $t$ -channel. It is important to emphasize that the dynamical equations for the reggeon amplitudes are coupled, i. e. there are transition vertices from  $n$  to  $m$  reggeons and the reggeon number in the  $t$ -channel is not conserved.

The starting point in this formalism is the two reggeon amplitude  $D_2(\omega)$  determined by the BFKL equation which can be written in the form [4]

$$[\omega + \beta(\mathbf{k}) + \beta(\mathbf{q} - \mathbf{k})] D_2^I(\omega; \mathbf{k}, \mathbf{q} - \mathbf{k}) = D_{2,0}^I + \left[ K_{(2,2)}^I \otimes D_2^I(\omega) \right] (\mathbf{k}, \mathbf{q} - \mathbf{k}) \quad (4.1)$$

Here  $D_{2,0}^I$  is an elementary particle-gluon vertex,  $K_{(2,2)}^I$  and  $\beta(\mathbf{k})$  are the kernel and the trajectory function (4.6) of the BFKL equation and the index  $I$  labels the irreducible representation of the gauge group. The function  $\omega + \beta(\mathbf{k}) + \beta(\mathbf{q} - \mathbf{k})$  can be interpreted as the inverse reggeon propagator. The equation (4.1) then admits the interpretation as a two reggeon integral equation where the kernel  $K_{(2,2)}^I$  represents the reggeon interaction. The kernel has the form

$$K_{(2,2)}^I(\mathbf{q}; \mathbf{k}, \mathbf{k}') = \frac{N_c}{2} g^2 \frac{c_I}{\mathbf{k}'^2 (\mathbf{q} - \mathbf{k}')^2} \left[ -\mathbf{q}^2 + \frac{\mathbf{k}^2 (\mathbf{q} - \mathbf{k}')^2 + \mathbf{k}'^2 (\mathbf{q} - \mathbf{k})^2}{(\mathbf{k} - \mathbf{k}')^2} \right] \quad (4.2)$$

and the symbol  $\otimes$  in eq. (4.1) represents integration w. r. t. the measure  $d^2 \mathbf{k}' / (2\pi)^3$ . The weight  $c_I$  is a real number depending on the irreducible representation ( $g$  is the gauge coupling). In terms of  $D_2(\omega)$  the partial wave amplitude  $A(\omega, t)$  can be calculated as

$$A^I(\omega, t) = \int \frac{d^2 \mathbf{k}}{(2\pi)^3} \frac{1}{\mathbf{k}^2 (\mathbf{q} - \mathbf{k})^2} D_{2,0}^I \cdot D_2^I(\mathbf{k} - \mathbf{q} - \mathbf{k}) \quad , \quad -\mathbf{q}^2 = t \quad (4.3)$$

When  $I$  corresponds to the color octet representation in QCD we have  $c_I = 1$  and the solution of eq. (4.1) is [3]

$$D_2^{8A}(\mathbf{k}, \mathbf{q} - \mathbf{k}) = \frac{D_{2,0}^{8A}}{\omega + \beta(\mathbf{q}^2)} \quad (4.4)$$

---

<sup>17</sup>Unlike otherwise stated the term 'reggeons' in the following always refers to reggeized gluons.

from which follows

$$A^{8_A}(\omega, t) = \frac{2}{3g^2} (D_{2,0}^{8_A})^2 \frac{\beta(\mathbf{q}^2)}{\omega + \beta(\mathbf{q}^2)} \quad (4.5)$$

This is the manifestation of the reggeization of the gluon. The partial wave amplitude has a Regge pole in the complex angular momentum plane. Of course the solution (4.4) is infrared divergent. In a nonabelian gauge theory with a massless gauge boson, amplitudes with nonsinglet exchange always contain infrared divergencies. Since the reggeization is such a fundamental property in the present approach it is desirable to give a meaning to the solution in eq. (4.4). To this end one has to perform a regularization. In the following we assume a mass regularization, i. e. the gluon has acquired a mass  $\lambda$ . To do this consistently one has to add scalar particles to the theory which give additional contributions to the kernel in eq. (4.2). We will not consider these additional terms in detail since they do not play any role in the following.

#### 4.1.1 Unitarity relations from the BFKL equation

In this short interlude we want to show that a set of unitarity equations can be derived from the integral equation (4.1) which could in principle serve to calculate the partial wave amplitude. The unitarity corrections which are the objective of this chapter will provide generalizations of the reggeon integral equations to higher numbers of reggeons. This formalism does however not give a generalization to eq. (4.3). It is therefore not clear in which way the  $n$ -reggeon amplitudes contribute to the partial wave amplitude. The idea is to use  $t$ -channel unitarity to construct the partial wave from the reggeon amplitudes. The following considerations should serve as an illustration of  $t$ -channel unitarity relations. For the use of unitarity in the  $t$ -channel it is first of all necessary to continue the amplitudes to the physical region of the  $t$ -channel, i. e. the region of positive  $t$ . In this region the trajectory function  $\beta(\mathbf{q}^2)$  has a cut starting at  $t = -\mathbf{q}^2 > 4\lambda^2$ . For the discontinuity along this cut one finds

$$\begin{aligned} \text{disc}_t \beta(\mathbf{q}^2) &= \text{disc}_t \frac{3}{2} g^2 \int \frac{d^2 \mathbf{k}}{(2\pi)^3} \frac{\mathbf{q}^2 + \lambda^2}{[\mathbf{k}^2 + \lambda^2][(\mathbf{q} - \mathbf{k})^2 + \lambda^2]} \\ &= \frac{3}{2} \frac{g^2}{(2\pi)^3} 2\pi^2 i \frac{t - \lambda^2}{\sqrt{t^2 - 4t\lambda^2}} \end{aligned} \quad (4.6)$$

$$= \frac{3}{2} \frac{g^2}{(2\pi)^3} (t - \lambda^2) \int \prod_{i=1}^2 [d^2 \mathbf{k}_i 2\pi \delta(\mathbf{k}_i^2 - \lambda^2)] \delta^{(2)}(\mathbf{q} - \sum_{i=1}^2 \mathbf{k}_i) \quad (4.7)$$

The last expression shows that this discontinuity can be associated with two  $t$ -channel particles going on the mass-shell. It is then possible to derive from eqs. (4.1), (4.3) the following equation for the discontinuity of the partial wave amplitude (continued to the region of positive  $t$ )

$$\text{disc}_t A^I(\omega, t) = \frac{\omega}{(2\pi)^3} \int \prod_{i=1}^2 [d^2 \mathbf{k}_i 2\pi \delta(\mathbf{k}_i^2 - \lambda^2)] \delta^{(2)}(\mathbf{q} - \sum_{i=1}^2 \mathbf{k}_i) D_2^I(\omega; \mathbf{k}_1, \mathbf{k}_2) D_2^{I*}(\omega; \mathbf{k}_1, \mathbf{k}_2) \quad (4.8)$$

The right hand side of this equation can be regarded as an unitarity integral for the two reggeon amplitude  $D_2(\omega)$ . The partial wave amplitude has further discontinuities corresponding to the thresholds for the production of  $n$  particles in the  $t$ -channel ( $n \geq 3$ ). The three particle cut starts at  $-\mathbf{q}^2 = 9\lambda^2$  and the corresponding unitarity condition can be expressed in terms of the two reggeon amplitude as

$$\begin{aligned} \text{disc}_t A^I(\omega, t) &= \frac{3}{2} \frac{g^2}{(2\pi)^6} \int \prod_{i=1}^3 [d^2 \mathbf{k}_i 2\pi \delta(\mathbf{k}_i^2 - \lambda^2)] \delta^{(2)}(\mathbf{q} - \sum_{i=1}^3 \mathbf{k}_i) \\ &\quad \cdot 2 [D_2^I(\mathbf{k}_1 + \mathbf{k}_2, \mathbf{k}_3) D_2^{I*}(\mathbf{k}_1 + \mathbf{k}_2, \mathbf{k}_3) - c_I D_2^I(\mathbf{k}_1 + \mathbf{k}_2, \mathbf{k}_3) D_2^{I*}(\mathbf{k}_1, \mathbf{k}_2 + \mathbf{k}_3)] \end{aligned} \quad (4.9)$$

The first term comes from cutting two virtual lines from a trajectory function whereas the second term comes from cutting a real line from the interaction kernel. The two and three particle unitarity relations have been

first discussed in [4]. Similarly one finds for the four particle unitarity relation for  $t = -\mathbf{q}^2 > 16\lambda^2$

$$\begin{aligned} \text{disc}_t A^I(\omega, t) = & \frac{9}{4} \frac{g^2}{(2\pi)^9} \int \prod_{i=1}^4 [d^2 \mathbf{k}_i \delta(\mathbf{k}_i^2 - \lambda^2)] \delta^{(2)}(\mathbf{q} - \sum_{i=1}^4 \mathbf{k}_i) \\ & [-2D_2^I(\mathbf{k}_1 + \mathbf{k}_2, \mathbf{k}_3 + \mathbf{k}_4) D_2^{I*}(\mathbf{k}_1 + \mathbf{k}_2, \mathbf{k}_3 + \mathbf{k}_4) \\ & - 2c_I^2 D_2^I(\mathbf{k}_1, \mathbf{k}_2 + \mathbf{k}_3 + \mathbf{k}_4) D_2^{I*}(\mathbf{k}_1 + \mathbf{k}_2 + \mathbf{k}_3, \mathbf{k}_4) \\ & + 2c_I D_2^I(\mathbf{k}_1 + \mathbf{k}_2, \mathbf{k}_3 + \mathbf{k}_4) D_2^{I*}(\mathbf{k}_1 + \mathbf{k}_2 + \mathbf{k}_3, \mathbf{k}_4) \\ & + 2c_I D_2^I(\mathbf{k}_1 + \mathbf{k}_2 + \mathbf{k}_3, \mathbf{k}_4) D_2^{I*}(\mathbf{k}_1 + \mathbf{k}_2, \mathbf{k}_3 + \mathbf{k}_4)] \end{aligned} \quad (4.10)$$

Due to the reggeization the  $n$ -particle cuts of the partial wave amplitude in the color octet channel have to vanish for  $n > 2$ . This can easily be shown to be true from eqs. (4.9), (4.10) since the solution (4.5) of the integral equation for the color octet representation depends only on  $\mathbf{q}^2$  and we have  $c_{8_A} = 1$ .

#### 4.1.2 Higher order equations

In this part we turn to the higher order reggeon amplitudes. For the generalization of the two reggeon integral equation (4.1) particle number nonconserving vertices  $K_{(2,n)}$  of order  $g^n$  are needed. These kernels generalize the BFKL kernel and they are calculated in perturbation theory. They have been obtained in [30] for the massive gauge theory and they are given in [19] for QCD. With these kernels the integral equations for the three and four reggeon amplitudes read

$$\begin{aligned} \left[ \omega + \sum_{i=1}^3 \beta(\mathbf{k}_i) \right] D_3(\omega; \{\mathbf{k}_i\}) &= D_{3,0} + [K_{(2,3)} \otimes D_2(\omega)](\{\mathbf{k}_i\}) + \sum_{1 \leq i < j \leq 3} [K_{(2,2)}^{(i,j)} \otimes D_3(\omega)](\{\mathbf{k}_i\}) \quad (4.11) \\ \left[ \omega + \sum_{i=1}^4 \beta(\mathbf{k}_i) \right] D_4(\omega; \{\mathbf{k}_i\}) &= D_{4,0} + [K_{(2,4)} \otimes D_2(\omega)](\{\mathbf{k}_i\}) + \sum_{1 \leq i < j \leq 3} [K_{(2,3)}^{(i,j)} \otimes D_3(\omega)](\{\mathbf{k}_i\}) \\ &+ \sum_{1 \leq i < j \leq 4} [K_{(2,2)}^{(i,j)} \otimes D_4(\omega)](\{\mathbf{k}_i\}) \quad (4.12) \end{aligned}$$

The summation indicates that all pairwise interactions have to be summed up. The relation  $\sum_{i=1}^n \mathbf{k}_i = \mathbf{q}$  is implicitly assumed. The construction principle for these equations is easy to understand. On the left hand side we have the inverse  $n$ -reggeon propagator and on the right hand side the kernels  $K_{(2,n)}$  are used to construct all contributions with  $n$  reggeons in the  $t$ -channel. It is clear from the construction that the reggeon number in the  $t$ -channel never decreases. In the above equations we have completely suppressed the color structure. Each reggeon amplitude  $D_n(\omega)$  carries  $n$  color indices and each interaction kernel carries  $n + 2$  color indices which are not displayed. All following considerations are restricted to total color zero in the  $t$ -channel, i. e. the four gluon state is in the color singlet representation. For this case it has been shown [18] that eqs. (4.11) and (4.12) are infrared finite, i. e. all divergencies cancel mutually.

It turned out that solutions to the above integral equations can be found [30, 18, 19]. The three reggeon amplitude can be determined exactly

$$D_3^{a_1 a_2 a_3}(\omega; \{\mathbf{k}_i\}) = g c_3 f^{a_1 a_2 a_3} [D_2(\omega; \mathbf{k}_1 + \mathbf{k}_2, \mathbf{k}_3) - D_2(\omega; \mathbf{k}_1 + \mathbf{k}_3, \mathbf{k}_2) + D_2(\omega; \mathbf{k}_1, \mathbf{k}_2 + \mathbf{k}_3)] \quad (4.13)$$

Here  $g$  is the gauge coupling,  $c_3$  is a normalization and  $f^{a_1 a_2 a_3}$  are the structure constants of  $SU(3)$ . What is observed here is again the reggeization of the gluon in QCD. Each single reggeon line is in a color octet state with negative signature. But since the total system is in a color singlet state the remaining pair also has to be in the negative signature color octet state. Due to the bootstrap property of the BFKL equation each two reggeon state in the color octet collapses into one reggeon and the three reggeon system can be reduced to the two reggeon system.

The four reggeon equation can be solved only partially [18, 19]. The amplitude  $D_4(\omega)$  can be decomposed into two terms the first of which can be reduced again to the two reggeon amplitude. The second one can be

written as a convolution of a two reggeon system and a four reggeon system with a transition vertex  $V_{(2,4)}$ . We have

$$D_4(\omega; \{\mathbf{k}_i\}) = D_4^R(\omega; \{\mathbf{k}_i\}) + D_4^I(\omega; \{\mathbf{k}_i\}) \quad (4.14)$$

with

$$\begin{aligned} D_4^{R, a_1 a_2 a_3 a_4}(\omega; \{\mathbf{k}_i\}) &= g^2 c_4 [-d^{a_2 a_1 a_3 a_4} (D_2(\omega; \mathbf{k}_{12}, \mathbf{k}_{34}) + D_2(\omega; \mathbf{k}_{13}, \mathbf{k}_{24})) - d^{a_1 a_2 a_3 a_4} D_2(\omega; \mathbf{k}_{14}, \mathbf{k}_{23}) \\ &\quad + d^{a_1 a_2 a_3 a_4} (D_2(\omega; \mathbf{k}_1, \mathbf{k}_{234}) + D_2(\omega; \mathbf{k}_4, \mathbf{k}_{123})) \\ &\quad + d^{a_2 a_1 a_3 a_4} (D_2(\omega; \mathbf{k}_2, \mathbf{k}_{134}) + D_2(\omega; \mathbf{k}_3, \mathbf{k}_{124}))] \end{aligned} \quad (4.15)$$

$$D_4^I, a_1 a_2 a_3 a_4(\omega; \{\mathbf{k}_i\}) = [G_4(\omega) \otimes V_{(2,4)} \otimes D_2(\omega)]^{a_1 a_2 a_3 a_4}(\{\mathbf{k}_i\}) \quad (4.16)$$

Here  $c_4$  is again a normalization constant and we have defined  $\mathbf{k}_{ij} = \mathbf{k}_i + \mathbf{k}_j$ . The convolution  $\otimes$  now also contains a summation over color indices. The color tensor  $d^{a_1 a_2 a_3 a_4}$  is defined as

$$d^{a_1 a_2 a_3 a_4} = Tr[T^{a_1} T^{a_2} T^{a_3} T^{a_4}] + Tr[T^{a_4} T^{a_3} T^{a_2} T^{a_1}] \quad (4.17)$$

where the  $T^a$  are the generators of  $SU(3)$  in the fundamental (three-dimensional) representation. There are two new elements which appear in the above solution of the four reggeon integral equation. The first is the two-to-four reggeon vertex  $V_{(2,4)}$ . It is an effective vertex which emerges after summation of different elementary interactions. It must not be confused with the elementary transition kernels  $K_{(2,n)}$ . An explicit representation and an investigation of some of its properties will be given in the next section. The second new element which deserves interest is the fully interacting four reggeon amplitude  $G_4$ . This function is a solution of the BKP equation [29, 36] for four reggeized gluons. The BKP equation is of the Bethe Salpeter type with pairwise interactions specified by the BFKL kernel  $K_{(2,2)}$ . It resums the pairwise interactions of four reggeized gluons in the  $t$ -channel. This equation will be formulated and investigated in section 4.3. The important feature of the decomposition in eq. (4.16) is the fact that all particle number nonconserving contributions have been absorbed in the function  $V_{(2,4)}$ . The problem which remains to be solved is one with fixed particle number.

Let us close this introductory part with a remark on the reggeized contributions  $D_3(\omega)$  and  $D_4^R(\omega)$ . One notices that these amplitudes are expressed through terms which appear in the unitarity relations (4.9) and (4.10) for the BFKL amplitude. This means that if one plugs in  $D_3(\omega)$  and  $D_4^R(\omega)$  into  $t$ -channel unitarity equations then certain parts of the result with the correct color quantum numbers should in fact be identified with the results that follow from the BFKL equation. Contributions with correct color quantum numbers in this sense are those for which the group of gluons which momenta appear summed in the respective  $D_2$ -amplitude is in the antisymmetric color octet representation, i. e. their color quantum number coincides with that of the gluon. It follows that one should associate the complete  $D_3$ -amplitude with contributions that are already contained in the BFKL equation. To show this consistently one has to formulate rules to construct  $t$ -channel unitarity integrals from the three reggeon amplitude. These rules have to reproduce the correct weight factors in eq. (4.9). In the case of  $D_4^R(\omega)$ , the construction of the  $t$ -channel unitarity integrals with the appropriate rules should yield one contribution with the correct color quantum numbers that corresponds to eq. (4.10). The remaining part could be associated with a part of the next-to-leading order corrections to the BFKL kernel as done by White and Coriano [94]. From our point of view, however, a consistent set of  $t$ -channel unitarity rules has not yet been found. It should be remarked, in any case, that a complete interpretation of the  $n$ -reggeon amplitudes requires still some work to be done. In particular it is important to separate the true corrections that arise from the  $n$ -reggeon amplitudes from terms which are already contained in the BFKL equation.

## 4.2 The transition vertex

The starting point is the expression for the irreducible part of the four reggeon amplitude (4.16). We assume that we convolute this amplitude from below with some kind of impact factor. This gives then rise to the

amplitude

$$\mathcal{A}_4 = \prod_{i=1}^2 d^2 \mathbf{q}_i \prod_{i=1}^4 d^2 \mathbf{k}_i \Phi_{\omega,2}(\mathbf{q}_1, \mathbf{q}_2) V_{(2,4)}^{a_1 a_2 a_3 a_4}(\{\mathbf{q}_i\}; \{\mathbf{k}_i\}) \Phi_{\omega,4}^{a_1 a_2 a_3 a_4}(\mathbf{k}_1, \mathbf{k}_2, \mathbf{k}_3, \mathbf{k}_4) \delta^{(2)}\left(\sum_{i=1}^2 \mathbf{q}_i - \sum_{i=1}^4 \mathbf{k}_i\right) \quad (4.18)$$

where we have slightly changed our notation and introduced the two reggeon amplitude  $\Phi_{\omega,2}$  which is a solution of the BFKL equation and the four reggeon amplitude  $\Phi_{\omega,4}$  which is a solution of the four-particle BKP equation. The vertex has the structure [19]

$$\begin{aligned} V_{(2,4)}^{a_1 a_2 a_3 a_4}(\{\mathbf{q}_i\}; \{\mathbf{k}_i\}) &= \delta^{a_1 a_2} \delta^{a_3 a_4} V(\{\mathbf{q}_i\}; \mathbf{k}_1, \mathbf{k}_2, \mathbf{k}_3, \mathbf{k}_4) \\ &+ \delta^{a_1 a_3} \delta^{a_2 a_4} V(\{\mathbf{q}_i\}; \mathbf{k}_1, \mathbf{k}_3, \mathbf{k}_2, \mathbf{k}_4) \\ &+ \delta^{a_1 a_4} \delta^{a_2 a_3} V(\{\mathbf{q}_i\}; \mathbf{k}_1, \mathbf{k}_4, \mathbf{k}_2, \mathbf{k}_3) \end{aligned} \quad (4.19)$$

From this representation it is clear that the vertex  $V_{(2,4)}$  is completely symmetric under the interchange of the outgoing gluons since  $V$  will be shown to be symmetric w. r. t. the exchange of the first and the second momentum argument, respectively the third and the fourth momentum argument. The momentum space representation of the function  $V$  is given explicitly in [19] and can be represented graphically as in fig. 4.1. Here for each line with momentum  $\mathbf{k}_i$  we have a propagator  $1/\mathbf{k}_i^2$  and for each vertex we have a factor  $\mathbf{q}^2$  with  $\mathbf{q}^2$  denoting the sum of momenta above or below the vertex. All momenta are integrated according to eq. (4.18) and for each momentum integration we have a factor  $1/(2\pi)^3$ . As indicated all permutations have to be summed finally and one has to multiply with the global factor  $g^4 \sqrt{2}/8$ . The grouping in fig. (4.1) is organized in such a way that for each group the  $\mathbf{q}_1, \mathbf{q}_2$ -integration in eq. (4.18) is infrared finite separately. It should be noted that the two gluon state  $\Phi_{\omega,2}$  vanishes if either  $\mathbf{q}_1 = 0$  or  $\mathbf{q}_2 = 0$ . Besides this infrared finiteness the function  $V$  fulfills another important consistency condition. If we absorb the propagators of the four outgoing gluons in the four gluon state  $\Phi_{\omega,4}$  the function  $V$  vanishes whenever one outgoing momentum or a group of outgoing momenta is set equal to zero. In this case cancellation takes place between terms of different groups and it is not possible to find a subgroup for which this property holds separately.

#### 4.2.1 The operator representation

In [34] the configuration space representation of the above introduced function  $V$  was derived and it was proven that this function is conformally invariant, i. e. it has the same symmetry properties as the BFKL kernel. The techniques employed in [34] are identical to the ones that were used in chapter 1 of this work to prove the conformal invariance of the BFKL kernel. In this section we derive an alternative representation for the transition vertex  $V$  which permits a more direct proof of conformal symmetry. From this representation we can furthermore address the important question of holomorphic separability of the vertex.

Lipatov has shown [35] that beyond conformal symmetry the BFKL kernel possesses the further property of being holomorphic separable. He developed a representation of the BFKL kernel in terms of pseudodifferential operators. In this representation the kernel decomposes into a sum of two terms which are complex conjugates of each other. The first one acts only on the coordinates  $\rho_1, \rho_2$ , whereas the second one acts only on the complex conjugate coordinates  $\rho_1^*, \rho_2^*$ . This property is termed holomorphic separability. Consequently the eigenfunctions of the kernel factorize into a part depending on  $\rho_1, \rho_2$  and a second part depending on  $\rho_1^*, \rho_2^*$ . The real eigenvalues come as a sum of two mutually complex conjugate contributions. The explicit representation of the kernel reads

$$\mathcal{K} = \frac{N_c g^2}{8\pi^2} (K + K^*) \quad (4.20)$$



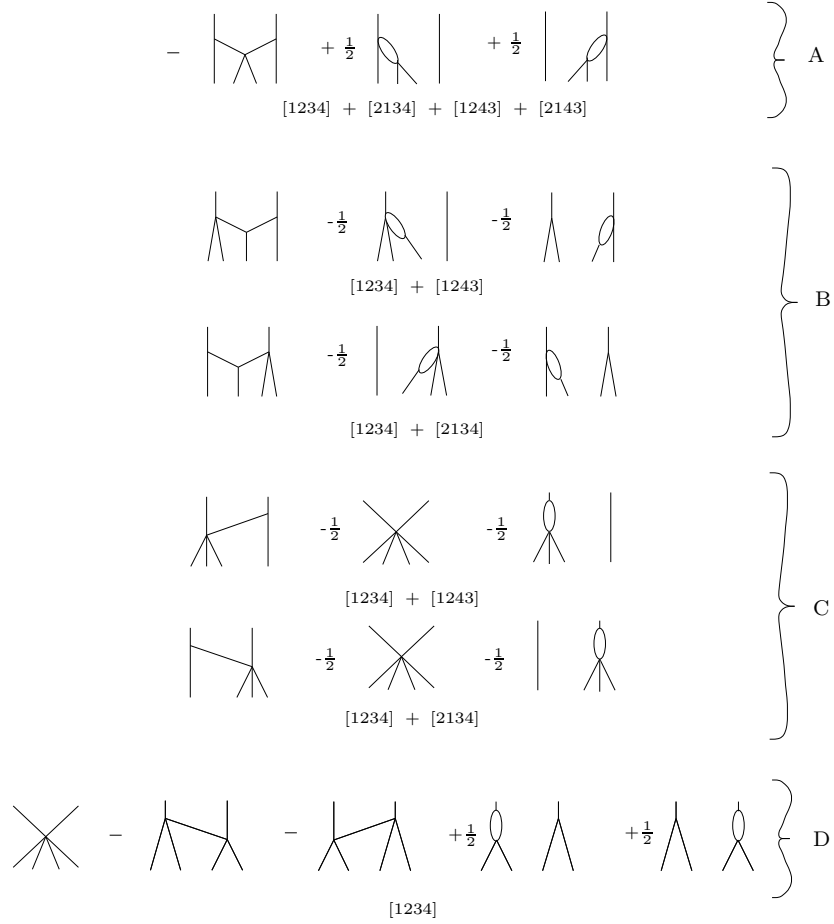


Figure 4.1: Graphical representation of the transition vertex function  $V$ . The notation is explained in the text. The brackets indicate the permutations.

with

$$K = \log(\rho_{12}^2 \partial_1) + \log(\rho_{12}^2 \partial_2) - 2 \log \rho_{12} - 2\psi(1) \quad (4.21)$$

$$= \frac{1}{2} \sum_{l=0}^{\infty} \left( \frac{2l+1}{l(l+1) + \rho_{12}^2 \partial_1 \partial_2} - \frac{2}{l+1} \right) \quad (4.22)$$

The second representation is of particular interest since it expresses the BFKL kernel in terms of the Casimir operators  $L^2 = \rho_{12}^2 \partial_1 \partial_2$ ,  $L^{*2} = \rho_{12}^{*2} \partial_1^* \partial_2^*$  (cf. eq. (4.34)) of the conformal group. In this representation the conformal symmetry becomes manifest. The equivalence of the representation (4.22) with the BFKL kernel can be proven using eq. (4.34) and the series representation (4.27) of the BFKL eigenvalue  $\chi(\nu, n)$ . The way in which the representation (4.21) is obtained will become clear below. In the operator representation the BFKL kernel becomes formally local<sup>18</sup> and can be interpreted as a Hamilton operator of a two-particle system. The corresponding stationary Schrödinger equation with the energy  $\omega$  reads

$$-\omega \Phi_\omega(\rho_1 \rho_2) = \mathcal{K} \Phi_\omega(\rho_1 \rho_2) \quad (4.23)$$

<sup>18</sup>  $\mathcal{K}$  is of course only formally local. In representation (4.21) appears the pseudodifferential operator  $\log \rho^2 \partial$  which is defined through Fourier transformation. In representation (4.22) an infinite summation over a differential operator is implied. This means that mathematically  $\mathcal{K}$  is a nonlocal operator.

The maximal eigenvalue of  $\mathcal{K}$  corresponds to the ground state energy of the two particle system. In section 4.3 we will meet the four-particle generalization of this Schrödinger equation.

In the following we derive a representation similar to (4.21) for the transition vertex  $V$ . We start with the group D in fig. 4.1 which has the form of the BFKL kernel. Using complex notation and mass regularization and omitting the global factors we have the following expression for this group

$$\begin{aligned} \mathcal{A}_4^D = & - \int d^2 \mathbf{q}_1 |\mathbf{q}_1|^2 |\mathbf{q}_2|^2 \hat{\Phi}_{\omega,2}(\mathbf{q}_1, \mathbf{q}_2) \prod_{i=1}^4 d^2 \mathbf{k}_i \left[ \frac{1}{|\mathbf{q}_1 - \mathbf{k}_1 - \mathbf{k}_2|^2 + \lambda^2} \left( \frac{(k_1 + k_2)(k_3 + k_4)^*}{q_1^* q_2} + \text{h.c.} \right) \right. \\ & \left. - \pi \left( \log \frac{|\mathbf{q}_1|^2}{\lambda^2} \delta^{(2)}(\mathbf{q}_1 - \mathbf{k}_1 - \mathbf{k}_2) + \log \frac{|\mathbf{q}_1|^2}{\lambda^2} \delta^{(2)}(\mathbf{q}_1 - \mathbf{k}_3 - \mathbf{k}_4) \right) \right] \hat{\Phi}_{\omega,4}(\mathbf{k}_1, \mathbf{k}_2, \mathbf{k}_3, \mathbf{k}_4)_{|\mathbf{q}_2 = \sum_{i=1}^4 \mathbf{k}_i - \mathbf{q}_1} \end{aligned} \quad (4.24)$$

The propagators of the incoming and outgoing gluons are now absorbed in the functions  $\hat{\Phi}_{\omega,2}$  and  $\hat{\Phi}_{\omega,4}$ . The momentum integration of the bubbles has already been performed leading to the logarithms. Now we switch to the configuration space representation by inserting

$$\hat{\Phi}_{\omega,2}(\mathbf{q}_1, \mathbf{q}_2) = \prod_{i=1}^2 [d^2 \rho_{i'} e^{-i \mathbf{q}_i \rho_{i'}}] \Phi_{\omega,2}(\rho_{1'}, \rho_{2'}) \quad (4.25)$$

$$\hat{\Phi}_{\omega,4}(\mathbf{k}_1, \mathbf{k}_2, \mathbf{k}_3, \mathbf{k}_4) = \prod_{i=1}^4 [d^2 \rho_i e^{-i \mathbf{k}_i \rho_i}] \Phi_{\omega,4}(\rho_1, \rho_2, \rho_3, \rho_4) \quad (4.26)$$

and obtain <sup>19</sup> upon integration of the momentum variables

$$\begin{aligned} \mathcal{A}_4^D = & - \int d^2 \rho_1 d^2 \rho_2 [\Delta_1 \Delta_2 \Phi_{\omega,2}(\rho_1, \rho_2)] \left[ \frac{1}{\partial_1 \partial_2^*} \int d^2 \mathbf{q} \frac{e^{-i \mathbf{q} \rho_{12}}}{|\mathbf{q}|^2 + \lambda^2} \partial_1^* \partial_2 + \text{h.c.} \right. \\ & \left. - \pi (\log(4|\partial_1|^2) + \log(4|\partial_2|^2)) + 2\pi \log \lambda^2 \right] \Phi_{\omega,4}(\rho_1, \rho_1, \rho_2, \rho_2) \end{aligned} \quad (4.27)$$

Here  $\Delta$  is the 2-d Laplace operator and the product  $\Delta_1 \Delta_2$  acts only on  $\Phi_{\omega,2}$  but not further to the right. The pseudodifferential operators  $\partial^{-1}$  and  $\log |\partial|^2$  have been introduced which are defined by the relations

$$\frac{1}{\partial} \phi(\rho, \rho^*) = \int d^2 \mathbf{q} \frac{2}{i \mathbf{q}^*} e^{i \mathbf{q} \rho} \hat{\phi}(\mathbf{q}) \quad (4.28)$$

$$\log(4|\partial|^2) \phi(\rho, \rho^*) = \int d^2 \mathbf{q} \log |\mathbf{q}|^2 e^{i \mathbf{q} \rho} \hat{\phi}(\mathbf{q}) \quad (4.29)$$

$$\text{where :} \quad \phi(\rho, \rho^*) = \int d^2 \mathbf{q} e^{i \mathbf{q} \rho} \hat{\phi}(\mathbf{q}) \quad (4.30)$$

An explicit integral operator representation can be found in eq. (4.6) in the appendix. The  $\mathbf{q}$ -integral is also calculated in the appendix. It yields

$$\int d^2 \mathbf{q} \frac{e^{-i \mathbf{q} \rho_{12}}}{|\mathbf{q}|^2 + \lambda^2} = \pi [-\log |\rho_{12}|^2 + \log 4 - \log \lambda^2 + 2\psi(1)] \quad (4.31)$$

and we end with the result

$$\begin{aligned} \mathcal{A}_4^D = & \pi \int d^2 \rho_1 d^2 \rho_2 \Delta_1 \Delta_2 \Phi_{\omega,2}(\rho_1, \rho_2) \left[ \frac{1}{\partial_1 \partial_2^*} \log |\rho_{12}|^2 \partial_1^* \partial_2 + \text{h.c.} \right. \\ & \left. + \log \partial_1 \partial_1^* + \log \partial_2 \partial_2^* - 4\psi(1) \right] \Phi_{\omega,4}(\rho_1, \rho_1, \rho_2, \rho_2) \end{aligned} \quad (4.32)$$

---

<sup>19</sup>A global factor  $(4\pi^2)^4$  from the fourfold  $\mathbf{k}$ -integration which appears here and in the following contributions has been omitted. Furthermore we have omitted a global factor which results from the color contraction of the vertex and the four gluon function.

From this representation one can already conclude that the operator  $\mathcal{K}_D$  acting on  $\Phi_{\omega,4}$  is holomorphic separable. Simple manipulations give

$$\mathcal{K} = K_D + K_D^* \quad (4.33)$$

$$K_D = \partial_1^{-1} \log \rho_{12} \partial_1 + \partial_2^{-1} \log \rho_{12} \partial_2 + \log \partial_1 \partial_2 - 2\psi(1) \quad (4.34)$$

$$= \rho_{12} \log(\partial_1 \partial_2) \rho_{12}^{-1} + 2 \log \rho_{12} - 2\psi(1) \quad (4.35)$$

where the last line follows from the identity  $[\rho_{12}, \log \partial_1] = -1/\partial_1$ .

To arrive at a representation which is manifest conformally invariant additional steps are required. It is useful to collect the noncommuting operators  $\partial_1$  and  $\rho_{12}^2$  in the form  $\rho_{12}^2 \partial_1$  in the argument of the logarithm. This can be achieved by using the commutator identity given above and the operator identities [95]

$$\log \partial + \log \rho = \frac{1}{2} [\psi(-\rho \partial) + \psi(1 + \rho \partial)] \quad (4.36)$$

$$\log \rho^2 \partial - \log \rho = \frac{1}{2} [\psi(\rho \partial) + \psi(1 - \rho \partial)] \quad (4.37)$$

The holomorphic part of  $K_D$  can then finally be represented as

$$K_D = \log(\rho_{12} \partial_1) + \log(\rho_{12} \partial_2) - 2 \log \rho_{12} - 2\psi(1) \quad (4.38)$$

Comparison with eq. (4.21) shows that  $K_D$  is identical with the BFKL kernel. It follows immediately that the group D of the transition vertex  $V$  is conformally invariant and holomorphic separable.

Now we turn to the group C in fig. 4.1 and start with the permutation [1234] in the first line. For the moment we omit the second term (the contact term) which will be considered separately below. The corresponding momentum space expression reads

$$\begin{aligned} \mathcal{A}_4^{C_1} = & \int d^2 \mathbf{q}_1 d^2 \mathbf{q}_2 |\mathbf{q}_1|^2 |\mathbf{q}_2|^2 \hat{\Phi}_{\omega,2}(\mathbf{q}_1, \mathbf{q}_2) \prod_{i=1}^4 d^2 \mathbf{k}_i \left[ \frac{(\mathbf{k}_1 + \mathbf{k}_2 + \mathbf{k}_3)^2}{[|\mathbf{q}_1 - \mathbf{k}_1 - \mathbf{k}_2 - \mathbf{k}_3|^2 + \lambda^2]} \frac{1}{|\mathbf{q}_1|^2} \right. \\ & \left. - \pi \log \frac{|\mathbf{q}_1|^2}{\lambda^2} \delta^{(2)}(\mathbf{q}_1 - \mathbf{k}_1 - \mathbf{k}_2 - \mathbf{k}_3) \right] \hat{\Phi}_{\omega,4}(\mathbf{k}_1, \mathbf{k}_2, \mathbf{k}_3, \mathbf{k}_4)_{|\mathbf{q}_2 = \sum_{i=1}^4 \mathbf{k}_i - \mathbf{q}_1} \end{aligned} \quad (4.39)$$

Fourier transformation along the lines above then leads to

$$\mathcal{A}_4^{C_1} = -\pi \int d^2 \rho_1 d^2 \rho_2 [\Delta_1 \Delta_2 \Phi_{\omega,2}(\rho_1, \rho_2)] \left[ \frac{1}{\partial_1 \partial_1^*} \log(|\rho_{12}|^2) \partial_1 \partial_1^* + \log \partial_1 \partial_1^* - 2\psi(1) \right] \Phi_{\omega,4}(\rho_1, \rho_1, \rho_1, \rho_2) \quad (4.40)$$

If we associate an operator  $\mathcal{K}_{C_1}$  with these terms we find that we can decompose it again into a holomorphic and an antiholomorphic part

$$-\mathcal{K}_{C_1} = K_{C_1} + K_{C_1}^* \quad (4.41)$$

$$K_{C_1} = \partial_1^{-1} \log(\rho_{12}) \partial_1 + \log \partial_1 - \psi(1) \quad (4.42)$$

$$= \log(\rho_{12}^2 \partial_1) - \log \rho_{12} - \psi(1) \quad (4.43)$$

where the last line follows again after application of the operator identities (4.36) and (4.37). This representation proves to be useful when investigating the conformal properties of the group C. For the second line of group C and the permutation [1234] we get a similar contribution the holomorphic part of which reads (again we omit the contact term)

$$K_{C_2} = \log(\rho_{12}^2 \partial_2) - \log \rho_{12} - \psi(1) \quad (4.44)$$

and this operator and its conjugate act on the function  $\Phi_{\omega,4}(\rho_1, \rho_2, \rho_2, \rho_2)$ .

Next we consider the contact term which appears with the weight  $-2$  in group C. In group D it was possible

to combine this term in a very compact way with the remaining contributions. In group C it is not possible to obtain such a combination and the term has to be treated separately. In momentum space we have

$$\mathcal{A}_4^0 = -2 \int d^2 \mathbf{q}_1 d^2 \mathbf{q}_2 |\mathbf{q}_1|^2 |\mathbf{q}_2|^2 \hat{\Phi}_{\omega,2}(\mathbf{q}_1, \mathbf{q}_2) \frac{(\mathbf{q}_1 + \mathbf{q}_2)^2}{|\mathbf{q}_1|^2 |\mathbf{q}_2|^2} \prod_{i=1}^4 d^2 \mathbf{k}_i \hat{\Phi}_{\omega,4}(\mathbf{k}_1, \mathbf{k}_2, \mathbf{k}_3, \mathbf{k}_4)_{|\mathbf{q}_2 = \sum_{i=1}^4 \mathbf{k}_i - \mathbf{q}_1} \quad (4.45)$$

Explicit Fourier transformation leads to

$$\begin{aligned} \mathcal{A}_4^0 = -2 \int d^2 \rho_1 d^2 \rho_2 [\Delta_1 \Delta_2 \Phi_{\omega,2}(\rho_1, \rho_2)] \int d^2 \rho_0 \left[ -\pi \left( \delta^{(2)}(\rho_{10}) + \delta^{(2)}(\rho_{20}) \right) (\log |\rho_{12}|^2) \right. \\ \left. - 2 \nabla_1 \cdot \nabla_2 \log |\rho_{10}| \log |\rho_{20}| \right] \Phi_{\omega,4}(\rho_0, \rho_0, \rho_0, \rho_0) \end{aligned} \quad (4.46)$$

which can be rewritten as

$$\begin{aligned} \mathcal{A}_4^0 = & 2\pi \int d^2 \rho_1 d^2 \rho_2 [\Delta_1 \Delta_2 \Phi_{\omega,2}(\rho_1, \rho_2)] \log \frac{|\rho_{12}|^2}{\epsilon^2} (\Phi_{\omega,4}(\rho_1, \rho_1, \rho_1, \rho_1) + \Phi_{\omega,4}(\rho_2, \rho_2, \rho_2, \rho_2)) \\ & - 2 \int d^2 \rho_1 d^2 \rho_2 [\Delta_1 \Delta_2 \Phi_{\omega,2}(\rho_1, \rho_2)] \int d^2 \rho_0 \frac{|\rho_{12}|^2}{(|\rho_{10}|^2 + \epsilon^2)(|\rho_{20}|^2 + \epsilon^2)} \Phi_{\omega,4}(\rho_0, \rho_0, \rho_0, \rho_0) \end{aligned} \quad (4.47)$$

Here we have used that  $\int d^2 \rho_1 \Delta_1 \Phi_{\omega,2}(\rho_1, \rho_2) = 0$  (and equivalently for  $\rho_2$ ). This property is valid since we have required  $\Phi_{\omega,2}(\mathbf{q}_1, \mathbf{q}_2)$  - which is obtained from  $\hat{\Phi}_{\omega,2}$  by amputation of the propagators - to vanish if either  $\mathbf{q}_1 = 0$  or  $\mathbf{q}_2 = 0$ . The fictitious parameter  $\epsilon$  has been introduced to regularize the singularity of the  $\rho_0$ -integration in the second line. It is not possible to decompose the second line in eq. (4.47) into a holomorphic and an antiholomorphic part. Group C thus contains a contribution which is not holomorphic separable. Now we use the identity

$$\frac{1}{2} \nabla_0^2 \log^2 \frac{|\rho_{10}|}{|\rho_{20}|} = 2\pi \log \frac{\epsilon}{|\rho_{12}|} \left( \delta^{(2)}(\rho_{10}) + \delta^{(2)}(\rho_{20}) \right) + \frac{|\rho_{12}|^2}{(|\rho_{10}|^2 + \epsilon^2)(|\rho_{20}|^2 + \epsilon^2)} \quad (4.48)$$

to combine the two terms in eq. (4.47) in the compact expression.

$$\mathcal{A}_4^0 = - \int d^2 \rho_1 d^2 \rho_2 \Delta_1 \Delta_2 \Phi_{\omega,2}(\rho_1, \rho_2) \int d^2 \rho_0 \Delta_0 \log^2 \frac{|\rho_{10}|}{|\rho_{20}|} \Phi_{\omega,4}(\rho_0, \rho_0, \rho_0, \rho_0) \quad (4.49)$$

This finishes the discussion of the contact term.

Finally we come to the terms in groups A and B. Consider first group A with the permutation [1234]. We omit the momentum space representation and turn directly to configuration space where the sum of the three terms can be written as

$$\begin{aligned} \mathcal{A}_4^A = \int d^2 \rho_1 d^2 \rho_2 [\Delta_1 \Delta_2 \Phi_{\omega,2}(\rho_1, \rho_2)] \int d^2 \rho_0 \left[ \pi \log \frac{|\rho_{12}|^2}{\epsilon^2} \left( \delta^{(2)}(\rho_{10}) + \delta^{(2)}(\rho_{20}) \right) \right. \\ \left. - \frac{|\rho_{12}|^2}{(|\rho_{10}|^2 + \epsilon^2)(|\rho_{20}|^2 + \epsilon^2)} \right] \Phi_{\omega,4}(\rho_1, \rho_0, \rho_0, \rho_2) \end{aligned} \quad (4.50)$$

We make again use of the identity (4.48) to bring this in the final form

$$\mathcal{A}_4^A = -\frac{1}{2} \int d^2 \rho_1 d^2 \rho_2 [\Delta_1 \Delta_2 \Phi_{\omega,2}(\rho_1, \rho_2)] \int d^2 \rho_0 \log^2 \frac{|\rho_{10}|}{|\rho_{20}|} \Delta_0 \Phi_{\omega,4}(\rho_1, \rho_0, \rho_0, \rho_2) \quad (4.51)$$

where we have used integration by parts to shift the  $\Delta_0$ -operator to the right. All permutations in group A and B can be cast into this form. Hence we can represent all terms in group A and B as well as the remaining contact term from group C through an integral operator with the kernel

$$\mathcal{K}_A = \log^2 \frac{|\rho_{10}|}{|\rho_{20}|} \Delta_0 \quad (4.52)$$

As to the holomorphic separability we find that this integral operator can not be decomposed into a holomorphic and an antiholomorphic part. Consequently we have to conclude from our analysis that the transition vertex  $V$  is not holomorphic separable.

### 4.2.2 Conformal invariance

With the expressions which have been found above the conformal invariance of the transition vertex can be shown in a rather straightforward way. We collect all terms and find for the operator representation of  $V$  acting on the four-gluon function  $\Phi_{\omega,4}$

$$\begin{aligned}
& - \frac{1}{2} \int d^2 \rho_0 \log^2 \frac{|\rho_{10}|}{|\rho_{20}|} \Delta_0 [\Phi_{\omega,4}(1, 0, 0, 2) + \Phi_{\omega,4}(1, 0, 2, 0) + \Phi_{\omega,4}(0, 1, 0, 2) + \Phi_{\omega,4}(0, 1, 2, 0)] \\
& + \frac{1}{2} \int d^2 \rho_0 \log^2 \frac{|\rho_{10}|}{|\rho_{20}|} \Delta_0 [\Phi_{\omega,4}(1, 1, 0, 2) + \Phi_{\omega,4}(1, 1, 2, 0) + \Phi_{\omega,4}(0, 1, 2, 2) + \Phi_{\omega,4}(1, 0, 2, 2)] \\
& - \int d^2 \rho_0 \log^2 \frac{|\rho_{10}|}{|\rho_{20}|} \Delta_0 \Phi_{\omega,4}(0, 0, 0, 0) \\
& - \pi [\log(\rho_{12}^2 \partial_1) - \log \rho_{12} - \psi(1) + \text{h.c.}] [\Phi_{\omega,4}(1, 1, 1, 2) + \Phi_{\omega,4}(1, 1, 2, 1)] \\
& - \pi [\log(\rho_{12}^2 \partial_2) - \log \rho_{12} - \psi(1) + \text{h.c.}] [\Phi_{\omega,4}(1, 2, 2, 2) + \Phi_{\omega,4}(2, 1, 2, 2)] \\
& + \pi [\log(\rho_{12}^2 \partial_1) + \log(\rho_{12}^2 \partial_2) - 2 \log \rho_{12} - 2\psi(1) + \text{h.c.}] \Phi_{\omega,4}(1, 1, 2, 2)
\end{aligned} \tag{4.53}$$

The amplitude  $\mathcal{A}_4$  is obtained by multiplying with  $\int d^2 \rho_1 d^2 \rho_2 [\Delta_1 \Delta_2 \Phi_{\omega,2}]$ . The invariance of the above structure under rotation, translation and dilatation is obvious. It remains to investigate the behavior under the inversion transformation  $\rho_i \rightarrow 1/\rho_i, \rho_i^* \rightarrow 1/\rho_i^*$ . The last line corresponds to the BFKL kernel and we already know that it is invariant. For the terms in the fourth and fifth line we find under inversion

$$\log \rho_{12}^2 \partial_1 - \log \rho_{12} \longrightarrow \log \rho_{12}^2 \partial_1 - \log \rho_{12} + \log \frac{\rho_1}{\rho_2} \tag{4.54}$$

and conclude that under inversion we produce the original structure and get the additional terms

$$- \pi \log \frac{|\rho_1|^2}{|\rho_2|^2} [\Phi_{\omega,4}(1, 1, 1, 2) + \Phi_{\omega,4}(1, 1, 2, 1) - \Phi_{\omega,4}(1, 2, 2, 2) - \Phi_{\omega,4}(2, 1, 2, 2)] \tag{4.55}$$

For the first three lines the transformation properties of the operator  $\mathcal{K}_A$  have to be considered

$$\begin{aligned}
\mathcal{K}_A = \Delta_0 \log^2 \frac{|\rho_{10}|}{|\rho_{20}|} & \rightarrow |\rho_0|^4 \Delta_0 \log^2 \frac{|\rho_{10}| |\rho_2|}{|\rho_{20}| |\rho_1|} \\
& = \Delta_0 \log^2 \frac{|\rho_{10}|}{|\rho_{20}|} + 2\pi \log \frac{|\rho_2|^2}{|\rho_1|^2} \left( \delta^{(2)}(\rho_{10}) - \delta^{(2)}(\rho_{20}) \right)
\end{aligned} \tag{4.56}$$

Upon inversion we therefore obtain from the first and second line after some cancellations besides the original structure the additional terms

$$\pi \log \frac{|\rho_1|^2}{|\rho_2|^2} [\Phi_{\omega,4}(1, 1, 1, 2) - \Phi_{\omega,4}(1, 2, 2, 2) + \Phi_{\omega,4}(1, 1, 2, 1) - \Phi_{\omega,4}(2, 1, 2, 2)] \tag{4.57}$$

These terms cancel exactly against the additional terms in the expression (4.55). The contact term in the third line of expression (4.53) is invariant in itself. The additional terms vanish here since they depend only on either  $\rho_1$  or  $\rho_2$  and one can use the property discussed after eq. (4.47). This finishes the proof of conformal invariance of the transition vertex function  $V$  and in turn of the two-to-four vertex  $V_{2,4}$ .

To summarize, the transition vertex  $V$  has three important properties. It is infrared finite, it vanishes whenever the momentum of one of the outgoing gluons vanishes (zeropoint property) and it is symmetric under conformal transformations. The question arises whether these properties are independent or if conformal symmetry follows from the other ones. The presence of the isolated contact term which is invariant in itself shows that conformal symmetry is independent from the zeropoint property. The contact term is not necessary for conformal invariance but it is needed to have the zeropoint property. It is remarkable that the first term in the first line of fig. 4.1 representing the new element that appears when one considers four gluons can be written in configuration space - up to regularization - as  $\int d^2 \rho_0 |\rho_{12}|^2 / (|\rho_{10}|^2 |\rho_{20}|^2)$  (cf. eq. (4.50)).

From this one might have concluded that this term together with its infrared regulators is conformally invariant separately. The above results however show that this conjecture is not true. To render group A conformally invariant one inevitably has to add group C which is independent from A as far as infrared finiteness is concerned. This shows that when one starts from momentum space the conformal symmetry of the vertex is a quite nontrivial property which emerges from a very specific combination of momentum space structures. It is not possible to see from the present analysis if this property persists in higher orders, i. e. when the five and six reggeon system [96] is considered.

### 4.2.3 Projection on conformal three-point functions

In this part we show that the two-to-four vertex  $V_{(2,4)}$  has a nice interpretation in terms of the three-point function of the conformal field  $O_{h\bar{h}}$  which was introduced in eq. (4.45) to describe the bound state of two reggeized gluons. To this end we perform the projection of the vertex on three conformal eigenfunctions  $E^{(\nu)}(\rho_{10}, \rho_{20})$ . This means that we calculate the amplitude  $\mathcal{A}_4$  and use for the configuration space representation of the functions  $\Phi_{2,\omega}$  and  $\Phi_{4,\omega}$  the expressions

$$\begin{aligned}\Phi_{2,\omega}(\rho_{1'}, \rho_{2'}) &= E^{(\nu_c)}(\rho_{1'c}, \rho_{2'c}) \\ \Phi_{4,\omega}^{a_1 a_2 a_3 a_4}(\rho_1, \rho_2, \rho_3, \rho_4) &= \delta^{a_1 a_2} \delta^{a_3 a_4} E^{(\nu_a)*}(\rho_{1a}, \rho_{2a}) \cdot E^{(\nu_b)*}(\rho_{3b}, \rho_{4b})\end{aligned}\quad (4.58)$$

The color projection corresponds to color singlet states in the (12) and (34) subsystems of the outgoing gluons. The amplitude  $\mathcal{A}_4$  then depends on the three conformal dimensions and the respective bound-state coordinates  $\rho_a, \rho_b, \rho_c$ . Let us consider again the transition vertex function  $V$  which is displayed in fig. 4.1. In configuration space each vertex corresponds to a configuration space point  $\rho$ . Consequently for each pair of outgoing gluon lines  $i, j$  which merge into the same vertex we have a  $\delta$ -function  $\delta^{(2)}(\rho_{ij})$ . If we assume  $\text{Re}(1/2 + i\nu_a), \text{Re}(1/2 + i\nu_b) > 0$  then all contributions vanish in which either the gluons (12) or the gluons (34) merge into the same vertex. This is exactly the same argument that was used in the discussion of diffractive vector meson production in section 3.2 and diffractive  $q\bar{q}$  production in section 3.3. It follows that after projection only the group A of the vertex function  $V$  in fig. 4.1 gives a finite contribution. The function  $V$  as displayed in fig. 4.1 corresponds to the color structure  $\delta^{a_1 a_2} \delta^{a_3 a_4}$  of the vertex. For the other two color structures, however, also B and D give contributions.

Let us first have a closer look at group A. The configuration space representation of the permutation [1234] is given in eq. (4.50). With the same argument as given just before the logarithmic terms corresponding to the bubble diagrams can be shown to vanish. In the remaining term the regulator  $\epsilon^2$  can be omitted since with the above constraint on the conformal dimensions the  $\rho_0$ -integration is finite. All what is left from the vertex after projection is the first term in the first line of group A. The integral associated with this term reads

$$\mathcal{A}_4^A = - \int d^2\rho_1 d^2\rho_2 \left[ \Delta_1 \Delta_2 \left( \frac{|\rho_{12}|^2}{|\rho_{1c}|^2 |\rho_{2c}|^2} \right)^{\frac{1}{2} - i\nu_c} \right] \int d^2\rho_0 \frac{|\rho_{12}|^2}{|\rho_{10}|^2 |\rho_{20}|^2} \left( \frac{|\rho_{10}|^2}{|\rho_{1a}|^2 |\rho_{0a}|^2} \right)^{\frac{1}{2} + i\nu_a} \left( \frac{|\rho_{20}|^2}{|\rho_{0b}|^2 |\rho_{2b}|^2} \right)^{\frac{1}{2} + i\nu_b} \quad (4.59)$$

When acting on the conformal eigenfunction the twofold Laplace operator yields a factor  $|\rho_{12}|^{-4}$ . It is then possible with the repeated use of Feynman parameter techniques and the Mellin Barnes representation for the hypergeometric function to perform the integral in (4.59). An important condition for this to be possible is that for every  $i \in \{0, 1, 2\}$  the sum of the powers of all monomials  $|\rho_{ik}|^2$  which contain the index  $i$  is -2. The result then reads

$$\mathcal{A}_4^A = (|\rho_{ab}|^2)^{-\frac{1}{2} - i\nu_c - i\nu_a - i\nu_b} (|\rho_{bc}|^2)^{-\frac{1}{2} + i\nu_c + i\nu_a - i\nu_b} (|\rho_{ac}|^2)^{-\frac{1}{2} + i\nu_c - i\nu_a + i\nu_b} \cdot \Omega(\nu_a, \nu_b, \nu_c) \quad (4.60)$$

The function  $\Omega(\nu_a, \nu_b, \nu_c)$  is too complicated to display it explicitly here. It can be written as a sum of strings of iterated contour integrals over fractions of  $\Gamma$ -functions. What is important is that the dependence of  $\mathcal{A}_4$  upon the coordinates is completely explicit and turns out to be very simple. It can be checked easily that (4.59) and (4.60) transform identically under conformal transformations. By comparison with the general form of a three-point function of conformal fields (4.43) one finds that  $\mathcal{A}_4^A$  as given above can be associated

with the three point function of the field  $O_{h,\bar{h}}$

$$\langle O_{h_a,\bar{h}_a}^*(\rho_a) O_{h_b,\bar{h}_b}^*(\rho_b) O_{h_c,\bar{h}_c}(\rho_c) \rangle = \mathcal{A}_4^A + \dots \quad (4.61)$$

where  $h_k = \bar{h}_k$  is given as  $h_k = 1/2 + i\nu_k$  for  $k = a, b$  and  $h_k = 1/2 - i\nu_k$  for  $k = c$  and the dots indicate further contributions. We have  $h = \bar{h}$  here since we have considered zero conformal spin only. Without doubt the above relation also generalizes to nonzero conformal spin.

It would of course be desirable to obtain more information on the function  $\Omega(\nu_a, \nu_b, \nu_c)$ . It would e. g. be interesting to isolate the singularity which implements the conservation of the conformal dimensions as it was done for the disconnected vertex (which results from the reggeized part of  $D_4$ ) in section 3.3. Another point of interest is the triple pomeron point  $\nu_a = \nu_b = \nu_c = 0$ . Since the coordinate dependence of  $\mathcal{A}_4$  is explicitly known one could use the points  $\rho_a = 0, \rho_b = 1, \rho_c = \infty$  to calculate the function  $\Omega$ . But even with this simplification applied  $\Omega(\nu_a, \nu_b, \nu_c)$  presently cannot be expressed in a transparent way. As to the point  $\nu_a = \nu_b = \nu_c = 0$  one could of course think of a numerical Monte Carlo integration to determine the value  $\Omega(0, 0, 0)$ .

So far we have only considered one part of the vertex  $V_{(2,4)}$  which belongs to the color structure  $\delta^{a_1 a_2} \delta^{a_3 a_4}$ . If we turn to the other two contributions then different terms give a nonzero result after projection. The momentum space structure which accompanies the color structure  $\delta^{a_1 a_3} \delta^{a_2 a_4}$  is obtained from the function  $V$  displayed in fig. 4.1 by interchanging the momenta of gluons (2) and (3). Projecting then in the same way as above on the (12) and (34) subsystems one finds that from group A the permutations [1234] and [2143] give a nonzero result which corresponds to  $\mathcal{A}_4^A$  given in eq. (4.59). As to the group B the situation is more complicated. With the same arguments as given above the second term in each line can be shown to vanish for all four permutations. The other two terms, however, have to be kept. We consider all four permutations together and find after projection the following expression

$$\begin{aligned} \mathcal{A}_4^B = & \int \frac{d^2 \rho_1 d^2 \rho_2}{|\rho_{12}|^4} \left( \frac{|\rho_{12}|^2}{|\rho_{1c}|^2 |\rho_{2c}|^2} \right)^{\frac{1}{2} - i\nu_c} \left( \frac{|\rho_{12}|^2}{|\rho_{1b}|^2 |\rho_{2b}|^2} \right)^{\frac{1}{2} + i\nu_b} \\ & \int d^2 \rho_0 \left[ \frac{|\rho_{12}|^2}{|\rho_{10}|^2 |\rho_{20}|^2} \theta \left( \frac{|\rho_{20}|}{|\rho_{12}|} - \epsilon \right) + \pi \delta^{(2)}(\rho_{20}) \log \epsilon^2 \right] \left( \frac{|\rho_{10}|^2}{|\rho_{1a}|^2 |\rho_{0a}|^2} \right)^{\frac{1}{2} + i\nu_a} \\ & + [(\nu_a, \rho_a) \longleftrightarrow (\nu_b, \rho_b)] \\ & + [\rho_2 \longleftrightarrow \rho_1] \\ & + [(\nu_a, \rho_a) \longleftrightarrow (\nu_b, \rho_b) \wedge \rho_2 \longleftrightarrow \rho_1] \end{aligned} \quad (4.62)$$

Note that here the regularization is needed since the conformal dimension regulates only one singularity of the  $\rho_0$ -integration. We have chosen the  $\theta$ -function regularization since this is convenient for the following steps. One can show that the  $\rho_0$ -integral in the second line together with the one obtained after interchange of the coordinates  $\rho_1$  and  $\rho_2$  (fourth line) is conformally invariant. The logarithms obtained after transformation of the argument of the  $\theta$ -function cancel between the two terms due to antisymmetry. This works in the same way as in the proof of conformal invariance of the BFKL kernel. From this we conclude that the conformal three-point function which appears in the  $\rho_0$ -integral is an eigenfunction of the integral operator associated with this integral. For the remaining terms in (4.62) the same is true with  $(\nu_a, \rho_a)$  and  $(\nu_b, \rho_b)$  interchanged. We thus find the interesting feature that after interchange of the outgoing gluons (2) and (3) the operator which is associated with group B decomposes into two terms which are diagonalized by conformal eigenfunctions in the (12) subsystem and (34) subsystem, respectively.  $\mathcal{A}_4^B$  can therefore be expressed as

$$\mathcal{A}_4^B = \int \frac{d^2 \rho_1 d^2 \rho_2}{|\rho_{12}|^4} \left( \frac{|\rho_{12}|^2}{|\rho_{1c}|^2 |\rho_{2c}|^2} \right)^{\frac{1}{2} - i\nu_c} \left( \frac{|\rho_{12}|^2}{|\rho_{1b}|^2 |\rho_{2b}|^2} \right)^{\frac{1}{2} + i\nu_b} \left( \frac{|\rho_{12}|^2}{|\rho_{1a}|^2 |\rho_{2a}|^2} \right)^{\frac{1}{2} + i\nu_a} [\xi(\nu_a) + \xi(\nu_b)] \quad (4.63)$$

An explicit calculation yields for the function  $\xi$

$$\xi(\nu) = 2\pi \left[ 2\psi(1) - \psi\left(\frac{1}{2} + i\nu\right) - \psi\left(\frac{1}{2} - i\nu\right) \right] \quad (4.64)$$

which coincides with the eigenvalue of the BFKL kernel <sup>20</sup>. We have thus found the striking result that after a permutation of the outgoing gluons the group B from the vertex function V acts as the BFKL kernel on pairs of the outgoing gluons. The integration over  $\rho_1$  and  $\rho_2$  can now be performed with the result

$$\mathcal{A}_4^B = (|\rho_{ab}|^2)^{-\frac{1}{2}-i\nu_c-i\nu_a-i\nu_b} (|\rho_{bc}|^2)^{-\frac{1}{2}+i\nu_c+i\nu_a-i\nu_b} (|\rho_{ac}|^2)^{-\frac{1}{2}+i\nu_c-i\nu_a+i\nu_b} \cdot \Lambda(\nu_a, \nu_b, \nu_c) [\xi(\nu_a) + \xi(\nu_b)] \quad (4.65)$$

We conclude that also this term has the general form of a conformal three-point function of the field  $O_{h,\bar{h}}$ . It gives a contribution to the terms which are indicated as dots in eq. (4.61). Before we have a closer look at the function  $\Lambda(\nu_a, \nu_b, \nu_c)$  we discuss the contribution of the group D. This group has the structure of the BFKL kernel and it is clear that this kernel is diagonal in the conformal eigenfunction used for projection from above. The  $\rho_0$ -integration hence yields the familiar BFKL eigenvalue and the remaining  $\rho_1, \rho_2$ -integration is exactly the same as in eq. (4.63) above. The result for the group D thus reads

$$\mathcal{A}_4^D = -(|\rho_{ab}|^2)^{-\frac{1}{2}-i\nu_c-i\nu_a-i\nu_b} (|\rho_{bc}|^2)^{-\frac{1}{2}+i\nu_c+i\nu_a-i\nu_b} (|\rho_{ac}|^2)^{-\frac{1}{2}+i\nu_c-i\nu_a+i\nu_b} \Lambda(\nu_a, \nu_b, \nu_c) \xi(\nu_c) \quad (4.66)$$

with  $\xi(\nu)$  as given above. As to the function  $\Lambda(\nu_a, \nu_b, \nu_c)$  we can make use of the fact that the coordinate dependence of the integral in eq. (4.63) is known and therefore use the coordinates  $\rho_a = 0, \rho_b = 1, \rho_c = \infty$  to determine  $\Lambda$ . In this way we are able to extract the singularity which expresses the conservation of conformal dimensions from the function  $\Lambda$ . We obtain

$$\Lambda(\nu_a, \nu_b, \nu_c) = \frac{\Gamma(\frac{1}{2} + i\nu_a + i\nu_b - i\nu_c)}{\Gamma(\frac{1}{2} - i\nu_a - i\nu_b + i\nu_c)} \lambda(\nu_a, \nu_b, \nu_c) \quad (4.67)$$

The function  $\lambda$  can be expressed as a twofold Mellin Barnes integral over a rational function of  $\Gamma$ -functions. The  $\Gamma$ -function which we have extracted expresses in the same way as discussed in section 3.3 the conservation of conformal dimensions at the two-to-four transition vertex. It is easy to see that this singularity is associated with the region  $|\rho_{12}| \sim 0$  of the integral in eq. (4.63).

Finally one has to consider the third part of the vertex  $V_{(2,4)}$  which belongs to the color structure  $\delta^{a_1 a_4} \delta^{a_2 a_3}$ . One immediately realizes that here the situation is the same as in the case discussed just before, i. e. we have to multiply the above results for the color structure  $\delta^{a_1 a_3} \delta^{a_2 a_4}$  with a factor of two.

If we collect all terms we find the following result for the  $V_{(2,4)}$  vertex projected on conformal eigenfunctions in the subsystems of the gluon pairs  $(1'2')$ ,  $(12)$  and  $(34)$

$$\begin{aligned} \mathcal{A}_4 &= \frac{1}{64} \int \prod_{i=1}^2 d^2 \rho_{i'} E^{(\nu_c)}(\rho_{1'c} \rho_{2'c}) \int \prod_{i=1}^4 d^2 \rho_i V_{(2,4)}^{a_1 a_2 a_3 a_4}(\{\rho_{i'}\}; \{\rho_i\}) \delta^{a_1 a_2} \delta^{a_3 a_4} E^{(\nu_a)*}(\rho_{1a} \rho_{2a}) E^{(\nu_b)*}(\rho_{3b} \rho_{4b}) \\ &= (|\rho_{ab}|^2)^{-\frac{1}{2}-i\nu_c-i\nu_a-i\nu_b} (|\rho_{bc}|^2)^{-\frac{1}{2}+i\nu_c+i\nu_a-i\nu_b} (|\rho_{ac}|^2)^{-\frac{1}{2}+i\nu_c-i\nu_a+i\nu_b} \\ &\quad \left[ 4\Omega(\nu_a, \nu_b, \nu_c) + \frac{1}{4} [2\Omega(\nu_a, \nu_b, \nu_c) + \Lambda(\nu_a, \nu_b, \nu_c) (\xi(\nu_a) + \xi(\nu_b) - \xi(\nu_c))] \right] \end{aligned} \quad (4.68)$$

The factor  $1/4$  results from the two identical contributions which have a color factor of  $1/8$  relative to the first term whose color structure matches the color structure of the projection operator. The factor  $1/64$  is a convenient normalization of the color projector.

The above equation states that one can consistently interpret the amplitude  $\mathcal{A}_4$  as a three point function of three fields of a conformal field theory with conformal dimensions  $\nu_a, \nu_b, \nu_c$

$$\mathcal{A}_4 = \langle O_{h_a, \bar{h}_a}^*(\rho_a) O_{h_b, \bar{h}_b}^*(\rho_b) O_{h_c, \bar{h}_c}(\rho_c) \rangle \quad (4.69)$$

In chapter 2 we have seen that the results of the BFKL theory fit into the framework of a general conformal field theory. Here we have demonstrated that the first nontrivial unitarity corrections - the effective two-to-four - vertex also has a natural interpretation in this setup. This strongly supports the expectation that the concept of an effective conformal field theory might serve as a powerful guideline in the investigation of the

<sup>20</sup>We do not use the symbol  $\chi$  here since this was defined to include a coefficient  $N_c \alpha_s / (2\pi^2)$ .



Regge limit of QCD.

$\mathcal{A}_4$  is not yet the complete three point function of the conformal field  $O_{h,\bar{h}}$  since we have not taken into account the four-reggeon state which follows below the vertex. Since this state is constructed from conformally invariant elements it is however clear that the coordinate dependence of the full three point function will be identical with the one in eq. (4.68). The four reggeon state will therefore only modify the coefficient which depends on the conformal dimensions. We turn to this problem in the next section.

### 4.3 The four gluon state I: Introduction, Motivation and Examples

In this section we investigate the second new element which arises from the study of subleading unitarity corrections to the BFKL pomeron, the fully interacting four reggeon amplitude  $G_4(\omega)$ . This amplitude is determined through the following generalized Bethe-Salpeter equation

$$\omega G_4^{\{a_i\},\{a'_j\}}(\omega; \{\mathbf{k}_i\}, \{\mathbf{k}'_j\}) = \prod_{i'=1}^4 \delta^{a_{i'} a'_{i'}} \delta^{(2)}(\mathbf{k}_{i'} - \mathbf{k}'_{i'}) + \sum_{1 \leq i' < j' \leq 4} (\mathcal{K}_{i'j'} \otimes G_4(\omega))^{\{a_i\},\{a'_j\}}(\{\mathbf{k}_i\}, \{\mathbf{k}'_j\}) \quad (4.70)$$

where the operator  $\mathcal{K}_{ij}$  describes the two reggeon interaction, i. e. it acts on the reggeons with the indices  $i$  and  $j$  and leaves the others unchanged. The interaction kernel acts on the reggeons  $i$  and  $j$  according to

$$(\mathcal{K}_{ij} \otimes \phi)^{a_1 a_2}(\mathbf{k}_1, \mathbf{k}_2) = \frac{1}{3} f^{a'_1 c a_1} f^{c a_2 a'_2} \left[ \left( K_{(2,2)}^0 \otimes \phi^{a'_1 a'_2} \right) (\mathbf{k}_1, \mathbf{k}_2) - (\beta(\mathbf{k}_1) + \beta(\mathbf{k}_2)) \phi^{a'_1 a'_2}(\mathbf{k}_1, \mathbf{k}_2) \right] \quad (4.71)$$

where  $K_{(2,2)}^0$  is the operator which is given in eq. (4.2) ( $c_0 = 2$ ),  $\beta(\mathbf{k})$  is the trajectory function of the gluon and the  $f^{ijk}$  are the generators of  $SU(3)$  in the adjoint representation, i. e. the structure constants. It is assumed that the total color of the four reggeon system is zero. The momentum structure of the two reggeon interaction corresponds to the one of the BFKL kernel in the color singlet channel. This has the immediate consequence that  $G_4(\omega)$  contains no infrared singularities. The coefficient of the interaction kernel depends on the color state of the two reggeon system. For the moment we keep the color structure in the explicit tensor form. The coefficient of the respective color state can be obtained by applying the corresponding projection operators.

If one compares the equations above with the initial equation (4.12) for the four reggeon amplitude  $D_4(\omega)$  one should note that a nontrivial step has been done to arrive at the form (4.71) of the interaction kernel. The original equation contains one trajectory function for each reggeon. Above, each trajectory function appears three times, multiplied with a nontrivial color structure which is normally associated with an  $s$ -channel gluon-production diagram. That eqs. (4.70) and (4.12) are indeed equivalent follows from the consideration of the infrared behavior. It has been shown in [18] that eq. (4.12) is free from infrared singularities, i. e. all divergencies cancel mutually, provided that the four reggeon system is in a color singlet state. The kernel  $K_{(2,2)}^0$  in (4.71) including the color structure is identical with the one that appears in (4.12). Since the kernel (4.71) and in turn eq. (4.70) are manifestly infrared finite it follows that the distribution of the trajectory functions into two-particle interaction kernels<sup>21</sup> in (4.70) is equivalent to the representation in terms of a reggeon propagator in eq. (4.12). If it were not equivalent there would appear isolated infrared singularities in (4.71). The advantage of the representation above is its manifest infrared finiteness and the appearance of the BFKL kernel. The symmetry properties of the latter facilitate to a large extent the analysis of the four reggeon system.

#### 4.3.1 The onset of unitarity

The ultimate aim is to solve eq. (4.70) or, equivalently, to diagonalize the four-particle operator which appears on the right hand side. Let us first sketch schematically the significance of such a solution. Assume that a complete set of eigenfunctions of the four-particle operator is known. We denote these eigenfunctions by  $\psi_{\{\alpha\}}(\{\mathbf{k}_i\})$  where the  $\mathbf{k}_i$  ( $i = 1, 2, 3, 4$ ) are the momentum space arguments and the set  $\{\alpha\}$  represents a

<sup>21</sup> This interaction is not a reggeon interaction any more, since the corresponding equation contains no reggeon propagator. Nevertheless we will use the term 'four-reggeon system' in the following to denote the system which is described by eq. (4.70).

collection of quantum numbers that parameterize the solutions. These quantum numbers will be related to the different symmetries of the problem. These symmetries include the color symmetry and the conformal symmetry. This means that there will be at least one quantum number related to the irreducible representations of the color group  $SU(3)$  and quantum numbers related to the representation of the conformal group, i. e. conformal dimension and conformal spin. In addition, quantum numbers belonging to extra symmetries are expected. The functions  $\psi_{\{\alpha\}}(\{\mathbf{k}_i\})$  diagonalize the four particle operator

$$\sum_{1 \leq i' < j' \leq 4} (\mathcal{K}_{i'j'} \otimes \psi_{\{\alpha\}})(\{\mathbf{k}_i\}) = \chi_4(\{\alpha\}) \psi_{\{\alpha\}}(\{\mathbf{k}_i\}) \quad (4.72)$$

with eigenvalues  $\chi_4(\{\alpha\})$ . Now the formal solution of eq. (4.70) reads

$$G_4(\omega, \{\mathbf{k}_i\}, \{\mathbf{k}'_j\}) = \sum_{\{\alpha\}} \frac{\psi_{\{\alpha\}}(\{\mathbf{k}_i\}) \psi_{\{\alpha\}}^*(\{\mathbf{k}'_j\})}{\omega - \chi_4(\{\alpha\})} \quad (4.73)$$

where the summation symbol stands for summation of discrete and integration of continuous quantum numbers. We have implicitly assumed that the functions  $\psi_{\{\alpha\}}$  satisfy suitable completeness and orthonormalization conditions. The color index of  $G_4(\omega)$  is suppressed here and in the following. We have assumed that  $\psi_{\{\alpha\}}$  is a tensor in color space.

This formal solution can now be inserted into eq. (4.16) to obtain the result for the irreducible part of the four reggeon amplitude  $D_4^I(\omega; \{\mathbf{k}_i\})$ . We use the fact that the solution for the two reggeon amplitude  $D_2(\omega)$  is known to be given by the BFKL pomeron and represent  $D_4^I(\omega)$  in the form

$$D_4^I(\omega; \{\mathbf{k}_i\}) = \int_{-\infty}^{+\infty} \frac{d\nu}{2\pi} \frac{D_{2,0}(\nu)}{\omega - \chi_2(\nu)} \sum_{\{\alpha\}} V_{(2,4)}(\nu, \{\alpha\}) \frac{1}{\omega - \chi_4(\{\alpha\})} \psi_{\{\alpha\}}(\{\mathbf{k}_i\}) \quad (4.74)$$

The function  $\chi_2(\nu)$  is the BFKL eigenvalue, formerly denoted by  $\chi(\nu)$ .  $D_{2,0}(\nu)$  is an impact factor in the Mellin representation which couples the two reggeon state to colorless external particles. The function  $V_{(2,4)}(\nu, \{\alpha\})$  arises from integrating the two to four transition vertex studied in the last section with the eigenfunctions  $E^{(\nu)}$  of the BFKL equation from above and the eigenfunctions  $\psi_{\{\alpha\}}$  of the four reggeon system from below. The momentum space integration which is involved here is expected to lead to nontrivial correlations between the quantum number  $\nu$  associated with the two reggeon state and the quantum numbers of the four reggeon system which are related to the conformal symmetry. As an example of such a correlation we have already discussed the conservation of conformal dimensions at the triple pomeron vertex at an earlier stage of this work 3.3.

Now, for simplicity, we construct the partial wave amplitude  $A(\omega, t)$  from  $D_4^I(\omega)$  by convoluting eq. (4.74) from below with a phenomenological impact factor  $B$  that depends on the four gluon momenta and contracts the color indices<sup>22</sup>. Having constructed the partial wave amplitude one gets the energy dependence of the amplitude by performing the  $\omega$ -integration. Taking the residues at  $\omega = \chi_2(\nu)$  and  $\omega = \chi_4(\{\alpha\})$  one obtains a sum of two terms<sup>23</sup>

$$A(s, t) = is \int \frac{d\nu}{2\pi} \sum_{\{\alpha\}} D_{2,0}(\nu) V_{(2,4)}(\nu, \{\alpha\}) B(\{\alpha\}) \left[ \frac{s^{\chi_2(\nu)}}{\chi_2(\nu) - \chi_4(\{\alpha\})} + \frac{s^{\chi_4(\{\alpha\})}}{\chi_4(\{\alpha\}) - \chi_2(\nu)} \right] \quad (4.75)$$

For large energy  $s$  the first term will be dominated by the region near  $\nu = 0$  and one obtains the usual energy behavior of the BFKL amplitude  $A(s, t) \sim s^{N_c \alpha_s / \pi 4 \log 2}$  with a coefficient proportional to  $\alpha_s^2$ . Recall that the transition vertex  $V_{(2,4)}$  is proportional to  $\alpha_s^2$ . With regard to the energy dependence the first contribution is therefore on the same level as the part of the amplitude that arises from the reggeizing part  $D_4^R$  of the four reggeon amplitude. The latter can be expressed in terms of the two reggeon amplitude  $D_2$  with a global coefficient of order  $\alpha_s$  (cf. eq. (4.15)). Consequently it has the same energy dependence as the first

<sup>22</sup>In this way one would proceed when this formalism is applied to inclusive deep inelastic scattering.

<sup>23</sup>The energy  $s$  is measured in units of a mass scale of the process.

term in (4.75). Both terms therefore lead to a higher order renormalization of the coefficient function of the BFKL amplitude. The second contribution in eq. (4.74) is of greater significance. If we assume that  $\hat{\chi}_4 = \chi_4(\{\hat{\alpha}\}) = \max_{\{\alpha\}} \chi_4(\{\alpha\})$  exists then this term introduces a new energy dependence in next-to-leading order in  $\alpha_s$

$$A(s, t) = i s^{1+\hat{\chi}_4} \int \frac{d\nu}{2\pi} \frac{D_{2,0}(\nu) V_{(2,4)}(\nu, \{\hat{\alpha}\}) B(\{\hat{\alpha}\})}{\chi_4(\{\hat{\alpha}\}) - \chi_2(\nu)} \quad (4.76)$$

This contribution now defines the first unitarity correction to the BFKL pomeron. Let us assume that the relation  $\hat{\chi}_4 > \hat{\chi}_2 = N_c \alpha_s / \pi 4 \log 2$  holds and furthermore that the coefficient of the term (4.76) turns out to be negative. By taking into account the contribution (4.76) and the contribution that is obtained from the two reggeon amplitude  $D_2(\omega)$  we find the following structure of the scattering amplitude

$$A(s, t) = i s [c_0 s^{\hat{\chi}_2} - \alpha_s^2 c_1 s^{\hat{\chi}_4}] \quad (4.77)$$

This demonstrates the effect of the unitarity corrections which are encoded in the second term. If the energy  $s$  starts to increase the first term dominates and the amplitude will rise as a function of  $s$  with the power given by the BFKL exponent. With a further increase of the energy the  $O(\alpha_s^2)$ -suppressed second term will gradually become important. This term will damp the rise of the amplitude and ultimately stop it. Clearly, for even larger energies also this term violates unitarity since it induces a power dependence on  $s$ . This shows the necessity to take into account all higher order reggeon amplitudes. For each  $n$ -reggeon amplitude a reasoning along the lines above leads to a new contribution to the amplitude which has a coefficient<sup>24</sup> of order  $\alpha_s^{\frac{n}{2}}$  and depends on the energy according to the power behavior  $s^{\hat{\chi}_n}$ . Each of these terms individually violates unitarity. Since, however, the formalism from which these results are obtained was designed from the beginning to provide a unitary scattering amplitude, unitarity is expected to be restored when all terms are summed up. As an example [97] of a series with such properties consider

$$\sum_{n=0}^{\infty} \frac{(-\alpha_s)^n}{n+1} s^{(n+1)\lambda} = \frac{1}{\alpha_s} \log(1 + \alpha_s s^\lambda) \approx \frac{\lambda}{\alpha_s} \log s \quad (4.78)$$

where the last expression is obtained in the limit of asymptotically large  $s$ . This example is intended to demonstrate that from a summation of powers a logarithm can be obtained. It is clear from this discussion that the solution of the four reggeon problem constitutes only one step on the path towards an unitary amplitude. From a phenomenological point of view, however, it is of great significance. Without it, it is impossible to decide at which energies the first modifications of the leading-log behavior become important. With the knowledge of at least the four reggeon correction a much more consistent comparison than presently can be made of experimental data with the results of the BFKL theory. It would e. g. be highly interesting to see if a satisfactory description of the behavior of the deep inelastic structure function  $F_2$  as measured in the small  $x$  regime of the HERA collider is possible by adding the four reggeon contribution to the BFKL pomeron. From eq. (4.76) we see that the transition vertex  $V_{(2,4)}$  plays an important role in this context. It contributes to the coefficient function which ultimately determines the sign of the correction.

### 4.3.2 Correlation functions, short distance limit and the BFKL amplitude as an example

In the last subsection the new energy dependence which is obtained from the four reggeon state was considered. The focus of the present section is the transverse momentum or, equivalently, the coordinate dependence of the reggeon amplitudes. This will ultimately lead us to an approach towards the four reggeon spectrum  $\chi_4(\{\alpha\})$  which is pursued in the subsequent sections of this chapter.

In eq. (4.69) of the preceding section we have already discussed the three point correlation function of the field  $O_{h\bar{h}}(\rho)$  that has been introduced to describe a compound state of two reggeons (reggeized gluons). At that point the calculation of the coefficient of this correlation function remained incomplete, but with the knowledge of the four reggeon amplitude  $G_4(\omega)$  this function can be completely determined within the

<sup>24</sup>For some  $n$  the coefficient might be zero. See e. g.  $n = 3$  above and the discussion in [96].

approximation scheme that takes into account up to four reggeons. It is clear in which way the three point function is calculated. First one has to convolute the function  $G_4(\omega)$  with the transition vertex  $V_{(2,4)}$ . Then the vertex is convoluted from above with the conformal eigenfunction  $E^{(\nu_c)}$ . Simultaneously the four gluons at the lower end of  $G_4(\omega)$  are grouped into two pairs, e. g. (12) and (34), and the corresponding legs are convoluted with conformal eigenfunctions  $E^{(\nu_a)*}$  and  $E^{(\nu_b)*}$ . In the configuration space representation the result <sup>25</sup> reads

$$\langle O_{h_c \bar{h}_c}(\rho_c) O_{h_a \bar{h}_a}^*(\rho_a) O_{h_b \bar{h}_b}^*(\rho_b) \rangle = \left[ \prod_{\substack{(i,j \in \{a,b,c\}) \\ i \neq j}} (|\rho_{ij}|^2)^{-h_i - h_j + 2 \sum_k h_k} \right] \sum_{\{\alpha\}} \frac{V_{(2,4)}(\nu_c, \{\alpha\}) g_4(\{\alpha\}, \nu_a, \nu_b)}{\omega - \chi_4(\{\alpha\})} \quad (4.79)$$

The relation between the conformal weights and the conformal dimension of the field  $O_{h\bar{h}}(\rho)$  is in each case  $h_i = \bar{h}_i = 1/2 - i\nu_i$  since we have restricted ourselves to zero conformal spin. For the conjugate field  $O_{h\bar{h}}^*(\rho)$  we have  $h_i = \bar{h}_i = 1/2 + i\nu_i$ . The residue functions  $V(\nu_c, \{\alpha\})$  and  $g_4(\{\alpha\}, \nu_a, \nu_b)$  arise from the convolution of the conformal eigenfunctions with the momentum space dependent part of the vertex function  $V_{(2,4)}$  and the amplitude  $G_4(\omega)$ .

From the function  $G_4(\omega)$  also the four point function of the field  $O_{h\bar{h}}(\rho)$  can be constructed. This can be done by grouping the four gluons at the upper end of  $G_4(\omega)$  into two pairs (1'2') and (3'4') and convoluting these pairs with conformal eigenfunctions  $E^{(\nu_c)}$  and  $E^{(\nu_d)}$ . The lower end of  $G_4(\omega)$  is convoluted in the same way as for the three point function. This defines the four point correlation function

$$\begin{aligned} \langle O_{h_c \bar{h}_c}(\rho_c) O_{h_d \bar{h}_d}(\rho_d) O_{h_a \bar{h}_a}^*(\rho_a) O_{h_b \bar{h}_b}^*(\rho_b) \rangle = & \left[ \prod_{\substack{(i,j \in \{a,b,c,d\}) \\ i \neq j}} (|\rho_{ij}|^2)^{-h_i - h_j + \frac{1}{3} \sum_k h_k} \right] \\ & \cdot \sum_{\{\alpha\}} \frac{g_4^*(\{\alpha\}, \nu_c, \nu_d) g_4(\{\alpha\}, \nu_a, \nu_b)}{\omega - \chi_4(\{\alpha\})} \Psi(\{\nu\}, \{\alpha\}; \eta, \eta^*) \end{aligned} \quad (4.80)$$

Here  $\eta$  denotes the anharmonic ratio  $(\rho_{ab}\rho_{cd})/(\rho_{ac}\rho_{bd})$  and  $\Psi$  is an unknown function. The construction of the four point and the three point correlation function is illustrated in fig. 4.2. For both cases the coordinate dependence follows entirely from conformal covariance.

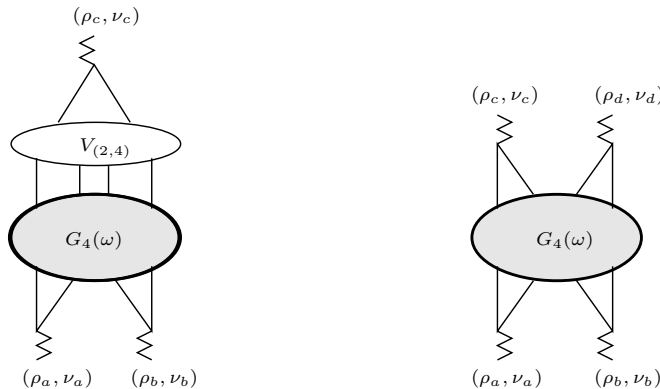


Figure 4.2: Construction of the three point and the four point function of the field  $O_{h\bar{h}}(\rho)$  from the four reggeon amplitude  $G_4(\omega)$  and the vertex  $V_{(2,4)}$ .

Having found the four point function of the field  $O_{h\bar{h}}$  one is able to derive the operator algebra of this field.

<sup>25</sup> Note that we do not include a two reggeon state above the vertex in our definition of the three point function. Likewise we do not include a full two reggeon amplitude in the subsystems (12) and (34) at the lower end.

In general the operator algebra [52, 42, 98] is contained in expansions of the form <sup>26</sup>

$$O_i(\rho_i)O_j(\rho_j) = \sum_k \frac{C_k^{ij}}{|\rho_{ij}|^{\Delta_i+\Delta_j-\Delta_k}} O_k(\rho_i) \quad (4.81)$$

which holds when the operators are inserted into some correlation function. The quantities  $\Delta_i$  are usually called the scaling dimensions <sup>27</sup> of the fields  $O_i$ . It is clear from the transformation properties of (4.81) that they coincide with the conformal dimensions, i. e. they are related to the conformal weights  $h, \bar{h}$  through  $\Delta_i = h_i + \bar{h}_i$ . The summation on the rhs extends over an infinite set of operators. From the point of view of conformal field theory [42, 52], the scaling dimensions  $\Delta$  and the expansion coefficients (fusion coefficients)  $C_k^{ij}$  contain the whole information on the theory. The knowledge of all anomalous dimensions and all fusion coefficients in (4.81) is hence equivalent to having the explicit representation of the four point function. In particular the operator algebra contains the information on the spectrum  $\chi_4(\alpha)$

The operator algebra in (4.81) can be determined from the four point function by performing short distance limits w. r. t. the coordinates.

Since the relation between the operator algebra and the spectrum is the central idea of what follows below we will illustrate it using the BFKL four point function as an example.

Let us consider the four point function of the field  $\phi_{00}$  associated with the reggeized gluon. This function was calculated explicitly in section 2.2 and we found the result (cf. eq. (4.47))

$$\begin{aligned} < \phi_{00}(\rho_1)\phi_{00}(\rho_2)\phi_{00}(\rho_{1'})\phi_{00}(\rho_{2'}) > = \int_{-\infty}^{+\infty} d\nu \frac{1}{\omega - \chi_2(\nu)} \\ & \cdot \left[ c(\nu)\eta^{\frac{1}{2}+i\nu}\eta^{*\frac{1}{2}+i\nu}F(\nu, \eta)F(\nu, \eta^*) + c(-\nu)\eta^{\frac{1}{2}-i\nu}\eta^{*\frac{1}{2}-i\nu}F(-\nu, \eta)F(-\nu, \eta^*) \right] \end{aligned} \quad (4.82)$$

where  $\eta = (\rho_{12}\rho_{1'2'})/(\rho_{11'}\rho_{22'})$  and  $F(\nu, \eta)$  is a shorthand notation for  ${}_2F_1(1/2 + i\nu, 1/2 + i\nu, 1 + 2i\nu; \eta)$ . We examine the short-distance limit  $|\rho_{12}| \ll |\rho_{1'2'}| \sim |\rho_{12'}| \sim |\rho_{1'2}|$ . In this limit the hypergeometric function is regular and we replace it with unity. More interesting are the factors  $|\rho_{12}|^{i\nu}, |\rho_{12}|^{-i\nu}$ . From these factors we obtain an expansion in  $|\rho_{12}|$  by shifting the contour of the  $\nu$ -integration past the singularities of the  $\nu$ -dependent coefficient. We restrict our considerations to the singularities generated by the factor  $1/(\omega - \chi_2(\nu))$ . The singularities of this term are obtained from the solution of the equation

$$\omega = \chi_2(\nu) \quad (4.83)$$

If we assume  $\alpha_s \ll \omega$ , i. e. we are not in the limit of asymptotically large energies, solutions of this equation can be found at

$$\nu_k = \pm \frac{1}{i} \left( \frac{1}{2} + k - \frac{N_c \alpha_s}{\pi \omega} \right) + O(\alpha_s^2), \quad k \in \mathbb{N} \quad (4.84)$$

To obtain the series representation of the four point function we close the  $\nu$ -contour in the lower half plane for the first term in eq. (4.82) and in the upper half plane for the second term. Retaining only terms of order  $\alpha_s$  in the solution (4.84) the resulting series reads

$$< \phi(\rho_1)\phi(\rho_2)\phi(\rho_{1'})\phi(\rho_{2'}) > \stackrel{|\rho_{12}| \rightarrow 0}{=} \sum_{k=0}^{\infty} C_k(\alpha_s) |\rho_{12}|^{2+2k-2\frac{N_c \alpha_s}{\pi \omega}} \left( \frac{|\rho_{1'2'}|}{|\rho_{11'}||\rho_{22'}|} \right)^{2+2k-2\frac{N_c \alpha_s}{\pi \omega}} \quad (4.85)$$

where the constants  $C_k(\alpha_s)$  are calculated from the coefficients  $c(\nu)$  and the function  $F$ . Note that in the limit  $|\rho_{12}| \rightarrow 0$  the coefficients of the expansion have the approximate form

$$\left( \frac{|\rho_{1'2'}|}{|\rho_{11'}||\rho_{22'}|} \right)^{2+2k-2\frac{N_c \alpha_s}{\pi \omega}} = < \phi(\rho_{1'})\phi(\rho_{2'})O_{h_k \bar{h}_k}(\rho_1) > [1 + O(|\rho_{12}|)] \quad (4.86)$$

<sup>26</sup> This is a shorthand notation. The operator  $O_k$  represents a whole series of operators, belonging to a conformal family [42]. The term which is denoted in eq. (4.81) represents the most singular term (in  $|\rho_{ij}|$ ) of each conformal family.

<sup>27</sup> We assume here that the conformal spin of the operators is zero. For the general case compare [42].

with  $h_k = \bar{h}_k = 1 + k - N_c \alpha_s / (\pi \omega)$ . We want to interpret the result in the following way. We have realized an expansion of the product  $\phi(\rho_1)\phi(\rho_2)$  in a series<sup>28</sup> over the operators  $O_{h_k \bar{h}_k}$  where the scaling dimension  $\nu_k$  is determined by eq. (4.83). Note that the  $O(\alpha_s)$  deviation of the scaling dimensions from a half integer value is degenerate, i. e. identical for all  $k$ . This degeneracy is lifted in higher orders. As discussed in section 2.2 the scaling dimensions of the field  $\phi$  are zero.

It is clear that the scaling dimensions of the operators  $O_{h\bar{h}}$  which appear in the expansion of the operator product of the fields  $\phi$  are intimately related to the spectrum  $\chi_2(\nu)$  of the bound state of two  $\phi$  fields. The scaling dimensions in order  $O(\alpha_s)$  correspond to the residues of the singularities of  $\chi_2(\nu)$ . In other words, if we knew all scaling dimensions we could determine the spectrum  $\chi_2(\nu)$  by means of a dispersion relation. In the case discussed here, one subtraction constant is needed to formulate the dispersion relation. To determine the subtraction constant one could use e. g. an higher order (in  $\alpha_s$ ) coefficient of a scaling dimension, which corresponds mathematically to a nonsingular contribution in the Laurent expansion of the function  $\chi_2(\nu)$  around one of its singularities.

We have considered here one particular short distance limit. Other limits such as e. g.  $|\rho_{12'}| \rightarrow 0$  can be easily performed after using analytic continuations for the hypergeometric function  $F$  in eq. (4.82) [95]. In the BPZ [42] approach to two dimensional conformal field theory associativity of the operator algebra is an important principle. It leads to relations between the coefficients  $C_k^{ij}$  of different expansions. It would be an interesting subject for future work to study these relations for the BFKL amplitude. This could lead to a better understanding of the connection between the two dimensional BFKL theory and the general theory with infinite dimensional conformal symmetry of [42].

Using the BFKL amplitude as an example we have demonstrated that the knowledge of the operator algebra suffices to determine the spectrum of the compound state of two reggeized gluons. The transfer of this connection to the four reggeon system defines the basis of our approach to the spectrum of the four reggeon problem. We will develop a method with which the operator algebra of this system can be constructed. More precisely, we show how to calculate the scaling dimensions of the relevant operators up to order  $\alpha_s$ . Equipped with this information one could in the next step try to determine the function  $\chi_4$  and in turn the energy dependence of the four reggeon system.

### 4.3.3 The twist expansion

In the preceding section we have discussed short-distance expansions in configuration space where conformal covariance dictates to a large extent the coordinate dependence of the amplitudes. For our actual computation we find it easier to use the momentum space representation. The short-distance expansion discussed above then transforms into the twist expansion.

Consider again the BFKL amplitude, which we now convolute with impact factors  $T(Q^2)$ ,  $B(\Lambda^2)$  of colorless particles which are characterized by mass scales  $Q^2$  and  $\Lambda^2$ . For simplicity we consider the forward direction ( $t = 0$ ) and obtain for the partial wave amplitude

$$\Phi_\omega(Q^2, \Lambda^2) = \frac{1}{\sqrt{Q^2 \Lambda^2}} \int \frac{d\nu}{2\pi} \left( \frac{Q^2}{\Lambda^2} \right)^{i\nu} \frac{T(\nu)B(\nu)}{\omega - \chi_2(\nu)} \quad (4.87)$$

with the Mellin transformed impact factors  $T(\nu)$  and  $B(\nu)$ . We assume  $Q^2 \gg \Lambda^2$  and expand the amplitude in powers of the ratio  $\Lambda^2/Q^2$ . This works exactly as described above by closing the  $\nu$ -contour in the upper half plane and taking the residues of the poles of  $(\omega - \chi_2(\nu))^{-1}$ . This leads to

$$\Phi_\omega(Q^2, \Lambda^2) = \frac{1}{\omega Q^2} \sum_{k=1}^{\infty} T_k B_k \gamma_k(\omega) \cdot \left( \frac{Q^2}{\Lambda^2} \right)^{1-k+\gamma_k(\omega)} \quad (4.88)$$

where the  $\gamma_k(\omega)$  are obtained from the equation  $\omega = \chi_2(\nu)$  as the solutions in  $\nu$ . To leading order we have again  $\gamma_k(\omega) = N_c \alpha_s / (\pi \omega)$  for all  $k$ . Eq. (4.88) constitutes the twist expansion of the partial wave

<sup>28</sup>We have made two approximations. In eq. (4.86) we have neglected higher orders and we have not considered the contributions that arise from higher orders of the expansion of the  $F$ -function in eq. (4.82). Both neglected groups give contributions with an integer power of  $|\rho_{12}|$ . One might identify these terms with contributions from secondary fields [42].

amplitude, i. e. the expansion in inverse powers of a large momentum scale. The quantities  $\gamma_k$  correspond to the anomalous dimensions of operators constructed from the quark and gluon fields with twist  $1 + k$ . In the present case only gluonic operators appear since quark operators do not contribute in the leading logarithmic approximation. Comparison with the results from the last subsection shows that the anomalous dimensions are related to the scaling dimensions of the fields  $O_{h_k \bar{h}_k}$ . The expansion (4.88) reveals that the BFKL equation contains contributions from an infinite number of operators with different twist. In leading order all anomalous dimensions which exactly correspond to the residues of the  $\chi_2$  function are degenerate. So far we have constructed the twist (or short-distance) expansion by making use of our complete knowledge of the BFKL four point function. In the four reggeon case the latter is of course not known and we have to develop an alternative method to obtain the expansion and especially the anomalous dimensions. The basic idea is the following. The solutions of the reggeon integral equations can be represented as an infinite series of nested momentum loop integrations. The latter arise from iteratively applying interaction kernels to some initial condition. For each individual loop integration a twist expansion can be performed by expanding the kernel of the corresponding loop in the ratio of the inner and the outer momentum scale (or alternatively the inverse ratio). The assertion is then that the  $O(\alpha_s)$ -contribution to the anomalous dimension of the operator with twist  $l$  can be found by retaining in each single loop the term with the corresponding twist and iterating this procedure through the whole succession of nested loops. Let us demonstrate this for the example of the partial wave amplitude  $\Phi_\omega(Q^2, \Lambda^2)$  calculated before. We can represent  $\Phi_\omega$  in the form

$$\Phi_\omega(Q^2, \Lambda^2) = B(\Lambda^2) \otimes \sum_{n=0}^{\infty} \left( \frac{\mathcal{K}_{\text{BFKL}}}{\omega} \right)^n \otimes \frac{1}{\omega} T(Q^2) \quad (4.89)$$

where the symbol  $\otimes$  denotes momentum integration and  $\mathcal{K}_{\text{BFKL}}$  is the forward BFKL kernel including the gluon trajectory function  $\beta(\mathbf{k}^2)$ . Using a Mellin representation for  $T(Q^2)$  the first momentum loop has the form

$$\int_0^\infty d^2 \mathbf{k}' \left[ \frac{N_c \alpha_s}{\pi} \frac{\mathbf{k}^2}{\mathbf{k}'^2 |\mathbf{k}^2 - \mathbf{k}'^2|} - \delta(\mathbf{k}'^2 - \mathbf{k}^2) \beta(\mathbf{k}^2) \right] \left( \frac{\mathbf{k}'^2}{Q^2} \right)^{\frac{1}{2} - i\nu} T(\nu) \quad (4.90)$$

Now we expand the kernel in the ratio  $\mathbf{k}^2/\mathbf{k}'^2$ , assuming  $\mathbf{k}^2 \ll \mathbf{k}'^2$  (strong ordering). The trajectory function gives no contribution since in the strong ordering limit the  $\delta$ -function yields zero. From the first term we get

$$\frac{N_c \alpha_s}{\pi} \sum_{k=1}^{\infty} \int_{\mathbf{k}^2}^{\infty} \frac{d\mathbf{k}'^2}{\mathbf{k}'^2} \left( \frac{\mathbf{k}^2}{\mathbf{k}'^2} \right)^k \left( \frac{\mathbf{k}'^2}{Q^2} \right)^{\frac{1}{2} - i\nu} T(\nu) = \frac{N_c \alpha_s}{\pi} \left( \frac{\mathbf{k}^2}{Q^2} \right)^{\frac{1}{2} - i\nu} \sum_{k=1}^{\infty} \frac{1}{i\nu + k - 1/2} T(\nu) \quad (4.91)$$

We take the  $l$ -th term in the sum and repeat this in each following loop. The last convolution yields  $\int d\mathbf{k}^2/\mathbf{k}^4 B(\Lambda^2) (\mathbf{k}^2/Q^2)^{\frac{1}{2} - i\nu} = (Q^2 \Lambda^2)^{-\frac{1}{2}} (Q^2/\Lambda^2)^{i\nu} B(\nu)$  and the corresponding contribution to the partial wave amplitude reads

$$\Phi_\omega^{(l)} = \frac{1}{\sqrt{Q^2 \Lambda^2}} \int \frac{d\nu}{2\pi} B(\nu) T(\nu) \frac{1}{\omega} \left( \frac{Q^2}{\Lambda^2} \right)^{i\nu} \sum_{n=0}^{\infty} \left( \frac{\frac{N_c \alpha_s}{\pi \omega}}{i\nu + l - 1/2} \right)^n \quad (4.92)$$

$$= \frac{1}{\sqrt{Q^2 \Lambda^2}} \int \frac{d\nu}{2\pi} B(\nu) T(\nu) \frac{1}{\omega} \left( \frac{Q^2}{\Lambda^2} \right)^{i\nu} \frac{1}{1 - \frac{N_c \alpha_s}{\pi \omega} \frac{1}{i\nu + l - 1/2}} \quad (4.93)$$

By taking the residue at  $i\nu = 1/2 + N_c \alpha_s/(\pi \omega) - l$  we obtain exactly the  $l$ -th term in the series in eq. (4.88) with the anomalous dimension determined to  $O(\alpha_s)$ . Repeating this procedure for each  $l$  we generate the whole twist expansion. In fact, we were able to obtain the whole set of anomalous dimensions to order  $\alpha_s$  without knowledge of the explicit form of the BFKL eigenvalue  $\chi_2(\nu)$ .

The same procedure is in the next section applied to the four gluon state.

#### 4.4 The four gluon state II: Beginning of the Twist Expansion

We now turn back to the Bethe Salpeter equation (4.70) which defines the central problem of the present chapter. As anticipated in the preceding section our aim is the twist expansion of the four reggeon amplitude  $G_4^{\{a_i\},\{a'_j\}}(\omega; \{\mathbf{k}_i\}, \{\mathbf{k}'_j\})$ . In order to analyze the singularity structure of the Mellin transformed amplitude we follow the approach of Bartels [18] by reordering the interaction kernels  $\mathcal{K}_{ij}$  according to a method developed by Faddeev [43]. The idea is to rearrange the infinite summation which is obtained by iteratively solving eq. (4.70). One combines the four reggeons into two pairs, e. g. (12) and (34). Then the interactions of each pair are resummed separately. After this infinite resummation one puts the first cross pair interaction, e. g. of reggeons (13). Then one performs the infinite resummation of interactions in the corresponding coupling scheme (13) and (24). This procedure is infinitely iterated. The virtue of this method lies in the fact that the infinite resummation of interactions in one fixed coupling scheme can be compactly expressed by the BFKL amplitude.

Before we realize this idea in terms of mathematical expressions we change the initial condition of the equation (4.70). To get rid of the  $\delta$ -functions in momentum and color space it is convenient to convolute the primed arguments of  $G_4(\omega)$  with an impact factor. The natural impact factor for the four reggeon state is of course the transition vertex  $V_{(2,4)}^{\{a'_j\}}(\{\mathbf{q}_i\}, \{\mathbf{k}'_j\})$  and from now on we take  $G_4^{\{a_i\}}(\omega; \{\mathbf{k}_i\})$  to be the four reggeon amplitude with the vertex as the initial condition.

Next we have to discuss the color structure. Since the color structure of the interaction kernel (4.71) can be expressed through projection operators of irreducible representations of  $SU(3)$  according to [18, 99]

$$f^{a'_1 c a_1} f^{c a_2 a'_2} = 3P_1 + \frac{3}{2}P_{8_A} + \frac{3}{2}P_{8_S} - P_{27} \quad (4.94)$$

it is sensible to decompose the amplitude  $G_4^{\{a_i\}}(\omega; \{\mathbf{k}_i\})$  w. r. t. the color states of the two pairs of reggeized gluons. The total color of the system is zero, hence the color states of the two pairs are identical. After the color decomposition has been performed the iteration of pairwise interactions within a fixed coupling scheme is simple. The infinite resummation leads to the BFKL amplitude with the eigenvalue  $\chi_2^{(i)}(\nu, n)$  where the index  $i = 1, 2, 3, 4$  labels the respective color state (1,  $8_A$ ,  $8_S$ , 27) and  $\chi_2^{(i)}$  is obtained by multiplying  $\chi_2^{(i)}$  in eq. (4.8) with  $a_i = 1/N_c \cdot (N_c, N_c/2, N_c/2, -1)$ . It is clear that when the coupling scheme is changed, i. e. when the first cross-pair interaction occurs, the basis in color space has to be changed. This basis change is implemented by a  $4 \times 4$  matrix  $\Lambda$  (cf. eq. (4.97)).

When the Faddeev method is applied the four reggeon amplitude decomposes into three parts

$$G_4^{(i)}(\omega; \{\mathbf{k}_j\}) = G_{4(12)}^{(i)}(\omega; (\mathbf{k}_1, \mathbf{k}_2); (\mathbf{k}_3, \mathbf{k}_4)) + G_{4(13)}^{(i)}(\omega; (\mathbf{k}_1, \mathbf{k}_3); (\mathbf{k}_2, \mathbf{k}_4)) + G_{4(14)}^{(i)}(\omega; (\mathbf{k}_1, \mathbf{k}_4); (\mathbf{k}_2, \mathbf{k}_3)) \quad (4.95)$$

where the index  $i$  indicates that from now on  $G_4(\omega; \{\mathbf{k}_i\})$  is a vector in the four dimensional color state space. The function  $G_{4(jk)}^{(i)}(\omega; (\mathbf{k}_j, \mathbf{k}_k), (\mathbf{k}_l, \mathbf{k}_m))$  contains all contributions in which the last pairwise interaction was in the  $(jk), (lm)$  coupling scheme. Now the 12 amplitudes on the rhs of eq. (4.95) can be collected into a 12 dimensional vector  $\mathbf{G}_4$  with elements

$$\mathbf{G}_4 = \text{diag} \left( G_{4(12)}^{(i)}((1, 2); (3, 4)), G_{4(13)}^{(i)}((1, 3); (2, 4)), G_{4(14)}^{(i)}((1, 4); (2, 3)) \right) \quad (4.96)$$

The solution of the Bethe Salpeter equation can now be expressed in a very compact form as

$$\mathbf{G}_4 = \Phi_\omega \otimes \sum_{n=0}^{\infty} (\mathbf{S}(\Lambda) \Phi_\omega)^n \otimes V + \mathbf{1}V \quad (4.97)$$

On the right hand side  $\Phi_\omega$  and  $\mathbf{S}(\Lambda)$  are  $12 \times 12$  matrices and  $V$  is a 12-dimensional vector ( $\mathbf{1}$  is the unit matrix). The first four elements of  $V$  are obtained by applying the projection operators  $P_1, P_{8_A}, P_{8_S}, P_{27}$  in the coupling scheme (12), (34) to the transition vertex  $V_{(2,4)}^{\{a_i\}}$ , the next four elements by applying the projection operators in the coupling scheme (13), (24) and the last four by projecting in coupling scheme



(14), (23). The explicit expressions for the projection operators can be found in [18]. The matrix  $\mathbf{S}$  describes the transition between different coupling schemes. It has the form [100]

$$\mathbf{S} = \begin{pmatrix} 0 & \Lambda & P\Lambda P \\ \Lambda^T & 0 & \Lambda^T P\Lambda P \\ P\Lambda P^T & P\Lambda^T P\Lambda & 0 \end{pmatrix}, \quad \Lambda = \begin{pmatrix} \frac{1}{8} & \frac{1}{\sqrt{8}} & \frac{1}{\sqrt{8}} & \sqrt{\frac{3}{8}} \\ \frac{1}{\sqrt{8}} & 1/2 & 1/2 & -\frac{1}{2}\sqrt{\frac{3}{2}} \\ \frac{1}{\sqrt{8}} & \frac{1}{2} & -\frac{3}{10} & \frac{3}{10}\sqrt{\frac{3}{2}} \\ \sqrt{\frac{3}{8}} & -\frac{1}{2}\sqrt{\frac{3}{2}} & \frac{3}{10}\sqrt{\frac{3}{2}} & \frac{7}{40} \end{pmatrix}, \quad P = \text{diag}(1, -1, 1, 1) \quad (4.98)$$

The matrix  $\Phi_\omega$  represents the infinite summation of interactions within a fixed coupling scheme. It can be written in the form

$$\Phi_\omega = \text{diag} \left( \Phi_\omega^{(i)}(\mathbf{k}_1, \mathbf{k}_2; \mathbf{k}_3, \mathbf{k}_4), \Phi_\omega^{(i)}(\mathbf{k}_1, \mathbf{k}_3; \mathbf{k}_2, \mathbf{k}_4), \Phi_\omega^{(i)}(\mathbf{k}_1, \mathbf{k}_4; \mathbf{k}_2, \mathbf{k}_3) \right) \quad (4.99)$$

with

$$\begin{aligned} \Phi_\omega^{(i)}(\mathbf{k}_1, \mathbf{k}_2; \mathbf{k}_3, \mathbf{k}_4) &= \sum_{n_1, n_2=-\infty}^{+\infty} \int_{-\infty}^{+\infty} \frac{d\nu_1}{2\pi} \int_{-\infty}^{+\infty} \frac{d\nu_2}{2\pi} \left[ \frac{\omega}{\omega - \chi_2^{(i)}(\nu_1, n_1) - \chi_2^{(i)}(\nu_2, n_2)} - 1 \right] \\ &\quad E^{(\nu_1, n_1)*}(\mathbf{k}'_1, \mathbf{k}'_2) E^{(\nu_1, n_1)}(\mathbf{k}_1, \mathbf{k}_2) E^{(\nu_2, n_2)*}(\mathbf{k}'_3, \mathbf{k}'_4) E^{(\nu_2, n_2)}(\mathbf{k}_3, \mathbf{k}_4) \prod_{i=1}^4 \mathbf{k}_i^2 \end{aligned} \quad (4.100)$$

This expression corresponds to the product of two BFKL amplitudes with the respective color coefficient  $a_i$  in nonforward direction in the momentum space representation. The functions  $E^{(\nu_j, n_j)}$  are the momentum space eigenfunctions which have been calculated in section 2.3. One has to subtract unity in the first line of (4.124) since at least one interaction has to take place for the coupling scheme to be defined. The no-interaction contribution is restored by the extra term in (4.97). The symbol  $\otimes$  in eq. (4.97) represents momentum integration w. r. t. the measure  $d^2\mathbf{k}/(2\pi)^3$ .

The first line of eq. (4.100) can be regarded as a two reggeon propagator with the trajectory function of the reggeon given by  $\chi_2^{(i)}(\nu_j, n_j)$ . When the Faddeev procedure is applied to the four reggeized gluon system, new reggeons<sup>29</sup> appear naturally as bound states of pairs of reggeized gluons. From this point of view the right hand side of (4.97) can be regarded as the iteration of two intermediate reggeon states. There appear four different types of reggeons corresponding to the four color projections and each state is threefold degenerate corresponding to the three different coupling schemes. In total we therefore have a 12 dimensional reggeon state space. Each intermediate state is described by a matrix  $\Phi_\omega$  as given in eq. (4.99).

It is clear that the momentum space integration associated with the change of the coupling scheme constitutes the essential complication in the iteration of the two reggeon state. This momentum space integration can be cast into an effective reggeon-reggeon interaction vertex. To this end we contract the lower part of the two reggeon function  $\Phi_\omega^{(i)}(\mathbf{k}_1, \mathbf{k}_2; \mathbf{k}_3, \mathbf{k}_4)$  (these are by definition the factors with the unprimed momentum arguments in eq. (4.100)) with the upper part of the two reggeon function  $\Phi_\omega^{(i)}(\mathbf{l}_1, \mathbf{l}_3; \mathbf{l}_2, \mathbf{l}_4)$  belonging to a different coupling scheme. This defines the vertex function

$$\begin{aligned} \Theta_{(\nu'_1, n'_1; \nu'_2, n'_2)}^{(\nu_1, n_1; \nu_2, n_2)}(\mathbf{q}, \mathbf{q}') &= \int \frac{d^2\mathbf{k}}{(2\pi)^3} E^{(\nu_1, n_1)}(\mathbf{k}, \mathbf{q} - \mathbf{k}) E^{(\nu_2, n_2)}(\mathbf{q}' - \mathbf{k}, -\mathbf{q} - \mathbf{q}' + \mathbf{k}) \\ &\quad E^{(\nu'_1, n'_1)*}(\mathbf{k}, \mathbf{q}' - \mathbf{k}) E^{(\nu'_2, n'_2)*}(\mathbf{q} - \mathbf{k}, -\mathbf{q} - \mathbf{q}' + \mathbf{k}) \mathbf{k}^2 (\mathbf{q} - \mathbf{k})^2 (\mathbf{q}' - \mathbf{k})^2 (-\mathbf{q} - \mathbf{q}' + \mathbf{k})^2 \end{aligned} \quad (4.101)$$

We have introduced momenta  $\mathbf{q} = \mathbf{k}_1 + \mathbf{k}_2$ ,  $\mathbf{q}' = \mathbf{l}'_1 + \mathbf{l}'_2$ . Note that the total system is in the forward direction  $\sum_{i=1}^4 \mathbf{k}_i = 0$ . A graphical representation for the vertex function is given in fig. 4.3. Having defined the vertex function  $\Theta$  we can simplify the structure of our above expressions essentially. The matrix  $\Phi_\omega$  is replaced by

$$\Phi(\omega) = \text{diag} \left( \Phi^{(i)}(\omega), \Phi^{(i)}(\omega), \Phi^{(i)}(\omega) \right) \quad (4.102)$$

<sup>29</sup>Note that by now we generalize the terminology. Up to now the term 'reggeon' was exclusively reserved for reggeized gluons. From now on the term refers to bound states of two reggeized gluons with different color states.

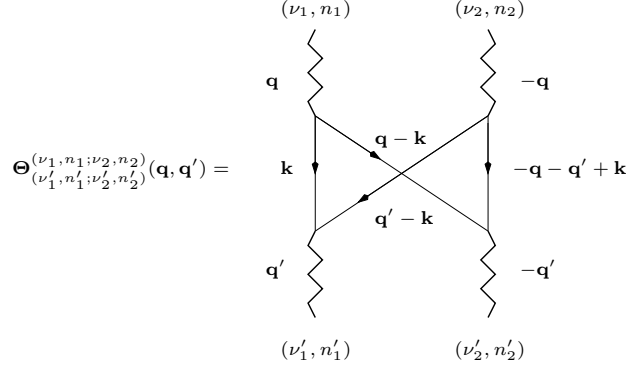


Figure 4.3: Definition of the effective reggeon interaction vertex  $\Theta$ .

with

$$\Phi^{(i)}(\omega) = \sum_{n_1, n_2 = -\infty}^{+\infty} \int_{-\infty}^{+\infty} \frac{d\nu_1}{2\pi} \int_{-\infty}^{+\infty} \frac{d\nu_2}{2\pi} \left[ \frac{\omega}{\omega - \chi_2^{(i)}(\nu_1, n_1) - \chi_2^{(i)}(\nu_2, n_2)} - 1 \right] \quad (4.103)$$

and equation (4.97) can be expressed as

$$\mathbf{G}_4 = \mathbf{E} \Phi(\omega) \otimes \sum_{n=0}^{\infty} (\mathbf{S}(\Lambda) \Theta \Phi(\omega))^n \otimes \hat{V} + \mathbf{1}V \quad (4.104)$$

Note that  $\Theta$  is only a coefficient, not a matrix. The virtue of eq. (4.104) is that the matrix  $\Phi(\omega)$  is simplified and the momentum space integrations have been plugged into the coefficient  $\Theta$ . The integration over the momenta  $\mathbf{q}$  which can be regarded as loop momenta of the intermediate two reggeon states are still contained in the convolution  $\otimes$ . The diagonal matrix  $\mathbf{E}$  at the end of the iteration in (4.104) restores the momentum dependence of the lowest two reggeon states. It can be written as

$$\mathbf{E} = \text{diag} \left( \hat{E}^{(\nu_1, n_1)}(\mathbf{k}_1, \mathbf{k}_2) \hat{E}^{(\nu_2, n_2)}(\mathbf{k}_3, \mathbf{k}_4), \hat{E}^{(\nu_1, n_1)}(\mathbf{k}_1, \mathbf{k}_3) \hat{E}^{(\nu_2, n_2)}(\mathbf{k}_2, \mathbf{k}_4), \hat{E}^{(\nu_1, n_1)}(\mathbf{k}_1, \mathbf{k}_4) \hat{E}^{(\nu_2, n_2)}(\mathbf{k}_2, \mathbf{k}_3) \right) \quad (4.105)$$

where each element represents a  $4 \times 4$  diagonal matrix and the hat on  $E^{(\nu, n)}$  means that the lower gluon propagators have been amputated, i. e.  $\hat{E}^{(\nu, n)}(\mathbf{k}_1, \mathbf{k}_2) = \mathbf{k}_1^2 \mathbf{k}_2^2 E^{(\nu, n)}(\mathbf{k}_1, \mathbf{k}_2)$ . The vertex  $V$  has been changed to  $\hat{V}$  in (4.104) to indicate that it is now not only color but also momentum projected, i. e. convoluted with a product of eigenfunctions  $E^{(\nu'_1, n'_1)*} E^{(\nu'_2, n'_2)*}$  according to the respective coupling scheme. A graphical representation of the structure of the four reggeized gluon amplitude can be found in fig. 4.4.

Having applied the Faddeev procedure we arrive at a ladder-like structure (fig. 4.4) for the four reggeized gluon state. This is quite welcome since ladder cells are easy to iterate. The elements of the ladder, however, are quite complicated. Each cell consists of a two reggeon intermediate state and an effective reggeon interaction vertex. This effective vertex is defined through an integral over four conformal eigenfunctions  $E^{(\nu, n)}$ . In order to obtain the twist expansion of  $G_4(\omega)$  with the method introduced for the BFKL amplitude in the preceding section, we have to isolate all sources of singularities of the amplitude. For each ladder cell we have an integration over a loop momentum  $\mathbf{q}$ . This loop momentum can be identified with the momentum that is carried by the two reggeons in that cell. Furthermore we have for each two reggeon intermediate state the integration over the conformal dimensions  $\nu_j$  associated with the two reggeons. As a first important result it turns out that the integration over the loop momentum  $\mathbf{q}$  generates a singularity which implies the conservation of the sum of the conformal dimensions of a ladder cell according to the conservation law  $\frac{1}{2} + i\nu_1 + \frac{1}{2} + i\nu_2 = \frac{1}{2} + i\nu$ . This is the first conserved quantity which characterizes the four gluon system. It is clear that this quantity is related to the conformal dimension of the operator which will be associated with

the four gluon state. In particular, we expect the singularities of  $G_4(\omega)$  in the  $\nu$ -plane to be associated with the residues of the spectrum  $\chi_4(\nu, \{\alpha'\})$ . Keeping  $\nu$  fixed, we still have one conformal dimension for each loop which has to be integrated. This integration leads to nontrivial singularities of  $\Phi^{(i)}(\omega)$  in the  $\nu$ -plane. The main complication arises from the effective interaction vertex  $\Theta$ . Since this vertex has an inner momentum loop we will also get a singularity from the vertex which has to be combined with the singularities from the two reggeon intermediate state.

In the next subsection we will first discuss the singularities arising from the integration of the conformal dimension of a single ladder cell. The singularities of the vertex will be considered in the next but one subsection.

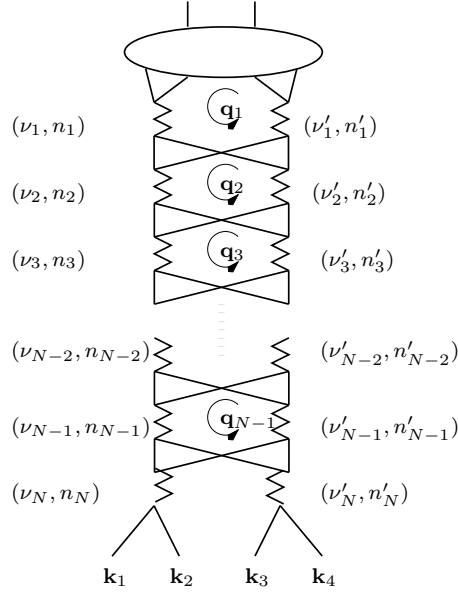


Figure 4.4: Schematic representation of the four reggeized gluon amplitude after the Faddeev procedure has been applied. The bubble on top denotes the vertex, the vertical curly lines represent the reggeons and the crossed box stands for the effective vertex. Indicated are the conformal dimensions and spins of the reggeons as well as the loop momenta.

#### 4.4.1 The two reggeon intermediate state

For each two reggeon intermediate state we have a function

$$\Phi^{(i)}(\omega, \nu) = \sum_{n_1, n_2=-\infty}^{+\infty} \int_{-\infty}^{+\infty} \frac{d\nu_1}{2\pi} \frac{\omega}{\omega - \chi_2^{(i)}(\nu_1, n_1) - \chi_2^{(i)}(\nu_2, n_2)} \quad (4.106)$$

where the index  $i$  labels the color of the exchanged reggeon and  $\nu_1, \nu_2$  are related to the conserved conformal weight  $1/2 + i\nu$  of the four (reggeized) gluon system by  $1/2 + i\nu_1 + 1/2 + i\nu_2 = 1/2 + i\nu$ . The additive constant  $(-1)$  has been omitted from the two reggeon propagator since it contains no singularities. We aim at extracting the singularities of  $\Phi^{(i)}(\omega, \nu)$  (in  $\nu$  at fixed  $\omega$ ) from the integral. Since the contour is closed (on  $S^2$ ), end-point singularities are absent and one only expects pinch singularities. Let us illustrate the origin of these pinch singularities. For simplicity we take  $n_1 = n_2 = 0$ . It is convenient to introduce the new variables  $\mu_i = 1/2 + i\nu_i$  because the conservation law for the conformal weights then reduces to the simple form  $\mu_1 + \mu_2 = \mu$ . The  $\mu_1$ -contour then runs along the imaginary axis and intersects the real axis to the right of  $\mu_1 = 0$  and to the left of  $\mu_1 = \mu$ . We require from the beginning  $0 < \text{Re}(\mu) < 1$  and we

are interested in the singularities in  $\mu$  which are located in the left half plane  $\text{Re}(\mu) \leq 0$ . It is clear how the pinching occurs. If  $\mu$  approaches zero, the  $\mu_1$ -contour is pinched between the singularities of  $\chi_2^{(i)}(\mu_1)$  at  $\mu_1 = 0$  and  $\chi_2^{(i)}(\mu - \mu_1)$  at  $\mu_1 = \mu$ . Expanding around these singularities and taking the pole in  $\mu_1$  one finds

$$\Phi^{(i)}(\omega, \mu) = \int_{\mathcal{C}} \frac{d\mu_1}{2\pi i} \frac{\omega}{\omega - a_i\alpha_s/(\pi\mu_1) - a_i\alpha_s/(\pi(\mu - \mu_1))} = \frac{a_i\alpha_s}{\pi\omega} \frac{1}{\sqrt{1 - \frac{4a_i\alpha_s}{\pi\omega\mu}}} \quad (4.107)$$

It follows that for each two reggeon intermediate state we have a square-root singularity (a cut) starting at  $\mu = a_i\alpha_s/(\pi\omega)$ . For the case of color zero ( $i = 1$ ) this singularity is known as the two-pomeron cut. If the effective reggeon-reggeon vertex were absent, this cut would already determine the anomalous dimension. This was the case in the analysis of Gribov, Levin and Ryskin [28] in which only noninteracting multi-reggeon states (fan diagrams) appeared as the corrections to the BFKL amplitude.

If we shift  $\mu$  further to the left additional singularities appear due to the pinching of different poles of the functions  $\chi_2^{(i)}(\mu_1)$  and  $\chi_2^{(i)}(\mu - \mu_1)$ . In the following we want to classify these singularities. To this end we make use of the Landau equations which are usually exploited to extract singularities of contour integrals (see e. g. [101]). Keeping still  $n_1 = n_2 = 0$  we define the function

$$\phi_{(0,0)}^{(i)}(\mu_1, \mu) = \omega - \chi_2^{(i)}(\mu_1, 0) - \chi_2^{(i)}(\mu - \mu_1, 0) \quad (4.108)$$

The Landau equations then read

$$\phi_{(0,0)}^{(i)}(\mu_1, \mu) = 0 \quad (4.109)$$

$$\frac{\partial}{\partial \mu_1} \phi_{(0,0)}^{(i)}(\mu_1, \mu) = 0 \quad (4.110)$$

We use the familiar form of  $\chi_2^{(i)}$  and write the second equation explicitly

$$\psi'(\mu_1) - \psi'(1 - \mu_1) - \psi'(\mu - \mu_1) + \psi'(1 - \mu + \mu_1) = 0 \quad (4.111)$$

where the prime denotes differentiation w. r. t.  $\mu_1$ . This equation is solved if we set  $\mu_1 = \mu/2$ . When inserting this solution into the first Landau equation we obtain

$$\omega = 2\chi_2^{(i)}\left(\frac{\mu}{2}, 0\right) \quad (4.112)$$

and through this equation we define a function  $\omega_{(0,0)}^{(i)} = 2\chi_2^{(i)}(\frac{\mu}{2}, 0)$  where the upper index of  $\omega$  refers to the color state and the lower ones to the conformal spins of the two intermediate reggeons. Now we express  $\Phi^{(i)}(\omega, \mu)$  in term of this function. We expand the function  $\phi_{(0,0)}^{(i)}$  around  $\mu_1 = \mu/2$

$$\phi_{(0,0)}^{(i)}(\mu, \mu_1) = \omega - 2\chi_2^{(i)}\left(\frac{\mu}{2}\right) + \frac{1}{2}\left(\mu_1 - \frac{\mu}{2}\right)^2 \xi^{(i)}(\mu) \quad , \quad \xi^{(i)}(\mu) = \frac{\partial^2}{\partial \mu_1^2} [-\chi_2^{(i)}(\mu_1) - \chi_2^{(i)}(\mu - \mu_1)]|_{\mu_1=\frac{\mu}{2}} \quad (4.113)$$

This is inserted into the  $\mu_1$ -integral in eq. (4.106) and the integration is performed by taking one of the poles. The result is

$$\Phi^{(i)}(\omega, \mu) = \frac{\omega}{\sqrt{2\xi^{(i)}(\mu) \left(2\chi_2^{(i)}\left(\frac{\mu}{2}\right) - \omega\right)}} \quad (4.114)$$

In order to investigate the singularity in the vicinity of  $\mu = 0$  we use  $\chi_2^{(i)}(\frac{\mu}{2}) \simeq 2a_i\alpha_s/(\pi\mu)$  and  $\xi(\mu) \simeq -32a_i\alpha_s/(\pi\mu^3)$  and find

$$\Phi^{(i)}(\omega, \mu) \simeq \sqrt{\frac{\mu^3\omega\pi}{64a_i\alpha_s}} \frac{1}{\sqrt{1 - \frac{4a_i\alpha_s}{\pi\omega\mu}}} \quad (4.115)$$

In the vicinity of the tip of the cut we have  $\mu = 4a_i\alpha_s/(\pi\omega)$  and one recognizes that (4.115) behaves exactly like (4.107). This demonstrates that we can correctly reproduce the pinching from the solution of the Landau equations. One can easily read off further singularities from eq. (4.114). These are determined by the poles of  $\chi_2^{(i)}(\frac{\mu}{2})$  which are located at (we restrict ourselves to the left halfplane)  $\mu = 0, -2, -4, \dots$ . These poles lead to cuts of  $\Phi^{(i)}(\omega, \mu)$  in the  $\mu$ -plane, starting at  $\mu = -k + 4a_i\alpha_s/(\pi\omega)$ ,  $k = 0, 2, 4, \dots$ . This means that from the solution (4.112) of the Landau equations we have obtained a whole string of singularities in  $\mu$ .

Let us now have a closer look at the vicinity of  $\mu = -2$ . From the reasoning above we find a pole of  $\chi_2^{(i)}(\frac{\mu}{2})$  which transforms into a cut of  $\Phi^{(i)}(\omega, \mu)$ . We can associate this singularity with the pinching of the poles at  $\mu_1 = -1$  of  $\chi_2^{(i)}(\mu_1)$  and at  $\mu - \mu_1 = -1$  of  $\chi_2^{(i)}(\mu - \mu_1)$ . But at  $\mu = -2$  also other types of pinching are possible, namely  $\mu_1 = -2$  with  $\mu - \mu_1 = 0$  and conversely  $\mu_1 = 0$  with  $\mu - \mu_1 = -2$ . By using the same method as in eq. (4.106) one can show that all three pinchings lead to the same type of square-root singularity. We conclude that the singularity at  $\mu = -2$  is degenerate. This can be understood as soon as one recognizes that due to the quasiperiodicity<sup>30</sup> of  $\psi(x)$  the Landau equations have infinitely many solutions. We start again from the second Landau equation

$$\partial_{\mu_1}[\psi(\mu_1) + \psi(1 - \mu_1) + \psi(\mu - \mu_1) + \psi(1 - \mu + \mu_1)] = 0 \quad (4.116)$$

By using the functional equation  $\psi(x+1) = \psi(x) + 1/x$  one can shift the arguments of the first two terms on the left hand side

$$\begin{aligned} & \partial_{\mu_1}[\psi(\mu_1 + k) + \psi(1 - \mu_1 - k) - 2 \sum_{l=0}^{k-1} (\mu_1 + l)^{-1} + \psi(\mu - \mu_1) + \psi(1 - \mu + \mu_1)] \\ &= [\psi'(\mu_1 + k) - \psi'(1 - \mu_1 - k) + 2 \sum_{l=0}^{k-1} (\mu_1 + l)^{-2} - \psi'(\mu - \mu_1) + \psi'(1 - \mu + \mu_1)] \end{aligned} \quad (4.117)$$

Equivalently one can shift the arguments of the last two terms

$$\begin{aligned} & \partial_{\mu_1}[\psi(\mu_1) + \psi(1 - \mu_1) + \psi(\mu - \mu_1 + k) + \psi(1 - \mu + \mu_1 - k) - 2 \sum_{l=0}^{k-1} (\mu - \mu_1 + l)^{-1}] \\ &= [\psi'(\mu_1) - \psi'(1 - \mu_1) - \psi'(\mu - \mu_1 + k) + \psi'(1 - \mu + \mu_1 - k) + 2 \sum_{l=0}^{k-1} (\mu - \mu_1 + l)^{-2}] \end{aligned} \quad (4.118)$$

We have already discussed that the pinching is due to the poles of the  $\psi$ -functions. Then, neglecting the nonsingular double poles in the sum, the following solution of eq. (4.117) can be found

$$\mu_1 = \frac{\mu - k}{2} + \Delta_{-k}(\mu) \quad (4.119)$$

Similarly a solution of eq. (4.118) reads

$$\mu_1 = \frac{\mu + k}{2} + \Delta_k(\mu) \quad (4.120)$$

By inserting these solutions into eqs. (4.117) and (4.118) resp., one finds that near the integer points  $\mu = -k - 2m$ ,  $m = 0, 2, 4, \dots$  the functions  $\Delta_{-k}(\mu)$  and  $\Delta_k(\mu)$  both behave as  $\Delta(\mu) \sim \text{const.}(\mu + k + 2m)^3$ . Now we can again insert the above solutions into the first Landau equation and define in analogy to the previously discussed case ( $k = 0$ ) functions  $\omega_{(0,0)-k}^{(i)}$  and  $\omega_{(0,0)k}^{(i)}$  through the equations

$$\omega_{(0,0)-k}^{(i)}(\mu) = \chi_2^{(i)}\left(\frac{\mu - k}{2} + \Delta_{-k}(\mu), 0\right) + \chi_2^{(i)}\left(\frac{\mu + k}{2} - \Delta_{-k}(\mu), 0\right) \quad (4.121)$$

$$\omega_{(0,0)k}^{(i)}(\mu) = \chi_2^{(i)}\left(\frac{\mu + k}{2} + \Delta_k(\mu), 0\right) + \chi_2^{(i)}\left(\frac{\mu - k}{2} - \Delta_k(\mu), 0\right) \quad (4.122)$$

---

<sup>30</sup> Quasiperiodicity here means that  $\psi$  has an infinite periodic series of poles.

These functions have a quite simple singularity structure in the left half plane. Both  $\omega_{(0,0)-k}^{(i)}$  and  $\omega_{(0,0)k}^{(i)}$  have simple poles at  $\mu = -k - 2m$ ,  $m = 0, 2, 4, \dots$  with identical residues  $4a_i\alpha_s/\pi$ . All these poles have their origin in the pinching of the  $\mu_1$ -contour by the poles of the two  $\chi_2$ -functions in the denominator in eq. (4.106). Introducing the functions  $\omega_{(0,0)\pm k}^{(i)}$  ( $k \in \mathbb{N}$ ) we have thus obtained a classification of the singularities of the two reggeon intermediate state. Each function  $\omega_{(0,0)k}^{(i)}$  introduces at most one square root singularity of  $\Phi(\omega, \mu)$  in the vicinity of an integer point  $\mu = -m$ . For each integer point  $\mu = -m$  we find a  $m + 1$ -fold degeneracy, i. e.  $\Phi(\omega, \mu)$  has  $m + 1$  cuts starting at  $\mu = -m + 4a_i\alpha_s/(\pi\omega)$ .

The functions  $\omega_{(0,0)k}^{(i)}$  are degenerate on the poles, i. e. they have identical residues. This degeneracy is lifted when the finite parts are taken into account. The finite parts can easily be calculated by applying the functional equation of the  $\psi$ -function. Since  $\Delta_{\pm k}(\mu)$  vanishes in the vicinity of the integer points  $\mu = -m$  proportional to  $(\mu + m)^3$  it can be neglected in the calculation of the finite part. Now at a fixed integer point  $\mu = -m$  a pole appears in the functions  $\omega_{(0,0)\pm l}^{(i)}(\mu)$  with  $l = m, m - 2, m - 4, \dots, 0(1)$  for  $m$  even (odd). The expansion of  $\omega_{(0,0)\pm l}^{(i)}(\mu)$  around the integer point up to the finite part then reads

$$\omega_{(0,0)\pm l}^{(i)}(\mu) = \frac{4a_i\alpha_s}{\pi(\mu + m)} + c_l, \quad c_l = -4\frac{a_i\alpha_s}{\pi} \left[ \sum_{i=0}^{(m+l)/2-1} \frac{2}{(m+l)/2-i} + \sum_{i=0}^{(m-l)/2-1} \frac{2}{(m-l)/2-i} \right] \quad (4.123)$$

which shows that the finite parts are different for different  $k$ .

So far we have only considered the contribution with zero conformal spin ( $n_1 = n_2 = 0$ ) for both reggeons. The same analysis can be repeated for nonzero spin. Without going into the details we only give the results. For each pair  $(n_1, n_2)$  functions  $\omega_{(n_1, n_2)\pm k}^{(i)}(\mu)$  can be defined from the solutions of the Landau equations. In the left half of the  $\mu$ -plane each function has an infinite string of simple poles located at  $\mu = -2k - (|n_1| + |n_2|)/2$ ,  $k = 0, 1, 2, \dots$  with residues  $4a_i\alpha_s/\pi$ . The degeneracy of the residues is lifted by the finite parts. These poles can again be related to the pinching of the  $\mu_1$ -contour by poles from the two  $\chi_2$ -functions in the denominator in eq. (4.106). In the vicinity of (half)integer points  $\mu = -l - (|n_1| + |n_2|)/2$  the poles of  $\omega_{(n_1, n_2)\pm k}^{(i)}(\mu)$  for  $k = l, l - 2, l - 4, \dots, 0(1)$  lead to square root singularities of  $\Phi(\omega, \mu)$  at  $\mu = -l - (|n_1| + |n_2|)/2 + 4a_i\alpha_s/(\pi\omega)$ .

It is obvious that by taking nonzero  $n_1, n_2$  into account, the degeneracy of the singularities increases strongly. Let us consider e. g. a fixed even integer point  $\mu = -m < 0$ . Simple counting then shows that there are  $m(m + 2)$  functions  $\omega_{(n_1, n_2)\pm k}^{(i)}(\mu)$  having a pole with residue  $4a_i\alpha_s/\pi$  at that point.

To summarize the results of this subsection, we have derived the following representation for the two reggeon intermediate state

$$\Phi^{(i)}(\mu, \omega) = \sum_{n_1, n_2 = -\infty}^{+\infty} \sum_{k = -\infty}^{+\infty} \frac{\omega}{\left[ \left( \omega - \omega_{(n_1, n_2)k}^{(i)}(\mu) \right) |2\xi_{(n_1, n_2)k}^{(i)}| \right]^{\frac{1}{2}}} \quad (4.124)$$

where  $\xi_{(n_1, n_2)k}^{(i)}$  is related to the second derivative of  $\omega_{(n_1, n_2)k}^{(i)}$ . We expect the representation (4.124) to be correct up to nonsingular terms. In particular it reproduces the behavior of  $\Phi^{(i)}(\mu, \omega)$  in the vicinity of integer and half-integer points in the left half of the  $\mu$ -plane. The most interesting result is that we could relate the singularities of  $\Phi^{(i)}(\mu, \omega)$  to strings of poles of an infinite number of different functions  $\omega_k(\mu)$ . It is of course tempting to identify the label  $k$  as a discrete quantum number of the noninteracting two reggeon system. It is, however, not clear from the present analysis if this quantum number can be associated with a symmetry. In addition to this new quantum number  $k$  we have to sum in (4.124) over the quantum numbers  $n_1, n_2$  which are associated with the conformal symmetry.

Now the two reggeon state has to be iterated. Let us first assume that the effective reggeon interaction vertex  $\Theta$  is diagonal in all quantum numbers  $k, n_1, n_2$  and its only effect is the conservation of the conformal dimension parameter  $\mu$ . In this case  $k$  could even be interpreted as a quantum number of the interacting two reggeon system. Let us furthermore assume for the sake of the argument that the matrix structure of the

iteration in (4.104) is completely ignored, i. e. we consider only one color state <sup>31</sup> and one coupling scheme and assume the vertex to be diagonal both in color and in the coupling scheme <sup>32</sup>. Then one can iterate each term in the sum in eq. (4.124) separately with the result

$$\sum_{j=0}^{\infty} \left( \frac{\omega_{\theta_{(n_1, n_2)k}(\mu)}}{[(\omega - \omega_{(n_1, n_2)k}(\mu)) |2\xi_{(n_1, n_2)k}(\mu)|]^{\frac{1}{2}}} \right)^j \frac{\omega}{[(\omega - \omega_{(n_1, n_2)k}(\mu)) |2\xi_{(n_1, n_2)k}(\mu)|]^{\frac{1}{2}}} = \frac{\omega}{[(\omega - \omega_{(n_1, n_2)k}(\mu)) |2\xi_{(n_1, n_2)k}(\mu)|]^{\frac{1}{2}} - \omega_{\theta_{(n_1, n_2)k}(\mu)}} \quad (4.125)$$

The function  $\theta_{(n_1, n_2)k}(\mu)$  is the coefficient which comes from the vertex. Now we use the fact that in the vicinity of the (half)integer point  $\mu = -m$  the function  $\omega_{(n_1, n_2)k}(\mu)$  behaves as  $\omega_{(n_1, n_2)k}(\mu) \sim 4a_i\alpha_s/(\pi(\mu+m))$ . Expanding around that point we find from eq. (4.125) the analogue of eq. (4.93) which was derived for the BFKL amplitude. In the present case in addition to a cut starting at  $\mu = -m + 4a_i\alpha_s/(\pi\omega)$  we find a pole <sup>33</sup> at  $\mu = -m + 4a_i\alpha_s/(\pi\omega) \cdot 1/(1 - \omega\theta_{(n_1, n_2)k}^2/(2\xi_{(n_1, n_2)k}))$  where  $\theta_{(n_1, n_2)k}$  is obtained from the expansion of  $\theta_{(n_1, n_2)k}(\mu)$  around  $\mu = -m$  and  $\xi_{(n_1, n_2)k}$  is a remainder from  $\xi_{(n_1, n_2)k}(\mu)$ . One finds that the singularity structure in the  $\mu$ -plane, even in this highly simplified case, is quite complicated. Near the (half)integer point there are a pole and a cut the distance of which is determined by the parameter  $\theta_{(n_1, n_2)k}$ . In particular the cut might be difficult to interpret when the twist expansion is considered. It is, however, encouraging that a pole in the  $\mu$ -plane appears. One can conjecture that this pole belongs to a meromorphic function  $\chi_4(\mu; n_1, n_2, k)$  which can be identified with an eigenvalue of the four (reggeized) gluon system. The further poles and residues of the function  $\chi_4(\mu; n_1, n_2, k)$  could also be easily calculated from the known properties of the function  $\omega_{(n_1, n_2)k}^{(i)}(\mu)$ .

Unfortunately things are not so easy as considered here since the interaction vertex is neither diagonal in color space, nor in the quantum numbers  $k, n_1, n_2$ . The nontrivial color structure is not too problematic since the color state space is finite dimensional, which leads to reformulating eq. (4.125) in matrix form. This is not the case for the other quantum numbers which are unbounded.

#### 4.4.2 The effective interaction vertex

This section is devoted to the effective reggeon interaction vertex defined in eq. (4.101) and in particular to an attempt to extract its singularities. For the following discussion it is helpful to recall the definition of the vertex here

$$\Theta_{(\nu'_1, n'_1; \nu'_2, n'_2)}^{(\nu_1, n_1; \nu_2, n_2)}(\mathbf{q}, \mathbf{q}') = \int \frac{d^2\mathbf{k}}{(2\pi)^3} E^{(\nu_1, n_1)}(\mathbf{k}, \mathbf{q} - \mathbf{k}) E^{(\nu_2, n_2)}(\mathbf{q}' - \mathbf{k}, -\mathbf{q} - \mathbf{q}' + \mathbf{k}) \\ E^{(\nu'_1, n'_1)*}(\mathbf{k}, \mathbf{q}' - \mathbf{k}) E^{(\nu'_2, n'_2)*}(\mathbf{q} - \mathbf{k}, -\mathbf{q} - \mathbf{q}' + \mathbf{k}) \cdot \mathbf{k}^2(\mathbf{q} - \mathbf{k})^2(\mathbf{q}' - \mathbf{k})^2(-\mathbf{q} - \mathbf{q}' + \mathbf{k})^2 \quad (4.126)$$

From which region of the momentum integration can we expect singularities? One possibility is that a singularity arises from the upper limit of the integration, i. e. the region  $\mathbf{k}^2 \rightarrow \infty$ . The other basic possibility is that a singularity appears when one of the momenta of the propagators in the crossed box diagram in fig. 4.3 vanishes, i. e. one of the arguments of the  $E^{(\nu, n)}$ -functions in (4.126) goes to zero.

Let us investigate the first possibility. In the case  $\mathbf{k} \rightarrow \infty$  we can neglect the momenta  $\mathbf{q}, \mathbf{q}'$  of the external reggeons, i. e. we can take the zero momentum transfer limit of  $E^{(\nu, n)}$  which was discussed in section 2.3. In this limit  $E^{(\nu, n)}(\mathbf{k}, \mathbf{q} - \mathbf{k})$  behaves as  $(\mathbf{k}^2)^{-\frac{3}{2}-i\nu}$ . From this we find the following behavior of the integrand  $I(\mathbf{k}^2)$  in (4.126)

$$I(\mathbf{k}^2) \xrightarrow{\mathbf{k} \rightarrow \infty} (\mathbf{k}^2)^{-2-i\nu_1-i\nu_2+i\nu'_1+i\nu'_2} \quad (4.127)$$

<sup>31</sup>Consequently we drop the index  $i$  referring to the color state in the following.

<sup>32</sup>Of course this simplification is paradoxical since if we had only one coupling scheme we would not have a vertex. The toy model which we use here for illustration is intended to capture all aspects which arise from the iteration of  $\mu$ -plane singularities while avoiding the complications associated with the matrix structure.

<sup>33</sup>If we had retained the constant  $(-1)$  in the definition of the two reggeon propagator the location of the pole had been slightly different. For the present qualitative discussion, however, this does not play any role.

In the last but one subsection we have anticipated that from the  $\mathbf{q}$ -integration we obtain a conservation law for the conformal dimensions in the form  $i\nu_1 + i\nu_2 = i\nu'_1 + i\nu'_2$ . Using, this we see that  $I(\mathbf{k}^2)$  effectively behaves as  $(\mathbf{k}^2)^{-2}$  and the upper limit of the  $\mathbf{k}$ -integration is convergent, i. e. does not produce a singularity. We therefore turn to the second possibility, the vanishing of one propagator momentum. This implies a technical difficulty since we have to investigate the behavior of  $E^{(\nu,n)}(\mathbf{k}, \mathbf{q} - \mathbf{k})$  for small argument. Starting from the explicit expression (4.53) one can derive the following expansion for the simplest case  $n = 0$

$$\begin{aligned}
E^{(\nu,0)}(\mathbf{k}, \mathbf{q} - \mathbf{k}) &= c(\nu, 0)(\mathbf{q}^2)^{-\frac{1}{2}-i\nu} \frac{1}{\mathbf{k}^2} \left[ b_1 \frac{|\mathbf{k}|}{|\mathbf{q}|} + b_2 \frac{|\mathbf{k}|^2}{|\mathbf{q}|^2} + b_3 \frac{|\mathbf{k}|^3}{|\mathbf{q}|^3} + O\left(\frac{|\mathbf{k}|^4}{|\mathbf{q}|^4}\right) \right] \\
\text{with} \quad b_1 &= b(\nu, 0) \cdot 2 \cos \phi \\
b_2 &= b(\nu, 0) \cdot \left[ \left( \nu^2 + \frac{1}{4} \right) \left( 2 \left( \log \frac{|\mathbf{k}|}{|\mathbf{q}|} - \xi(\nu) \right) - 3 \right) + \frac{1}{2} (4\nu^2 + 9) \cos^2 \phi \right] \\
b_3 &= b(\nu, 0) \cdot \left[ \left( 2 \left( \log \frac{|\mathbf{k}|}{|\mathbf{q}|} - \xi(\nu) \right) \left( \nu^2 + \frac{1}{4} \right) \left( \nu^2 + \frac{9}{4} \right) - 4 \left( \nu^2 + \frac{3}{4} \right) \left( \nu^2 + \frac{5}{4} \right) \right) \cos \phi \right. \\
&\quad \left. + \frac{2}{3} \left( \nu^2 + \frac{9}{4} \right) \left( \nu^2 + \frac{25}{4} \right) \cos^3 \phi \right]
\end{aligned} \tag{4.128}$$

The coefficient  $c(\nu, 0)$  is given in eq. (4.59),  $b(\nu, 0)$  is defined as  $b(\nu, 0) = 8\pi^2 4^{i\nu} \Gamma(3/2 + i\nu) \Gamma(3/2 - i\nu) / \Gamma^2(1/2 - i\nu)$  and  $\xi(\nu) = 2\psi(1) - \psi(1/2 + i\nu) - \psi(1/2 - i\nu)$  is the same as in eq. (4.64). The angle  $\phi$  is defined through  $\cos \phi = (\mathbf{k} \cdot \mathbf{q}) / (|\mathbf{k}| |\mathbf{q}|)$ . Due to symmetry the same expansion is obtained for the argument  $(\mathbf{q} - \mathbf{k})$ . The derivation of the coefficients in (4.128) requires considerable effort the basic steps of which are given in appendix A.4. Since there are two  $E^{(\nu)}$ -functions in (4.101) which have the momentum  $\mathbf{k}$  as an argument we find from the leading term in (4.128) for the small- $\mathbf{k}$  behavior of the integrand  $I(\mathbf{k}^2) \simeq \text{const.}$  One concludes that the vertex function  $\Theta$  is also regular when one of the propagator momenta vanishes.

This shows that we cannot expect a singularity from the effective vertex if both external momenta  $\mathbf{q}, \mathbf{q}'$  are different from zero.

The situation changes if one of the the momentum transfers e. g.  $\mathbf{q}'$  is set equal to zero. Inserting the expression (4.7) for the eigenfunctions in forward direction we then obtain the following simplified form of the vertex

$$\begin{aligned}
\Theta_{(\nu'_1, n'_1; \nu'_2, n'_2)}^{(\nu_1, n_1; \nu_2, n_2)}(\mathbf{q}, 0) &= \int \frac{d^2 \mathbf{k}}{(2\pi)^3} (2\pi\sqrt{2})^2 (\mathbf{k}^2)^{\frac{1}{2}+i\nu'_1} ((\mathbf{q} - \mathbf{k})^2)^{\frac{1}{2}+i\nu'_2} \left( \frac{k^*}{k} \right)^{\frac{n'_1}{2}} \left( \frac{(q-k)^*}{(q-k)} \right)^{\frac{n'_2}{2}} \\
&\quad \cdot E^{(\nu_1, n_1)}(\mathbf{k}, \mathbf{q} - \mathbf{k}) E^{(\nu_2, n_2)}(-\mathbf{k}, -\mathbf{q} + \mathbf{k})
\end{aligned} \tag{4.129}$$

Here the complex notation (cf. eq. (4.14)) was used to display the angular dependence of the eigenfunctions. Considering again the limit  $\mathbf{k} \rightarrow 0$  we find, using the leading term of the expansion (4.128), the following behavior of the integrand (for  $n_1 = n_2 = 0$ )

$$I(\mathbf{k}^2) \stackrel{\mathbf{k} \rightarrow 0}{\simeq} (\mathbf{k}^2)^{-\frac{1}{2}+i\nu'_1} \cdot \text{const.} \cdot (\mathbf{q}^2)^{\frac{3}{2}+i\nu'_2-i\nu_1-i\nu_2} \tag{4.130}$$

The  $\mathbf{k}$ -integration now leads to a pole in the  $\nu'_1$  plane

$$(\mathbf{q}^2)^{-\frac{3}{2}+i\nu'_2-i\nu_1-i\nu_2} \int_0^{\mathbf{q}^2} \frac{d\mathbf{k}^2}{\mathbf{k}^2} (\mathbf{k}^2)^{\frac{1}{2}+i\nu'_1} = \frac{1}{\frac{1}{2} + i\nu'_1} (\mathbf{q}^2)^{-1+i\nu'_1+i\nu'_2-i\nu_1-i\nu_2} \tag{4.131}$$

where the upper limit of the integration is required from consistency with the expansion in powers of  $|\mathbf{k}|/|\mathbf{q}|$ . Equivalently a pole in the  $\nu'_2$  plane can be obtained when the limit  $\mathbf{k} \rightarrow \mathbf{q}$  is considered.

By setting  $\mathbf{q}' = 0$  we have extracted a singularity of the vertex function in the lower half of the  $\nu'_1$  and the  $\nu'_2$  plane. It is easily seen that further singularities in the respective  $\nu'_j$ -planes can be obtained by expanding the integrand in (4.129) to higher orders in  $|\mathbf{k}|/|\mathbf{q}|$ . These are exactly the singularities we look for since they are of the same type as the singularities which appear in the  $\chi_2^{(i)}(\nu'_j)$ -functions belonging to the two reggeons below the vertex.



From the above observations we formulate the following conjecture. The relevant singularities of the vertex function  $\Theta(\mathbf{q}, \mathbf{q}')$  which can be consistently combined with the singularities of the reggeon states below the vertex are obtained by setting the momentum transfer  $\mathbf{q}'$  of the lower reggeons to zero and expanding the integrand in the vertex function around the singular points  $\mathbf{k} = 0$  and  $\mathbf{k} = \mathbf{q}$ , respectively, where  $\mathbf{q}$  is the momentum transfer of the upper reggeons. If the momentum transfer  $\mathbf{q}'$  of the lower reggeons is different from zero it acts as an effective regularization which prevents the integration from becoming singular.

It remains to discuss the integration of the momentum transfer. After  $\mathbf{q}'$  has been set to zero the  $\mathbf{q}$ -dependence of the vertex function follows from scaling arguments and is as given in eq. (4.131). Obviously, after integration of  $\mathbf{q}^2$  a function  $\delta(i\nu'_1 + i\nu'_2 - i\nu_1 - i\nu_2)$  is obtained which expresses the conservation of conformal dimensions.

Now let us consider in more detail in which way the singularities from the lower two reggeon state and the singularities from the vertex function are combined. We start with the leading poles which were discussed above. Adding the poles at  $i\nu'_1 = -1/2$  and  $i\nu'_2 = -1/2$  and restoring all coefficients correctly we obtain for eq. (4.129) integrated over  $\mathbf{q}$

$$\Theta_{(\frac{i}{2}, 0; \frac{i}{2}, 0)}^{(\nu_1, 0; \nu_2, 0)} = \frac{\mu}{\mu'_1(\mu - \mu'_1)} \frac{1}{4\pi^2} c(\nu_1, 0) b(\nu_1, 0) c(\nu_2, 0) b(\nu_2, 0) \quad (4.132)$$

We have considered the simplest case  $n_1 = n_2 = n'_1 = n'_2 = 0$ . Furthermore we have again introduced the variables  $\mu'_1 = 1/2 + i\nu'_1$  and  $\mu - \mu'_1 = 1/2 + i\nu'_2$ . Multiplying with the reggeon propagator  $\Phi^{(i)}(\omega, \mu)$  which has been expanded around the corresponding singularities (cf. eq. (4.107)) from below and performing the  $\mu'_1$ -integration we obtain

$$\frac{1}{\sqrt{1 - 4\frac{a_i \alpha_s}{\pi \omega \mu}}} \frac{1}{4\pi^2} c(\nu_1, 0) b(\nu_1, 0) c(\nu_2, 0) b(\nu_2, 0) \quad (4.133)$$

One recognizes that due to the singularities arising from the vertex the result on the right hand side of eq. (4.107) has been slightly modified. At this point all singularities associated with the two reggeon state below the vertex have been treated and we turn to the upper reggeons with quantum numbers  $\nu_1, \nu_2$ .

From the lower reggeon state the singularity at  $\mu \simeq 0$  has been extracted. Conservation of conformal dimensions hence implies  $1/2 + i\nu_1 + 1/2 + i\nu_2 = \mu_1 + \mu_2 \simeq 0$ . There is only one possibility to fulfill this equation and to simultaneously generate singularities in the upper reggeon state, namely  $i\nu_1 = i\nu_2 \simeq -1/2$ , corresponding to  $\mu_1 = \mu_2 \simeq 0$ . Conservation of conformal dimensions near the point  $\mu \simeq 0$  thus implies that one has to expand the upper two reggeon state around  $i\nu_1 = -1/2$  and  $i\nu_2 = -1/2$ , respectively. In particular the coefficients  $c(\nu_1, 0)$  and  $b(\nu_i, 0)$  have to be evaluated at these points. Using the explicit expressions for these functions we then obtain for eq. (4.132)

$$\Theta_{(\frac{i}{2}, 0; \frac{i}{2}, 0)}^{(\frac{i}{2}, 0; \frac{i}{2}, 0)} = \frac{1}{2} \frac{\mu}{\mu'_1(\mu - \mu'_1)} \quad (4.134)$$

We find that evaluated near the singular points of the upper two reggeon state the vertex function  $\Theta$  integrated over the momentum transfer of the upper two reggeon state reduces to the factor  $1/2$ . This is the famous factor  $1/2$  which has been found with a different method in [18]. Consequently if one is interested in the singularity of the four reggeized gluon state near the point  $\mu = 0$  the following structure has to be iterated

$$\frac{1}{2} \left[ \frac{1}{\sqrt{1 - \frac{4a_1}{\omega \mu}}} - 1 \right] \quad (4.135)$$

In [18] it was shown that when the full structure of the recoupling matrix  $\mathbf{S}$  is taken into account the iteration leads to a pole in the  $\mu$ -plane. This pole which was found to the right of the two pomeron cut was identified as the anomalous dimension of the twist four operator associated with the four gluon state.

So far we have extracted the rightmost poles in the left half of the  $\mu'_1$  and  $\mu'_2$  plane. It is clear how one

has to proceed further in our setup. By expanding the integrand in (4.129) to higher orders in  $|\mathbf{k}|/|\mathbf{q}|$  one generates further singularities at  $\mu'_1, \mu'_2 = -2, -3, -4, \dots$  (we still keep  $n_i, n'_i = 0$ ). These singularities are combined in the way described above with the poles from the two reggeon propagator. Finally one applies the conservation of conformal dimensions and evaluates the coefficients  $c(\nu_i), b(\nu_i)$  at the respective integer points.

There appears to arise a problem when the integrand is expanded to higher orders since the next-to-leading terms in the expansion (4.128) contain logarithms in  $|\mathbf{k}|$ . This seems to indicate the appearance of double poles. Closer inspection however shows that these logarithms disappear when the coefficients  $c(\nu_i), b(\nu_i)$  are evaluated on the integer points. The same is true for the additional poles which one could expect from the  $\xi$ -functions in (4.128). In fact it can be shown that the functions  $E^{(\nu, n)}(\mathbf{k}, \mathbf{q} - \mathbf{k})$  can be evaluated explicitly on the integer points  $i\nu = -(1 + |n|)/2 - k$  and turn out to be rational functions of  $|\mathbf{k}|$  and  $|\mathbf{q}|$ . This then proves that only single poles appear in the vertex as long as the conformal dimensions of the upper reggeon state are near the integer points.

It is nevertheless obvious that for the poles which are found to the left of the ones discussed above a new complication arises due to the degeneracy of singularities at a fixed integer point. We have seen in the preceding subsection that at an integer point  $\mu = -m$  several functions  $\omega_{\pm k}^{(i)}(\mu)$  have a singularity corresponding to the different types of possible pinchings. For all these contributions the respective poles have to be extracted from the vertex. The same degeneracy is of course also present in the upper two reggeon state. Conservation of conformal dimensions tells us that  $\mu$  is fixed but it does not determine which combination of poles builds up the singularity in  $\mu$  in the upper reggeon state given a particular type of pinching in the lower two reggeon state. Different choices of combinations will clearly lead to different results for the coefficients  $c(\nu_i), b(\nu_i)$ . Consequently, the vertex function  $\Theta$  is not diagonal in the quantum number  $k$  which was introduced to label the different types of possible pinchings. W. r. t. this quantum number the vertex has a matrix structure. It is clear that the dimension of this matrix becomes even higher if nonzero conformal spins  $n_i, n'_i$  are taken into account.

Let us consider an example which displays the full complexity. We are interested in the behavior near the singular point  $\mu = -2$ . The following table shows the different combinations of quantum numbers which lead to a singularity at  $\mu = -2$  in the lower two reggeon state.

$ n'_1 $	$ n'_2 $	$\mu'_1$	$\mu'_2$
0	0	-2	0
0	0	-1	-1
0	0	0	-2
1	1	-3/2	-1/2
1	1	-1/2	-3/2
2	0	-1	-1
2	0	-2	0
0	2	-1	-1
0	2	0	-2
3	1	-3/2	-1/2
1	3	-1/2	-3/2
2	2	-1	-1
4	0	-2	0
0	4	0	-2

We have 56 combinations of quantum numbers which lead to a singularity at  $\mu = -2$ . Corresponding to this 56-fold degeneracy we have a  $56 \times 56$  matrix associated with the vertex function  $\Theta$ . This matrix can be obtained from the representation 4.129 with the following steps.

- Fix  $n'_1$  and  $n'_2$  according to the first two columns in the table.
- Find the poles in  $\mu'_1$  and  $\mu'_2$  by expanding the integrand in (4.129) to the respective order.
- With  $\mu_1 = 1/2 + i\nu_1, \mu_2 = 1/2 + i\nu_2$ , calculate the coefficients  $c(\nu_1, n_1), c(\nu_2, n_2)$  and  $b(\nu_1, n_1), b(\nu_2, n_2)$  for all combinations of  $n_1, n_2, \mu_1, \mu_2$  which appear in the table above.

We see that in order to calculate the complete matrix we need in principle the explicit momentum space representation of the functions  $E^{(\nu,n)}(\mathbf{k}, \mathbf{q} - \mathbf{k})$  for general  $n$  and moreover their expansion in powers of  $|\mathbf{k}|/|\mathbf{q}|$ . In section 2.3 we have considered these functions for nonzero  $n$  and we have recognized that their calculation is an extremely arduous task. What is really needed, however, is not the complete dependence of the function  $E^{(\nu,n)}(\mathbf{k}, \mathbf{q} - \mathbf{k})$  on  $\nu$  but only the value at specific points  $i\nu = -(1 + |n|)/2 - k$ . It turns out that these quantities, the eigenfunctions evaluated on the integer points, can be obtained in a much simpler way. To see this, we have to recall the result for the coefficients  $c(\nu, n)$  which have been calculated for general  $n$  in section 2.3

$$c(\nu, n) = i^n \frac{\sqrt{2}}{2\pi} 4^{i\nu} \frac{\Gamma(1 + i\nu + \frac{|n|}{2}) \Gamma(-\frac{1}{2} - i\nu + \frac{|n|}{2}) \Gamma(\frac{1}{2} - i\nu + \frac{|n|}{2})}{\Gamma(-i\nu + \frac{|n|}{2}) \Gamma(\frac{1}{2} + i\nu + \frac{|n|}{2}) \Gamma(\frac{3}{2} + i\nu + \frac{|n|}{2})} \quad (4.136)$$

Inspection shows that for  $|n| \neq 0$  this coefficient has a zero for  $i\nu = -1/2 - |n|/2$  and a double zero for  $i\nu = -1/2 - |n|/2 - k, k = 1, 2, 3, \dots$ . Consequently the function which multiplies these coefficients must have a single, respectively a double pole at the corresponding points, otherwise the value of the function  $E^{(\nu,n)}(\mathbf{k}, \mathbf{q} - \mathbf{k})$  on the integer point  $i\nu = -1/2 - |n|/2 - k$  would be zero. It follows that to calculate  $E^{(\nu,n)}(\mathbf{k}, \mathbf{q} - \mathbf{k})$  on the integer points we just have to extract the residues from the function multiplying the coefficient  $c(\nu, n)$  in eq. (4.136). Returning to the basic equation (4.48) we find that this function is just the ordinary Fourier integral of the conformal three point function in configuration space

$$\int d^2\rho_1 d^2\rho_2 e^{i\mathbf{k}\rho_1 + i(\mathbf{q}-\mathbf{k})\rho_2} \left( \frac{\rho_{12}}{\rho_1\rho_2} \right)^{\frac{1+|n|}{2} - i\nu} \left( \frac{\rho_{12}^*}{\rho_1^*\rho_2^*} \right)^{\frac{1-|n|}{2} - i\nu} \quad (4.137)$$

Now to extract the respective poles which cancel the zeroes of  $c(\nu, n)$  from this integral is far simpler than performing the Fourier transformation explicitly. The origin of these poles is clear. They arise when either  $\rho_1$  or  $\rho_2$  (or both) go to zero. They can be extracted from the integral by isolating the factors  $1/(|\rho_1|^2)^{\frac{1}{2} - i\nu}$  and  $1/(|\rho_2|^2)^{\frac{1}{2} - i\nu}$  and successively performing integration by parts. Without going into the details we give here a list of results <sup>34</sup> for the first integer points and the cases  $|n| = 0, 1, 2$ .

$$\begin{aligned} E^{(i\frac{1}{2}, 0)}(\mathbf{k}, \mathbf{q} - \mathbf{k}) &= \sqrt{2}\pi \left[ \frac{1}{\mathbf{k}^2} + \frac{1}{(\mathbf{q} - \mathbf{k})^2} - \frac{\mathbf{q}^2}{\mathbf{k}^2(\mathbf{q} - \mathbf{k})^2} \right] \\ E^{(i\frac{3}{2}, 0)}(\mathbf{k}, \mathbf{q} - \mathbf{k}) &= 2\sqrt{2}\pi \\ E^{(i\frac{5}{2}, 0)}(\mathbf{k}, \mathbf{q} - \mathbf{k}) &= \frac{1}{2}2\sqrt{2}\pi (4\mathbf{k}^2 - 4|\mathbf{k}||\mathbf{q}|\cos\phi + \mathbf{q}^2) \end{aligned} \quad (4.138)$$

$$\begin{aligned} E^{(i1, \pm 1)}(\mathbf{k}, \mathbf{q} - \mathbf{k}) &= \sqrt{2}\pi e^{\mp i\alpha} \frac{(2|\mathbf{k}| - |\mathbf{q}|e^{\pm i\phi})}{|\mathbf{k}|(|\mathbf{k}| - |\mathbf{q}|e^{\pm i\phi})} \\ E^{(i2, \pm 1)}(\mathbf{k}, \mathbf{q} - \mathbf{k}) &= \sqrt{2}\pi e^{\mp i\alpha} (2|\mathbf{k}| - |\mathbf{q}|e^{\pm i\phi}) \\ E^{(i\frac{3}{2}, \pm 2)}(\mathbf{k}, \mathbf{q} - \mathbf{k}) &= \frac{1}{2}\sqrt{2}\pi e^{\mp 2i\alpha} \frac{(2|\mathbf{k}| - |\mathbf{q}|e^{\pm i\phi})(2|\mathbf{k}| - |\mathbf{q}|e^{\mp i\phi})}{|\mathbf{k}|(|\mathbf{k}| - |\mathbf{q}|e^{\pm i\phi})} \end{aligned} \quad (4.139)$$

$$E^{(i\frac{5}{2}, \pm 2)}(\mathbf{k}, \mathbf{q} - \mathbf{k}) = \frac{2}{5}\sqrt{2}\pi e^{\mp 2i\alpha} (5\mathbf{k}^2 - 5|\mathbf{k}||\mathbf{q}|e^{\mp i\phi} + \mathbf{q}^2 e^{\mp 2i\phi}) \quad (4.140)$$

Here  $\phi$  is defined as in eq. (4.128) and  $\exp(i\alpha) = \sqrt{k/k^*}$ . A check of these results is the forward direction limit  $\mathbf{q} = 0$ . In this case the above results are consistent with eq. (4.7).

Starting from these expressions, the values of the expansion coefficients of  $E^{(\nu,n)}(\mathbf{k}, \mathbf{q} - \mathbf{k})$  in the  $|\mathbf{k}|/|\mathbf{q}|$ -expansion can be obtained without recurrence to the explicit representation of the momentum space functions. This offers the possibility to calculate the elements of the matrix  $\Theta$  for nonzero  $n_1, n_2$ . In this respect the calculation of the coefficients  $c(\nu, n)$  in section 2.3 has been very important.

<sup>34</sup>For  $n = 0$  and the first integer point  $i\nu = -1/2$  there is no zero in the coefficient  $c(\nu, 0)$  in eq. (4.136). For this case the result can be obtained directly from the momentum space representation by putting  $i\nu = -1/2$ .

#### 4.4.3 Concluding remarks

Since the section 4.4 has become increasingly technical it appears advisable to recall our starting point, the results that have been obtained and the difficulties we have encountered.

The aim was to formulate the twist expansion of the four (reggeized) gluon amplitude  $G_4(\omega)$ . The background motivation, inspired by the analysis of the BFKL amplitude, is to construct from the series of anomalous dimensions, supplemented by a number of subtraction constants, the spectrum  $\chi_4(\{\alpha\})$  of the four gluon state by means of a dispersion relation. The function  $\chi_4$  is the fundamental new quantity governing the energy and the scaling behavior of  $G_4(\omega)$ . We have argued that in terms of  $\chi_4$ ,  $G_4(\omega)$  can be expressed as

$$G_4(\omega) = \sum_{\{\alpha\}} \frac{\psi_{\{\alpha\}} \psi_{\{\alpha\}}^*}{\omega - \chi_4(\{\alpha\})} \quad (4.141)$$

with quantum numbers  $\{\alpha\}$  and eigenfunctions  $\psi_{\{\alpha\}}$ . The fundamental observation is that the anomalous dimensions which appear in the twist expansion of  $G_4(\omega)$  are related to the residues of the singularities of  $\chi_4$  in the vicinity of the integer points in the  $\nu$ -plane, with  $\nu$  being a conformal dimension parameter. Guided by the experience from the BFKL amplitude we have argued that the twist expansion can be accomplished by a loopwise extraction of logarithms (corresponding to poles in the conformal dimension plane) and iteration of these singular terms. To this end we have used the Faddeev method to construct a solution of the defining equation for  $G_4(\omega)$  in terms of an infinite iteration of two basic elements, namely a two reggeon intermediate state and an effective reggeon interaction vertex. It is important to emphasize that the two reggeons which make up the intermediate state are bound states of two reggeized gluons. In the present context it is essential to distinguish between these reggeons and the reggeized gluons. In our approach the four reggeized gluons are grouped into intermediate two reggeon states. These reggeons can be expressed through the BFKL amplitude with a generalized color coefficient. Consequently we associate a two dimensional momentum transfer  $\mathbf{q}$  as well as three quantum numbers, namely color and conformal dimension and spin with them. Within the Faddeev formalism both the intermediate state and the vertex are  $12 \times 12$ -matrices which substantially complicates the analysis of the analytic structure. The momentum dependence, however, can be collected into a single loop integral  $\Theta$  which is extracted from the vertex matrix. The further analysis concentrated on extracting the singularities from the two reggeon intermediate state and the vertex function  $\Theta$ .

The singularities of the two reggeon intermediate state were obtained and classified by employing the Landau equations. In addition to the quantum numbers  $i$  (color),  $n_1, n_2$  (conformal spins of the two intermediate reggeons) and  $\mu$  (the sum  $\mu = 1/2 + i\nu_1 + 1/2 + i\nu_2$  of conformal dimensions) a new quantum number  $k$  was identified. With each  $k$  an analytic function  $\omega_{(n_1, n_2)k}^{(i)}(\mu)$  could be associated which contains an infinite number of single poles with degenerate residues at the integer points of the left half of the  $\mu$  plane. The outcome of these considerations was that the singularities of the two reggeon intermediate state in the  $\mu$ -plane are degenerate. In the vicinity of an integer point  $\mu = -m$  a definite number (depending on  $m$ ) of different cuts at  $\mu = -m + 4a_i\alpha_s/(\pi\omega)$  have their origin. These different cuts can be associated with different combinations of the quantum numbers  $n_1, n_2$  and  $k$ . The number of degenerate cuts increases with increasing  $m$ .

Associated with each iteration are two momentum integrals, the one contained in the vertex function  $\Theta$  and the integration over the momentum transfer of the intermediate reggeons. The latter can be shown to lead to a conservation of the sum of conformal dimensions  $\mu$  associated with the two reggeon state. The former can be demonstrated to generate an infinite string of poles in the  $\mu'_1$  and  $\mu'_2$  planes where  $\mu'_1$  and  $\mu'_2$  are related to the conformal dimensions of the two intermediate reggeons below the vertex by  $\mu'_i = 1/2 + i\nu'_i$ . These singularities can be obtained by expanding the integrand of the vertex in powers of the ratio of the loop momentum and the momentum transfer of the upper two reggeon state. They are combined in a straightforward way with the corresponding singularities of the lower reggeon state. For the leading singularity which is found near  $\mu = 0$  the vertex function  $\Theta$  then reduces to the coefficient  $1/2$ . The iteration of singularities near  $\mu = 0$  is rather easy and finally leads to a pole of the four gluon amplitude in the  $\mu$ -plane to the right of the two pomeron cut. For the singularities located to the left of  $\mu = 0$  the situation becomes more complicated. Here the vertex function becomes a matrix in the space which is spanned by the set of the quantum numbers  $n_1, n_2, k$  which lead to the same singularity in the  $\mu$ -plane. This matrix can in principle be calculated. An

important information which is needed then is the value of the conformal momentum space eigenfunctions  $E^{(\nu,n)}$  on the integer points  $i\nu = (1 + |n|)/2 - k$ . The iteration of singularities near the integer points to the left of  $\mu = 0$  has to take into account the matrix structure. The appearance of this matrix means that the quantum numbers  $n_1, n_2$  and  $k$  which were identified for the two reggeon state do not correspond to the true quantum numbers of the four reggeized gluon system. One can not identify  $k$  as a label of the eigenvalues  $\chi_4$ . It is in fact questionable if the quantum numbers of the four reggeized gluon system can be identified with the method presented here. The appearance of the quantum number  $k$  in the two reggeon intermediate state however indicates that  $\chi_4$  has extra discrete quantum numbers in addition to the quantum numbers related to the conformal symmetry. The investigation of the singularity structure is of course complicated by the additional matrix structure but it is at least in principle clear how to proceed. For each integer point  $\mu = -m$  which is considered one could diagonalize the matrix and iterate the eigenvalues in analogy to the factor  $1/2$  for the nondegenerate point  $\mu = 0$ . For each eigenvalue this will lead after iteration to a different singularity of the function  $G_4(\omega)$  in the  $\mu$ -plane. These singularities can be identified as contributions to the twist expansion of  $G_4(\omega)$ . The technical problem is the rather rapid increase of the dimension of the matrix when going farther to the left in the  $\mu$ -plane. A principle problem is the classification of the resulting singularities. One would like to collect them into groups corresponding to different quantum numbers of the potential function  $\chi_4(\{\alpha\})$ . From the present point of view it is not yet clear according to which principles this grouping should be performed. The quite regular pattern of singularities which appeared in both the reggeon intermediate state through the functions  $\omega_{(n_1, n_2)k}^{(i)}(\mu)$  and in the vertex function  $\Theta$  gives rise to the hope that there exists some underlying structure which eventually could be identified using an additional information.

## 5 Conclusions

In the introduction we raised two questions concerning the phenomenological and theoretical significance of the BFKL pomeron. We want to summarize the results of this thesis with reference to these issues.

The first question points to the phenomenological relevance of the BFKL pomeron, i. e. the perturbative resummation of leading logarithms in  $1/x$ . To address this question we investigated in chapter 2 four different processes in deep inelastic scattering on the basis of BFKL pomeron exchange. The aim was to work out specific properties of the cross sections and to check the theoretical consistence. DIS is well-suited for this purpose since the large virtuality of the photon allows to start from perturbation theory.

First we performed a calculation of the inclusive structure function  $F_2$  based on a numerical solution of the BFKL equation and the high energy factorization formalism. Special attention was paid to the distribution of transverse momenta in the evolution. The point was made that due to the diffusion mechanism inherent in the BFKL evolution the contribution of transverse momenta from the infrared region where perturbation theory cannot be consistently applied is large. We have discussed a modification of the equation which suppresses the region of low transverse momenta. With such a modification it is possible to obtain good agreement with the experimental data but due to the arbitrariness inherent in the modification it is not conclusive. In summary one can say that the strong rise of  $F_2$  at low  $x$  indicates the importance of the large logarithms of  $1/x$  but a consistent application of the BFKL pomeron to this observable has to take into account higher order corrections.

Since it is difficult to trace the BFKL pomeron in the  $x$ -dependence of the inclusive structure function, exclusive observables like e. g. the transverse energy distribution in the final state have been proposed for this purpose. We have studied some characteristic features of the transverse energy distribution of the gluons in the BFKL evolution. The idea behind this is that the broad distribution of transverse momenta typical for the diffusion behavior transforms into some broad distribution of the transverse energy of the final state. The problem with this observable, however, is that it is strongly affected by hadronization effects [102].

To overcome the infrared problem of the BFKL equation one can consider a process in which the infrared momentum region is naturally suppressed by the kinematical requirements. As an example of such a process we have discussed diffractive production of vector mesons with a large momentum transfer in DIS. This process provides an interesting application of the BFKL pomeron in the nonforward direction. We have derived an explicit formula for the cross section which has been evaluated numerically and analytically in some limiting cases. Based on this evaluation we have obtained estimates for the cross section of the process in the HERA region. The result is of the order of  $10^2$  nbarn, i. e. the prospects to observe this process at HERA are not bad. Being  $t$ -dependent this process also allows to study the slope of the Regge trajectory associated with the BFKL pomeron. We have defined an effective slope parameter  $\alpha'_{\text{eff}}$  which turned out to be quite small compared to the slope of the soft pomeron. This smallness can be traced back to the conformal symmetry of the BFKL pomeron which is only weakly broken by mass scales associated with the impact factors of the physical particles.

BFKL pomeron exchange has then been applied to inclusive photon diffractive dissociation. First, the situation has been studied in which the hadronic state is made out of a quark-antiquark pair. For this case a complete expression for the cross section has been derived. Simple expressions have been found for the  $t = 0$  and the large- $t$  limit. The large  $t$ -limit is interesting since it allows a discussion of the Mueller-Tang effective prescription for the coupling of the BFKL pomeron to quarks. It was demonstrated that for the inclusive case in which the final state of the quarks is integrated the Mueller-Tang prescription stating to couple the two gluons from the BFKL pomeron to a single quark is correct. Using the effective photon-meson transition vertex from the preceding calculation it has been shown that this prescription does not hold in general. In this case where the quark-antiquark pair forms a specific final state (exclusive situation) the effective prescription fails. In any case, for the consistent application of the BFKL pomeron one should try to work out a gauge invariant coupling of the gluons.

When the invariant mass of the diffractively produced hadronic system increases final states with additional gluons have to be taken into account. In the triple Regge limit these corrections decompose into two parts. A reggeizing part which resembles a triple pomeron situation and an irreducible part in which a four gluon state appears as a new element.

The first part of these corrections has been investigated in this thesis by generalizing the calculation for the

quark-antiquark case. It was shown that the zero momentum transfer limit is finite in contradiction to a result by Mueller and Patel. The calculation reveals a conservation law for the conformal dimensions of the three BFKL pomerons at the effective triple ladder vertex in the limit  $t = 0$ . This conservation law has important consequences for the energy dependence. In particular it is not possible to couple three ladders which are in the BFKL limit with the anomalous dimension  $-1/2$ . Instead, if the two lower ladders are in the BFKL limit the upper ladder is forced into the double logarithmic limit of strongly ordered transverse momenta. As a consequence the transverse momentum decreases rapidly from the photon virtuality  $Q^2$  to the effective scale at the vertex. The latter is shifted deep into the infrared.

The same is true if the BFKL pomeron couples to the quark-antiquark pair directly. The photon virtuality  $Q^2$  does not act as an effective hard scale. On the contrary the scale which determines the gluon coupling to the quarks is soft. This shows that corrections to the BFKL pomeron which operate in the infrared region are very important in diffractive dissociation.

The scale at the effective photon-pomeron vertex can be increased by imposing restrictions on the final state of the quark-antiquark pair. As an example we have considered in this thesis a large transverse momentum or a large mass of the (anti)quark. Indeed the effective scale was found to be  $(\mathbf{k}^2 + m^2)/(1 - \beta)$  where  $\mathbf{k}^2$  and  $m^2$  are the transverse momentum and the mass of the (anti)quark and  $\beta$  is the familiar variable used in diffraction. This scale is perturbative if either  $\mathbf{k}^2$  or/and  $m^2$  are larger than  $1 \text{ GeV}^2$ . The cross section of the process has been obtained in the framework of high energy factorization and expressed through the unintegrated gluon structure function. Performing the double-logarithmic approximation in the result we have been able to express the cross section in terms of the square of the gluon density evaluated at the momentum scale  $(\mathbf{k}^2 + m^2)/(1 - \beta)$ . This result displays the explicit violation of Regge factorization. Extensive numerical studies on the dependences on the different kinematical parameters have been performed. Characteristic features are the steep rise at small  $x$  and the rapid decrease with increasing transverse momentum (higher twist behavior). For kinematical cuts corresponding to the HERA characteristics a total cross section of the order of  $10^2 \text{ pbarn}$  has been estimated. One should however keep in mind that our calculations are based on a leading logarithmic approximation and are therefore subject to normalization uncertainties. An interesting observable turned out to be the azimuthal angle  $\phi$  between the quark-antiquark plane and the scattering plane of the electron. The  $\phi$ -spectrum peaks at  $\phi = \pi/2$  quite in contrast to one gluon exchange models which peak at  $\phi = 0$  and  $\phi = \pi$ . This might serve as a signal to reveal the two gluon exchange nature of the process.

For charm quarks the contribution to the diffractive structure function has been obtained in this model by integration over the transverse momentum. In the  $\beta$ -spectrum a zero at  $\beta = 0$  is found both for the transverse and the longitudinal cross section. This behavior is in contrast to the data which is flat in the low  $\beta$  region. This highlights the necessity to extend the model by taking into account production of additional gluons. With one additional gluon being produced in the final state the cross section becomes constant for  $\beta = 0$ .

The theoretical aspects of the BFKL pomeron have been the focus of the second part of this thesis. Starting from the observation that both the violation of unitarity and the infrared consistency problems require to take into account higher order corrections beyond the leading logarithmic approximation we have investigated the first unitarity corrections. The basis of our study was the approach of Bartels [29, 30, 18] in which an effective two-to-four gluon vertex and the interacting four (reggeized) gluon state appear as the important elements of the first unitarity corrections. The analysis of both elements is urgently needed: from the phenomenological point of view to estimate in which region of  $x$  subleading corrections leading to a saturation of parton densities become important, and from the theoretical point of view to obtain indications of how unitarization in perturbation theory could work.

As to the transition vertex we have concentrated our investigations on the properties of this element under conformal transformations. We have obtained a symbolic operator representation of the vertex which was then used to give a simplified proof of conformal invariance of the vertex. The question of holomorphic separability has been addressed and it turned out that in our representation the vertex could not be decomposed into a holomorphic and an antiholomorphic part. We have then projected the vertex on conformal eigenfunctions. These eigenfunctions have been interpreted before as conformal three point functions of two fields associated with the reggeized gluon and one composite field associated with the BFKL pomeron. We

denote this field composite since it appears as a bound state of the two reggeized gluons. What we have obtained after projection of the vertex could be interpreted as the three point function of this composite field. This is a very encouraging result. It indicates that it could be fruitful to associate fields of a conformal field theory with the reggeons that appear after resummation of elementary Feynman diagrams. The elements that appear as unitarity corrections could then be identified as correlation function of this conformal field theory.

This approach has also been pursued with regard to the four gluon state. We have demonstrated in which way the corresponding amplitude can be identified as the four point function of the composite field mentioned above. Important information on the structure of the theory can be expected from the operator algebra of these fields. The operator algebra, i. e. the operator product expansion contains encoded in the fusion coefficients and the anomalous dimensions the whole information on a conformal field theory. This initiated our interest in the operator product expansion of the four (reggeized) gluon amplitude.

The aim of our approach is the calculation of the anomalous dimensions. From these the spectrum of the integral operator of the Bethe Salpeter equation of the four gluon system can eventually be obtained. The spectrum of the system is encoded in the new function  $\chi_4(\{\alpha\})$  which depends on a set of quantum numbers  $\{\alpha\}$  associated with the symmetries of the system. We have derived a close relation between the anomalous dimensions and the spectrum of the respective integral operator of the BFKL equation encoded in the well-known function  $\chi_2(\nu, n)$ . Inspired by this relation we have initiated a similar approach for the four gluon system. This means that in our analysis we focus on the behaviour of this function near the integer points in the conformal dimension plane. The virtue of the method lies in the fact that this behavior can be interpreted physically in terms of the anomalous dimensions of the four gluon state.

Following Bartels [18] we have used the Faddeev method to transform the equation for the four gluon amplitude into an effective two reggeon equation defined in momentum space. We have argued that in order to obtain the short distance expansion corresponding to the twist expansion in momentum space the singularities of the elements (reggeon propagators and vertices) of this equation have to be isolated and iterated. We succeeded in classifying the singularities which arise from the reggeon intermediate states and the effective reggeon interaction vertex. With this classification at hand it is possible to see in which way these elementary singularities have to be iterated. The singularities that are generated upon iteration of the elementary singularities can be identified with the anomalous dimensions of new composite fields associated with the four (reggeized) gluon state. As a result of the iteration a very complex singularity structure of the four gluon amplitude is found containing poles as well as cuts. So far we have gained insight into the structural properties of the four gluon state. In our setup we could understand the origin of the singularity structure of the corresponding amplitude.

With our method we were able to reproduce the result of [18] for the anomalous dimension of the four gluon operator belonging to the twist four. With this anomalous dimension we associate a pole of the function  $\chi_4$  in the complex conformal dimension plane. We expect further poles being associated with the anomalous dimension of higher twist operators. The calculation of the anomalous dimensions belonging to the higher twists faces the complication that the extraction of singularities from the reggeon vertices turns out to be quite difficult. This is a problem of technical nature. As a possible way out one could investigate whether in configuration space the relevant information, namely the singularities of the effective reggeon-reggeon interaction, can be obtained more easily. In the last chapter we have demonstrated that the singularities belonging to the higher twists appear with a certain multiplicity. This multiplicity is associated with the quantum numbers of the function  $\chi_4$ . Ultimately with each complete set of quantum numbers one single singularity should be related. A conceptual problem arising here is that it is not easy to see in which way one should classify the resulting singularities with regard to the quantum numbers of the system. To classify the singularities according to the quantum numbers it is probably necessary to obtain more information on the mathematical structure of the problem. The identification of additional symmetries would of course be very helpful. Possibly, one has to restrict oneself to the large  $N_c$ -approximation in which the set of commuting operators can be identified in configuration space using quantum inverse scattering methods.

The specified problems constitute major challenges for future work. The analysis of the four gluon state certainly deserves further interest since it constitutes the next important step to be taken towards a unitary scattering amplitude in perturbative QCD.



## Acknowledgments

I would like to thank my supervisor Professor Jochen Bartels for constant guidance, encouragement and interest. I am very much indebted to him for countless helpful suggestions and discussions during all the years.

I thank Professor Wilfried Buchmüller for delivering his opinion on this thesis and Professor Gustav Kramer for the support of my applications for scholarships.

The discussions with Mark Wüsthoff were vital for my understanding of the Regge limit in QCD. I want to express my deep gratitude for his assistance and collaboration.

It was a great experience to meet Professor Lev Lipatov who generously explained us his ideas and shared some of his deep insights into QCD and field theory.

Special thanks to Jeff Forshaw for extraordinarily pleasant discussions and collaboration.

For fruitful collaboration I am indebted to Albert De Roeck, Markus Diehl, Carlo Ewerz, Professor Mikhail Ryskin and Matthias Vogt.

For the very careful reading of the manuscript and numerous helpful suggestions I would like to thank Carlo Ewerz. Helpful comments on the manuscript were also delivered by Claas Bontus.

Furthermore I would like to thank all participants of the seminar on perturbative aspects of QCD for creating such a nice atmosphere in the last four years.

The financial support of the Deutsche Forschungsgemeinschaft and the Studienstiftung des Deutschen Volkes is gratefully acknowledged.

This thesis would not have been possible without constant support from my parents. Finally thanks to Tanja for patience.

## A Appendix

### A.1 Fourier transformation of the Bethe-Salpeter equation

The non-trivial part is the transformation of the squared production vertex and the gluon trajectory. Regularizing the infrared singularities by a fictitious gluon mass  $\lambda$  and multiplying the whole equation (A.4) with  $\mathbf{k}^2(\mathbf{q} - \mathbf{k})^2$  the homogeneous part reads <sup>35</sup>

$$(\mathcal{K}\Phi_\omega)(\mathbf{k}, \mathbf{q} - \mathbf{k}) = \int d^2\mathbf{k}' \left( \frac{k(q-k)^* k'^*(q-k')}{|\mathbf{k} - \mathbf{k}'|^2 + \lambda^2} + \text{h.c.} \right) \Phi_\omega(\mathbf{k}', \mathbf{q} - \mathbf{k}') \\ - \pi \left( \log \frac{|\mathbf{k}|^2}{\lambda^2} + \log \frac{|\mathbf{q} - \mathbf{k}|^2}{\lambda^2} \right) \Phi_\omega(\mathbf{k}, \mathbf{q} - \mathbf{k}) \quad (\text{A.1})$$

Fourier transformation is defined as

$$\Phi_\omega(\rho_1, \rho_2) = \frac{1}{(2\pi)^4} \int d^2\mathbf{k} d^2\mathbf{q} e^{i\mathbf{k}\rho_1 + i(\mathbf{q}-\mathbf{k})\rho_2} \Phi_\omega(\mathbf{k}, \mathbf{q} - \mathbf{k}) \quad (\text{A.2})$$

Let us begin with the gluon trajectory. Performing the Fourier transformation and inserting

$$1 = \frac{1}{(2\pi)^2} \int d^2\rho_0 \int d^2\mathbf{l} e^{i\rho_0(\mathbf{l}-\mathbf{k})} \quad (\text{A.3})$$

we obtain

$$-16|\partial_1|^2|\partial_2|^2 \int d^2\rho_0 \left[ \frac{1}{(2\pi)^2} \int d^2\mathbf{l} e^{i\mathbf{l}(\rho_1-\rho_0)} \pi \log \frac{|\mathbf{l}|^2}{\lambda^2} \right] \Phi_\omega(\rho_0, \rho_2) \quad (\text{A.4})$$

For the integral in brackets we make the ansatz

$$- \left[ \frac{1}{(2\pi)^2} \int d^2\mathbf{l} e^{i\mathbf{l}(\rho_1-\rho_0)} \pi \log \frac{|\mathbf{l}|^2}{\lambda^2} \right] = \Gamma(\rho_1 - \rho_0) \quad (\text{A.5})$$

$$\Gamma(\rho_1 - \rho_0) = \frac{1}{|\rho_{10}|^2} \theta(|\rho_{10}| - \epsilon) + c(\epsilon, \lambda) \delta^{(2)}(\rho_{10}) \quad (\text{A.6})$$

and obtain

$$c(\epsilon, \lambda) = 2\pi[\log \lambda + \log \frac{\epsilon}{2} - 2\psi(1)] \quad (\text{A.7})$$

Here we have used

$$\int d^2\rho \frac{1}{|\rho|^2} \theta(|\rho| - \epsilon) e^{-i\rho} = 2\pi \int_\epsilon^\infty \frac{d|\rho|}{|\rho|} J_0(|\mathbf{l}||\rho|) \\ = 2\pi \left[ \log \frac{1}{\epsilon} + |\mathbf{l}| \int_0^\infty d|\rho| \log |\rho| J_1(|\mathbf{l}||\rho|) \right] + O(\epsilon) \\ = 2\pi \left[ \log \frac{1}{\epsilon} - \log \frac{|\mathbf{l}|}{2} + \psi(1) \right] + O(\epsilon) \quad (\text{A.8})$$

Now we turn to the squared production vertex. Applying Fourier transformation leads to

$$\int d^2\mathbf{k} d^2\mathbf{q} \frac{1}{(2\pi)^4} e^{i\mathbf{k}\rho_1 + i(\mathbf{q}-\mathbf{k})\rho_2} \int d^2\mathbf{k}' \left( \frac{k(q-k)^* k'^*(q-k')}{|\mathbf{k} - \mathbf{k}'|^2 + \lambda^2} + \text{h.c.} \right) \Phi_\omega(\mathbf{k}, \mathbf{q} - \mathbf{k}) \\ = \int d^2\rho_{1'} d^2\rho_{2'} \int d^2\mathbf{k} d^2\mathbf{q} \int d^2\hat{\mathbf{k}} \frac{16}{|\hat{\mathbf{k}}|^2 + \lambda^2} \partial_1^* \partial_2 e^{-i\hat{\mathbf{k}}(\rho_{1'} - \rho_{2'})} \\ \cdot \frac{1}{(2\pi)^4} e^{i\mathbf{k}(\rho_1 - \rho_{1'}) + i(\mathbf{q}-\mathbf{k})(\rho_2 - \rho_{2'})} \partial_1 \partial_2^* \Phi_\omega(\rho_{1'}, \rho_{2'}) + \text{h.c.} \\ = 16 \partial_1^* \partial_2 \int d^2\hat{\mathbf{k}} \frac{1}{|\hat{\mathbf{k}}|^2 + \lambda^2} e^{-i\hat{\mathbf{k}}(\rho_1 - \rho_2)} \partial_1 \partial_2^* \Phi_\omega(\rho_1, \rho_2) + \text{h.c.} \quad (\text{A.9})$$

---

<sup>35</sup>For simplicity we set  $\frac{N_c \alpha_s}{2\pi^2} = 1$  in this and the following section.

The  $\hat{\mathbf{k}}$  - integral gives

$$\begin{aligned}
\int d^2\hat{\mathbf{k}} \frac{e^{i\hat{\mathbf{k}}\rho}}{\hat{\mathbf{k}}^2 + \lambda^2} &= 2\pi \int_0^\infty d|\hat{\mathbf{k}}| \frac{|\hat{\mathbf{k}}| J_0(|\hat{\mathbf{k}}||\rho|)}{\hat{\mathbf{k}}^2 + \lambda^2} \\
&= 2\pi K_0(|\rho|\lambda) \\
&= 2\pi [\log \frac{2}{|\rho|} - \log \lambda + \psi(1)] + O(\lambda)
\end{aligned} \tag{A.10}$$

Comparing with eq. (A.7) we find that the combination  $\psi(1) - \log \lambda + \log 2$  cancels between the gluon production vertex and the trajectory function. The final form in configuration space reads

$$\begin{aligned}
|\partial_1|^2 |\partial_2|^2 (\mathcal{K}\Phi_\omega)(\rho_1, \rho_2) &= |\partial_1|^2 |\partial_2|^2 \int \frac{d^2\rho_0}{|\rho_{10}|^2} \theta(|\rho_{10}| - \epsilon) \Phi_\omega(\rho_0, \rho_2) \\
&\quad + |\partial_1|^2 |\partial_2|^2 \int \frac{d^2\rho_0}{|\rho_{20}|^2} \theta(|\rho_{20}| - \epsilon) \Phi_\omega(\rho_1, \rho_0) \\
&\quad + 2\pi \log \epsilon^2 |\partial_1|^2 |\partial_2|^2 \Phi_\omega(\rho_1, \rho_2) \\
&\quad - [\pi \partial_1^* \partial_2 \log |\rho_{12}|^2 \partial_1 \partial_2^* + \text{h.c.}] \Phi_\omega(\rho_1, \rho_2)
\end{aligned} \tag{A.11}$$

We rearrange the differential operators in the first two terms using integration by parts ( $g$  is a test function)

$$\begin{aligned}
\partial_1 \partial_1^* \int d^2\rho_0 g(|\rho_{10}|^2) \Phi_\omega(\rho_0, \rho_2) &= \partial_1 \int d^2\rho_0 \partial_1^* g(\rho_{10} \rho_{10}^*) \Phi_\omega(\rho_0, \rho_2) \\
&= \partial_1 \int d^2\rho_0 (-1) \partial_0^* g(\rho_{10} \rho_{10}^*) \Phi_\omega(\rho_0, \rho_2) = \partial_1 \int d^2\rho_0 g(|\rho_{10}|^2) \partial_0^* \Phi_\omega(\rho_0, \rho_2)
\end{aligned} \tag{A.12}$$

Distributing the derivatives in a symmetric way we end up with

$$\begin{aligned}
2 |\partial_1|^2 |\partial_2|^2 (\mathcal{K}\Phi_\omega)(\rho_1, \rho_2) &= \\
&\quad \partial_1 \partial_2^* \int d^2\rho_0 \left[ \frac{1}{|\rho_{10}|^2} \theta(|\rho_{10}| - \epsilon) - 2\pi \delta^{(2)}(\rho_{10}) \log |\rho_{12}| \right] \partial_0^* \partial_2 \Phi_\omega(\rho_0, \rho_2) \\
&\quad + \partial_1^* \partial_2 \int d^2\rho_0 \left[ \frac{1}{|\rho_{10}|^2} \theta(|\rho_{10}| - \epsilon) - 2\pi \delta^{(2)}(\rho_{10}) \log |\rho_{12}| \right] \partial_0 \partial_2^* \Phi_\omega(\rho_0, \rho_2) \\
&\quad + [1 \leftrightarrow 2] + \pi \log \epsilon^2 |\partial_1|^2 |\partial_2|^2 \Phi_\omega \\
&= \partial_1 \partial_2^* \int d^2\rho_0 \left[ \frac{1}{|\rho_{10}|^2} \theta(|\rho_{10}| - \epsilon) - 2\pi \delta^{(2)}(\rho_{10}) \log |\rho_{12}| \right] \partial_0^* \partial_2 \Phi_\omega(\rho_0, \rho_2) \\
&\quad + [\text{h.c.}] \\
&\quad + [1 \leftrightarrow 2] + \pi \log \epsilon^2 |\partial_1|^2 |\partial_2|^2 \Phi_\omega(\rho_1, \rho_2)
\end{aligned} \tag{A.13}$$

The final form is obtained by absorbing the logarithm into the argument of the  $\theta$ -function

$$\begin{aligned}
2 |\partial_1|^2 |\partial_2|^2 (\mathcal{K}\Phi_\omega)(\rho_1, \rho_2) &= \\
&\quad \partial_1 \partial_2^* \int \frac{d^2\rho_0}{|\rho_{10}|^2} \theta\left(\frac{|\rho_{10}|}{|\rho_{12}|} - \epsilon\right) \partial_0^* \partial_2 \Phi_\omega(\rho_0, \rho_2) + [\text{h.c.}] \\
&\quad + [1 \leftrightarrow 2] + \pi \log \epsilon^2 |\partial_1|^2 |\partial_2|^2 \Phi_\omega(\rho_1, \rho_2)
\end{aligned} \tag{A.14}$$

## A.2 The eigenvalue of the configuration space kernel

In this section we want to sketch how the eigenvalue of the BFKL-kernel can be obtained in configuration space. For our calculation we use the form of eq. (A.11) of the preceding section. We insert

$$\Phi_\omega(\rho_1, \rho_2) = \left( \frac{\rho_{12}}{\rho_{10'} \rho_{20'}} \right)^{\frac{1+n}{2} - i\nu} \left( \frac{\rho_{12}^*}{\rho_{10'}^* \rho_{20'}^*} \right)^{\frac{1-n}{2} - i\nu} \tag{A.15}$$

and use the fact that the kernel is conformally invariant. This allows to use as a special set of coordinates for which we calculate the eigenvalue the points  $\rho_1, \rho_2, \rho'_0 = \infty$ . It remains to calculate the integral

$$\int \frac{d^2 \rho_0}{|\rho_{10}|^2} \theta(|\rho_{10}| - \epsilon) (\rho_{20})^{\frac{1+n}{2} - i\nu} (\rho_{20}^*)^{\frac{1-n}{2} - i\nu} \quad (\text{A.16})$$

We use the following representation of the  $\theta$ -function ( $\delta \rightarrow +0$ )

$$\theta(|\rho_{10}| - \epsilon) = \frac{1}{2\pi i} \int_{-i\infty+\delta}^{i\infty+\delta} \frac{d\xi}{\xi} \left( \frac{|\rho_{10}|^2}{\epsilon^2} \right)^\xi \quad (\text{A.17})$$

and end with the configuration space integral

$$\begin{aligned} I(\nu, n; \xi) &= \int d^2 \rho_0 (|\rho_{10}|^2)^{\xi-1} (\rho_{20})^{\frac{1+n}{2} - i\nu} (\rho_{20}^*)^{\frac{1-n}{2} - i\nu} \\ &= (|\rho_{12}|^2)^{\frac{1}{2} - i\nu + \xi} \left( \frac{\rho_{12}}{\rho_{12}^*} \right)^{\frac{n}{2}} \int d^2 x x^{\xi-1} x^{*\xi-1} (x-1)^{\frac{1+n}{2} - i\nu} (x-1)^{* \frac{1-n}{2} - i\nu} \end{aligned} \quad (\text{A.18})$$

The two-dimensional integral which obviously depends only on  $|n|$  is calculated with a method which is described in detail in [52]. After a Wick-rotation, introduction of light-cone coordinates and deformation of contours we get

$$\begin{aligned} I(\nu, n; \xi) &= (|\rho_{12}|^2)^{\frac{1}{2} - i\nu + \xi} \left( \frac{\rho_{12}}{\rho_{12}^*} \right)^{\frac{|n|}{2}} \sin \pi \left( \frac{1-n}{2} - i\nu \right) \\ &\quad \int_0^1 du u^{\xi-1} (1-u)^{\frac{1+|n|}{2} - i\nu} \int_1^\infty dv v^{\xi-1} (v-1)^{\frac{1-|n|}{2} - i\nu} \\ &= \pi (|\rho_{12}|^2)^{\frac{1}{2} - i\nu + \xi} \left( \frac{\rho_{12}}{\rho_{12}^*} \right)^{\frac{|n|}{2}} \frac{\Gamma(\xi)}{\Gamma(1-\xi)} \frac{\Gamma(-\xi - \frac{1-|n|}{2} + i\nu)}{\Gamma(\xi + \frac{3+|n|}{2} - i\nu)} \frac{\Gamma(\frac{3+|n|}{2} - i\nu) \Gamma(\frac{3-|n|}{2} - i\nu)}{\Gamma(\frac{1+|n|}{2} + i\nu) \Gamma(\frac{1-|n|}{2} - i\nu)} \end{aligned} \quad (\text{A.19})$$

Now we can perform the  $\xi$ -integration by shifting the contour to the left. The first non-vanishing contribution comes from the double-pole at  $\xi = 0$ . All subsequent poles in the left half-plane vanish in the limit  $\epsilon \rightarrow 0$ . As the result we get for eq. (A.16)

$$\begin{aligned} &\pi (|\rho_{12}|^2)^{\frac{1}{2} - i\nu} \left( \frac{\rho_{12}}{\rho_{12}^*} \right)^{\frac{|n|}{2}} \left[ 2\psi(1) - \psi\left(\frac{3+|n|}{2} - i\nu\right) - \psi\left(-\frac{1-|n|}{2} + i\nu\right) - \log \frac{\epsilon^2}{|\rho_{12}|^2} \right] \\ &= (|\rho_{12}|^2)^{\frac{1}{2} - i\nu} \left( \frac{\rho_{12}}{\rho_{12}^*} \right)^{\frac{|n|}{2}} \left[ 2\psi(1) - \psi\left(\frac{1+|n|}{2} + i\nu\right) - \psi\left(\frac{1+|n|}{2} - i\nu\right) \right. \\ &\quad \left. - \frac{2i\nu - 1}{(\frac{1+|n|}{2} - i\nu)(\frac{1-|n|}{2} - i\nu)} - \log \frac{\epsilon^2}{|\rho_{12}|^2} \right] \end{aligned} \quad (\text{A.20})$$

After adding the term with  $\rho_1$  and  $\rho_2$  interchanged the  $\log \epsilon^2$ -contribution cancels in eq. (A.11). The fourth term in the bracket above and the  $\log |\rho_{12}|^2$  cancel against the remaining terms

$$- \pi [\partial_1^* \partial_2 \log |\rho_{12}|^2 \partial_1 \partial_2^* + \text{h.c.}] (|\rho_{12}|^2)^{\frac{1}{2} - i\nu} \left( \frac{\rho_{12}}{\rho_{12}^*} \right)^{\frac{|n|}{2}} \quad (\text{A.21})$$

after the derivatives are taken. After all we obtain for the action of the BFKL-kernel on the conformal three-point functions

$$\pi (|\rho_{12}|^2)^{\frac{1}{2} - i\nu} \left( \frac{\rho_{12}}{\rho_{12}^*} \right)^{\frac{|n|}{2}} \left[ 2\psi(1) - \psi\left(\frac{1+|n|}{2} + i\nu\right) - \psi\left(\frac{1+|n|}{2} - i\nu\right) \right] \quad (\text{A.22})$$

what was to be proved.

### A.3 Properties of the BFKL eigenvalue $\chi(\nu, n)$

For completeness some properties of the function  $\chi(\nu, n)$  used at different stages of this work are presented here. The eigenvalue of the BFKL kernel reads ( $\psi(x)$  is the logarithmic derivative of the  $\Gamma$ -function  $\psi(x) = \Gamma'(x)/\Gamma(x)$ )

$$\chi(\nu, n) = \frac{N_c \alpha_s}{\pi} \left[ 2\psi(1) - \psi\left(\frac{1+|n|}{2} + i\nu\right) - \psi\left(\frac{1+|n|}{2} - i\nu\right) \right] \quad (\text{A.23})$$

The function  $\chi(\nu, n)$  is a real function of  $\nu$  which is analytic in the strip  $-(1+|n|)/2 < \text{Im}(\nu) < (1+|n|)/2$ . As a function of  $\nu \in \mathbb{R}$ ,  $\chi(\nu, n)$  is symmetric w. r. t.  $\nu = 0$ , has a global maximum at  $\nu = 0$  and tends to  $-\infty$  for  $\nu \rightarrow \pm\infty$ . For the high-energy limit the expansion around  $\nu = 0$  up to quadratic order (harmonic approximation) is important

$$\chi(\nu, 0) = \frac{N_c \alpha_s}{\pi} [4\log 2 - 14\zeta(3)\nu^2 + O(\nu^6)] \quad (\text{A.24})$$

$$\chi(\nu, \pm 1) = \frac{N_c \alpha_s}{\pi} [-2\zeta(3)\nu^2 + O(\nu^6)] \quad (\text{A.25})$$

$$\chi(\nu, \pm 2) = \frac{N_c \alpha_s}{\pi} [-4 + 4\log 2 + (16 - 14\zeta(3))\nu^2 + O(\nu^6)] \quad (\text{A.26})$$

In this approximation the BFKL equation becomes equivalent to a diffusion equation, where the coefficient of the quadratic term determines the diffusion constant. Comparing the expansions with zero and nonzero conformal spin  $n$  we see that in the high-energy limit the contribution with zero conformal spin always dominates because it is the only one with a strictly positive intercept.

The singularities of  $\chi(\nu, n)$  are located on the imaginary  $\nu$ -axis. For each  $n$  there are integer spaced simple poles with identical residues. The singularity structure is most easily read off from the representation

$$\chi(\nu, n) = \frac{N_c \alpha_s}{\pi} \sum_{k=0}^{\infty} \left[ \frac{1}{k + \frac{1+|n|}{2} + i\nu} + \frac{1}{k + \frac{1+|n|}{2} - i\nu} - \frac{2}{k+1} \right] \quad (\text{A.27})$$

Likewise important is the Laurent expansion of  $\chi(\nu, 0)$  around the pole at  $i\nu = -1/2$ . It reads

$$\chi(\nu, 0) = \frac{N_c \alpha_s}{\pi} \frac{1}{i\nu + \frac{1}{2}} \left[ 1 + 2 \sum_{k=1}^{\infty} \zeta(2k+1) \left( i\nu + \frac{1}{2} \right)^{2k+1} \right] \quad (\text{A.28})$$

This expansion is used to calculate higher order contributions to the anomalous dimension matrix from the BFKL equation [9]. From the fact that the first subleading term in this expansion is of order  $(i\nu + \frac{1}{2})^2$  one concludes that the first subleading contribution to the gluon anomalous dimension which follows from the BFKL equation is of order  $\alpha_s^4$ .

### A.4 Expansion of the momentum space eigenfunction for small argument

In this appendix we show how the small argument expansion the beginning of which is given in eq. (A.128) can be derived starting from the momentum space expression (A.53)

$$E^{(\nu, 0)}(\mathbf{k}, \mathbf{q} - \mathbf{k}) = b(\nu, 0) \int_0^1 dx [x(1-x)]^{-\frac{1}{2} + i\nu} [\mathbf{k}^2 + x((\mathbf{q} - \mathbf{k})^2 - \mathbf{k}^2)]^{-\frac{3}{2} - i\nu} {}_2F_1\left(\frac{3}{2} + i\nu, -\frac{1}{2} + i\nu, 1; 1 - \frac{\mathbf{q}^2 x(1-x)}{\mathbf{k}^2 + x((\mathbf{q} - \mathbf{k})^2 - \mathbf{k}^2)}\right) \quad (\text{A.29})$$

where  $b(\nu, 0)$  collects some unimportant (for the moment) coefficients. It is necessary to perform first the  $x$ -integration. To this end an analytic transformation of the  ${}_2F_1$ -function is applied which changes the

argument from  $z$  to  $1 - z$ . In the two terms which are generated by this procedure the series representation for the hypergeometric function is used. This leads to

$$E^{(\nu,0)}(\mathbf{k}, \mathbf{q} - \mathbf{k}) = b(\nu, 0)(\mathbf{q}^2)^{-i\nu} \left[ \frac{(\mathbf{q}^2)^{i\nu}}{(\mathbf{k}^2)^{\frac{3}{2}+i\nu}} \frac{\Gamma(-2i\nu)}{\Gamma(-\frac{1}{2} - i\nu)\Gamma(\frac{3}{2} - i\nu)} \sum_{n=0}^{\infty} \frac{(\frac{3}{2} + i\nu)_n (-\frac{1}{2} + i\nu)_n}{n!(1 + 2i\nu)_n} \left( \frac{\mathbf{q}^2}{\mathbf{k}^2} \right)^n \right. \\ \left. \cdot \int_0^1 dx [x(1-x)]^{-\frac{1}{2}+i\nu+n} \left( 1 + x \frac{(\mathbf{k} - \mathbf{q})^2 - \mathbf{k}^2}{\mathbf{k}^2} \right)^{-n-\frac{3}{2}-i\nu} + (\text{h.c.}) \right] \quad (\text{A.30})$$

where the Pochhammer symbol  $(a)_n = \Gamma(a+n)/\Gamma(a)$  has been used. The  $x$ -integral in the second line can now be performed yielding

$$B\left(\frac{1}{2} + i\nu + n, \frac{1}{2} + i\nu + n\right) {}_2F_1\left(\frac{3}{2} + i\nu + n, \frac{1}{2} + i\nu + n, 1 + 2i\nu + 2n; \frac{\mathbf{k}^2 - (\mathbf{k} - \mathbf{q})^2}{\mathbf{k}^2}\right) \quad (\text{A.31})$$

and analogously for the complex conjugate. Now, unfortunately the argument of the hypergeometric function does not allow an expansion in powers of  $|\mathbf{k}|$ . To invert the argument one has to use another analytic continuation for the hypergeometric function which - since the first two arguments differ by unity - is logarithmic [53]. In this way one obtains

$$E^{(\nu,0)}(\mathbf{k}, \mathbf{q} - \mathbf{k}) = b(\nu, 0)(\mathbf{q}^2)^{-i\nu} \left[ \frac{\Gamma(-2i\nu)}{\Gamma(-\frac{1}{2} - i\nu)\Gamma(\frac{3}{2} - i\nu)} \sum_{n=0}^{\infty} \frac{(\frac{3}{2} + i\nu)_n (-\frac{1}{2} + i\nu)_n}{n!(1 + 2i\nu)_n} \frac{(\mathbf{q}^2)^{n+i\nu}}{((\mathbf{k} - \mathbf{q})^2 - \mathbf{k}^2)^{n+\frac{3}{2}+i\nu}} \right. \\ \left. \left(\frac{1}{2} + i\nu + n\right) \left( \sum_{l=0}^{\infty} \frac{(\frac{1}{2} + i\nu + n)_{l+1} (\frac{1}{2} - i\nu - n)_{l+1}}{l!(l+1)!} \left( \frac{\mathbf{k}^2}{(\mathbf{q} - \mathbf{k})^2 - \mathbf{k}^2} \right)^l \left[ \gamma_l - \log \frac{\mathbf{k}^2}{(\mathbf{q} - \mathbf{k})^2 - \mathbf{k}^2} \right] + \frac{(\mathbf{q} - \mathbf{k})^2 - \mathbf{k}^2}{\mathbf{k}^2} \right) \right. \\ \left. + (\text{h.c.}) \right] \quad (\text{A.32})$$

with

$$\gamma_l = \psi(2+l) + \psi(1+l) - \psi\left(\frac{3}{2} + i\nu + n + l\right) - \psi\left(\frac{3}{2} - i\nu - n + l\right) \quad (\text{A.33})$$

Starting from this expression the expansion in powers of  $|\mathbf{k}|/|\mathbf{q}|$  or alternatively  $|\mathbf{q} - \mathbf{k}|/|\mathbf{q}|$  is in principle straightforward. The main problem is to collect all terms which contribute to a given order. It is now clear where the logarithms and  $\psi$ -functions in eq. (A.128) have their origin. Note that the leading term in the expansion (A.128) comes from the very last term in the second line of (A.32).

## References

- [1] I.I.Balitskii, L.N.Lipatov, *Sov. J. Nucl. Phys.* **28** (1978) 822.
- [2] L.N.Lipatov, *Sov. J. Nucl. Phys.* **23** (1976) 642.
- [3] E.A.Kuraev, L.N.Lipatov, V.S.Fadin, *Sov. Phys. JETP* **44** (1976) 443.
- [4] E.A.Kuraev, L.N.Lipatov, V.S.Fadin, *Sov. Phys. JETP* **45** (1977) 199.
- [5] L.N.Lipatov, *Sov. Phys. JETP* **63** (1986) 904.
- [6] J.Bartels, A.DeRoeck, H.Lotter, hep-ph/9608401.
- [7] J.C.Collins, D.E.Soper, G.Sterman, in *Perturbative Quantum Chromodynamics*, A.H.Mueller (ed.), World Scientific, Singapore, 1989 and references therein.
- [8] V.N.Gribov, L.N.Lipatov, *Sov. J. Nucl. Phys.* **15** (1972) 438,675;  
G.Altarelli, G.Parisi, *Nucl. Phys.* **B 126** (1977) 297; Y.Dokshitzer, *Sov. Phys. JETP* **46** (1977) 641.
- [9] S.Catani, F.Hautmann, *Nucl. Phys.* **B 427** (1994) 475;  
S.Catani, M.Ciafaloni, F.Hautmann, *Phys. Lett.* **B 242** (1990) 97; *Nucl. Phys.* **B 366** (1991) 135.
- [10] H1 Collaboration, *Nucl. Phys.* **B 439** (1995) 471; *Nucl. Phys.* **B 470** (1996) 3.
- [11] ZEUS Collaboration, *Z. Phys.* **C 65** (1995) 379, *Z. Phys.* **C 69** (1996) 607.
- [12] R.K.Ellis, Z.Kunszt, E.M.Levin, *Nucl. Phys.* **B 420** (1994) 517, Erratum *Nucl. Phys.* **B 433** (1995) 498; R.K.Ellis, F.Hautmann, B.Webber, *Phys. Lett.* **B 348** (1995) 582; R.D.Ball, S.Forte, *Phys. Lett.* **B 351** (1995) 313.
- [13] A.H.Mueller, *Nucl. Phys.* **B** (Procc. Suppl.) **18 C** (1991) 125; W.K.Tang, *Phys. Lett.* **B 278** (1991) 363; J.Bartels, A.DeRoeck, M.Loewe, *Z. Phys.* **C 54** (1992) 635; J.Kwieciński, A.D.Martin, P.J.Sutton, *Phys. Lett.* **B 287** (1992) 254; *Phys. Rev.* **D 46** (1992) 921.
- [14] J.Bartels, H.Lotter, *Phys. Lett.* **B 309** (1993) 400.
- [15] J.Bartels, V.DelDuca, A.DeRoeck, D.Graudenz, M.Wüsthoff, *Phys. Lett.* **B 384** (1996) 300.
- [16] J.R.Forshaw, M.G.Ryskin, *Z. Phys.* **C 68** (1995) 137.
- [17] L.Frankfurt, M.Strikman, *Phys. Rev. Lett.* **63** (1989) 1914, Erratum *Phys. Rev. Lett.* **64** (1990) 815.
- [18] J.Bartels, *Phys. Lett.* **B 298** (1993) 204; *Z. Phys.* **C 62** (1994) 425.
- [19] J.Bartels, M.Wüsthoff, *Z. Phys.* **C 66** (1995) 157.
- [20] H1 Collaboration, *Phys. Lett.* **B 348** (1995) 681.
- [21] ZEUS Collaboration, *Z. Phys.* **C 70** (1996) 391.
- [22] J.Bartels, H.Lotter, M.Vogt, *Phys. Lett.* **B 373** (1996) 215;  
M.Vogt, Diploma – thesis, University of Hamburg 1995 (unpublished).
- [23] J.D.Bjorken, hep-ph/9601363 and references therein.
- [24] W.Buchmüller, A.Hebecker, *Nucl. Phys.* **B 463** (1996).
- [25] J.Bartels, H.Lotter, M.Wüsthoff, *Phys.Lett.* **B 379** (1996) 239;  
J.Bartels, C.Ewerz, H.Lotter, M.Wüsthoff, *Phys.Lett.* **B 386** (1996) 389.
- [26] M.Diehl, hep-ph/9610430.

- [27] A.H.Mueller, *QCD 20 years later*, Vol. 1 (edited by P.M.Zerwas, H.A.Kastrup), Singapore 1993; E.M.Levin, *Nucl. Phys.* **B 453** (1995) 303.
- [28] L.V.Gribov, E.M.Levin, M.G.Ryskin, *Phys. Rep.* **100** (1983) 1.
- [29] J.Bartels, *Nucl. Phys.* **B 151** (1979) 293; *Nucl. Phys.* **B 175** (1980) 365.
- [30] J.Bartels, DESY 91-074.
- [31] V.N.Gribov, *Sov. Phys. JETP* **26** (1968) 414.
- [32] H.D.I.Abarbanel, J.D.Bronzan, R.L.Sugar, A.R.White, *Phys. Rep.* **C 21** (1973) 120.
- [33] A.R.White, *Int. J. Mod. Phys.* **A 6** (1991) 1859.
- [34] J.Bartels, L.N.Lipatov, M.Wüsthoff, *Nucl. Phys.* **B 464** (1996) 298.
- [35] L.N.Lipatov, *Phys. Lett.* **B 251** (1990) 284.
- [36] J.Kwieciński, M.Praszałowicz, *Phys. Lett.* **B 94** (1980) 413.
- [37] L.N.Lipatov, *Phys. Lett.* **B 309** (1993) 394; *JETP Lett.* **59** (1994) 596.
- [38] L.D.Faddeev, G.P.Korchemsky, *Phys. Lett.* **B 342** (1995) 311.
- [39] V.O.Tarasov, L.A.Takhtajan, L.D.Faddeev, *Theor. Math. Phys.* **57** (1983) 163.
- [40] G.P.Korchemsky, *Nucl. Phys.* **B 443** (1995) 255; *Nucl. Phys.* **B 462** (1996) 333.
- [41] Z.Maassarani, S.Wallon, *J. Phys.* **A 28** (1995) 6423.
- [42] A.A.Belavin, A.M.Polyakov, A.B.Zamolodchikov, *Nucl. Phys.* **B 241** (1984) 333; *J. Statist. Phys.* **34** (1984) 763.
- [43] L.D.Faddeev, *Sov. Phys.* **12** (1961) 1014.
- [44] J.Bartels, H.Lotter, M.Wüsthoff, *Z. Phys.* **C 68** (1995) 121.
- [45] A.J.Askew, J.Kwieciński, A.D.Martin, P.J.Sutton, *Phys. Rev.* **D 47** (1993) 3775, *Phys. Rev.* **D 49** (1994) 4402;  
A.J.Askew, K.Golec-Biernat J.Kwieciński, A.D.Martin, P.J.Sutton, *Phys. Lett.* **B 325** (1994) 212.
- [46] J.Bartels, J.R.Forshaw, H.Lotter, M.Wüsthoff, *Phys. Lett.* **B 375** (1996) 301.
- [47] J.Bartels, J.R.Forshaw, H.Lotter, L.N.Lipatov, M.Ryskin, M.Wüsthoff, *Phys. Lett.* **B 348** (1995) 589.
- [48] J.Bartels, L.N.Lipatov, H.Lotter, DESY-preprint in preparation.
- [49] V.S.Fadin, L.N.Lipatov, hep-ph/9602287.
- [50] G.Mack, *Group theoretical approach to conformal invariant quantum field theory*, Journ. de Physique (Paris) **34** C11 (supplement au no. 10) 99 (1973), and in *Renormalization and invariance in quantum field theory*, E.R.Caianello (ed.), Plenum Press 1974.
- [51] A.M.Polyakov, *JETP Lett.* **12** (1970) 381.
- [52] V.I.S.Dotsenko, *Lectures on conformal field theory*, Advanced Studies in Pure Mathematics 16, 1988.
- [53] The Bateman manuscript project, A. Erdélyi (ed.), McGraw-Hill book company, 1953.
- [54] A.DeRujula, S.L.Glashow, H.D.Politzer, S.B.Treiman, F. Wilczek, A. Zee, *Phys. Rev.* **D 10** (1974) 1649.



- [55] R.D.Ball, S.Forte, *Phys. Lett.* **B 335** (1994) 77.
- [56] J.C.Collins, P.V.Landshoff, *Phys. Lett.* **B 276** (1992) 196.
- [57] J.R.Forshaw, P.N.Harriman, P.J.Sutton, *Nucl. Phys.* **B 416** (1994) 739;  
M.F.McDermott, J.R.Forshaw, G.G.Ross, *Phys. Lett.* **B 349** (1995) 189; M.F.McDermott, J.R.Forshaw,  
hep-ph/9606293.
- [58] R.E.Hancock, D.A.Ross, *Nucl. Phys.* **B 383** (1992) 575.
- [59] E.M.Levin, M.G.Ryskin, *Sov. J. Nucl. Phys.* **53** (1991) 653.
- [60] A.V.Kotval, E665 Collaboration, Fermilab-Conf-95/046-E, Presented at the XXXth Rencontres de  
Moriond, March 1995.
- [61] H1 Collaboration, *Phys. Lett.* **B 356** (1995) 118;  
K.Golec-Biernat, J.Kwieciński, A.D.Martin, P.J.Sutton, *Phys. Rev.* **D 50** (1994) 217, *Phys. Lett.* **B**  
**335** (1994) 220.
- [62] G.Marchesini, *Nucl. Phys.* **B 445** (1995) 49.
- [63] M.G.Ryskin, *Z. Phys.* **C 57** (1993) 89.
- [64] A.H.Mueller, W.K.Tang, *Phys. Lett.* **B 284** (1992) 123.
- [65] E.M.Levin, M.G.Ryskin, *Z. Phys.* **C 48** (1990) 231.
- [66] N.N.Nikolaev, B.G.Zakharov, V.R.Zoller, *Phys.Lett.* **B 366** (1996) 337.
- [67] A.Donnachie, P.V.Landshoff, *Phys.Lett.* **B 123** (1983) 345; *Nucl. Phys.* **B 231** (1984) 189; *Nucl. Phys.*  
**B 267** (1986) 690.
- [68] G.P.Lepage, *Journ. Comp. Phys.* **27** (1978) 192.
- [69] W.Buchmüller, D.Haidt, hep-ph/9605428.
- [70] A.L.Ayala, M.B. Gay Ducati, E.M.Levin, hep-ph/9607210.
- [71] A.H.Mueller, *Nucl. Phys.* **B 335** (1990) 115.
- [72] N.N.Nikolaev, B.G.Zakharov, *Z. Phys.* **C 53** (1992) 331.
- [73] E.M.Levin, M.Wüsthoff, *Phys. Rev.* **D 50** (1994) 4306.
- [74] M.Wüsthoff, PhD – thesis, University of Hamburg 1995, DESY 95-166.
- [75] A.H.Mueller, B.Patel, *Nucl. Phys.* **B 425** (1994) 471.
- [76] M.G.Ryskin, M.Besancon, Proceedings of the HERA workshop 'Physics at HERA', Vol. 1 (edited by  
W.Buchmüller, G.Engelman), Hamburg 1991.
- [77] N.N.Nikolaev, B.G.Zakharov, *Phys.Lett.* **B 332** (1994) 177;  
M.Genovese, N.N.Nikolaev, B.G.Zakharov, *Phys.Lett.* **B 378** (1996) 347.
- [78] M.Diehl, *Z. Phys.* **C 66** (1995) 181.
- [79] W.Buchmüller, M.McDermott, A.Hebecker, hep-ph/9607290.
- [80] E.M.Levin, M.G.Ryskin, A.D.Martin, T.Teubner, hep-ph/9604443.
- [81] G.Engelman, P.Schlein, *Phys.Lett.* **B 152** (1985) 256.

- [82] A.Donnachie, P.V.Landshoff, *Nucl. Phys.* **B 244** (1984) 322; *Nucl. Phys.* **B 303** (1988) 634.
- [83] M.Glück, E.Reya, A.Vogt, *Z. Phys.* **C 67** (1995) 433.
- [84] S.Brodsky, L.Frankfurt, J.F.Gunion, A.H.Mueller, M.Strikman, *Phys. Rev.* **D 50** (1994) 3134;  
L.Frankfurt, W.Koepf, M.Strikman, *Phys. Rev.* **D 54** (1996) 3194;  
M.G.Ryskin, R.G.Roberts, A.D.Martin, E.M.Levin, hep-ph/9511228.
- [85] H.Georgi, J.Sheiman, *Phys. Rev.* **D 20** (1979) 111;  
C.Rumpf, G.Kramer, *Phys.Lett.* **B 89** (1980) 380;  
C.Rumpf, G.Kramer, J.Willrodt, *Z. Phys.* **C 7** (1981) 337.
- [86] V.Hedberg, G.Ingelman, C.Jacobsson, L.Jönsson, Proceedings of the HERA workshop 'Physics at HERA', Vol. 1 (edited by W.Buchmüller, G.Ingelman), Hamburg 1991.
- [87] ZEUS collaboration, *Z. Phys.* **C 70** (1996) 391.
- [88] M.Froissart, *Phys. Rev.* **12** (1961) 1053.
- [89] L.N.Lipatov *Nucl. Phys.* **B 365** (1991) 614;  
R.Kirschner, L.N.Lipatov, L.Szymanowski, *Nucl. Phys.* **B 425** (1994) 579; *Phys. Rev.* **D 51** (1995) 838;  
L.N.Lipatov *Nucl. Phys.* **B 452** (1995) 369.
- [90] H.Verlinde, E.Verlinde, hep-th/9302104.
- [91] O.Nachtmann, *Ann. Phys.* **209** (1991) 436.
- [92] I.I.Balitskii, *Nucl. Phys.* **B 463** (1996) 99.
- [93] G.t'Hooft, *Nucl. Phys.* **B 72** (1974) 461; *Nucl. Phys.* **B 75** (1974) 461;
- [94] A.R.White, *Phys. Lett.* **B 334** (1994) 87; A.R.White, C.Coriano, *Phys. Rev. Lett.* **74** (1995) 4980; *Nucl. Phys.* **B 451** (1995) 231; *Nucl. Phys.* **B 468** (1996) 175.
- [95] L.N.Lipatov, DESY 96-132, hep-ph/9610276, and private communication.
- [96] C.Ewerz, PhD thesis in preparation.
- [97] G.P.Korchemsky, *Nucl. Phys.* **B 443** (1995) 225.
- [98] K.G.Wilson, *Phys. Rev.* **179** (1969) 1499.
- [99] E.M.Levin, M.G.Ryskin, A.G.Shuvaev, *Nucl. Phys.* **B 387** (1992) 589.
- [100] J.Bartels, M.G.Ryskin, *Z. Phys.* **C 62** (1994) 425.
- [101] C.Itzykson, J.B.Zuber, Quantum Field Theory, Singapore 1985.
- [102] M.Kuhlen, private communication.